PHOTOCHEMISTRY AND BIO-EVALUATION OF 1, 4- DISUBSTITUTED TETRAZOLETHIONES AND SYNTHESIS OF 2-(2-(PHENYLIMINO) VINYL)BENZONITRILE

by

RADHIKA CHHABRA

M. S., University of Delhi, Delhi, India, 2003

A THESIS

Submitted in partial fulfillment of the

Requirements for the degree

MASTER OF SCIENCE

Department of Chemistry
College of Arts and Science

KANSAS STATE UNIVERSITY
Manhattan, Kansas

2007

Approved by:

Major Professor

Dr. Sundeep Rayat

ABSTRACT

Compounds containing the tetrazole scaffold have wide variety of applications in medicine, food industry, automobile industry, photography, agriculture. As a result, the structure and reactivity of these compounds have been studied. However, the related tetrazolethione scaffold has not been studied well. In our work presented in Chapter-1 (part-1), the synthesis, photochemical properties and reactivities of 1,4-disubstituted tetrazolethione analogs **20a-d** are described. The solvent effects on the photochemistry of compounds are discussed and; the rates and quantum yields for the photodecomposition of compounds are documented. The photodecomposition products for the photolysis of **20a-d** were analyzed by LCMS, GCMS and NMR spectroscopy; the results pertaining to their identification are also reported. Further, the multiphoton excitation of THF solution of1-methyl-4-(4-nitrophenyl)-1*H*-tetrazol-5(4*H*)-thione **20d** with Ti: Sapphire laser was also performed; however, the experiment was not successful. In Chapter-2 (part-1), the cytoxicity of the 1-methyl-4-(4-chlorophenyl)-1*H*-tetrazol-5(4*H*)-thione **20c** against human breast cancer cell is documented. MTT assays were performed for a time dependent study of the cytoxicity.

In part-2 which consists of Chapter-3, the synthesis of 2-(2-phenylimino)vinyl)benzonitirle is described. This was as a step towards our laboratory's goal of synthesizing a series of mono-, di- and tri- azaenyne-allenes and studying their Myers-Saito and Schmittel cyclizations. In future, if our

cyclization studies are successful, these cyclizations could be employed for synthesis of heteroaromatic rings found in many compounds of biological importance.

TABLE OF CONTENTS

LIST OF TABLES viii

LIST OF FIGURES ix

LIST OF SCHEMES xi

PART ONE

Chapter-1. Photochemistry of 1,4-Disubstituted Tetrazolethiones 2

- Introduction 2
- Results and Discussion 13
- Conclusions 38
- References 40
- Experimental Section 44

I. 1.Synthesis 44

1. 5-Chloro-1-phenyl-1H-tetrazole **(22)** 44
2. 1-Phenyl-1*H*-tetrazol-5(4*H*)-one **(23a)** 44
3. 1-(4-Methoxyphenyl)-1*H*-tetrazol-5(4*H*)-one **(23b)** 45
4. 1-(4-Chlorophenyl)-1*H*-tetrazol-5(4*H*)-one **(23c)** 46
5. 1-(4-Nitrophenyl)-1*H*-tetrazol-5(4*H*)-one **(23d)** 46
6. 1-Methyl-4-phenyl-1*H*-tetrazol-5(4*H*)-one **(25a)** 46
7. 1-Methyl-4-(4-methoxyphenyl)-1*H*-tetrazol-5(4*H*)-one **(25b)** 47
8. 1-Methyl-4-(4-chlorophenyl)-1H-tetrazol-5(4H)-one **(25c)** 47
9. 1-Methyl-4-(4-nitrophenyl)-1H-tetrazol-5(4H)-one **(25d)** 48
10. 1-Methyl-4-phenyl-1*H*-tetrazole-5(4*H*)-thione **(20a)** 48
11. 1-Methyl-4-(4-methoxyphenyl)-1*H*-tetrazole-5(4H)-thione**(20b)** 49

12. 1-Methyl-4-(4-chlorophenyl)-1*H*-tetrazole-5(4H)-thione**(20c)** 49

13. 1-Methyl-4-(4-nitrophenyl)-1H-tetrazole-5(4H)-thione **(20d)** 50

I. 2. Photolysis of tetrazolethione analogs 50

I. 3. Ferrioxalate Actinometry 51

I. 4. HPLC separation 52

I. 4. 1. Photolysis of THF solution of **20a** 52

I. 4. 2. Photolysis of MeCN solution of **20c** 53

Chapter-2. Bio- evaluation of cytotoxicity of 1-methyl-4-(4-chlorophenyl)-1*H*-tetrazol-5(4*H*)-thione against MCF-7 cell line 54

- Introduction 54
- Results and Discussion 55
- Conclusions 58
- References 59
- Experimental Section 60

I. 1. Cell Culture 60

I. 2. Drug Treatment 60

I. 2. 1. Time dependent study 60

I. 2. 3. 48 h Treatments 61

I. 3. 1. MTT cell proliferation assay 61

I. 3. 2 % Cell Viability versus Treatment plot for 48 h Treatments 62

PART TWO

Chapter-3. Synthesis of 2-(2-(phenylimino)vinyl)benzonitrile 64

- Introduction 64

- Results and Discussion 74
- Conclusions 76
- References 78
- Experimental Section 81

I. Synthesis 81

1. 2-(2-Cyanophenyl) acetic acid **(20)** 81

II. Unsuccessful Synthesis 81

1. 2-Cyanophenyl-2-ketene **(33)** 81

2. 2-Cyanophenyl-2-acetic acid chloride **(35)** 82

Appendix I: ^{1}H-NMR and ^{13}C-NMR spectra (Chapter -1) 83

Appendix II: IR spectra (Chapter -1) 110

Appendix III: Mass spectra (Chapter -1) 121

Appendix IV: Overlayed UV spectra of photolysis experiments (Chapter -1) 135

Appendix V: Overlayed HPLC chromatograms of photolysis Experiments (Chapter -1) 139

Appendix VI: LCMS spectra of photolysis products (Chapter -1) 144

Appendix VII:GCMS spectra of photolysis products (Chapter -1) 149

Appendix VIII:NMR spectra of photolysis products (Chapter -1) 170

Appendix IX: HRMS spectrum :

6-chloro-1,3-dihydro-1-methyl-2H-benzimidazole-2-thione **34c**

(Chapter -1) 175

Appendix X: Overlayed fluorescence spectra for photolysis experiments (Chapter -1) 177

Appendix XI: NMR spectra of 2-(2-cyanophenyl) acetic acid **(20)** (Chapter -3) 182

LIST OF TABLES

PART ONE

Chapter-1. Photochemistry of 1,4-Disubstituted Tetrazolethiones

Table 1. Absorption band positions and extinction coefficients 20

Table 2. Quantum Yields 26

LIST OF FIGURES

PART ONE

Chapter-1. Photochemistry of 1,4-Disubstituted Tetrazolethiones

Figure 1. Overlay of 1, 4- disubstitued tetrazolethiones spectra in (i) THF, (ii) Acetonitrile 19

Figure 2. Overlay of (i) UV spectra and (ii) HPLC chromatograms recorded during photolysis of 1-methyl-4-(4-nitrophenyl)-1H-tetrazol-5(4H)-thione(**20d**) in THF 21

Figure 3 (i). Photochemical decomposition of tetrazolethiones. ln (A/Ao) vs. Irradiation time plots for THF solutions 23

Figure 3 (ii). Photochemical decomposition of tetrazolethiones. ln (A/Ao) vs. Irradiation time plots for MeCN solutions 24

Figure 4. HPLC chromatogram of irradiated 1-methyl-4-phenyl-1H-tetrazol-5(4H)-thione **20a** 31

Figure 5. HPLC chromatogram of irradiated methyl-4-(4-chlorophenyl)-1H-tetrazol-5(4H)-thione **20c** 32

Figure 6. Mass spectrum of 6-chloro-1,3-dihydro-1-methyl-2H-Benzimidazole-2-thione **34c** 34

Figure 7. Multiphoton Excitation 36

Chapter-2. Bio- evaluation of cytotoxicity of 1-methyl-4-(4-chlorophenyl)-1*H*-tetrazol-5(4*H*)-thione against MCF-7 cell line

Figure 1. % cell viability of MCF-7 cells after 24 hr, 48hr and 72hr of treatment with 20c solutions. The bar on each data point represents ±SE for that data 57

Figure 2. Comparative plot for 24 hr, 48 hr and 72 hr of treatment 57

LIST OF SCHEMES

PART ONE

Chapter-1. Photochemistry of 1,4-Disubstituted Tetrazolethiones

Scheme 1. Naturally occurring antitumor antibiotics enediynes 2

Scheme 2. Bergman Cyclization 3

Scheme 3. Mechanism of action of Neocarzinostatin Chromophore 4

Scheme 4. Mechanism of DNA cleavage by enediynes via C (5)' hydrogen abstraction 5

Scheme 5. Myers- Saito and Schmittel cyclization in enyne- allenes 7

Scheme 6. Enyne Ketenimine and Enyne Carbodiimide 8

Scheme 7. Generation of active carbodiimide drug and DNA Cleavage 8

Scheme 8. Photochemical decomposition of tetrazolethione compounds 9

Scheme 9. Photochemical decomposition of 1-methyl-1H-tetrazole-5(4H)-thione 10

Scheme 10. 1, 4- disubstituted tetrazolethiones 11

Scheme 11. Key: (i) NaN_3, Bu_4NBr, toluene, r.t., 2.5 h; (ii) 10% NaOH, ethanol, 70^oC, 2 h; (iii) fuming HNO_3, 100^oC, 30 min; (iv) Me_3SiN_3, 100^oC, 24h; (v) Me_2SO_4/ CH_2Cl_2, Bu_4NBr, 10% NaOH/ CH_2Cl_2, r.t., 3h; (vi) Thionation 14

Scheme 12 . Lawesson's reagent 15

Scheme 13. Synthesis of **20a**. (i) thiourea, ethanol, 80^oC, 4 days; (ii) NEt_3, MeI, dry THF, 70^oC, 6 h 15

Scheme 14. Synthesis of **20a**. (i) NaN_3, water, 100^oC, 24 hr; (ii) NEt_3, MeI, dry THF, 80^oC, 6 h 16

Scheme 15. Methylation of 1-methyl-4-phenyl-1H- tetrazol-5(4H)-thione, **20a** 16

Scheme 16. Thionation of 25a-d. P_2S_5, dry toluene, 110^oC, (**25a**) 2 days, (**25b**) 20 h, (**25c**) 28 h, (**25d**) 24 h 17

Scheme 17. Intramolecular charge transfer in **20d** 21

Scheme 18. Formation of Ferrous- Phenanthroline complex 25

Scheme 19. Photolysis of tetrazolethiones **20a-c**. Hydrolysis of the photoproduct carbodiimide **29a-c** to urea **30a-c** 27

Scheme 20. Photochemical decomposition products 29

Chapter-2. Bio- evaluation of cytotoxicity of 1-methyl-4-(4-chlorophenyl)-1*H*-tetrazol-5(4*H*)-thione against MCF-7 cell line

Scheme 1. Tetrazole based compounds 54

Scheme 2. Tetrazolethione analogs 55

PART TWO

Chapter-3. Synthesis of 2-(2-(phenylimino)vinyl)benzonitrile

Scheme 1. Myers- Saito and Schmittel cyclization in enyne- allenes 65

Scheme 2. Enyne Ketenimine and Enyne Carbodiimide 65

Scheme 3. Schmittel (C^2- C^6) cyclization of ketenimine **2** followed by formal [4+2] cycloaddition 66

Scheme 4. Myer- Saito cyclization favored by presence of a small group at the alkyne terminus 67

Scheme 5. Photochemical cyclization of enyne- ketenimines (**9a, 10a**) with bulky groups at the alkyne terminus 67

Scheme 6. Schmittel (C^2- C^6) cyclization of carbodiimide **11a-b** followed by formal [4+2] cycloaddition 68

Scheme 7. Photochemical cyclization of enyne-carbodiimides 69

Scheme 8. Myers- Saito cyclization of C- alkynyl- N- allenyl imine **15** followed by H- abstraction from 1, 4- CHD 69

Scheme 9. Myers- Saito cyclization of benzannulated enyne isonitrile **17a-b** followed by [4+1] formal cycloaddition 70

Scheme 10. Photochemical cyclization of nitrile substituted allenes **24a-b** 71

Scheme 11. Cyclization of 2-(2-(phenylimino)vinyl)benzonitrile (**25**) to the anticipated product 11H-indeno [1, 2b] quinoxaline (**28**). 72

Scheme 12. Quinoxaline based compounds 73

Scheme 13. Plan for synthesis of 2-(2-(phenylimino)vinyl)benzonitrile, **25**. (i) [$(Ph_3P)_2PdCl_2$], $CHCl_3$/ 50% KOH, r.t., 24 h; (ii) $SOCl_2$, pyridine, toluene, 115^0C, 30 min; (iii) dry CH_2Cl_2, r.t., 30 min 74

Scheme 14. Synthesis of **21**. (i) [$(Ph3P)_2PdCl_2$], $CHCl_3$/ 50% KOH, r.t., 24 h; (ii) $SOCl_2$, pyridine, toluene, 115^0C, 30 min 75

Scheme 15. Synthesis of 2-(2-(phenylimino)vinyl)benzonitrile **25**. (i) neat $SOCl_2$, 80^0C, 30 min; (ii) n-BuLi, THF, -70^0C for 90 min → r.t. for 24 h 75

ACKNOWLEDGEMENT

I would like to thank Dr. Sundeep Rayat, my research advisor, for providing valuable guidance during my research at Kansas State University. I would also like to thank Dr. Stefan Bossman for providing valuable insight on photochemical studies of our compounds.

I would like to thank my committee members Dr. Hua and Dr. Smith. Thanks to Dr. Thu Nguyen for providing guidance for bioevaluation of cytotoxicity of our compounds and for letting us use her laboratory for conducting cytotoxicity experiments. Thanks to Dr. Nathan Leigh at University of Missouri, Columbia for LCMS analysis of our samples.

Thanks to University of Kansas for GCMS analysis of our samples during my research.

PART ONE

CHAPTER 1

Photochemistry of 1,4-Disubstituted Tetrazolethiones

I. INTRODUCTION

I. 1. Enediynes

Naturally occurring enediyne compounds form a class of very potent antitumor antibiotics. Neocarzinostatin (NCS) was the first enediyne to be isolated from *Streptomyces carzinostaticus* in 1965 (**Scheme 1**).[1] Since then, many enediynes have been discovered (*e.g.* calicheamicin r_1, **Scheme 1**). These compounds are divided into two groups based on the 9- or 10- membered ring structure.[2]

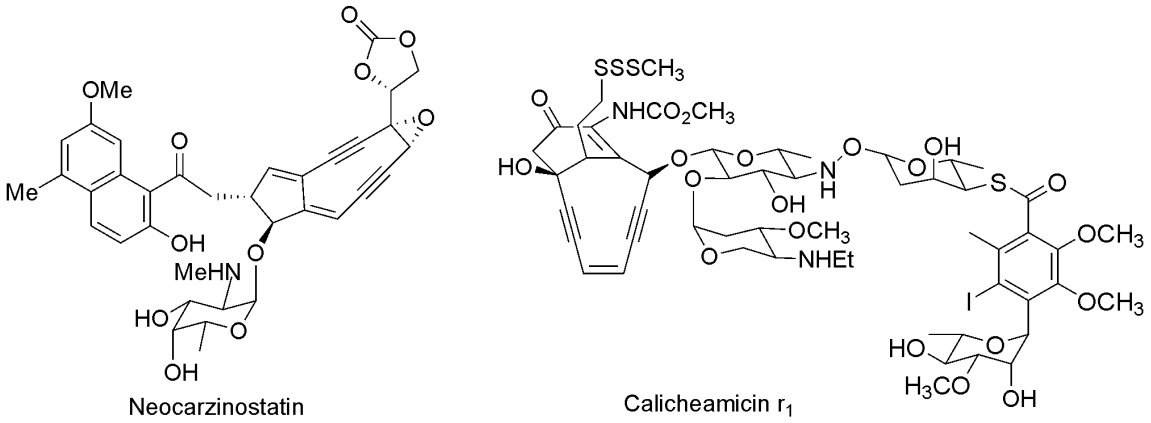

Scheme 1. Naturally occurring antitumor antibiotics enediynes.[2]

In 1972, Bergman showed with the help of model compounds that enediynes undergo thermally triggered cycloaromatization reaction to 1, 4-benzenoid biradical which abstracts hydrogens from the hydrogen donors (**Scheme 2**).[3] This cycloaromatization is known as Bergman cyclization and is thought to be responsible for the biological activity of these compounds.

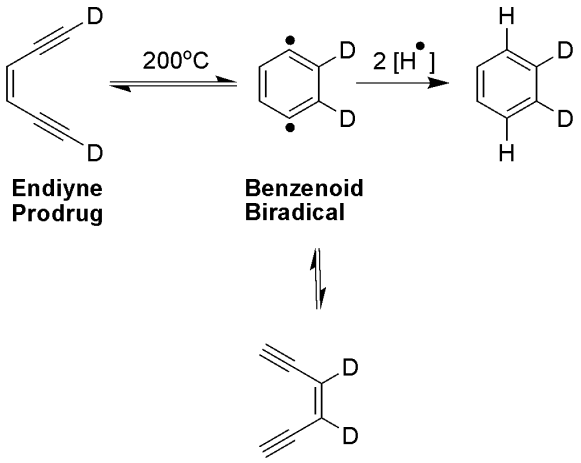

Scheme 2. Bergman Cyclization.[3]

It is well known that naturally occurring antitumor antibiotics enediynes consist of a chromophore which may or may not be associated with an apoprotein.[2] The apoprotein binds non- covalently to the chromophore and stabilizes it. In addition, this apoprotein delivers the chromophore into the minor groove of target cell's DNA where enediyne functionality of the chromophore is activated through Bergman cyclization as discussed above, (**Scheme 2**) to form the 1, 4- benzenoid biradical. This biradical is well placed to abstract the hydrogen atoms from the adjacent strands of DNA and cause scission of the DNA double helix.[3,4] It is this understanding of structure and mechanism of action of naturally occurring enediyne based compounds that revolutionalized the development of anticancer drugs in 1980s.

NCS also consists of 1:1 noncovalently associated mixture of an apoprotein and the chromophore, however, follows slightly different path to cleave DNA. The mechanism of DNA cleavage by NCS **1** is shown in **Scheme 3**. This mechanism was proposed by *Myers* in 1987.[5] The enediyne moiety goes

through a cascade of reactions to generate biradical **which is discussed as follows**.

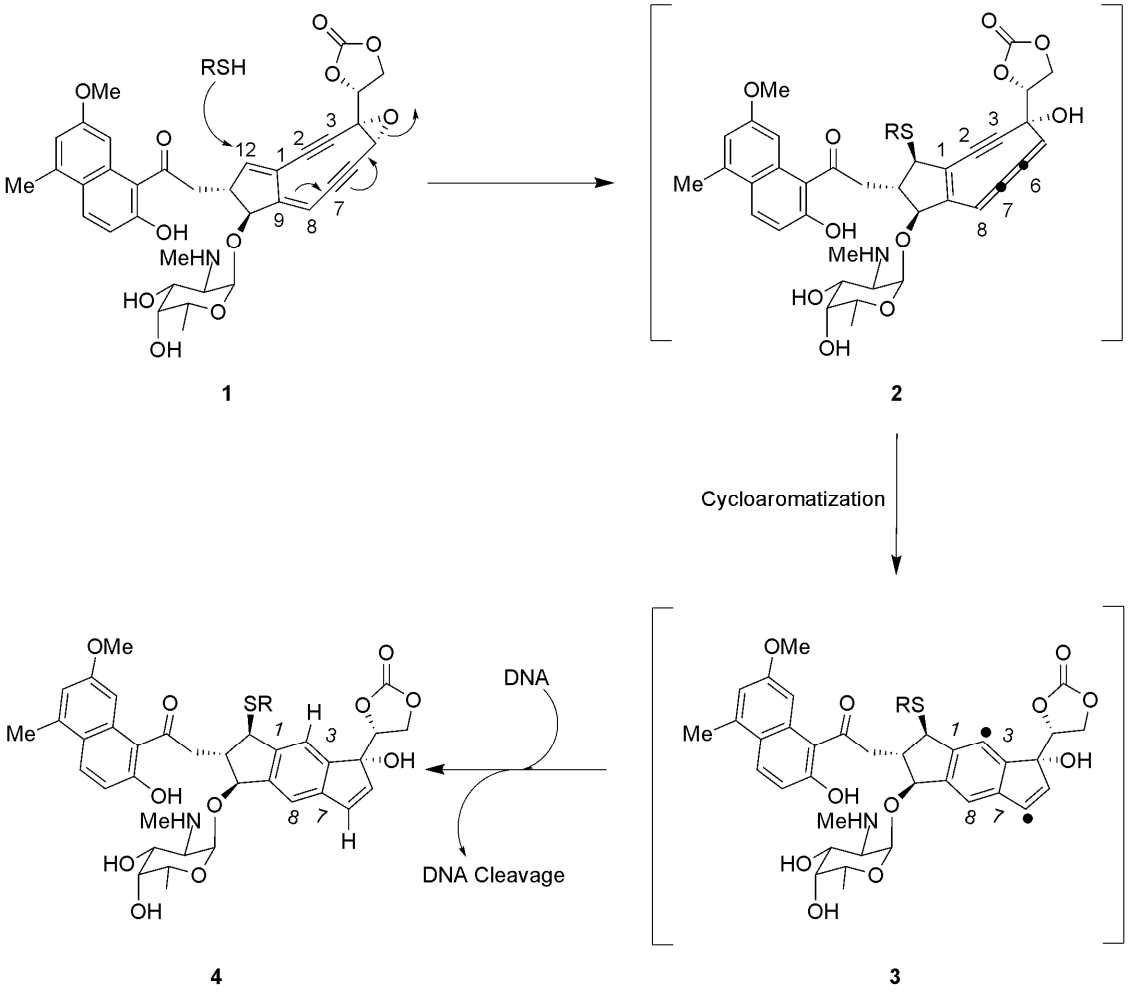

Scheme 3. Mechanism of action of Neocarzinostatin Chromophore. [4, 5]

The cyclization process is initiated by the stereospecific attack of thiol on C-12 of NCS. This leads to the rearrangement of the ring skeleton followed by opening of epoxide ring. As a result a cumulene intermediate **2** is formed which undergoes Myers- Saito cyclization to generate the biradical **3** which then abstracts hydrogen atoms from the sugar phosphate backbone of DNA and ultimately, leads to strand scission (**Scheme 3)**[4, 5]. The mechanism of DNA

strand scission is illustrated in **Scheme 4**. The generation of a radical on the DNA backbone is followed by the addition of molecular oxygen to form a hydroperoxide which then undergo reduction followed by the formation of aldehyde products as shown.[4]

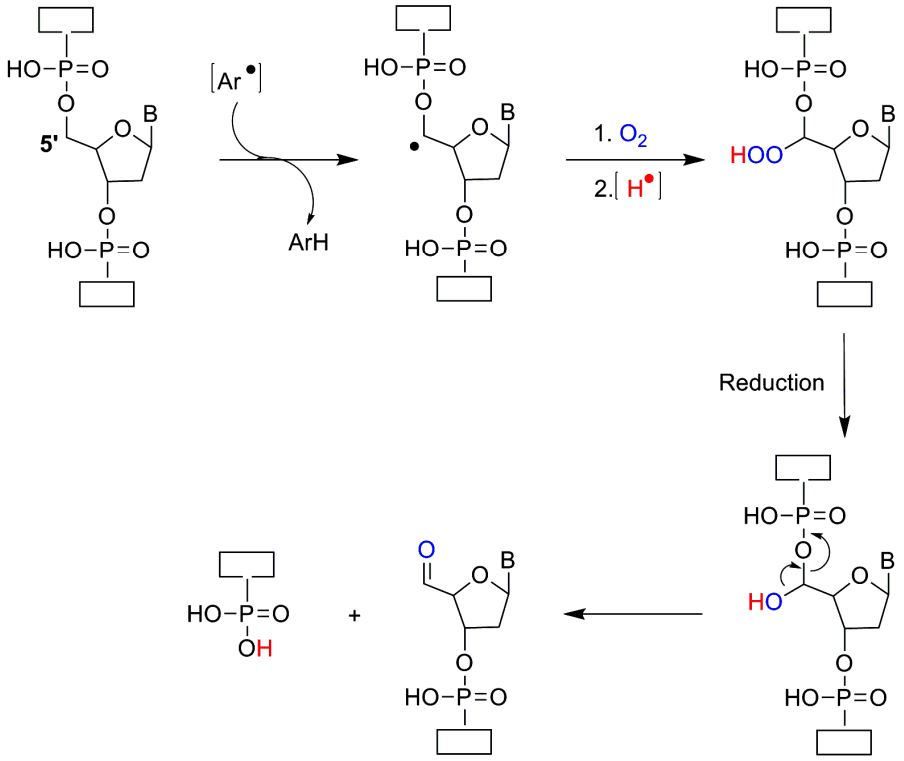

Scheme 4. Mechanism of DNA cleavage by enediynes via C (5)' hydrogen abstraction.[4]

The biradical in case of neocarzinostatin primarily attacks the adenine and thymine rich sites; this leads to single strand cleavage of DNA. Approximately 80% of the cleavage is caused as a result of attack of the C-6 radical of neocarzinostatin on the C-5' of deoxyribose sugar leading to formation of 5'-aldehydes of adenine and thymine.[4] Less than 20% of the cleavage is caused

due to double strand lesions, this requires additional abstraction of hydrogen by C-2 radical of NCS from the C-1' or C-4' of deoxyribose sugar present on the complementary strand.

I. 2. Enyne- Allenes and Hetero- Allenes

Over years many naturally occurring enediynes have been discovered; however, the non- specificity limits their use as anticancer drugs.[6-9] Since the discovery of enediynes, scientists have been working towards the development of new drugs which would mimic these drugs in their mode of action but would have fewer side effects. One class of drugs that is inspired by enediynes is enyne-allenes **5**. These compounds are known to undergo thermal and photochemical cyclization via two different pathways, the C^2- C^7 or Myers–Saito cyclization and the C^2-C^6 or Schmittel cyclization.[10-14] The Schmittel pathway is favored when a bulky group (R= Ph or *t*- Bu) is present at the alkyne end of the enyne-allenes.[15] The two cyclizations yield α, 3- dehydrotoluene **7** and fulvene-like biradicals **6**, respectively. The biradicals (**6** and **7**) are known to abstract hydrogen from the hydrogen donors like 1, 4- cyclohexadiene.[11, 15] The experiments have also shown that the generated biradicals mimic enediynes by cleaving DNA via hydrogen abstraction from the sugar phosphate backbone.[16, 17](**Scheme 5**)

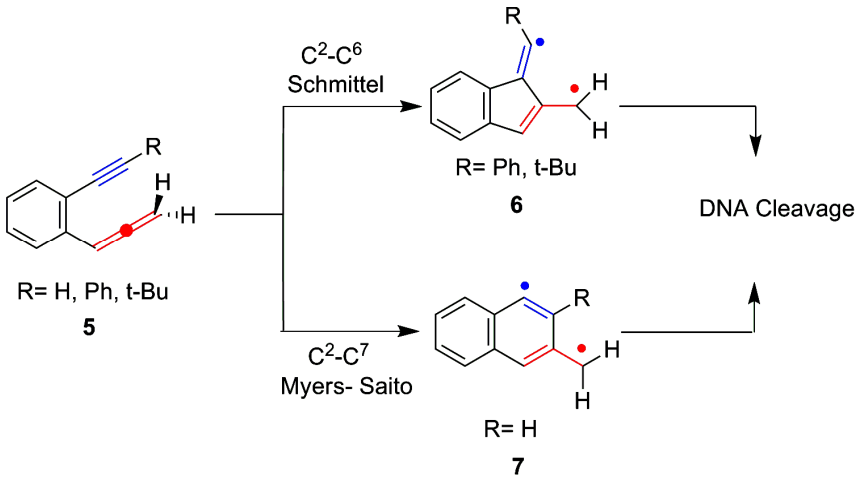

Scheme 5. Myers- Saito and Schmittel cyclization in enyne- allenes.

Similarly, hetero-allene based compounds have been synthesized. Replacement of one or two carbons in allene functionality of enyne-allenes gives rise to enyne ketenimines and enyne carbodiimides, respectively (**Scheme 6**). These compounds also undergo Myers- Saito and Schmittel cyclizations under thermal conditions to generate α, 3- dehydrotoluene and fulvene- like biradicals that are known to abstract hydrogen from 1, 4- cyclohexadiene (1,4-CHD), analogous to enyne-allenes **5**.[18- 21] Under photochemical conditions, only the Schmittel product is observed, irrespective of the substituent present on the alkyne terminus. However, it is not known if these compounds abstract hydrogen from deoxyribose of the sugar phosphate backbone of DNA and cause cleavage. One big drawback related to enyne carbodiimides or enyne-keteneimines is that they are highly reactive due to the presence of carbodiimide or keteneimine moiety which renders them susceptible to biological nucleophiles. This maybe the reason that no DNA cleaving studies related to these compounds have been reported so far. Evidently, in order to use these compounds as drugs one has to

protect the respective carbodiimide or the keteneimine functionality from biological nucleophiles. This may be achieved by masking these functionalities in a structure that could be easily unmasked photochemically, once the drug is localized in the target cell.

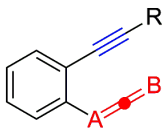

Enyne Ketenimine: A=N, B= CR_1R_2
Enyne Carbodiimide: A=N, B=NR_3

Scheme 6. Enyne Ketenimine and Enyne Carbodiimide

I. 3. Chemotherapeutive Drugs Based on Enyne-Carbodiimides

The objective of our research group is to develop chemotherapeutive drugs based on enyne-carbodiimides. In order to achieve this goal, we plan to develop masked enyne-carbodiimides **8** as prodrugs where the carbodiimide functionality will be protected in a tetrazolethione ring structure. Once absorbed in the body, **8** will be locally irradiated in cancer cells by an infrared laser through multiphoton excitation, to generate **9**, that is immediately expected to undergo cyclization to give **10** which will cause DNA strand scission leading to cell death.

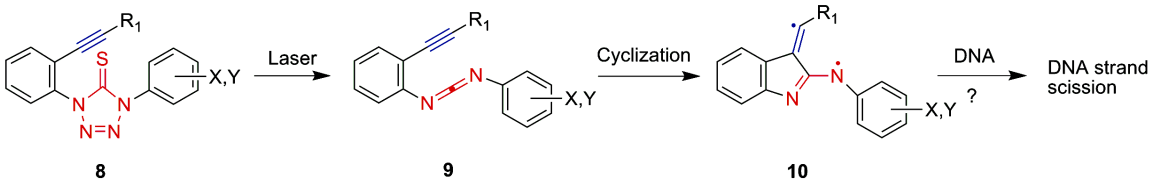

8 **9** **10**

Scheme 7. Generation of active carbodiimide drug and DNA Cleavage

I. 4. Previous Studies on the Photodecomposition of Tetrazolethiones and the Challenges to be Addressed

Quast and co-workers have reported that the photochemical decomposition of 1, 4-disubstituted tetrazolethiones **11** occur with the formation of carbodiimides **12**, and simultaneous expulsion of dinitrogen and molecular sulfur (**Scheme 8**)[22-24].

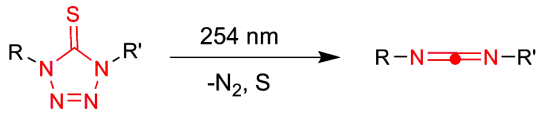

11 **12**

R, R' = alkyl, alkenyl, aromatic

Scheme 8. Photochemical decomposition of tetrazolethione compounds.

The photochemistry of tetrazolethiones has been revisited by Fausto and coworkers who reported that the photochemical decomposition 1-methyl-1H-tetrazole-5(4H)-thione, a monosubstituted tetrazolethione, occurs with the formation of a variety of products in addition to carbodiimides, *via* three decomposition pathways involving (1) the expulsion of dinitrogen to form 1-methyl-1H-diazirene-3-thiol, (2) the cleavage of the tetrazolethione ring to form methylisothiocyanate and azide, and (3) the concurrent expulsion of dinitrogen and sulfur to form N-methyl carbodiimide(**Scheme 9**).[46]

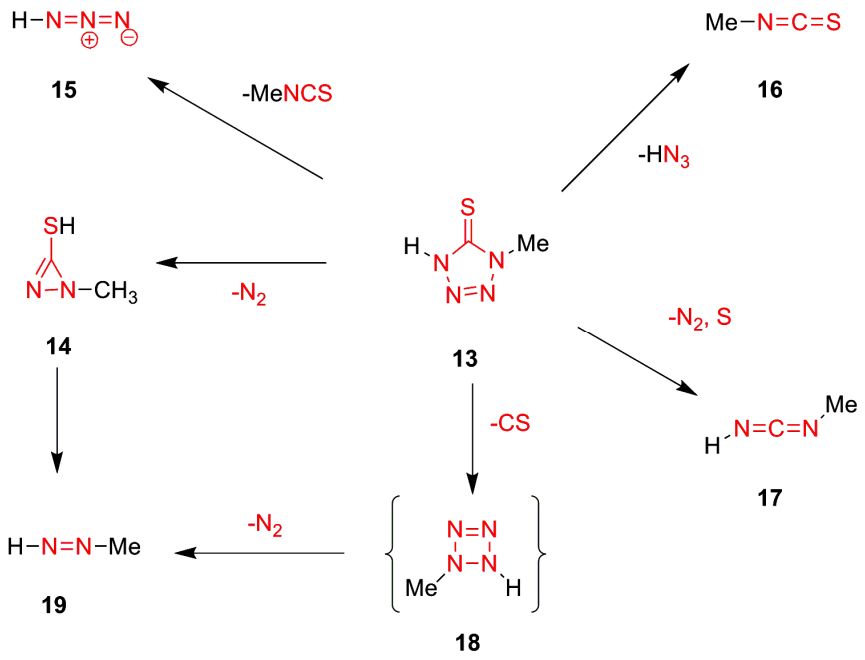

Scheme 9. Photochemical decomposition of 1-methyl-1H-tetrazole-5(4H)-thione.[46]

The authors also reported that the primary photoproducts undergo further reactions in the gas phase to form secondary photoproducts such as methyl diazene, carbon monosulfide and nitrogen hydride. Analogous to the monosubstituted tetrazolethione, the photodecomposition of 1,4-disubstituted tetrazole-5-thiones may also proceed with the formation of the products other than the carbodiimide as initially reported by Quast. No studies have been reported on the rate of the photodecomposition of tetrazolethiones to carbodiimides, their yields or the overall efficiencies of this conversion. *The ability to drive the photodecomposition in the direction of "carbodiimide" is critical to accomplishment of our goal.* Therefore, before the synthesis of prodrug (give number) could begun, the photochemistry of tetrazolethiones needs to be thoroughly investigated.

Secondly, the photochemical studies by Quast and Fausto have employed UV light at which the living cells are vulnerable to photodamage. In order to exploit this chemistry for activation of prodrug **8** (**Scheme 7**), in vivo, one needs to be able to use longer wavelength that will not damage the living cells. Therefore, we will use multiphoton excitation to convert tetrazolethiones to carbodiimides. This technique allows one to excite the UV absorbing chromophores by a laser in the 800-900nm range. This is important because cells are commonly transparent at 870 nm, but strongly absorbing at < 300 nm. The biological applications of multiphoton excitation have been well-documented in literature.[49, 50] Note that the conversion of a tetrazolethione ring to carbodiimide has not been studied under multiphoton excitation and needs to be established before the synthesis of prodrug **8** could commence.

We wanted to first investigate the photochemistry of the tetrazolethione ring via single photon excitation so that the information collected from the experiments could be employed to design the experimental conditions for the multiphoton excitation studies. Thus, our first goal was to synthesize four differently substituted 1, 4- disubstituted tetrazolethione analogs **20a-d** (**Scheme 10**) and to study the effect of substituents on photostability and photoliability of the tetrazolethione ring.

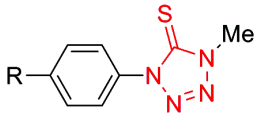

20a R= H
20b R= OMe
20c R= Cl
20d R= NO_2

Scheme 10. 1, 4- disubstituted tetrazolethiones

I. 5. Our approach

Since the nature of the substituents is known to affect the photochemical properties of the tetrazolethione ring,[25- 28] our goal is to synthesize a series of different 1-methyl-4-phenyl tetrazolethiones substituted with a variety of different electron-withdrawing or electron-donating groups at the phenyl ring and study their photophysical and photochemical properties. These studies will allow us to identify systems that will give the high yields of carbodiimides as well as show high rates of photodecomposition and quantum efficiencies upon UV irradiation. Once we have a better understanding of the tetrazolethione photochemistry under single-photon excitation, we will study the conversion of select tetrazolethiones to carbodiimides under multiphoton excitation.

Therefore, with this goal in mind, we synthesized four analogs of 1-methyl-4-phenyl tetrazolethiones **20a** with three different substituents at the phenyl ring **20b** - **c**. The substituents were; OMe group with strongly activating effect, Cl with weakly deactivating effect and NO_2 having the strongly deactivating effect. The photochemistry of these compounds was studied in THF and MeCN to investigate the effect of solvent polarity on the photochemical properties of the tetrazolethione system. The product mixtures were analyzed using LCMS and EI/GCMS.

II. RESULTS AND DISCUSSION

II. 1. Synthesis of 1, 4- disubstituted tetrazolethione 20a- d

Synthesis was carried out as follows. The literature reported procedures were followed for synthesis our tetrazolethione analogs (**Scheme 11**) and all products were analyzed by ^{1}H-NMR, ^{13}C-NMR and mass spectroscopy.

5-chloro-1- phenyl- 1*H*- tetrazole **22** was formed via 1, 3–dipolar cycloaddition of phenyl-1, 1-dichloroisocyanide **21** and sodium azide in the presence of tetrabutylammonium bromide in water-toluene suspension.[29] The reaction was carried out at room temperature for 2.5 h and yielded **22** in 73% yield. **22** was refluxed at 70^{o}C for 2 h in NaOH/ ethanol which resulted in the formation of 1-phenyl-1*H*- tetrazol-5(4*H*)-one **23a** in 95% yield.[30] Nitration of **23a** with fuming HNO_3 at 100^{o}C for 30 min gave 1-(4-nitrophenyl)-1*H*-tetrazol-5(4*H*)-one **23d** in 59% yield.[30] Remaining two tetrazolone analogs, 1-(4-methoxyphenyl)-1*H*-tetrazol-5(4*H*)-one **23b** and 1-(4-chlorophenyl)-1*H*-tetrazol-5(4*H*)-one **23c** were synthesized from their corresponding isocyanates **24b-c** by refluxing in neat trisilylazide (TMSA) under N_2 for 24 h at 100^{o}C.[31] **23b** was produced in 90% yield and **23c** was produced in 95% yield.

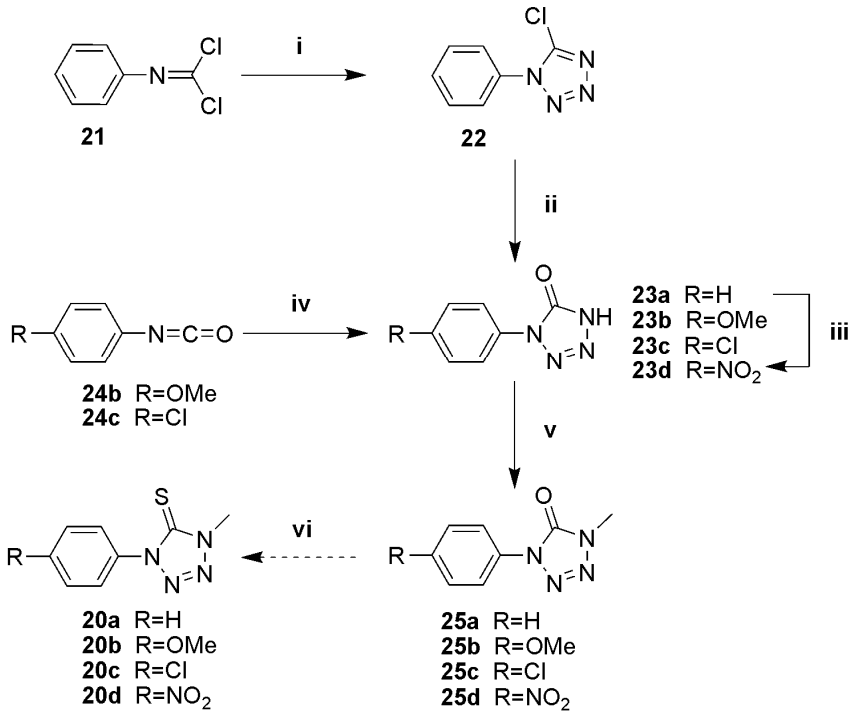

Scheme 11. Key: (i) NaN_3, Bu_4NBr, toluene, r.t., 2.5 h; (ii) 10% NaOH, ethanol, 70°C, 2 h; (iii) fuming HNO_3, 100°C, 30 min; (iv) Me_3SiN_3, 100°C, 24h; (v) Me_2SO_4/ CH_2Cl_2, Bu_4NBr, 10% NaOH/ CH_2Cl_2, r.t., 3h; (vi) thionation.

Methylation of **23a-d** with Me_2SO_4 in dichloromethane yielded the respective 1, 4-disubstituted tetrazolones **25a-d. 23a-d** were stirred at room temperature with Me_2SO_4 in dichloromethane in the presence of 10% NaOH and Bu_4NBr for 3 h.[32] **25a** was produced in 84%, **25b** in 92%, **25c** in 90% and **25d** in 96% yield. After Synthesis of 1, 4-disubstituted tetrazolones **25a-d** was accomplished, the last step involving thionation of these compounds remained (**Scheme 11**). We first tried this reaction for 1-methyl-4-phenyl-1*H*- tetrazol-5(4*H*)-one **20a. 25a** was first refluxed with P_2S_5 in dry pyridine under N_2 at 115.5°C.[33] Even after 4 days, the desired starting material **25a** was found unreacted. Therefore, we tried several other methods to synthesize the final

products **20a – d**. First, we attempted the synthesis of **20a** according to the method reported by Quast. According to this procedure, **25a** was refluxed with P_2S_5 in dry toluene under N_2 at 110^oC.[22] After 4 days, the desired product **20a** was obtained in 55% yield. Since the reaction took 4 days, we searched the literature for other methods requiring shorter reaction times. We tried the thionation of **25a** with Lawesson's reagent (**Scheme 12**) in dry toluene under N_2 at 110^oC.[34] Even after 4 days of refluxing, desired product was not obtained. We also tried refluxing **25a** and Lawesson's reagent in dry pyridine but our attempt was still unsuccessful.

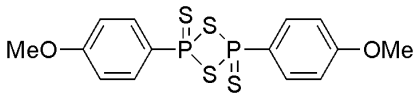

Scheme 12 . Lawesson's reagent

In our next attempt, we decided to synthesis **20a** by another method that involved first generating the monosubstituted tetrazolethione from **22** and then attempting methylation[37] as shown in **Scheme 13.**

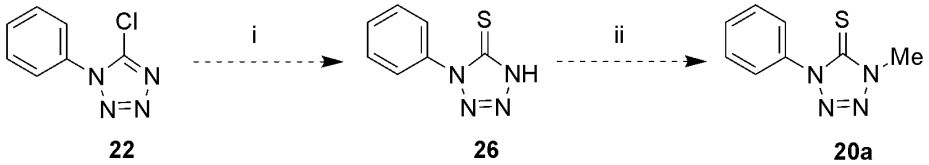

22 **26** **20a**

Scheme 13. Synthesis of 20a. (i) thiourea, ethanol, 80^oC, 4 days; (ii) NEt_3, MeI, dry THF, 70^oC, 6 h.

22 was refluxed with thiourea in ethanol at 80°C for 4 days.[35] The starting material was recovered unreacted. After failure of this attempt we planned another synthetic route (**Scheme 14**).

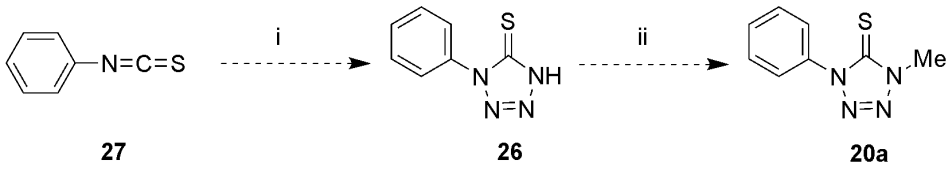

27 **26** **20a**

Scheme 14. Synthesis of 20a. (i) NaN_3, water, 100°C, 24 hr; (ii) NEt_3, MeI, dry THF, 80°C, 6 h.

The plan involved first refluxing isothiocyanate **27** with NaN_3 in water at 100°C for 24 h to yield **26** [36] followed by methylation to obtain **20a**. The first reaction was successful and **26** was obtained in 83% yield. However, the attempted methylation of **26** with triethyl amine and methyl iodide in THF at 80 °C for 6 h[37] yielded (methylthio)-1-phenyl-1H-tetrazole **28** instead of 1-methyl-4-phenyl-1*H*- tetrazol-5(4*H*)-thione **20a** owing to the greater nucleophilicity of sulfur. (**Scheme 15**).

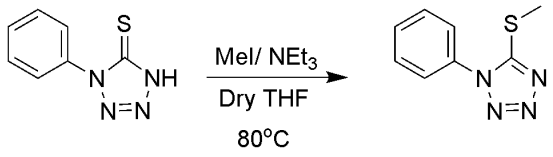

26 **28**

Scheme 15. Methylation of 1-methyl-4-phenyl-1H- tetrazol-5(4H)-thione, 20a.

We tried one last approach for methylation of **26** that involved stirring **26** with methyl benzoate in DMSO.[38] After 4 days, starting material was found unreacted.

After trying all possible methods for synthesis of 1-methyl-4-phenyl-1*H*-tetrazol-5(4*H*)-thione **20a**, we decided to follow our sole successful thionation with P_2S_5. Care was taken to ensure the dry conditions for this reaction by using freshly distilled toluene. Thus, 1, 4-disubstitued tetrazolone analogs **25a-d** were thionated by refluxing in dry toluene with P_2S_5 at 110 ^{o}C. [22] After work up, pure products were obtained by column chromatography. **25a** was refluxed for 2 days that gave 1-methyl-4-phenyl-1*H*- tetrazol-5(4*H*)-thione **5a** in 53% yield, **25b** was refluxed for 20 h to obtain 1-methyl-4-(4-methoxyphenyl)-1*H*-tetrazol-5(4*H*)-thione **20b** in 75% yield, **25c** was refluxed for 28 h to yield 1-methyl-4-(4-chlorophenyl)-1*H*-tetrazol-5(4*H*)-thione **20c** in 68% yield, and **25d** was refluxed for 24 h to obtain 1-methyl-4-(4-nitrophenyl)-1*H*-tetrazol-5(4*H*)-thione **20d** in 50% yield (**Scheme 16**)**.**

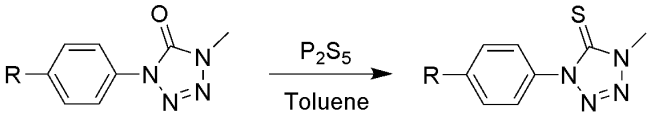

25a R=H
25b R=OMe
25c R=Cl
25d R=NO_2

20a R=H
20b R=OMe
20c R=Cl
20d R=NO_2

Scheme 16. Thionation of 25a-d. P_2S_5, dry toluene, 110^{o}C, (25a) 2 days, (25b) 20 h, (25c) 28 h, (25d) 24 h

II. 2. Photochemical Studies

We used THF and MeCN for the photochemical studies of compounds **20a-d**. The solubility of our compounds is good in these two solvents. Also, these two solvents do not absorb significantly beyond 200 nm where our compounds exhibit significant absorbance. **20a-d** were also soluble in acetone and dimethyl sulfoxide, however, these solvents were not used for our studies since they absorb significantly at 254 nm.

II. 2. 1. Absorption Spectra of Tetrazolethione Analogs

The absorption spectra of **20a-d** in THF and MeCN are shown in **Figure 1 (i)- (ii)**. Two absorption bands λ_1 and λ_2 were observed for all the compounds which underwent blue-shifts on going from less polar solvent THF to the more polar solvent MeCN. Comparing the effect of para substituents on the aromatic ring, it was observed that the presence of OMe group on aromatic ring in methyl-4-(4-methoxyphenyl)-1*H*-tetrazol-5(4*H*)-thione **20b** had negligible effect (a shift of 1-3 nm) on the position of both bands with respect to **20a**. The presence of Cl group did not have much effect on λ_1; however, λ_2 was red shifted by approximately 7 nm in both solvents. Significant effect on positions of λ_1 and λ_2 was observed in case of NO_2 substituent. The first band was blue shifted (11-13 nm) whereas the second band was significantly red shifted (40-44 nm) with respect to **20a** in both solvents.

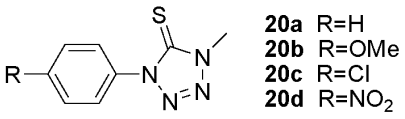

20a R=H
20b R=OMe
20c R=Cl
20d R=NO_2

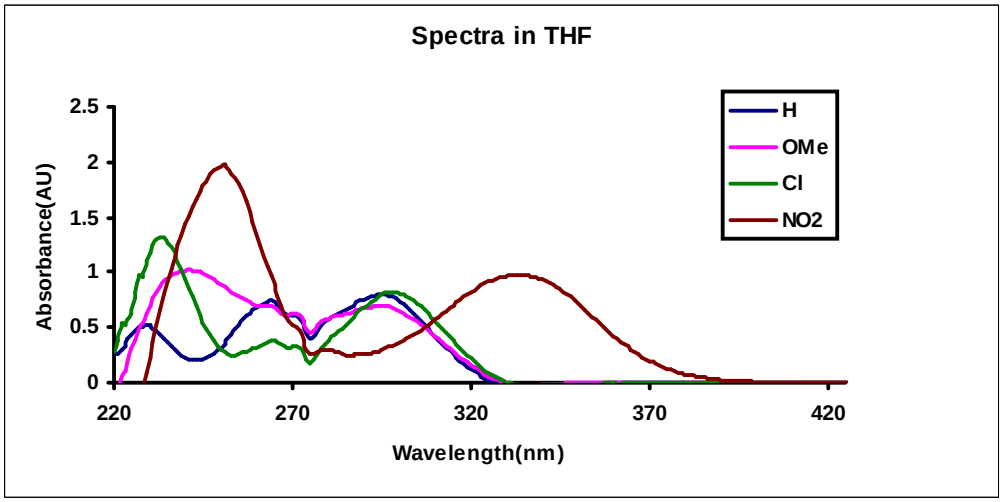

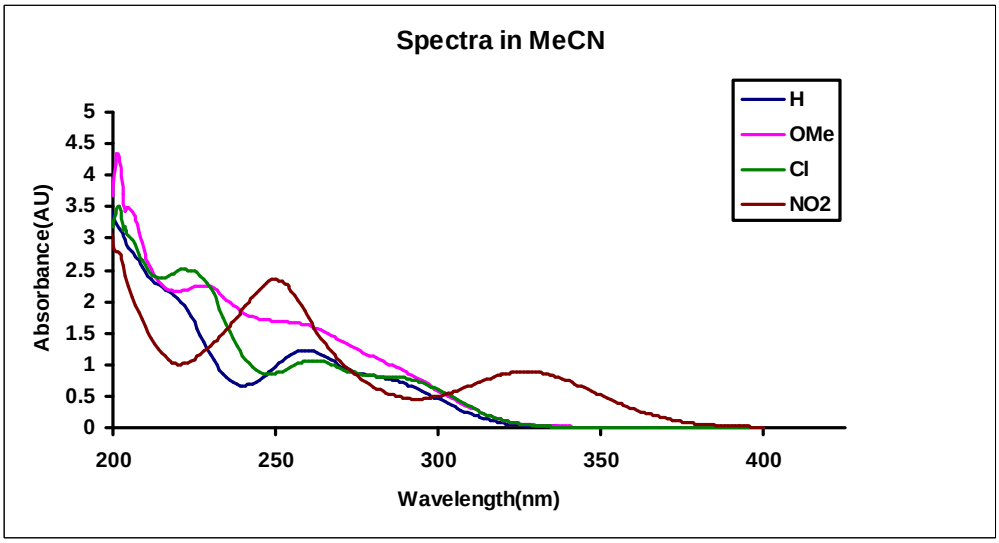

Figure 1. Overlay of 1, 4- disubstitued tetrazolethiones spectra in (i) THF, (ii) Acetonitrile.

Previous studies by Gosavi and Rao on substituted thioureas [39] suggest that λ_1 is due to $\pi \rightarrow \pi^*$ transition of the thione group of the tetrazolethione ring. The blue shift in λ_1 on going from less polar THF to more polar MeCN and the

extinction coefficients for this band are consistent with Gosavi and Rao's findings **(Table 1)**. λ_2 is due to an intramolecular negative charge transfer from the tetrazolethione ring nitrogen to the aromatic ring. This band is comparatively broad and sensitive to the substituents on the aromatic ring; this type of effect has been observed in donor- acceptor substituted aromatic compounds. [40-42]

	THF				MeCN			
	λ_1	log ε	λ_2	log ε	λ_1	log ε	λ_2	log ε
20a	**265**	**3.90**	**290**	**3.70**	**260**	**3.90**	**282**	**3.63**
20b	**267**	**3.95**	**287**	**3.72**	**261**	**3.90**	**281**	**3.81**
20c	**266**	**3.82**	**297**	**3.80**	**263**	**3.90**	**289**	**3.81**
20d	**251**	**4.20**	**336**	**3.80**	**250**	**4.30**	**328**	**3.90**

λ in nm; ε in M^{-1} cm^{-1}

Table 1. Absorption band positions and extinction coefficients

The increase in charge transfer is observed as the substituent changes from electron donating to electron withdrawing (OCH_3 < Cl < NO_2) on going from **20b** →**20c** → **20d**. The considerable red shift in case of **20d** is due to significant negative charge transfer to the NO_2 substituent which is not possible in case of **20b** and **20c (Scheme 17).** Further, a significant blue shift in λ_2 is observed in case of **20d** on going from less polar solvent THF to more polar solvent MeCN. This maybe due to the increased charge stabilization in more polar MeCN.

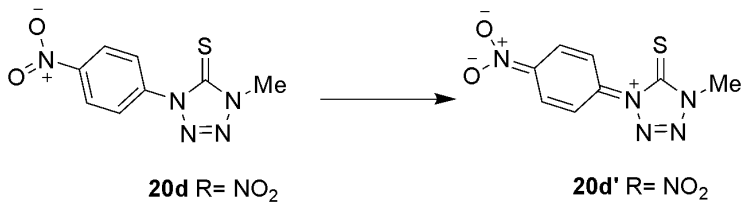

20d R= NO_2 **20d'** R= NO_2

Scheme 17. Intramolecular charge transfer in 20d

II. 2. 2. Photolysis of Tetrazolethiones

We used 100 W medium-pressure quartz mercury lamp for photolysis of THF and MeCN solutions of1, 4- disubstituted tetrazolethione analogs **20a-d**. The solutions were photolyzed at 254 nm. The change during photolysis of each solution was followed with UV and HPLC analyses. An aliquot was also taken out during irradiation of each solution for LCMS and GCMS analysis of the product mixture.

II. 2. 2. 1. UV and HPLC Analyses

UV and HPLC analyses were carried out to follow the photolysis experiments. The UV spectra were taken using UV- VIS spectrophotometer at Kansas State University. The HPLC chromatograms were obtained using the Shimadzu HPLC instrument. The chromatograms were recorded at 254 nm.

An overlay of UV spectra and HPLC chromatograms for irradiation of THF solution of 1-methyl-4-(4-nitrophenyl)-1H-tetrazol-5(4H)-thione **20d** is shown in **Figure 2.** The overlay of UV spectra and the HPLC chromatograms for photolysis of **20a-c** is shown in **Appendix III** and **IV**, Supporting Information.

(i)

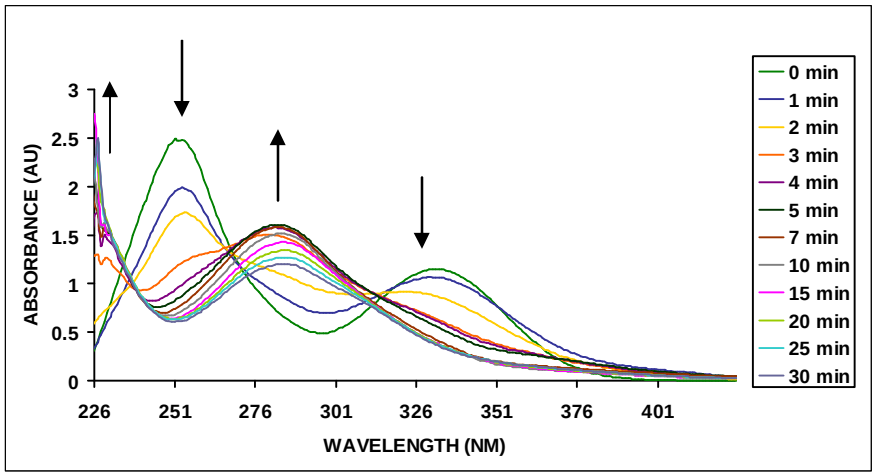

(ii)

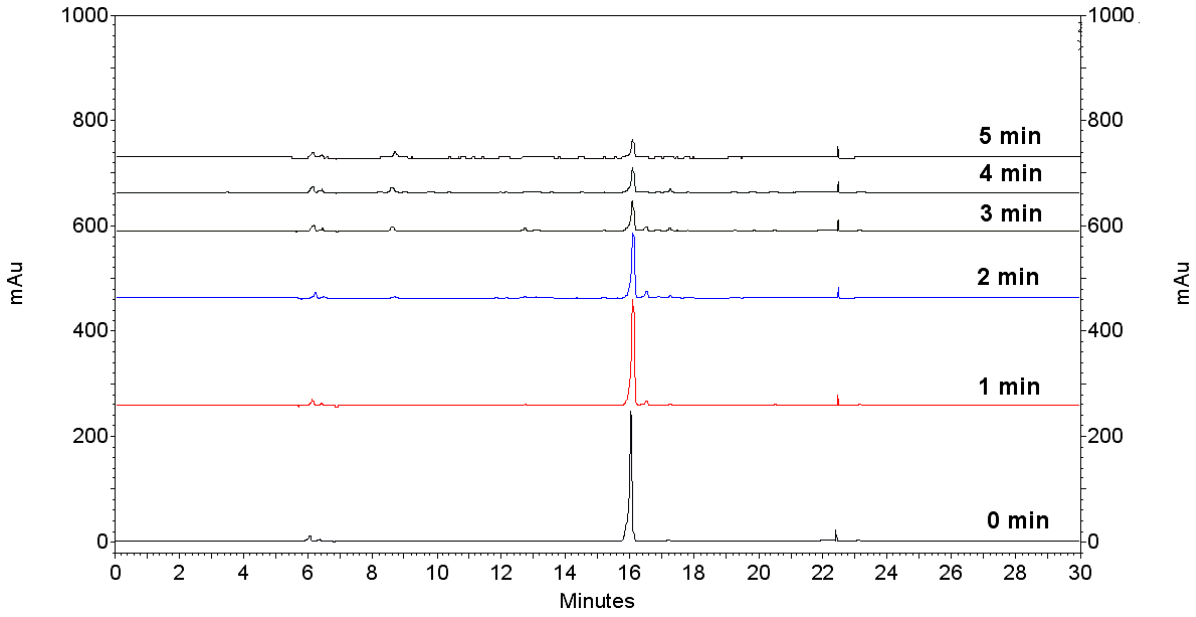

Figure 2. Overlay of (i) UV spectra and (ii) HPLC chromatograms recorded during photolysis of 1-methyl-4-(4-nitrophenyl)-1H-tetrazol-5(4H)-thione(20d) in THF.

It can be seen from the overlayed UV spectra and HPLC chromatograms that a mixture of products is formed during the photolysis of samples. Therefore, we do not observe a clear isobestic points in the overlayed UV spectra.

II. 2. 2. 2. Rate Constants

The overlayed UV spectra were used for determination of rate constants for photodecomposition of compounds **20a-d**. The absorbance of the second band, λ_2 observed in the UV spectra of each compound was followed for plotting ln (A/A_o) vs. irradiation time **Figure 3 (i)- (ii)**.

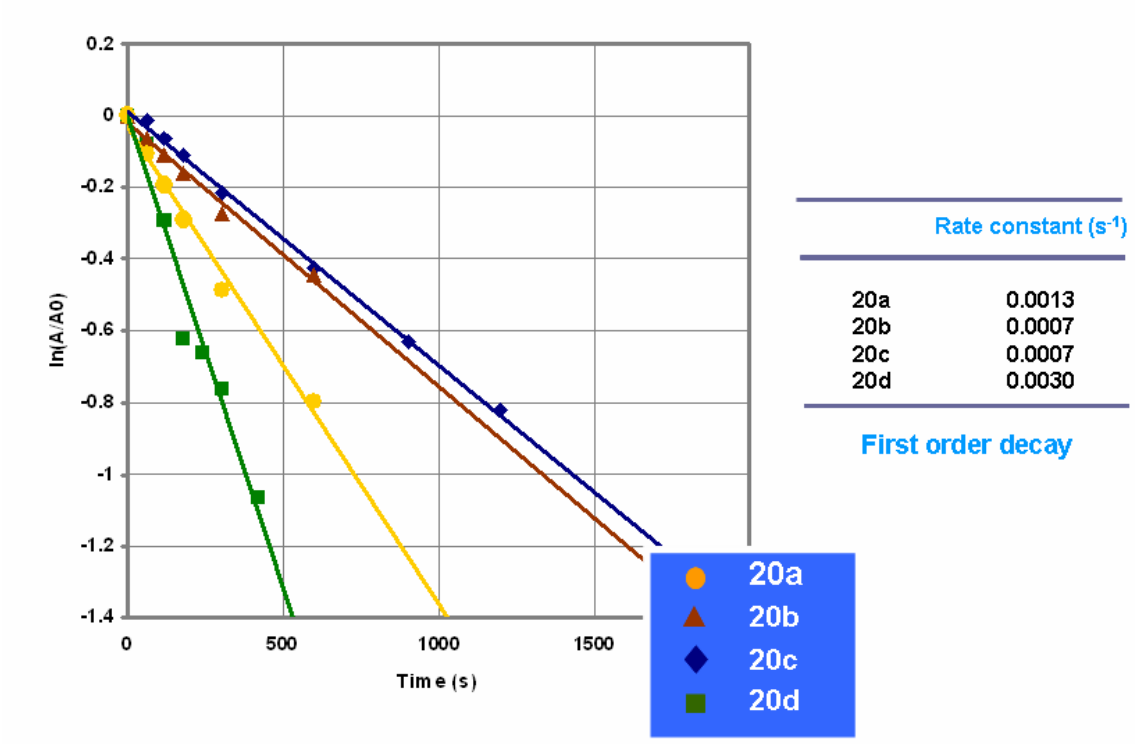

Figure 3 (i). Photochemical decomposition of tetrazolethiones. ln (A/A_o) vs. Irradiation time plots for THF solutions

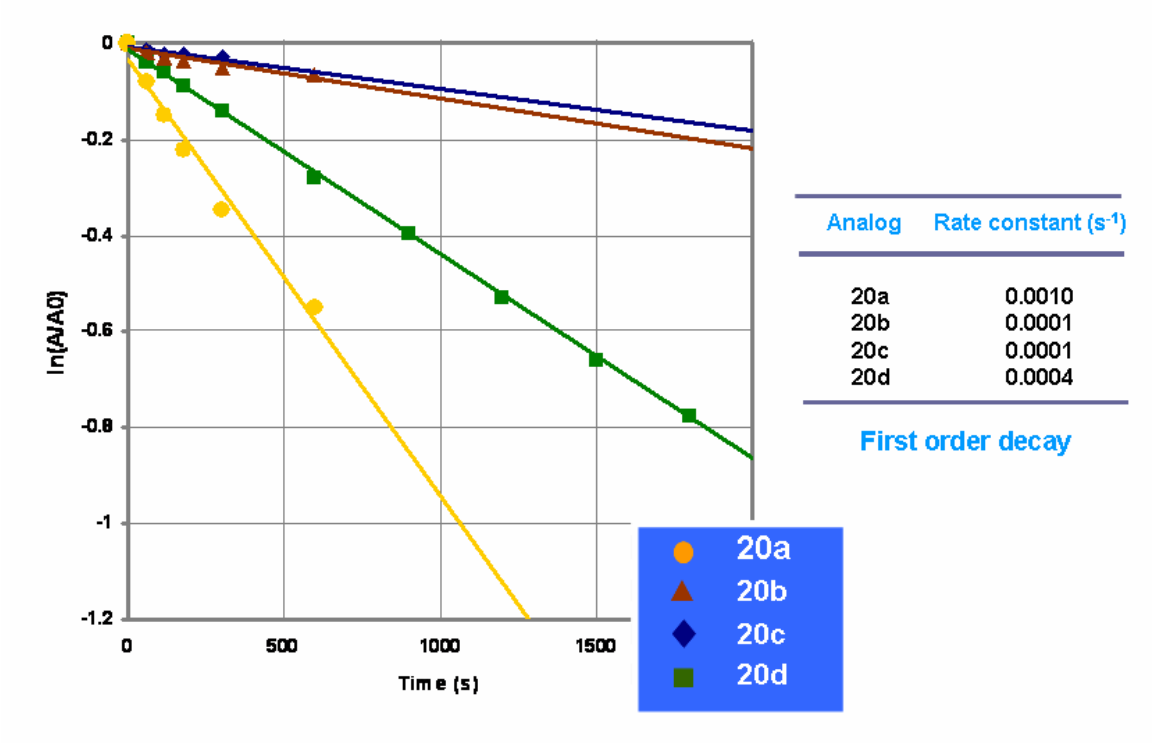

Figure 3 (ii). Photochemical decomposition of tetrazolethiones. ln (A/A_o) vs. Irradiation time plots for MeCN solutions.

The straight line in these plots indicates the first order kinetics for the photochemical decomposition reactions. The rate of decomposition was low for both THF and MeCN solutions of each compound; the rate in MeCN being lower than that in THF. We believe that λ_2 might be responsible for the photochemical decomposition of tetrazoelthiones. This is also supported by the fact that the rate of photodecomposition of **20d** was reduced to a great extent in more polar MeCN which may be explained by the greater stabilization of the intramolecular charge transfer (**20d' Scheme 17)** in this solvent.

II. 2. 2. 3. Quantum Yields

We used Ferrioxalate Actinometry [43-45] to calculate the quantum yields for the disappearance of starting materials **20a-d** during photolysis experiments. This experiment involves irradiation of mixtures of ferric sulfate and oxalic acid solutions. Upon irradiation ferric ions reduced to ferrous ions and carbon dioxide is produced. The net reaction equation is shown below:

$$2Fe^{3+} + C_2O_{10}^{2-} \longrightarrow 2Fe^{2+} + 2CO_2$$

The irradiated solutions are then mixed with 1, 10-pheanathroline solution to yield red colored solutions which are produced as a result of complexation of ferric ions with phenanthroline (**Scheme 18**). The ferrous-phenanthroline complex absorbs strongly at 510 nm; thus the amount of ferric ions produced during the irradiation is determined by obtaining absorption spectra which is used to calculate quantum yields for photolysis of compounds **20a-d**. The unreacted ferric ions complex weakly with phenanthroline and the little amount of complex thus produced is transparent at 510 nm.

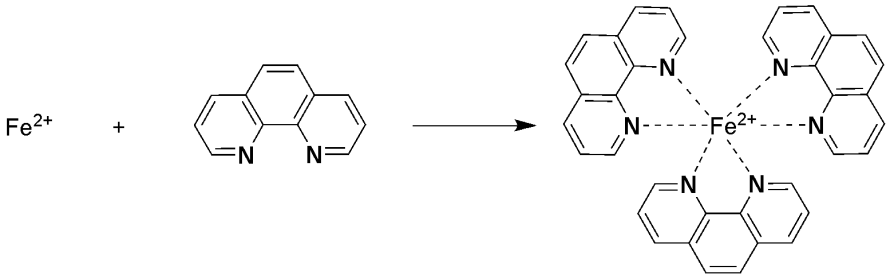

Scheme 18. Formation of Ferrous- Phenanthroline complex.

In our experiments 2.6 x 10^{-5} M s $^{-}$1 of Fe^{2+} was produced and the radiant power of our medium pressure mercury lamp was found to be 12.26 W at 254 nm.

The quantum yields were found to be low for our experiments (**Table 2**) Compared to that in THF, quantum yields were found to be lower in more polar MeCN. As explained for lower rates of photochemical decompositions in MeCN, lower quantum yields may also be due to the greater stabilization of the intramolecular charge transfer in more polar MeCN. Further, radiationless decay or fluorescence may also be responsible for these results.

	Φ (THF)	**Φ (MeCN)**
20a	**0.015**	**0.010**
20b	**0.030**	**0.015**
20c	**0.012**	**0.012**
20d	**0.020**	**0.004**

Table 2. Quantum yields

II. 2. 2. 4. LC/MS Analyses

The LCMS analyses of the irradiated THF and MeCN solutions were done at the University of Missouri-Columbia. A positive ion electronspray ionization mass spectroscopy (ESI) was performed on each photoproduct.

The ESI-MS of the samples revealed the presence of a urea in both THF and MeCN product mixtures for all compounds except for **20d** which suggests that during photolysis a carbodiimide product **29a-c** forms which is hydrolyzed to urea **30a-c** by water present in the mobile phase used for LCMS analysis (**Scheme 19)**

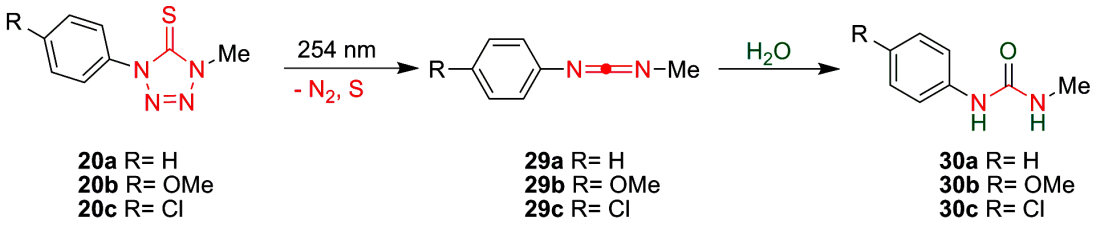

20a R= H
20b R= OMe
20c R= Cl

29a R= H
29b R= OMe
29c R= Cl

30a R= H
30b R= OMe
30c R= Cl

Scheme 19. Photolysis of tetrazolethiones 20a-c. Hydrolysis of the photoproduct carbodiimide 29a-c to urea 30a-c.

Only urea product was observed with LCMS analyses. Other peaks including the starting material could not be ionized by electrospray. However, the presence of remaining starting material is confirmed from HPLC chromatograms taken before and during irradiation of samples. Since we have difficulties in ionizing the samples with electrospray, we decided to analyze the reaction mixtures by GCMS analysis.

II. 2. 2. 5. GC/MS Analyses

An EI-GCMS analysis of photolyzed THF and MeCN reaction mixtures was carried out at University of Kansas. A mixture of five photoproducts and the remaining starting material was observed for each sample except for **20d**. The

five products were the diaziridine-3-thione, isothiocyanate, azide, carbodiimide and the hydrolyzed product of carbodiimide, the urea. In case of **20d**, azide was not observed for both THF and MeCN samples.

Irradiation of THF and MeCN solutions of 1-methyl-4-phenyl-1*H*-tetrazol-5(4*H*)-thione **20a** produced 1-methyl-2-phenyldiaziridine-3–thione **31a** (m/z = 164), 1-isothiocyanatobenzene **32a** (m/z = 135), 1-azidobenzene **33a** (m/z = 119), N-(methylcarbonimidoyl)-benzeamine **29a** and the hydrolyzed product of **29a**, 1-methyl-3-phenylurea **30a**. Similarly, EI-GCMS analysis of **20b** and **20c** indicated the formation of five products. As in case of **20a**, a peak for unreacted **20b** and **20c** was observed in the product mixtures. Upon irradiation, the THF and MeCN solutions of **20b** and **20c** yielded diaziridine-3-thiones **31b** and **31c** (m/z = 194 and m/z=198 respectively), isothiocyanates **32b** and **32c** (m/z = 165 and m/z = 169 respectively), azides **33b** and **33c** (m/z = 149 and m/z = 153 respectively), carbodiimides **29b** and **29c** (m/z = 162 and m/z = 166 respectively) and ureas **30b** and **30c** (m/z = 180 and m/z = 184 respectively). (**Scheme 20**)

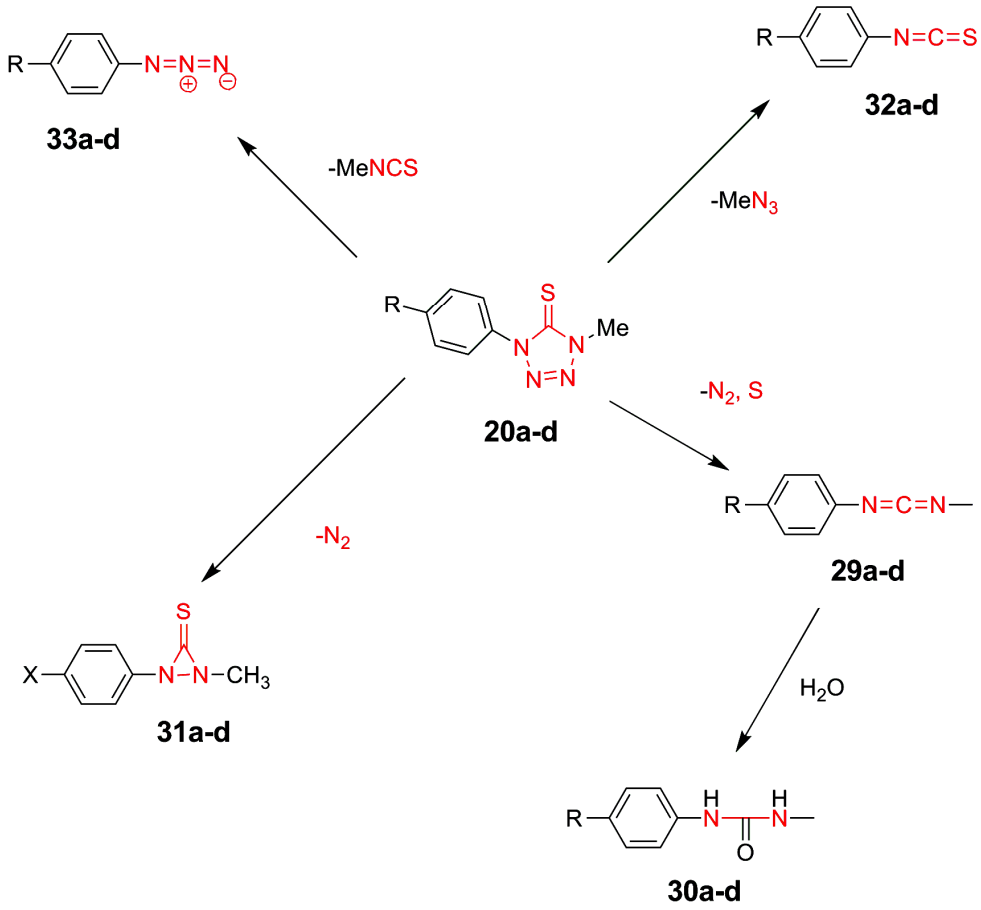

Scheme 20. Photochemical decomposition products

EI-GCMS analysis of irradiated THF and MeCN solutions of **20d** indicated that it may undergo photodecomposition analogous to other tetrazolethiones. However, only four products were observed along with unreacted **20d** for the MeCN reaction mixture. These products were 1-methyl-2-(4-nitrophenyl) diaziridine-3-thione **31d** (m/z = 209), 1-isothiocyanato-4-nitrobenzene **32d** (m/z = 180), N-(methylcarbonimidoyl)-4-nitrobenzenamine **29d** (m/z = 177) and 1-methyl-3-(4-nitrophenyl) urea **30d** (m/z = 195). **29d** was not observed in the THF sample. Also, 1-azido-4-nitrobenzene **33d** (m/z = 164) was not observed in both THF and MeCN samples. GCMS analysis suggested that the traces of products

were produced upon irradiation of **20d** compared to **20a- c**. These results were in agreement with the results found for photodecomposition of a monosubstituted tetrazolethione.[46] **Scheme 20** shows four different paths leading to 5 different products for photolysis of **20a-d**.

The trace amount of the photoproducts in case of **20d** may be due to the photoreduction[47] of nitro group to yield an amine under the experimental conditions. These formed amines may polymerize which would be difficult to identify by GCMS.

II. 2. 2. 6. HPLC separation and NMR analysis

In order to obtain further spectroscopic evidence for the formation of these photoproducts, we decided to separate the photoproducts using HPLC and analyze the products via ^{1}H-NMR and ^{13}C-NMR spectroscopy.

We first carried out large scale photolysis reaction for 1-methyl-4-phenyl-1*H*- tetrazol-5(4*H*)-thione **20a**. 100 mg of **20a** was dissolved in 150 ml of THF. The solution was irradiated for 1 h with a medium pressure mercury lamp in a quartz photochemical reactor. A sample of unirradiated solution of **20a** was analyzed by HPLC. After irradiation, another sample was analyzed by HPLC, The chromatogram of crude product mixture is shown in **Figure 4**

In the chromatogram of concentrated product mixture, the peak with retention time of 10.7 min corresponds to the unreacted starting material, 1-methyl-4-phenyl-1*H*-tetrazol-5(4*H*)-thione **20a** as confirmed from the chromatogram obtained for HPLC run of unirradiated sample.

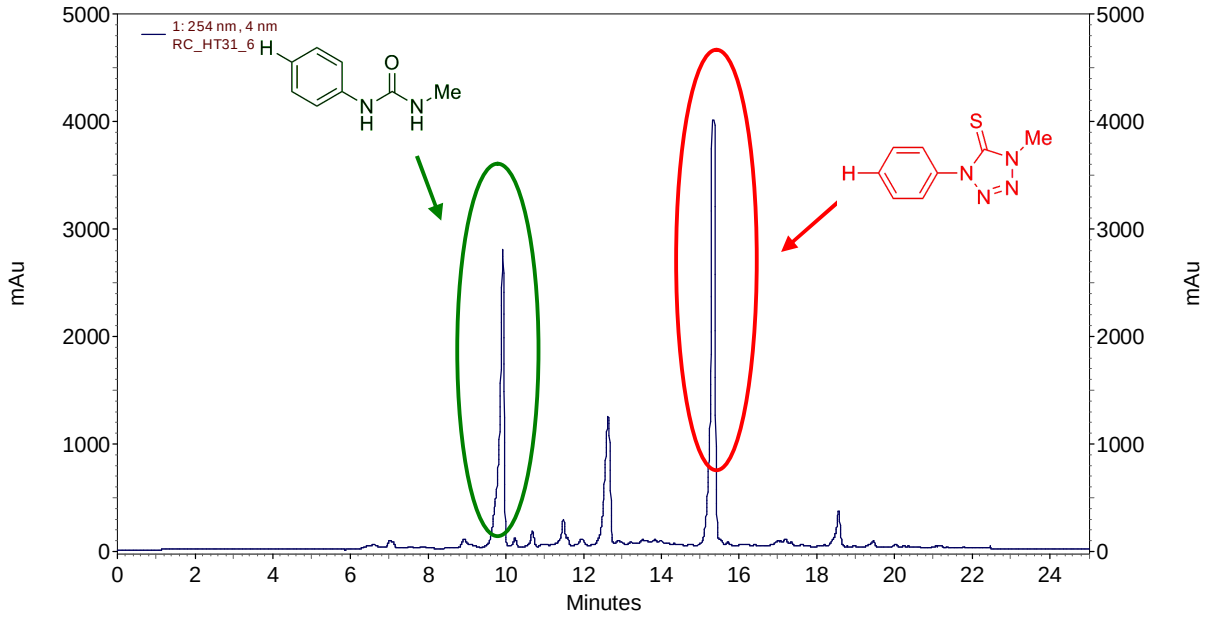

Figure 4. HPLC chromatogram of irradiated 1-methyl-4-phenyl-1H-tetrazol-5(4H)-thione 20a.

From the ^{1}H-NMR analysis, it was found that the peak with retention time of 5.1 min **(Figure 4)** corresponds to 1-methyl-3-phenylurea **30a**. This product was also found during LCMS and GCMS analyses. As explained earlier, this product is formed via hydrolysis of the photoproduct N-(methylcarbonimidoyl)-benzeamine **29a** during HPLC analysis (**Schemes 19 and 20)**. Thus, **29a** is not observed during LCMS or HPLC analyses but its hydrolyzed product **30a** is observed instead.

Similarly, we separated and analyzed products obtained during photolysis of methyl-4-(4-chlorophenyl)-1*H*-tetrazol-5(4*H*)-thione **20c**. The solution was made by dissolving 100mg of **20c** in 100 ml of MeCN and was irradiated in a

quartz photochemical reactor for 2 h and 5 min. The chromatogram for the crude irradiated solution is shown in **Figure 5**.

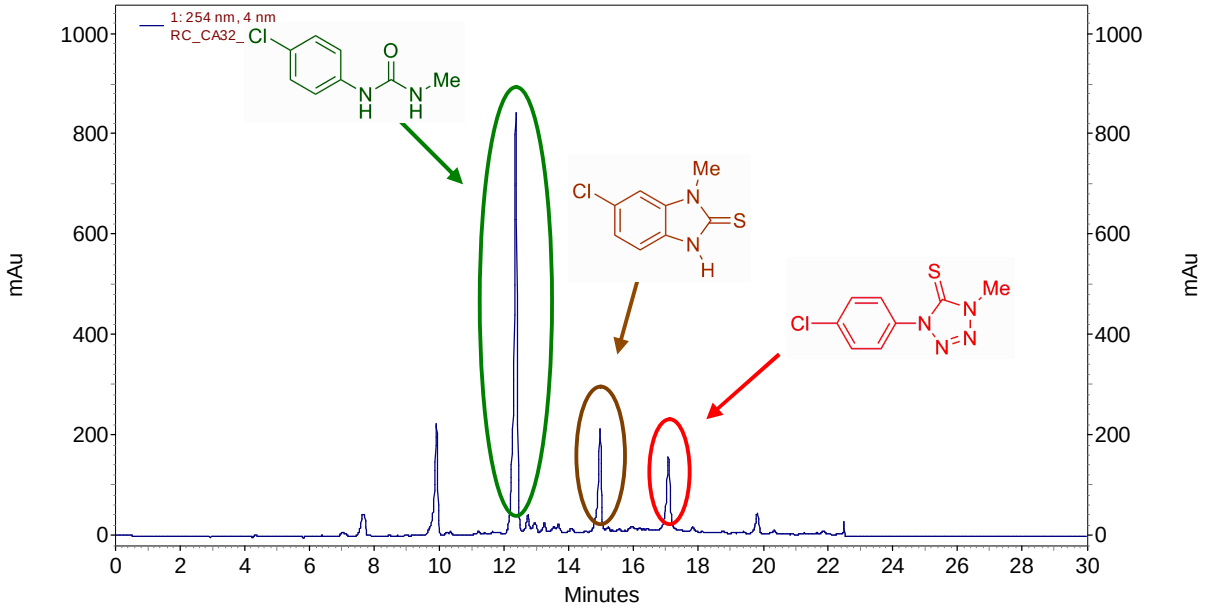

Figure 5. HPLC chromatogram of irradiated methyl-4-(4-chlorophenyl)-1H-tetrazol-5(4H)-thione 20c.

The separated products were analyzed by ^{1}H-NMR spectroscopy. Only two products along with the unreacted starting material were identified for photolyzed MeCN solution of **20c.**

As in case of **20a**, the unreacted starting material was identified by comparison of the chromatogram of crude product with the chromatogram obtained for the unirradiated MeCN solution of **20c (Figure 5).** The first photoproduct which was successfully identified had a retention time of 12.3 min in the crude product mixture chromatogram **(Figure 5)**; this product was found to be 1-methyl-3-(4-chlorophenyl) urea **30c** by ^{1}H-NMR analysis. This product was

also found during LCMS and GCMS analyses of the photolyzed MeCN solution of **20c.**

The second product which was identified by both ^{1}H-NMR and ^{13}C-NMR spectroscopy had a retention time of 15 min, it was identified to be 6-chloro-1,3-dihydro-1-methyl-2H-benzimidazole-2-thione **34c** (m/z = 198). We earlier hypothesized on the basis of GC-MS/MS analysis that this product was 1-methyl-2-(4-chlorophenyl) diaziridine-3-thione **31c** (m/z = 198). This type of product was also found by Fausto for the photolysis of 1-methyl-1*H*-tetrazole-5(4H)-thione. [46] However, our ^{1}H-NMR and ^{13}C-NMR spectra confirm that this product is not a diaziridine-3-thione but a benzimidazole-2-thione based compound. In case of 1-methyl-1*H*-tetrazole-5(4*H*)-thione, there is no phenyl group present on the tetrazolethione ring which will allow the benzimidazole-2-thione like product to form, therefore, in their case only diazridine-3-thione is produced. Note that these researchers identified this product using low temperature matrix-isolation IR spectroscopy as this highly unstable compound may be difficult to isolate in solution. In our GC- MS/MS spectrum, the fragmentation pattern of earlier hypothesized 1-methyl-2-(4-chlorophenyl)-diaziridine-3-thione **31c** could very well fit the fragmentation pattern of now confirmed 6-chloro-1,3-dihydro-1-methyl-2*H*-benzimidazole-2-thione **34c.** The two products would have essentially the same fragmentation pattern due to the formation of a 4- chloro-phenyl isothiocyanate type radical ion **(Figure 6).**

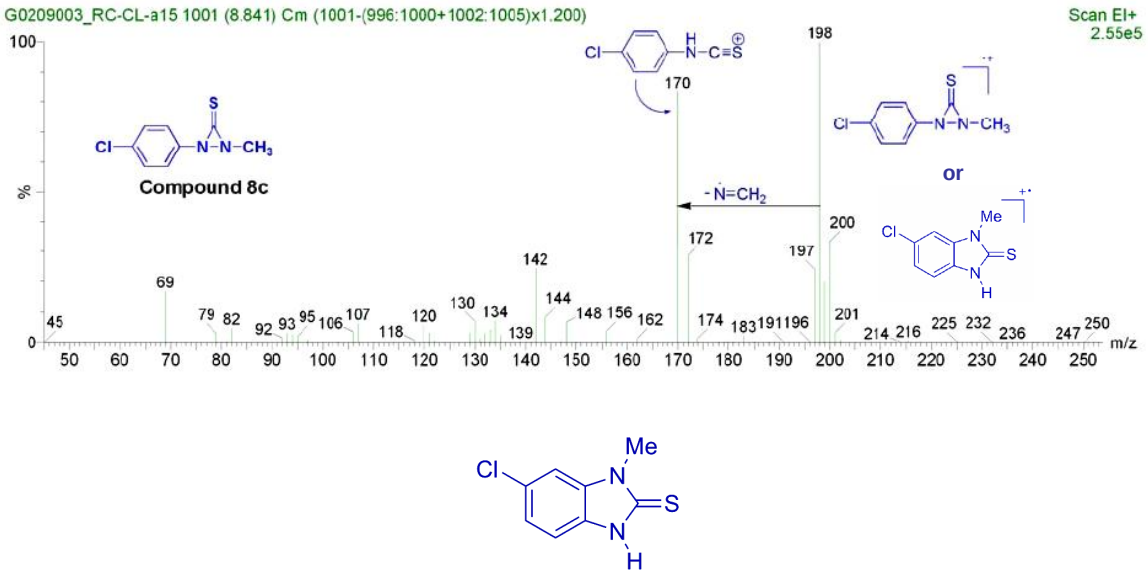

34c

Figure 6. Mass spectrum of 6-chloro-1,3-dihydro-1-methyl-2H-Benzimidazole-2-thione 34c.

The peak at 9.8 min (**Figure 6)** was also separated by preparatory HPLC, however, a clean ^{1}H-NMR was not obtained. Further, purification by HPLC is required to obtain any concrete data for analysis of this compound.

Similarly, a THF solution of **20c** was also irradiated under similar conditions. Again the solution was made by dissolving 100mg of **20c** in 100ml of THF. The solution was irradiated with medium pressure mercury lamp for 2 h 40 min. The irradiation time was longer than in MeCN solution. A dense liquid was obtained when irradiated sample was concentrated under vacuum. The TLC analysis showed a slow moving huge UV active spot. We believe that this dense liquid is a mixture of polymers formed by polymerization of THF during photolysis; all formed photoproducts are strongly embedded in this polymer

mixture which results in a single spot on the TLC plate. A column chromatography purification was also performed to remove the polymer mixture but this attempt was futile. As a result we could not carry out separation of the products using HPLC.

The work on separation and NMR analysis of the photoproducts obtained for photolysis of the remaining THF and/ or MeCN solutions of **20a-d** is intended in future.

II. 2. 2. 7. Multiphoton Excitation

Multiphoton experiments were carried out using Ti: sapphire laser at Kansas State University. As mentioned earlier, our goal was to develop masked enyne- carbodiimide prodrugs, the enynyl- *1H*- tetrazole- 5 (4H)- thiones **8** (**Scheme 7**) for photodynamic therapy of cancers. We wanted to study if the multiphoton excitation could be used to unmask the tetrazolethione scaffold in (give the number for the prodrug) to generate the active enyne- carbodiimide drug locally in cancer cells. This technique involves the use of 650-1050 nm laser to excite a UV active molecule. When an ultra fast laser (100 fs) is focused on a reaction mixture section, the high photon densities of the laser lead to excitation of the molecule due to simultaneous absorption of two or more photons.

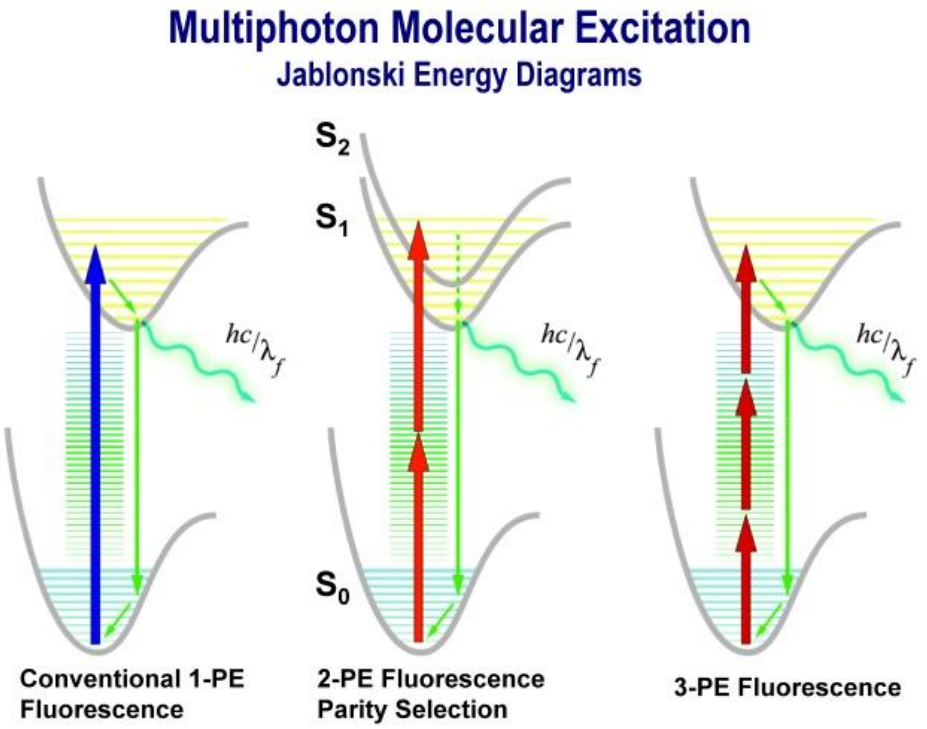

Figure 7. Multiphoton Excitation. [48]

Thus, two or more photons of longer wavelength provide together the same energy as a single photon in UV region (**Figure 11**)[48] This technique is very important for biological applications since a visible or near IR region photon is employed for the excitation of the molecules instead of a UV wavelength which is harmful to cells. [49, 50] The laser beam is focused at one point, therefore, there is no photodamage outside the focal plane.

We first tried photolysis of 1-methyl-4-(4-nitrophenyl)-1*H*-tetrazol-5(4*H*)-thione **20d** in THF using a 870 nm beam. In UV spectrum of **20d** in THF, the first absorption band λ_1 is at 251 nm and the second absorption band λ_2 is at 336 nm. Therefore, it was expected that **20d** would absorb three 870 nm photons during this experiment.

As in case of photolysis with UV light, a 4.2 ml of THF solution was kept at a distance of 10 cm from the laser source. The change during the experiment was followed with UV-VIS spectroscopy. The starting material **20d** was found unreacted even after 8 h of irradiation. The solution was again irradiated for 8h next day; this time the THF solution was placed as close as possible to the laser source. Again, no change was observed in the UV spectrum of **20d** after 8h. Since, "efficient multiphoton excitation requires the short pulses and high repetitive frequencies of the mode- locked lasers", it maybe that the Ti: sapphire laser used for our experiment is not strong enough to cause any reaction.[50] In that case, a stronger NdYAG laser with a shorter pulse width and higher repetitive rates could be useful for our experiments. It is also likely that our compound has a small three photon absorption cross-section; therefore, our compound is not excited during the experiment.

The fluorescence spectra of unirradiated **20a-d** in THF and MeCN, and that of their irradiated solutions were taken (see **supporting information**). This was to see if our multiphoton excitation experiments could be followed with fluorescence spectroscopy in future. The spectra were taken in Dr. Higgins' laboratory. However, the spectrometer recorded emission spectra starting at 330 nm. Near this region there was no significant difference between the fluorescence intensities of unirradiated and irradiated solutions of our 1, 4-disustitued tetrazolethione analogs. Therefore even if multiphoton excitation experiments are successful, they cannot be followed with fluorescence

spectroscopy since the fluorescence spectrometer records the emission spectra starting at 330 nm.

Considering all above described results, we conclude that there is a need for synthesis of new 1, 4-disubstiuted tetrazolethione analogs with UV absorption and fluorescence emission lying close to the visible region of light. This could be achieved by adding more electronically deactivating substituents on the phenyl ring subsituent of the tetrazolethione system. Also, instead of adding a methyl group on the tetrazolethione ring, some other substituents that could shift the UV absorption or the fluorescence emission closer to the visible region could be placed at the tetrazolethione ring. Thus, we could still use Ti- Sapphire laser for our experiments if our compounds have bigger two photon absorption cross-section.

III. CONCLUSIONS

The photolysis of THF and MeCN solutions of **20a-d** was performed using medium pressure mercury lamp. The rate of decomposition terazolethiones and the quantum yields of photoirradiation experiments depend upon the nature of substituents on the phenyl substituent. This effect is however not so pronounced.

The LCMS and GCMS analyses of irradiated THF and MeCN solutions of **20a-d** suggest the formation of isothiocyanates, azides, carbodiimides, ureas and benzeimidazole-2-thione. The analysis of THF solution could not be carried out since a polymeric mixture was formed during irradiation.

The experiments for THF solution of **20a** and MeCN solution of **20c** need to be repeated at larger scale to confirm the presence of any other products detected during GCMS analyses for UV irradiated solutions of these solutions**.** The experiments need to be conducted for spectroscopic analysis of products formed for the remaining MeCN solution of **20a** and THF solution of **20c** and; for the photolysis of **20b** and **20d** in THF and MeCN**.**

The multiphoton excitation experiment was not successful for the irradiation of **20d** which decomposes at a very fast rate with UV light. This experiment needs to be repeated with more powerful NdYAG laser. New analogs with different aromatic substituents need to be synthesized to further bring the UV absorption and the fluorescence emission bands closer to the visible region of light.

Our studies prove that it is possible to fine tune the photochemical properties of the tetrazolethione systems by modifying the substituents. The new analogs could be used for the development of a novel class of anticancer prodrugs for photodynamic therapy of cancers.

References:

1. Ishida, N.; Miyazaki, K.; Kumagai, K.; Rikimaru, M. J. *Journal of Antibiotics* **1965**, *18*, 68.

2. Dai, W. *Current Medicinal Chemistry* **2003**, *10*, 2265.

3. Bergman, R., G. *Accounts of Chemical Research* **1973**, *6*, 25.

4. Smith, A., L.; Nicolaou, K., C. *Journal of Medical Chemistry* **1996**, 39, 2103.

5. Myers, A., G. *Tetrahedron Letters* **1987**, *28*, 4493.

6. Zhao, K.; Reiner, J.; Xie, W. *Frontiers of Biotechnology & Pharmaceuticals* **2001***, 2*, 329-349

7. Bross, P. F.; Beitz, J.; Chen, G.; Chen, X. H.; Duffy, E.; Kieffer, L.; Roy, S.; Sridhara, R.; Rahman, A.; Williams, G.; Pazdur, R. *Clinical Cancer Research* **2001***, 7*, 1490-1496.

8. Abe, S.; Otsuki, M. *Current Medicinal Chemistry: Anti-Cancer Agents* **2002**, *2*, 715.

9. Naito, K.; Takeshita, A.; Shigeno, K.; Nakamura, S.; Fujisawa, S.; Shinjo, K.; Yoshida, H.; Ohnishi, K.; Mori, M.; Terakawa, S.; Ohno, R. *Leukemia* **2000***,14*, 1436.

10.. Myers, A., G.; Kuo, E., Y.; Finney, N., S. *Journal of the American Chemical Society* **1989**, *111*, 8057.

11. Nagata, R.; Yamanaka, H.; Okazaki, E.; Saito, I. *Tetrahedron Letters* **1989**, *30*, 4995.

12. Schmittel, M.; Strittmatter, M.; Kiau, S. *Tetrahedron Letters* **1995**, *36*, 4975.

13. Schmittel, M.; Kiau, S. *Liebigs Annalen* **1997**, 733.

14. Schmittel, M.; Mahajan, A., A.; Bucher, G. *Journal of the American Chemical Society* **2005**, *127*, 5324.

15. Engels, B.; Lennartz, C.; Hanrath, M.; Schmittel, M.; Strittmatter, M. *Angewandte Chemie, International Addition* **1998**, *37*, 1960.

16. Maier, M., E. *Synlett* **1995**, 13.

17. Nagata, R.; Yamanaka, H.; Murahashi, E.; Saito, I. *Tetrahedron Letters* **1990**, *31*, 2907.

18. Schmittel, M.; Steffen, J., P.; Angel, M., A., W.; Engels, B.; Lennartz, C.; Hanrath, M. *Angewandte Chemie, International Edition* **1998**, *37*, 1562.

19. Shi, C.; Wang, K., K. *Journal of Organic Chemistry* **1998**, *63*, 3517.

20. Schmittel, M.; Steffen, J., P.; Engels, B.; Lennartz, C.; Hanrath, M. *Angewandte Chemie, International Edition* **1998**, *37*, 2371.

21. Schmittel, M.; Rodriguez, D.; Steffen, J., P. *Angewandte Chemie, International Edition* **2000**, *39*, 2152.

22. Quast, H.; Nahr, U. *Chemische Berichte* **1985***, 118*, 526-540

23. Quast, H.; Nahr, U. *Chemische Berichte* **1983***, 116*, 3427-3437.

24. Quast, H.; Bieber, L. *Chemische Berichte* **1981***, 114*, 3253-3272.

25. Maier, G.; Eckwert, J.; Bothur, A.; Reisenauer, H., P.; Schmidt, C. *Liebigs Annalen* **1996**, 1041.

26. Dunkin, I., R.; Shields, C. J.; Quast, H. *Tetrahedron* **1989**, *45*, 259.

27. Chae, Y., B.; Chang, K., S.; Kim, S., S. *Taehan Hwahakhoe Chi* **1967**, *11*, 85.

28. Awadallah, A.; Kowski, K.; Rademacher, P *Journal of Heterocyclic Chemistry* **1997**, *34*, 85.

29. Philippon, A.; Tao, J.; Tetard, D.; Degueil-Castaing, M.; Maillard,B. *Synthetic Comunications* **1997**, *27*, 2651.

30. Johnstone, R. A. W.; Price, P. J. *J. Chem. Perkin Trans. 1: Organic and Bio-Organic Chemistry* **1987**, *5*, 1069.

31. Tsuge, O.; Urano, S.; Koji, O. *J. Org. Chem*. **1980**, *45*, 5130.

32. Poplavskaya, Y. V.; Alam, L. V.; Koldobskii, G. I. *Russian Journal of Organic Chemistry* **2000***, 36*, 1847.

33. Tullio, P., D,; Becker, B.; Boverie, S.; Dabrowski, M.; Wahl, P.; Antonie, M., H.; Somers, F.; Sebille, S.; Ouedraogo, R.; Hansen, J., B.; Lebrun, P.; Pirotte, B. *Journal of Medicinal Chemistry* **2003**, *46*, 3342.

34. Thomsen, I.; Clausen, K.; Scheibye, S.; Lawesson, S.-O. *Organic Syntheses* **1990**, *7*, 372.

35. Harrison, D.; Ralph, J., T. *Journal of the Chemical Society (Resumed)* **1965**, 3132.

36. Lieber, E.; Ramachandran, J. *Canadian Journal of Chemistry* **1959**, *37*, 101.

37. Labbe, G.; Vermeulen, G.; Flemal, J.; Toppet, S. *Journal of Organic Chemistry* **1976**, *41*, 1976.

38. Bukharov, S., V.; Litvinov, I., A.; Gubaidullin, A., T.; Chernova, A., V.; Shagidullin, R., R.; Nugumanova, G., N.; Mukmeneva, N., A. *Russian Journal of General Chemistry* **2004**, *74*, 1864.

39. Gosavi, R. K.; Rao C. N. R. *Canadian Journal of Chemistry* **1967**, *45*, 1897.

40. Moran, A. M.; Bartholomew, G. P.; Bazan, G. C.; Kelley, A. M. *Journal of Physical Chemistry A* **2002**, *106*, 4928.

41. Zuccarello, F.; Millefiori, S.; Buemi, G. *Spectrochimica Acta, Part A: Molecular and Biomolecular Spectroscopy* **1979**, *35A*, 223.

42. Sawamura, S.; Taniguchi, K.; Suzuki, K. *Bulletin of the Chemical Society of Japan* **1980**, *53*, 1898.

43. Hatchard, C., G.; Parker, C. A. *Proceedings of Royal Society (London)* **1966**, *88*, 5041.

44. *Parker, A., C. Proceedings of Royal Society (London)* **1956**, *A220*, 104.

45. Lei, L.; Hu, X.; Yue, P., L.; Bossmann, S., H.; Gob, S.; Braun , A. *Journal of Photochemistry and Photobiology, A: Chemistry* **1998,** *116,* 159.

46. Gomez- Zavaglia, A.; Reva, I. D.; Frija, L.; Critiano, M. L.; Fausto, R. *Journal of Molecular Structure* **2006**, *786*, 182.

47. Letsinger, R. L.; Wubbels, G. G. *Journal of American Chemical Society* **1966**, *88*, 5041. (GCMS photoreduction)

48. http://www.drbio.cornell.edu/MPE/mpe1.html

49. William, R., M.; Zipfel, W.; Webb, W., W. *Current opinion in Chemical Biology* **2001**, *5*, 603.

50.Denk, W.; Svoboda, K. *Neuron* **1997**, *18*, 351.

CHAPTER 1

Photochemistry of 1,4-Disubstituted Tetrazolethiones

EXPERIMENTAL SECTION

I. 1.Synthesis

5-Chloro-1-phenyl-1*H*-tetrazole (22)[29]**:** A mixture of sodium azide (3.0 g, 46.15 mmol) and tetrabutylammonium bromide (0.650 g, 2.02 mmol) in water (8.7 mL) was added to a solution of phenyl-1,1-dichloroisocyanide (**21**) (5.0 g, 28.73 mmol) in toluene (42.4 ml). The mixture was stirred at room temperature and monitored by TLC until the starting material disappeared. After 2.5 h the aqueous layer was saturated with NaCl and the organic layer was extracted with toluene thrice and dried over Na_2SO_4. The organic layer was concentrated under reduced pressure. The flask was then kept at -5^{o}C until the crystals of **22** started to appear (approximately 2 - 5 minutes) which were recovered by filteration. The supernatant was further concentrated, cooled to -5^{o}C to recover more crystals. The latter process was repeated twice. Compound **22** (3.8 g**,** 73% yield) was obtained as white crystalline material: R_f 0.3 (80:20 hexane:ethylacetate); ^{1}H-NMR (400 MHz, $CDCl_3$): δ 7.58-7.65 (m, 5H); ^{13}C NMR (400 MHz, $CDCl_3$): δ 124.70, 130.11, 131.11, 132.80, 145.73. LRMS (ESI): *m/z* 198 (M + NH_4^+), 181 (M + H^+), 153, 138, 118, 92, 77.

1-Phenyl-1*H*-tetrazol-5(4*H*)-one (23a)[30]**. 22** (3.7 g, 20.49 mmol) was added to a mixture of 2 M aqueous NaOH (55.7 mL) and ethanol (18.6 mL). The mixture

was refluxed at 70 ^{o}C until the starting material disappeared (approximately 2 h). The reaction mixture was cooled in ice that resulted in the separation of a side product in the form of a colorless solid that was removed by filteration. Acidification of the filterate with concentrated HCl (pH = 3-5) afforded a thick white precipitate that was filtered, washed with water and air dried. Compound **23a** (3.15 g, 95% yield) was obtained as a white solid: R_f 0.22 (40:60 hexane:ethylacetate); ^{1}H-NMR (400 MHz, DMSO): δ 7.42 (t, *J* = 7.51 Hz, 1H), 7.56 (t, *J* = 7.60 Hz, 2H), 7.85 (d, *J* = 7.68 Hz, 2H); ^{13}C NMR (400 MHz, DMSO): δ 119.48, 127.51, 129.39, 134.15, 150.17. LRMS (ESI): *m/z* 180 (M + NH_4^+), 163 (M + H^+), 135, 120, 107, 92, 80.

1-(4-Methoxyphenyl)-1*H*-tetrazol-5(4*H*)-one (23b)[31]: Trimethylsilyl azide (TMSA) (0.773 g, 6.7 mmol) was added to 4-methoxyphenylisocyanate (**24b**) (0.5 g, 3.35 mmol). The mixture was refluxed at 100^{o}C for 24 h. The unreacted TMSA was removed under reduced pressure and the white residue was dried under vacuum. Compound **23b** (0.581 g, 90% yield) was obtained as a white solid: R_f 0.45 (40:60 hexane:ethylacetate); ^{1}H NMR (400 MHz,, DMSO): δ 3.81 (s, 3H), 7.10 (d, *J* = 8.98 Hz, 2H), 7.71 (d, *J* = 9.17 Hz, 2H); ^{13}C-NMR (400 MHz, DMSO): δ 55.45, 114.53, 121.97, 127.08, 150.46, 158.50. LRMS (ESI): *m/z* 210 (M + NH_4^+**),** 193 (M + H^+), 165, 150, 137, 134, 122, 110.

Similarly, compound **23c** was prepared.

1-(4-Chlorophenyl)-1*H*-tetrazol-5(4*H*)-one (23c)[31]: Compound **23c** (0.605 g, 95% yield) was obtained from 4-chlorophenylisocyanate (**24c**) (0.5 g, 3.26 mmol) as a white solid: R_f 0.55 (40:60 hexane:ethylacetate); ^{1}H-NMR (400 MHz, DMSO): δ 7.89 (d, *J* **=** 8.72 Hz**,** 2H), 7.63 (d, *J* **=** 8.72 Hz**,** 2H); ^{13}C-NMR (400 MHz, DMSO): δ 120.98, 129.48, 131.67, 133.10, 150.13. LRMS (ESI): *m/z* 214 ($M + NH_4^+$**),** 197 ($M + H^+$), 173, 169, 158, 141, 134.

1-(4-Nitrophenyl)-1*H*-tetrazol-5(4*H*)-one (23d)[30]: Fuming HNO_3 (3.5 ml) was added to **23a** (1.0 g, 6.2 mmol). The mixture was refluxed at 100^{o}C for 30 min during which formation of a yellow solid was observed. The reaction mixture was poured over ice and cooled for 2 h to afford a thick yellow solid which was filtered, washed with plenty of water and air dried. Compound **23d** (0.749 g, 59% yield) was obtained as a yellow solid: R_f 0.18 (20:80 hexane:ethylacetate); IR (KBr) v: 587, 688, 704, 720, 751, 861, 1032, 1055, 1112, 1337, 1352, 1375, 1502, 1512, 1598, 1611, 1742, 3090, 3121, 3270cm^{-1}; 1H NMR (200 MHz, DMSO): δ 8.43 (d, *J* = 9.15 Hz, 2H), 8.19 (d, *J* = 9.17 Hz, 2H); ^{13}C NMR (400 MHz, DMSO): δ 118.85, 125.15, 139.20, 145.40, 150.00. LRMS (ESI): *m/z* 225 ($M + NH_4^+$**),** 208 ($M + H^+$), 165, 121, 105, 91.

1-Methyl-4-phenyl-1*H*-tetrazol-5(4*H*)-one (25a)[32]: A solution of dimethyl sulfate (0.83 g, 6.58 mmol) and methylene chloride (8.2 mL) was added to a mixture of **23a** (1 g**,** 6.17 mmol), tetrabutylammonium bromide (0.093 g, 0.29 mmol), 10% NaOH (12.4 mL) and methylene chloride (12.4 mL). The reaction mixture was

stirred at room temperature for 3 h. The organic layer was separated and washed with water thrice to remove tetrabutylammonium bromide and dried over Na_2SO_4. The dried organic layer was concentrated under reduced pressure and the residue dried under vacuum. Compound **25a** (0.91 g, 84% yield) was obtained as a crystalline colorless solid: R_f 0.81 (40:60 hexane:ethylacetate); ^{1}H NMR (400 MHz, DMSO): δ 3.62 (s, 3H), 7.44 (t, *J* = 7.40 Hz, 1H), 7.58 (t, *J* = 7.03 Hz, 2H), 7.85 (d, *J* = 8.27 Hz, 2H); ^{13}C NMR (400 MHz, DMSO): δ 31.16, 119.42, 127.73, 129.46, 134.23, 148.77. HRMS (ESI), exact mass calculated for (M + Na^+) $C_8H_8N_4ONa^+$ = 199.0596, found 199.0602.

Similarly, compounds **25b** – **d** were prepared.

1-Methyl-4-(4-methoxyphenyl)-1*H*-tetrazol-5(4*H*)-one (25b)[32]: Compound **25b** (0.396 g, 92% yield) was obtained from **23b** (0.4 g, 2.08 mmol) as a white crystalline solid: R_f 0.51 (40:60 hexane:ethylacetate); mp 98 – 99 ^{o}C; IR (KBr) v: 511, 574, 729, 744, 824, 1028, 1048, 1155, 1252, 1357, 1424, 1519, 1618, 1721, 2847, 2945, 2975, 3011, 3088 cm^{-1}; ^{1}H NMR (400 MHz, $CDCl_3$): δ 3.70 (s, 3H), 3.86 (s, 3H), 7.01 (d, *J* = 9.17 Hz, 2H), 7.80 (d, *J* = 9.17 Hz, 2H); ^{13}C NMR (200 MHz, $CDCl_3$): δ 31.63, 55.75, 114.70, 121.61, 127.87, 149.62, 159.22. HRMS (ESI), exact mass calculated for (M + Na^+) $C_9H_{10}N_4O_2Na^+$ = 229.0702, found 229.0712.

1-Methyl-4-(4-chlorophenyl)-1*H*-tetrazol-5(4*H*)-one (25c)[32]: Compound **25c** (0.48 g, 90% yield) was obtained from **23c** (0.5 g**,** 2.54 mmol) as a white solid: R_f

0.62 (40:60 hexane:ethylacetate); mp 91 – 93 ^{o}C; IR (KBr) v: 512, 575, 708, 729, 832, 839, 1014, 1092, 1138, 1387, 1423, 1496, 1597, 1732, 2854, 2928, 2958, 3054, 3106 cm^{-1}; ^{1}H NMR (200 MHz, $CDCl_3$) δ: 3.72 (s, 3H), 7.47 (d, *J* = 8.80 Hz, 2H), 7.93 (d, *J* = 8.80 Hz, 2H); ^{13}C NMR (400 MHz, $CDCl_3$): δ 31.69, 120.49, 129.78, 133.42, 133.55, 149.32. HRMS (ESI), exact mass calculated for (M + Na^+) $C_8H_7ClN_4ONa^+$ = 233.0206, found 233.0215.

1-Methyl-4-(4-nitrophenyl)-1*H*-tetrazol-5(4*H*)-one (25d)[32]: Compound **25d** (0.719 g, 96% yield) was obtained form **23d** (0.71 g**,** 3.38 mmol) as a yellow-brown solid: R_f 0.6 (20:80 Hexane:Ethylacetate); ^{1}H NMR (200 MHz, DMSO): δ 3.64 (s, 3H), 8.20 (d, *J* = 9.16 Hz, 2H), 8.45 (d, *J* = 9.15 Hz, 2H); ^{13}C NMR (400 MHz, DMSO): δ 31.32, 118.89, 125.29, 139.21, 145.61, 148.61. HRMS (ESI): exact mass calculated for (M + H^+) $C_8H_8N_5O_3^+$ = 222.0627, found 222.0634.

1-Methyl-4-phenyl-1*H*-tetrazole-5(4*H*)-thione (20a)[22]: P_2S_5 (12.0 g, 53.5 mmol) was added to a solution of **25a** (4.0 g**,** 22.7 mmol) in toluene (82 mL). The mixture was refluxed for 2 days at 110^{o}C until the starting material disappeared. The reaction mixture was filtered and the filtrate was dried over Na_2SO_4 and concentrated under reduced pressure. Purification by column chromatography (hexane:ethylacetate, 88:12) gave **20a** (2.3 g, 53% yield) as a yellow solid: R_f 0.77 (40:60 hexane:ethylacetate); ^{1}H-NMR (400 MHz, DMSO): δ 3.91 (s, 3H) 7.68-7.55 (m, 3H), 7.87 (d, *J* = 7.14 Hz, 2H); ^{13}C-NMR (400 MHz, DMSO): δ

34.68, 124.30, 129.29, 129.76, 134.45, 163.23. HRMS (ESI): exact mass calculated for (M + H^+) $C_8H_9N_4S^+$ = 193.0548, found 193.0545.

Similarly, Compounds **20b** - **d** were synthesized.

1-Methyl-4-(4-methoxyphenyl)-1*H*-tetrazole-5(4*H*)-thione (20b)[22]: Synthesis of **20b** was carried out from **25b** (0.3 g**,** 1.46 mmol). The refluxing time in P_2S_5 was 20 h. Purification by column chromatography (hexane:ethylacetate, 9:1) gave **20b** (0.243 g, 75% yield) as a white crystalline solid: R_f 0.56 (60:40 hexane:ethylacetate); mp 134 – 135 ^oC; IR (KBr) v: 543, 561, 742, 825, 1028, 1041, 1080, 1114, 1191, 1256, 1302, 1326, 1369, 1446, 1514, 1591, 1612, 2840, 2926, 2965, 2998, 3076 cm^{-1}; ^1H NMR (200 MHz, $CDCl_3$) δ: 7.82 (d, *J* = 9.16 Hz, 2H), 7.05 (d, *J* = 9.16 Hz, 2H), 3.98 (s, 3H), 3.88 (s, 3H); ^{13}C-NMR (200 MHz, $CDCl_3$) δ: 35.17, 55.83, 114.62, 125.67, 127.85, 160.53, 163.93. HRMS (ESI): exact mass calculated for (M + H^+) $C_9H_{11}N_4OS^+$ = 223.0654, found 223.0645.

1-Methyl-4-(4-chlorophenyl)-1*H*-tetrazole-5(4*H*)-thione (20c)[22]: Synthesis of **20c** was carried out from **25c** (0.32 g**,** 1.52 mmol). The refluxing time in P_2S_5 was 28 h. Purification by column chromatography (hexane:ethylacetate, 93:7) gave **20c** (0.235 g, 68% yield) as a white crystalline solid: R_f 0.62 (60:40 hexane:ethylacetate); mp 137 – 139 ^oC; IR (KBr) v: 544, 571, 718, 828, 1016, 1080, 1095, 1201, 1368, 1389, 1494, 1590, 1721, 2855, 2924, 2953, 3077, 3097 cm^{-1}; ^1H NMR (200 MHz, $CDCl_3$) δ: 3.98 (s, 3H), 7.53 (d, *J* = 9.15 Hz, 2H), 7.99 (d, *J* = 8.80 Hz, 2H); ^{13}C-NMR (200 MHz, $CDCl_3$) δ: 35.05, 124.71, 129.56,

133.36, 135.50, 163.57; HRMS (ESI): exact mass calculated for (M + H^+) $C_8H_8ClN_4S^+$ = 227.0158, found 227.0161.

1-Methyl-4-(4-nitrophenyl)-1*H*-tetrazole-5(4*H*)-thione (20d)[22]: Synthesis of **20d** was carried out from **25d** (0.561 g**,** 2.54 mmol). The refluxing time in P_2S_5 was 24 h. Purification by column chromatography (hexane:ethylacetate, 9:1) gave **20d** (0.303 g, 50% yield) as a yellow crystalline solid: R_f 0.73 (40:60 hexane:ethylacetate); mp 141 – 143 ^oC; IR (KBr) v: 549, 568, 684, 702, 749, 854, 1038, 1068, 1109, 1328, 1340, 1365, 1494, 1529, 1593, 1614, 2853, 2963, 3093, 3120 cm^{-1}; ^1H NMR (200 MHz, DMSO): δ 3.92 (s, 3H), 8.33 (d, *J* = 8.42 Hz, 2H), 8.49 (d, *J* = 8.42 Hz, 2H); ^{13}C-NMR (200 MHz, DMSO): δ 34.78, 124.61, 124.83, 139.22, 147.23, 163.23. HRMS (ESI): exact mass calculated for (M + H^+) $C_8H_8N_5O_2S^+$ = 238.0399, found 238.0387.

I. 2. Photolysis of tetrazolethione analogs

The solutions of **20a- d** were made in THF and MeCN and were irradiated at 254 nm. The initial concentrations of the unirradiated THF and MeCN solutions was 0.45 and 0.40 mM for **20a**, 0.28 and 0.22 mM for **20b**, 0.49 and 0.37 mM for **20c** and; 0.17 and 0.13 mM for **20d** respectively. The lamp was placed 10 cm away from the sample and was allowed to warm up for 5 min before the experiment was conducted. 4.2 ml of each solution was taken in a quartz cuvette and was irradiated in UV light. A UV spectrum was taken for each solution at 0, 2, 3, 5, 10, 15, 20, 25, 30 min intervals during irradiation. At these intervals, an

aliquot of 10µl was also taken out which was analyzed using HPLC. An external calibration curve for each solution was constructed using HPLC and the amount of starting material left after each interval of irradiation was determined by using these curves.

An aliquot was also taken out during irradiation of each solution for LCMS and GCMS analysis of the product mixture. The samples were collected after irradiation for 15 and 20 min for **20a**, 10 and 15 min for **20b**, 20 and 15 min for **20c** and; 20 and 15 min for **20d** solutions made in THF and MeCN respectively.

I. 3. Ferrioxalate Actinometry

We prepared 100 ml of 0.0113 M ferric sulfate 7-hydrate, 25 ml of 0. 356 M oxalic acid and 1, 10- phenanthroline solution obtained by dissolving 0.5g of phenanthroline in 1 ml glacial acetic acid and 24 ml water.

For this experiment, seven separate reaction mixtures were prepared by mixing 3.36 ml of ferric sulfate solution and 0.84ml of oxalic acid solution. These mixtures were irradiated in quartz cuvettes for 30, 60, 90, 120, 150 and 180 s. 0.2 ml of each irradiated mixture was mixed with 0.1 ml 1, 10- phenanthroline and 2.7 ml water and an absorption spectrum was taken at 510 nm. The amount of Fe^{2+} produced was calculated using the absorption spectra obtained from ferrioxalate actinometry experiment.

We used the data collected from HPLC analysis and ferrioxalate actinometry to calculate quantum yields for our photolysis experiments. As mentioned before (**Section: II. 2. 3.)**, we used HPLC to determine the change in

amount of starting materials during the irradiation of our THF and MeCN solutions of **20a-d**. This information was used to calculate the rate of disappearance of starting materials over time. Using this information along with the amount of Fe^{2+} produced from ferrioxalate actinometry, we calculated quantum yields for the disappearance of each starting material in THF and MeCN.

I. 4. HPLC separation

I. 4. 1. Photolysis of THF solution of 20a

100 mg of compound **20a** was dissolved in 150 ml of THF. The solution was irradiated for 1 h with a medium pressure mercury lamp in a quartz photochemical reactor. The irradiated solution was collected and concentrated under pressure. The contents were dissolved in 3ml of 50: 50 MeCN: H_2O mixture and a 10µl of this sample was injected for HPLC analysis. The mobile phase used for HPLC run was initially 100% water and concentration of MeCN was increased linearly from 0% to 100% over 20 min. The total flow rate was 1ml/ min. A sample of unirradiated solution of **20a** was also analyzed by HPLC.

TLC analysis of the crude irradiated sample was done to gather information about the components present in appreciable quantity in the product mixture. Thus, all components corresponding to the UV active spots were separated by column chromatography. The separated fractions were concentrated to dryness under pressure and were dissolved in 3ml of 50: 50 MeCN: H_2O mixtures for further analysis by HPLC to check for various

photoproducts. The photoproducts in each fraction were separated by preparatory HPLC. Since there were no products in the beginning of the HPLC run for the crude product mixture (as seen from chromatogram of crude product mixture) we decided to start the preparatory HPLC runs with an initial mobile phase of 30% water -70% MeCN mixture. The concentration of MeCN was increased linearly from 30% to 100% over 15 min. The total flow rate was 4.73 ml/ min. The separated product solutions were concentrated under pressure and dried under vacuum. The dried products were analyzed by ^{1}H-NMR spectroscopy. ^{13}C-NMR was also taken whenever required. We used d6-acetone or d-chloroform for preparing NMR solutions.

I. 4. 2. Photolysis of MeCN solution of 20c

Similarly, 100 mg of **20c** was dissolved and irradiated for 2h and 5 min. Chromatographic and HPLC separation was carried out as mentioned above for **20a**. The separated products were analyzed by ^{1}H-NMR. ^{13}C-NMR was taken whenever required.

CHAPTER 2

Bio- evaluation of cytotoxicity of 1-methyl-4-(4-chlorophenyl)-1H-tetrazol-5(4H)-thione against MCF-7 cell line

I. INTRODUCTION

Tetrazole based compounds have wide variety of applications. There are many known compounds which are potent pharmaceutical agents and many others with other useful applications. Some of the pharmaceutically important compounds are shown in **Scheme 1 .**The compound **1** is patented for treatment of pain, neurodegenerative diseases, addiction disorders, sexual dysfunction[1]; the compound **2** is antihypertensive drug[2]; the compound **3** is a potent HIV protease inhibitor[3] and; the compound **4** is anticarcinogenic[4].

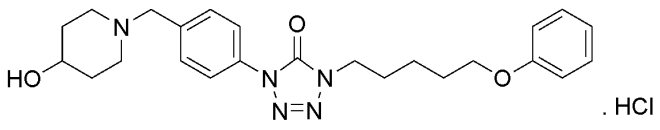

1

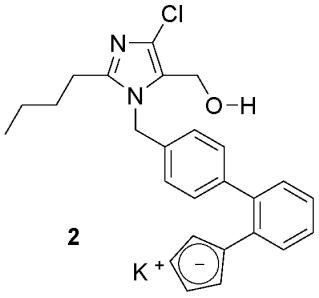

2

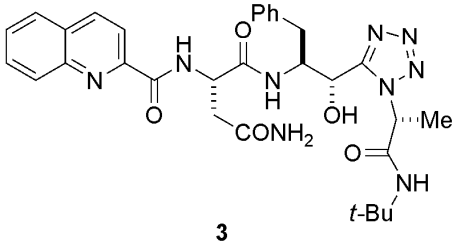

3

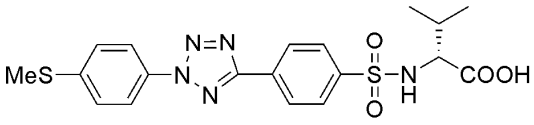

4

Scheme 1. Tetrazole based compounds

I. 1. Our Goal

Our goal was to test the tetrazolethione analogs **20a-d** (**Scheme 2**) synthesized in our laboratory (**Chapter-1**) for their cytotoxicity against MCF-7 cell line.

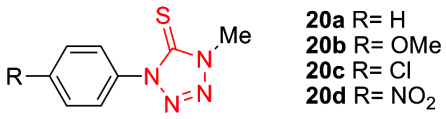

20a R= H
20b R= OMe
20c R= Cl
20d R= NO_2

Scheme 2. Tetrazolethione analogs

II RESULTS AND DISCUSSION

Initially, we tested only 1-methyl-4-(4-chlorophenyl)-1*H*-tetrazol-5(4*H*)-thione **20c** for it's cytotoxicity against MCF-7 cancer cell line via MTT (3-(4,5-dimethylthiazoyl-2-yl)2,5-diphenyltetrazolium-bromide) assay. 50,000 cells per well were seeded out in three 96-well plates carrying 100µl of 10% MEM per well. The plates were incubated at 37^{o}C in presence of 5% CO_2.

A time dependent study was performed for cytotoxicity of **20c** on MCF-7 cells. The cells in all three plates were dosed with 1 nm, 10 nm, 100nm, 500nm and 1µm of **20c** solution made in DMSO after 24 hr (second day) of incubation. Some wells were not dosed with compound solution for maintaining control. MTT assay was performed on one of the dosed plates on the third day. The cells in other two plates were again dosed with same concentration solutions. After 48 hr of dosing, i.e., on the fourth day, one of the remaining plates was used for MTT assay. This was to study the effect of different concentrations of **20c** after 48 hr of treatment. The remaining third plate was again dosed with the same

concentration solutions and incubated for another 24 hr. On the fifth day the MTT assay was performed to study the effect of our compound solutions after 72 hr of treatment.

The data collected for each MTT assay was used to plot % cell viability against the **20c** concentration. ±SE was also plotted for each data point. The plots thus obtained are shown in **Figure 1**. A comparative plot of % cell viability vs. treatment for three assays was also made (**Figure 2**)**.**

a)

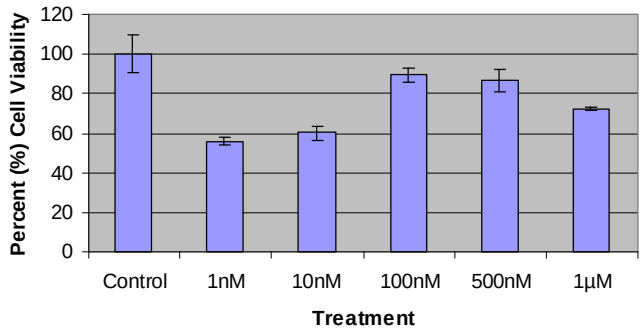

b)

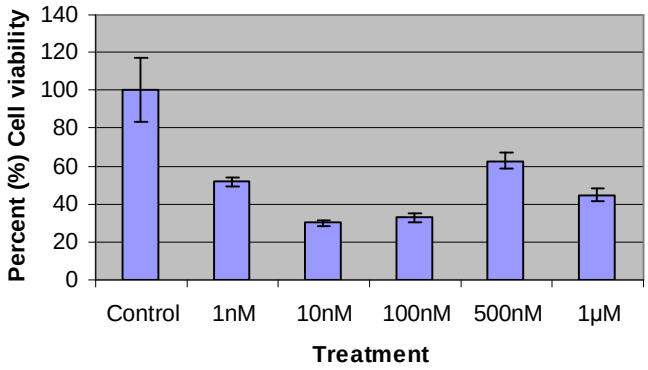

c)

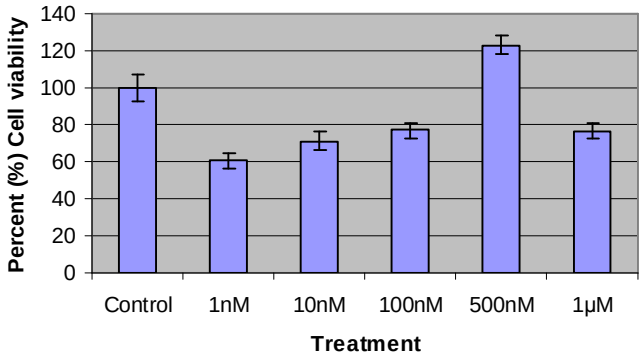

Figure 1. % cell viability of MCF-7 cells after 24 hr, 48hr and 72hr of treatment with 20c solutions. The bar on each data point represents ±SE for that data.

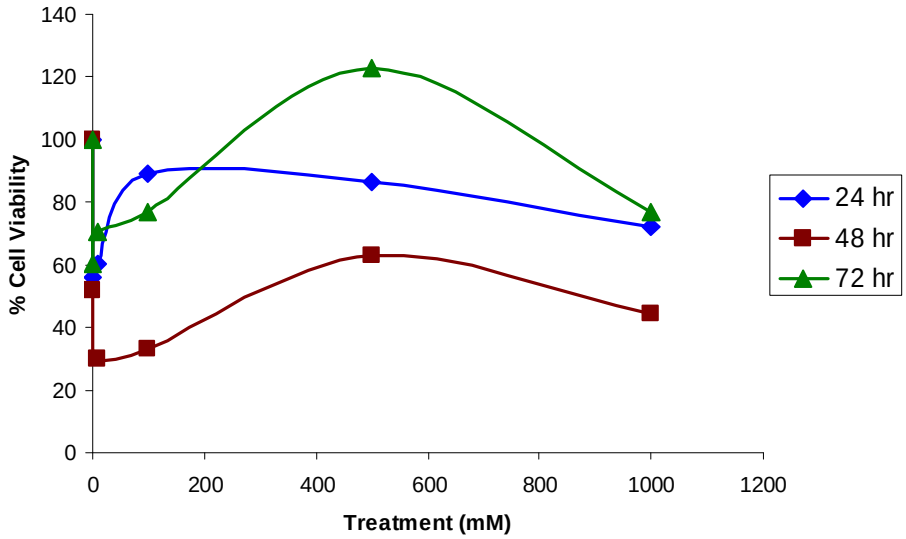

Figure 2. Comparative plot for 24 hr, 48 hr and 72 hr of treatment.

The % cell viability was found to be low for 48 hr treatment of MCF-7 cells with all concentrations of 1-methyl-4-(4-chlorophenyl)-1*H*-tetrazol-5(4*H*)-thione **20c** solutions. Further, 10nM was found to be the most effective concentration of

20c for inhibition of MCF-7 cells proliferation. The % cell viability for 48 hr treatment of this concentration solution was found to be 30% with 2% ±SE.

Three multiples of 48 hr treatment assays were also performed to confirm the above results. However, this time cells were dosed with 10nM, 100nM, 200nM and 500nM of **20c** solutions. The results were found to be different from the experiment; %cell viability was found to be 55% with a 5% ±SE for average obtained from three assays.

III. CONCLUSIONS

The time dependent study for treatment of **20c** solutions suggests the 48 hr treatment to be most effective for inhibition of MCF-7 cells proliferation. Among all concentrations of **20c** solutions, 10 nM is the most cytotoxic concentration for 48 hr treatment of MCF-7 cell line.

The above experiments need to be repeated before investigating the cytoxicity of **20c** against MCF-7 cells. Other tetrazolethione analogs **20a, b, d** need to be tested for their cytoxicity against MCF-7 cell line. MCF-7 cells are known to express both α_{2B} and α_{2C} adrenoceptors and tetrazolone based compounds are known to be effective α_{2C} antagonists. Studies to investigate the cytoxicity of **20c** and all other synthesized tetrazolethione analogs **20a, b, d** against MCF-7 and other cell lines with α_{2B} and/ or α_{2C} adrenoceptors would prove to be beneficial for the development of novel α_{2B} and/ or α_{2C} antagonist based drugs.

References:

1. Andres-Gil, Jose Ignacio; Alcazar-Vaca, Manuel Jesus ,*WO 2006/067139* .

2. Mavromoustakos, T.; Kolocouris, A.; Zervou, M.; Roumelioti, P.; Matsoukas, J.; Weisemann, R. *Journal of Medicinal Chemistry* **1999**, *42*, 1714.

3. Abell, A. D.; Foulds, J.G. *Journal of the Chemical Society, Perkin Transactions 1* **1997**, *17*, 2475.

4. Tamura, Y.; Fumihiko, W; Nakatani, T; Ohtani, M *J.Med. Chem.***1998**, *41*, 640-649

CHAPTER 2

Bio- evaluation of cytotoxicity of 1-methyl-4-(4-chlorophenyl)-1H-tetrazol-5(4H)-thione against MCF-7 cell line

EXPERIMENTAL SECTION

I. 1. Cell Culture

Cells were cultured in 10 % Minimum Essential Eagle's Medium (MEM). This media was prepared by mixing 9.53 g MEM, 1. 5g NaHCO3, 10 ml of 100 mM sodium pyruvate, 10 ml non-essential amino acids solution, 100ml fetal bovine serum, 10 ml antibiotic- antimycotic and 1 tube (0.01g/L) of insulin in 1L of water at room temperature.

I. 2. Drug Treatment

50,000 MCF-7 cells were seeded out in a 96 well plate and were incubated in 100 µl of 10 % MEM at 37^0C in presence of 5% CO_2 for 24 h.

I. 2. 1. Time dependent study

Old media was removed and 100 µl of new media was added to MCF-7 cells in three 96 well plates after 24 h of incubation. The cells were dosed with 1 µl of 1 nM, 10 nM, 100nM, 500nM and 1µM **20c** solutions made in DMSO after 24 hr (second day) of incubation. Some wells were not dosed with compound solution for maintaining control. On the third day, an MTT assay was performed on one of the dosed plates and the cells in other two plates were treated with **20c**

solutions as described. After 48 h of treatment, i.e., on the fourth day, one of the remaining plates was used for MTT assay. This was to study the effect of different concentrations of **20c** after 48 h of treatment. The remaining third plate was again dosed with the same concentration solutions and incubated for another 24 h. On the fifth day the MTT assay was performed to study the effect of **20c** after 72 hr of treatment.

I. 2. 3. 48 h Treatments

The incubated cells were treated with 10nM, 100nM, 200nM and 500nM of **20c** solutions for 48 h as described earlier. MTT assays were performed on three multiples of 48 h treatment assays.

I. 3.1 MTT cell proliferation assay

MTT (3-(4,5-dimethylthiazoyl-2-yl)2,5-diphenyltetrazolium-bromide) was used to determine the % cell viability after treatments with solutions of **20c**. The living cells metabolize MTT to formazan a purple colored compound which indicates the % cells surviving after treatment with a drug. After desired hours of treatment with **20c** solutions, old media was removed and replaced with 100 µl of new media. A 10 µl of MTT (5mg/ml, in PBS) was added to each well and cells were incubated at 37^0C in presence of 5% CO_2. After 2 h of incubation, formazan crystals were solubilized in each well by mixing with 100 µl solubilization solution (isopropanol in 0.04 N HCl). Absorbance was recorded using a plate reader. Two wavelength channels were used; 570 nm for recording the absorbance of each

well and 650 nm for recording the background absorbance. The net solution absorbance was obtained by subtracting the background absorbances from the absorbance of wells. % Cell viability was calculated according to the **equation 1**.

% cell viability= (absorbance of treated cells/ absorbance of control) * 100 **(1)**

% cell viability versus treatment plot for the average data of three multiples of 48 treatment assays was made.

I. 3. 2 % Cell Viability versus Treatment plot for 48 h Treatments

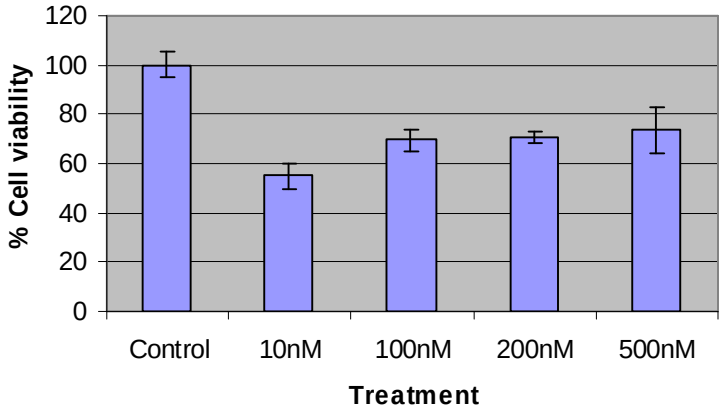

The % Cell Viability for 10 nM treatment was found to be 55% with 5% of ±SE.

PART TWO

CHAPTER 3

Synthesis of 2-(2-(phenylimino)vinyl)benzonitrile

I. INTRODUCTION

I. 1. Enyne- Allenes and Enyne- heteroallenes

In Chapter-1 we discussed that potent naturally occurring anticancer antibiotics, enediynes undergo bergman cyclization upon heating to generate a biradical which cleaves DNA by abstracting the hydrogen atom from it's sugar-phosphate back bone.[1, 2] These compounds though very potent antitumor agents are non-specific in their action and are known to exhibit high cytotoxicity towards normal cells.[3-6] Due to this limitation, the DNA cleaving properties of these naturally occurring compounds have been utilized for designing new anticancer drugs with fewer or no side effects.

One class of drugs that is inspired by enediynes is enyne-allene. Enyne-allenes undergo thermally and photochemically triggered C^2- C^7 or Myers–Saito and the C^2-C^6 or Schmittel cyclizations to generate α, 3- dehydrotoluene and fulvene-like biradicals respectively.[7-11] The Schmittel pathway is favored when a bulky group (R= Ph or t- Bu) is present at the alkyne end of the enyne-allenes.[12] The generated biradicals mimic enediynes in their mode of action by abstracting hydrogen from the sugar phosphate back bone of the DNA and causing it's cleavage[13, 14] (**Scheme 1**). These biradicals are also known to abstract hydrogen atoms from hydrogen donors like 1, 4- cyclohexadiene (CHD).[8, 12]

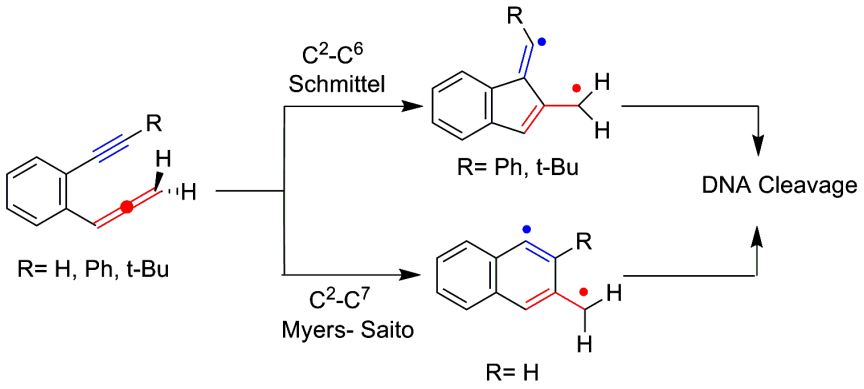

Scheme 1. Myers- Saito and Schmittel cyclization in enyne- allenes.

Similarly, hetero-allene based compounds have been synthesized. The replacements of one or more carbons in the allene moiety of the enyne-allenes gave rise to enyne ketenimines and enyne carbodiimides respectively (**Scheme 2**)

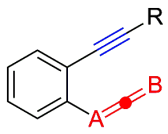

Enyne Ketenimine: A=N, B= CR_1R_2
Enyne Carbodiimide: A=N, B=NR_3

Scheme 2. Enyne Ketenimine and Enyne Carbodiimide

Enyne- ketenimines mimic enyne allenes by undergoing Myers- Saito and Schmittel cyclization to generate α, 3- dehydrotoluene **2** and azafulvene- like biradicals **3** respectively. The Schmittel pathway is favored when a bulky group (R = T-Bu, $SiMe_3$, Ph) is present at the alkyne terminus.[15- 17]

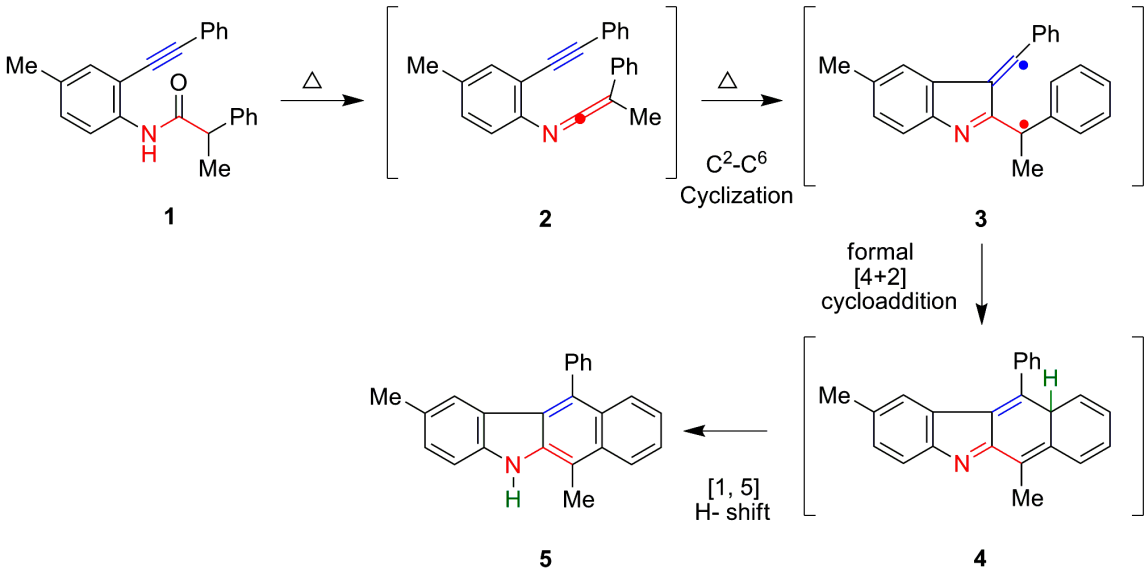

Scheme 3. Schmittel (C^2- C^6) cyclization of ketenimine 2 followed by formal [4+2] cycloaddition.[15]

Thermolysis studies have shown that in the presence of an aryl group at the ketenimine terminus, azafulvene- like biradical **2** undergoes formal [4+2] cycloaddition resulting in formation of a benzocarbazole product **5** (**Scheme 3**). However, Myers- Saito pathway is still favored if alkyne terminus is substituted with a small group (R= H) (**Scheme 4**).[15, 16]This is proved by detection of a quinoline product **9** formed as result of hydrogen abstraction from a hydrogen donor 1, 4- cyclohexadiene (1, 4- CHD).

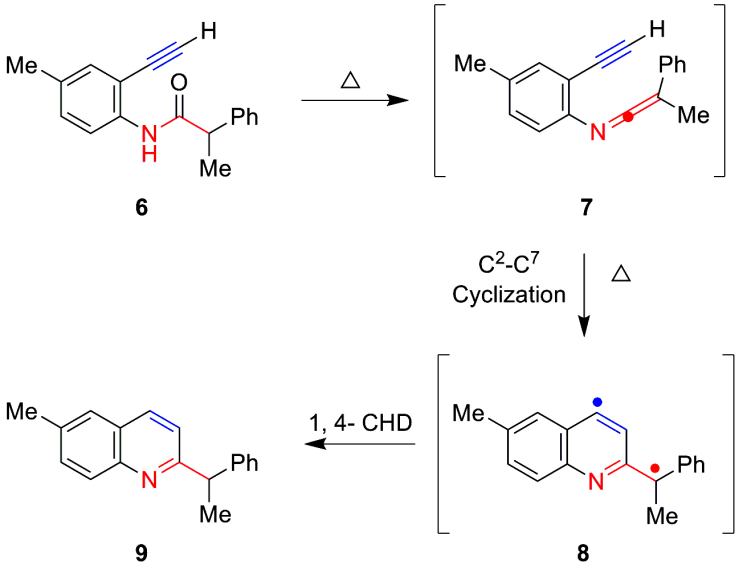

Scheme 4. Myer- Saito cyclization favored by presence of a small group at the alkyne terminus. [15]

Photochemical cyclization of enyne ketenimines with allenic aryl substituents has not been explored much. Only two compounds with bulky groups at the alkyne terminus are known to undergo formal [4+2] cycloadditions via azabenfulvene biradicals (**Scheme 5**).[17]

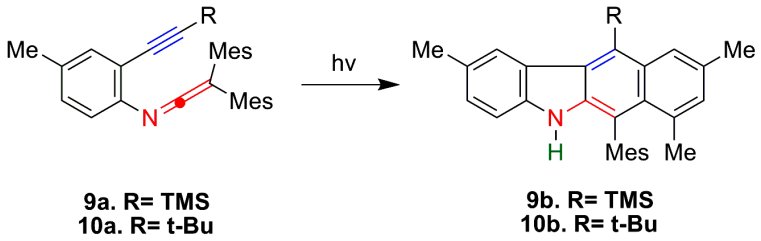

9a. R= TMS
10a. R= t-Bu

9b. R= TMS
10b. R= t-Bu

Scheme 5. Photochemical cyclization of enyne- ketenimines (9a, 10a) with bulky groups at the alkyne terminus.[17]

Upon photolysis, **9a** and **10a** are known to form the corresponding benzcarbazole products **9b** and **10b.** Some polymeric products were also detected along with benzocarbazoles. Theoretical studies have revealed that the Myers- Saito cyclization may be responsible for the formation of the polymeric products.[17, 18]

Similarly, carbodimides undergo thermally triggered Myers- Saito and Schmittel cyclization to generate α, 3- dehydropyridine and diazafulvene- like biradicals respectively. Again , the Schmittel pathway is favored when a bulky group (R = T-Bu, $SiMe_3$, Ph) is present at the alkyne terminus. [19, 20] Just as in case of ketenimines, diazafulvene- like biradical **12** undergoes formal [4+2] cycloaddition resulting in formation of an indoloquinoline product **14** in the presence of an aryl group at the carbodiimide terminus [19, 20] (**Scheme 6**).

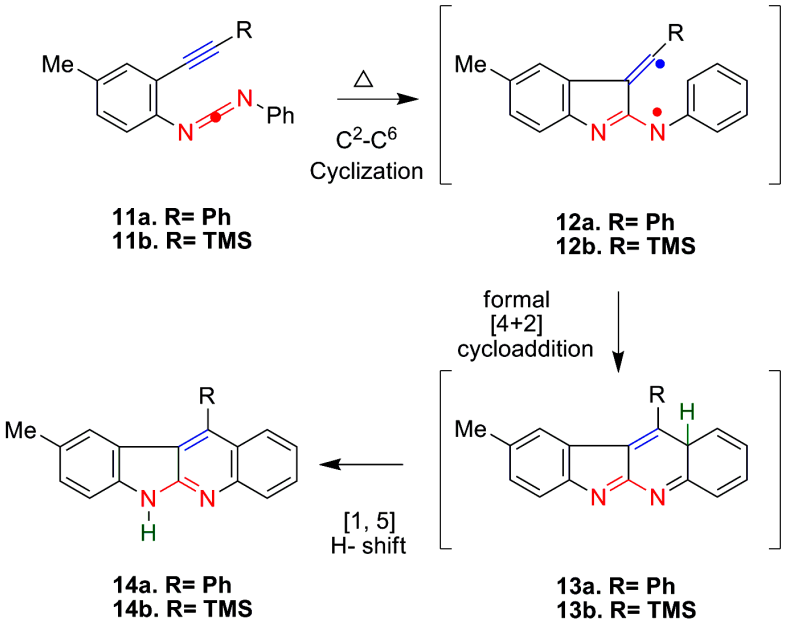

Scheme 6. Schmittel (C^2- C^6) cyclization of carbodiimide 11a-b followed by formal [4+2] cycloaddition.[20]

Under photochemical trigger, carbodiimides are known to undergo Schmittel cyclization independent of size of the substituents at the alkyne terminus[17] (**Scheme 7**). The Myers- Saito cyclization for photochemical reactions of carbodiimdes is unknown.

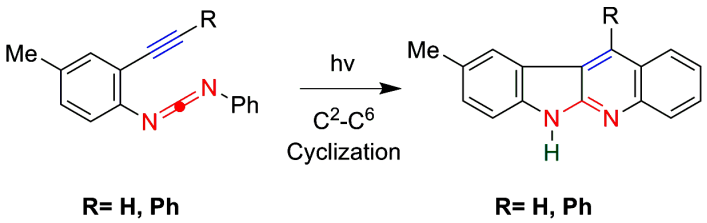

Scheme 7. Photochemical cyclization of enyne-carbodiimides.[17]

Apart form Enyne- ketenimines and enyne – carbodiimides, other hetero analogs of enyne- allenes have been synthesized and their thermal and or photochemical cyclizations have been studied. A C-alkynyl- N-allenyl imine **15** was synthesized and it's thermal and photochemical cyclization was studied. **15** undergoes facile Myers- Saito cyclization thermally and photochemically to generate an α, 5-didehydro-3-picoline biradical. The formation of this biradical was confirmed by formation of a product **17** via hydrogen abstraction from 1, 4- CHD (1, 4- cyclohexadiene) (**Scheme 8**).[21] It is believed that Schmittel cyclization results in formation of complex unidentified products.

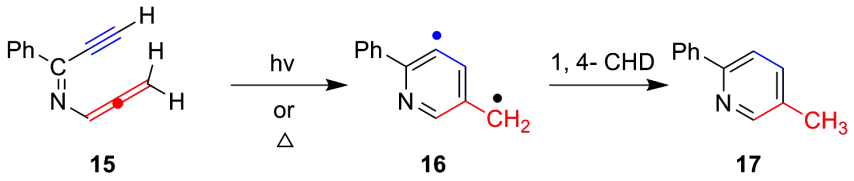

Scheme 8. Myers- Saito cyclization of C- alkynyl- N- allenyl imine 15 followed by H-abstraction from 1, 4- CHD. [21]

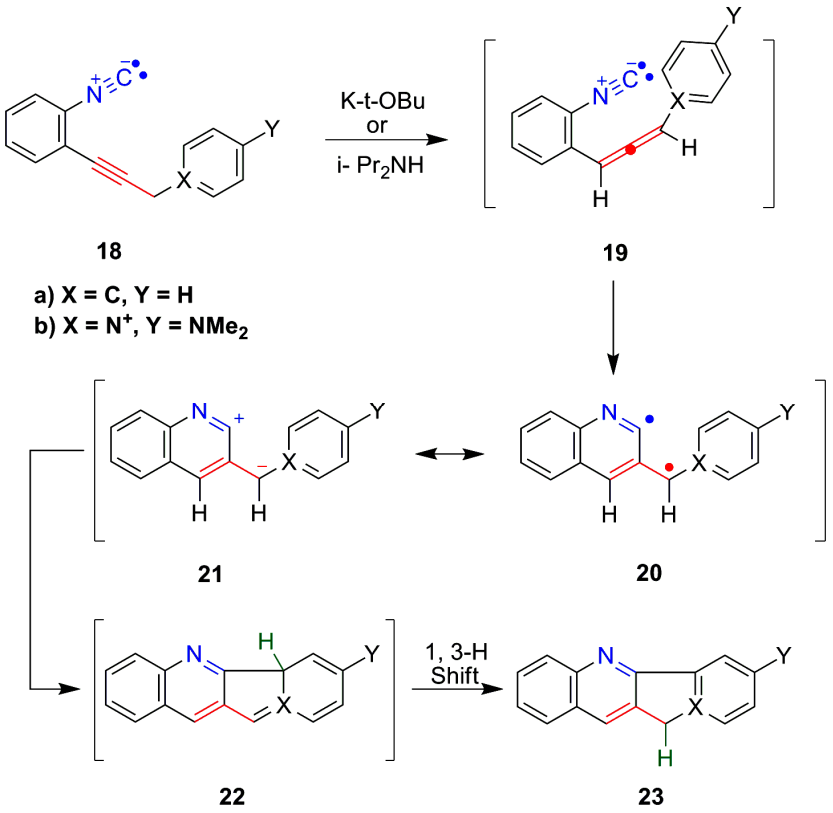

Scheme 9. Myers- Saito cyclization of benzannulated enyne isonitrile 17a-b followed by [4+1] formal cycloaddition.[22]

Thermal cyclizations of benzannulated enyne- isonitrile analogs **19** have also been studied. These analogs undergo Myers- Saito cyclization to generate a biradical **20** or a zwitterion **21**. A subsequent intramolecular radical- radical coupling of **20** or an intramolecular electrophilic substitution of **21** followed by 1, 3- H shift affords a 11*H*-indeno [1, 2b] quinoline product **23** (**Scheme 9**).[22] Both **20a** or **21a** maybe involved in formal [4+1] cycloaddition reaction of **17a** whereas only biradical **20b** is involved in formal [4+1] cycloaddition of **17b.**

In 1996 Wang tried the thermal cyclization of another type of aza analogs of enyne- allenes; these analogs had a nitrile group serving as an alkyne functionality.[16, 23] Compound **24a** and **24a** were expected to undergo the Myer-Saito cyclization to produce the corresponding substituted pyridine products **25b** and **25b** in the presence of hydrogen donor 1, 4- cyclohexadiene. However, the experiments were unsuccessful and resulted in the formation of unidentified mixture of products (**Scheme 10**). [16, 23]

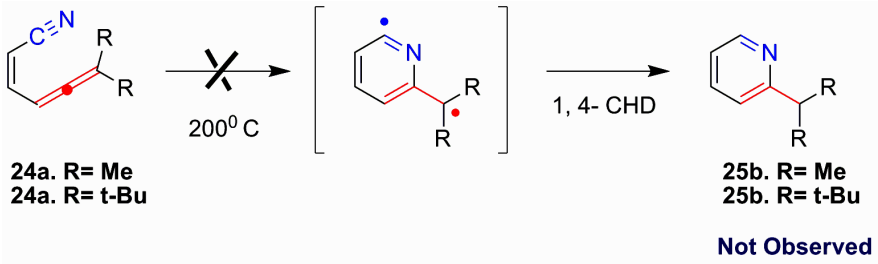

Scheme 10. Photochemical cyclization of nitrile substituted allenes 24a-b.[2, 5]

I. 2. Our Goal

The goal of our laboratory is to synthesize a series of mono, di and tri-azaenyne-allenes to study their Myers- Saito and Schmittel cyclizations. If our studies are successful, these cyclizations could be employed for synthesis of heteroaromatic rings found in many compounds of biological importance. As a step towards our studies, our goal was to synthesize a nitrile substituted keteneimine, 2-(2-(phenylimino)vinyl)benzonitrile **25** and to study its thermal and photochemical cyclizations. As observed in case of enyne- ketenimines this ketenimine is expected to undergo formal [4+2] cycloaddition via Schmittel cyclization pathway. This experiment if successful would then yield the

anticipated product 11*H*-indeno [1, 2b] quinoxaline **28** via a novel synthetic route (**Scheme 11**).

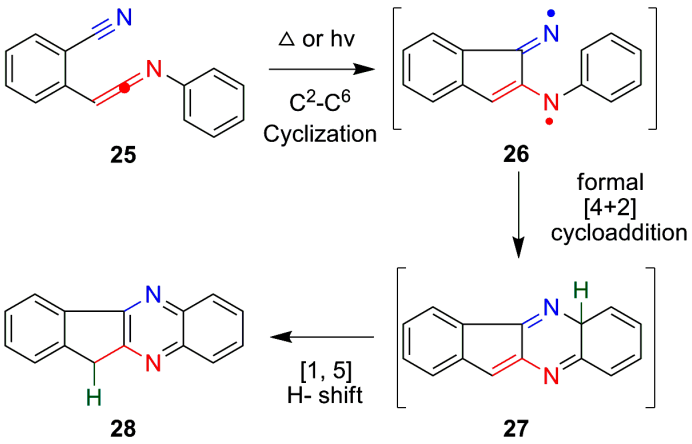

Scheme 11. Cyclization of 2-(2-(phenylimino)vinyl)benzonitrile (25) to the anticipated product 11*H*-indeno [1, 2b] quinoxaline (28).

Quinoxaline based compounds are known to have various applications. Compound **29** [24] in **Scheme 12** is known to have antitumor properties and compound **30** [25] is patented for its use for making organic light- emitting devices. Recently, synthesis of a pyrrole substituted quinoxaline compound was reported. The pyrrole substituted compounds are known to be important components of anti-inflammatory and antitumor agents, immunosuppressants.[26-28] If our experiments are successful, this synthesis pathway could be employed for synthesis of quinoxaline based compounds of diverse applications.

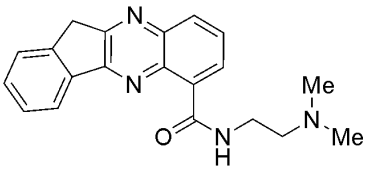

29

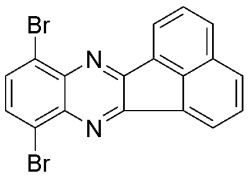

30

Scheme 12. Quinoxaline based compounds.[24, 25]

II RESULTS AND DISCUSSION

II. 1. Synthetic method

The synthetic plan was to first synthesize 2-(2-cyanophenyl) acetic acid **32** from 2- (bromomethyl) benzonitrile **31** [29] and then to convert it into a ketene **33.**[30] The desired product, 2-(2-(phenylimino)vinyl)benzonitrile **25** could then be synthesized by stirring **33** with a phosphorane **34** in CH_2Cl_2 (**Scheme 13**).[31]

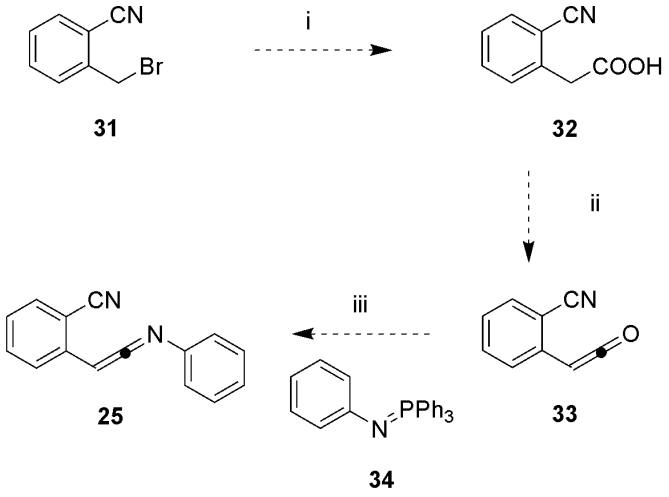

Scheme 13. Plan for synthesis of 2-(2-(phenylimino)vinyl)benzonitrile, 25. (i) $[(Ph_3P)_2PdCl_2]$, $CHCl_3$/ 50% KOH, r.t., 24 h; (ii) $SOCl_2$, pyridine, toluene, 115^{0}C, 30 min; (iii) dry CH_2Cl_2, r.t., 30 min.

2-(2-cyanophenyl) acetic acid **32** was synthesized by stirring under N_2 a mixture of 2- (bromomethyl) benzonitrile **31** and bis(triphenylphosphine)palladium (II) chloride in the presence of $CHCl_3$/ 50% KOH mixture. The reaction mixture was stirred at room temperature for 24 h and yielded 62% of **32**. [29]

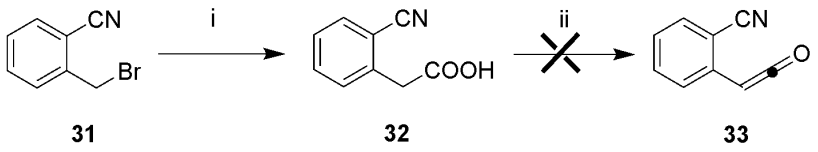

31 **32** **33**

Scheme 14. Synthesis of 21. (i) $[(Ph_3P)_2PdCl_2]$, $CHCl_3$/ 50% KOH, r.t., 24 h; (ii) $SOCl_2$, pyridine, toluene, 115^{0}C, 30 min.

2-(2-cyanophenyl) acetic acid **32** was refluxed at 115^{0}C in the presence of dry toluene/ pyridine and thionyl chloride to obtain ketene **33**. Starting material **32** disappeared in 30 min; however, the desired product **33** was not obtained (**Scheme 14**).

After this unsuccessful attempt to synthesize **33**, we decided to synthesize 2-(2-(phenylimino)vinyl)benzonitrile **25** via another route (**Scheme 15**). The plan was to first convert 2-(2-cyanophenyl) acetic acid **32** into an acid chloride **35**[32] and then synthesize the keteneimine **25** from it.

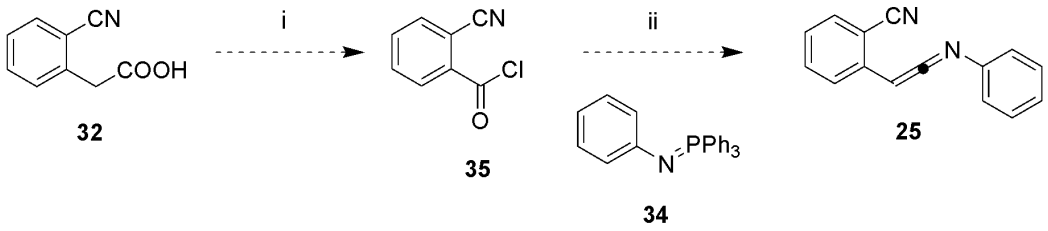

32 **35** **34** **25**

Scheme 15. Synthesis of 2-(2-(phenylimino)vinyl)benzonitrile 25. (i) neat $SOCl_2$, 80^{0}C, 30 min; (ii) n-BuLi, THF, -70^{0}C for 90 min → r.t. for 24 h

32 was refluxed under N_2 in neat thionyl chloride for 30 min at 80^0C. The reaction mixture was analyzed by ^{1}H-NMR before work up and it indicated formation of the desired acid chloride **35.** The unreacted thionyl chloride was removed under reduced pressure on rotary evaporator. However, during removal of thionyl chloride our product reacted with moisture from air and decomposed back to the starting acid **32**. The reaction was repeated and this time unreacted thionyl chloride was removed over vacuum line. The product stayed unreacted initially but started to decompose back to the starting material **32** over time. Repeated attempts to synthesize 2-(2-(phenylimino)vinyl)benzonitrile **25** were unsuccessful. The desired ketene **33** and acid chloride **35** were very unstable due to the presence of ortho nitrile substituent on the phenyl ring. **35** if formed decomposed back to yield the starting acid **32** by reacting with little moisture during removal of unreacted thionyl chloride.

III. CONCLUSIONS

The desired keteneimine, 2-(2-(phenylimino)vinyl)benzonitrile **25** could not be synthesized due to instability of the intermediate compound acid chloride **35** or ketene **33**. As result, the desired studies towards thermal and photochemical cyclization of **25** and thus development of a novel route for synthesis of 11*H*-indeno [1, 2b] quinoxaline **28** could not be carried out.

Studies towards synthesis of other azaenyne-allene analogs is going on in our laboratory. If synthesis is successful then thermal and photochemical cyclizations of these compounds could lead to development of new routes for

synthesis of heteroaromatic rings found in many compounds of biological importance.

References:

1. Dai, W. *Current Medicinal Chemistry* **2003**, *10*, 2265.

2. Bergman, R., G. *Accounts of Chemical Research* **1973**, *6*, 25.

3. Zhao, K.; Reiner, J.; Xie, W. *Frontiers of Biotechnology & Pharmaceuticals* **2001***, 2*, 329-349

4. Bross, P. F.; Beitz, J.; Chen, G.; Chen, X. H.; Duffy, E.; Kieffer, L.; Roy, S.; Sridhara, R.; Rahman, A.; Williams, G.; Pazdur, R. *Clinical Cancer Research* **2001***, 7*, 1490-1496.

5. Abe, S.; Otsuki, M. *Current Medicinal Chemistry: Anti-Cancer Agents* **2002**, *2*, 715.

6. Naito, K.; Takeshita, A.; Shigeno, K.; Nakamura, S.; Fujisawa, S.; Shinjo, K.; Yoshida, H.; Ohnishi, K.; Mori, M.; Terakawa, S.; Ohno, R. *Leukemia* **2000***,14*, 1436.

7. Myers, A., G.; Kuo, E., Y.; Finney, N., S. *Journal of the American Chemical Society* **1989**, *111*, 8057.

8. Nagata, R.; Yamanaka, H.; Okazaki, E.; Saito, I. *Tetrahedron Letters* **1989**, *30*, 4995.

9. Schmittel, M.; Strittmatter, M.; Kiau, S. *Tetrahedron Letters* **1995**, *36*, 4975.

10. Schmittel, M.; Kiau, S. *Liebigs Annalen* **1997**, 733.

11. Schmittel, M.; Mahajan, A., A.; Bucher, G. *Journal of the American Chemical Society* **2005**, *127*, 5324.

12. Engels, B.; Lennartz, C.; Hanrath, M.; Schmittel, M.; Strittmatter, M. *Angewandte Chemie, International Addition* **1998**, *37*, 1960.

13. Maier, M., E. *Synlett* **1995**, 13.

14. Nagata, R.; Yamanaka, H.; Murahashi, E.; Saito, I. *Tetrahedron Letters* **1990**, *31*, 2907.

15. Schmittel, M.; Steffen, J., P.; Angel, M., A., W.; Engels, B.; Lennartz, C.; Hanrath, M. *Angewandte Chemie, International Edition* **1998**, *37*, 1562.

16. Shi, C.; Wang, K., K. *Journal of Organic Chemistry* **1998**, *63*, 3517.

17. Schmittel, M.; Rodriguez, D.; Steffen, J., P*. Angewandte Chemie, International Edition* **2000**, *39*, 2152.

18. Spoler, C.; Engels, B. *Chemistry: A European Journal* **2003**, *9*, 4670.

19. Shi, C.; Zhang, Q.; Wang, K., K. *Journal of Organic Chemistry* **1999**, *64*, 925

20. Schmittel, M.; Steffen, J., P.; Engels, B.; Lennartz, C.; Hanrath, M. *Angewandte Chemie, International Edition* **1998**, *37*, 2371.

21. OL. Feng, L.; Kumar, D., M.; Kerwin, S., M. *Organic Letters* **2004**, *6*, 2059.

22. O.l. Lu, Xiaoling, Peterson, J., L.; Wang, K., K. *Organic Letters* **2003**, *18*, 3277.

23. Wang, K., K.; Wang, Z. *Journal of Organic Chemistry* **1996**, *61*, 1516.

24. Deady, L., W.; Kaye, A., J.; Finlay, G., J.; Baguley, B., C.; Denny, W. A. *Journal of Medicinal Chemistry* **1997**, *40*, 2040.

25. Inoue, T.; Watanabe, M.; Kondo, H. *WO 2007/060795*.

26. Yadav, J., S.; Reddy, B., V., S.; Jain, R.; Reddy, S. *Tetrahedron Letters* **2007**, *48*, 3295.

27. Schann, S.; Mayer, S.; Gardan, S. *WO 2007/*071379.

28. Grushin, V., V.; Alper, H. *Organomettalics* **1993**, *12*, 3846.

29. Furstner, A.; Szillat, H.; Gabor, B.; Mynott, R. *Journal of the American Chemical Society* **1998**, *120*, 8305.

.30. Allen, B., M.; Hegarty, A., F.; Neill, P., O.; Nguyen, M., T. *Journal of the Chemical Society, Perkin Transactions 2* **1992**, 927.

31. Alajarin, M.; Vidal, A.; Ortin, M., -M. *Organic and Biomolecular Chemistry* **2003**, *1*, 4282.

32. Cristau, H., -J.; Jouanin, I.; Taillefer, M. *Journal of Organometallic Chemistry* **1999**, *584,* 68.

CHAPTER 3

Synthesis of 2-(2-(phenylimino)vinyl)benzonitrile

EXPERIMENTAL SECTION

I. Synthesis

2-(2-Cyanophenyl) acetic acid (20)[29]: 50% KOH (13.08 ml) was added to $CHCl_3$ (2.5 ml) and the resulting mixture was degassed. 2-(2-cyanophenyl) acetic acid **20** (2 g, 10.20 mmol) and bis(triphenylphosphine)palladium (II) chloride (0 .074 g, 0.105 mmol) were added to the degassed reaction mixture. The reaction mixture was stirred under N_2 at room temperature for 24 h. water (10 ml) and ethylacetate (7 ml) was added to the reaction mixture. The aqueous layer was separated, acidified with 20% HCl and extracted with ethylacetate thrice. The collected solution was dried over Na2SO4, concentrated under reduced pressure. Purification by column chromatography (hexane:ethylacetate, 60:40) gave **13** (1.015 g, 62% yield) as a light brown solid: R_f 0.28 (40:60 hexane:ethylacetate); ^{1}H-NMR (200 MHz, CD_3COCD_3): δ 3.95 (s, 2H), δ 7.47-7.82 (m, 4H); ^{13}C NMR (200MHz, CD_3COCD_3): δ 39.73, 114.46, 118.28, 128.73, 132.05, 133.54, 133.85, 139. 60, 171.25.

II. Unsucessful Synthesis

2-Cyanophenyl-2-ketene (33)[30]: 2-(2-cyanophenyl) acetic acid **32** (0.050g, 0.3103 mmol) was added to a mixture of thionyl chloride (0.13 ml), toluene (2 ml) and pyridine (0.030 ml). The reaction mixture was refluxed under N_2 at 115^0C for

30 min. Activated charcoal was added to the reaction mixture and the reaction mixture was filtered. The collected solution was dried over Na2SO4, concentrated under reduced pressure to yield a sticky solid. Acetonitrile (2 ml) was added to the sticky solid and the resulting solution was left for recrystallization overnight. TLC analysis revealed presence of a mixture of products. The non-polar products were extracted with hexane, concentrated under reduced pressure and dried over vacuum. The non-polar component was analyzed by ^{1}H-NMR and the remaining polar solution was analyzed by IR spectroscopy. ^{1}H-NMR (200 MHz, $CDCl_3$): Nothing about the identity of compound could be deduced from the nmr; IR (NaBr) v: No band for ketene functionality observed.

2-Cyanophenyl-2-acetic acid chloride (35)[32]**:** 2-(2-cyanophenyl) acetic acid **32** (0.050g, 0.3103 mmol) was added to neat thionyl chloride (3 ml). the reaction mixture was refluxed under N_2 for 30 min at 80^0C. The reaction mixture was analyzed by ^{1}H-NMR before work up and it indicated formation of the desired acid chloride **35.** Excess of thionyl chloride was removed under reduced pressure. ^{1}H-NMR (200 MHz, CD_3COCD_3): Only the starting material **32** was found present, acid chloride **35** had hydrolyzed back to **32**.

APPENDIX I

^{1}H-NMR AND ^{13}C-NMR SPECTRA

(Chapter-1)

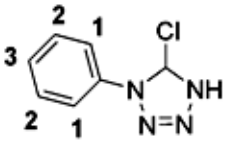
2
1
Cl
3
N
NH
2
1
N=N

22

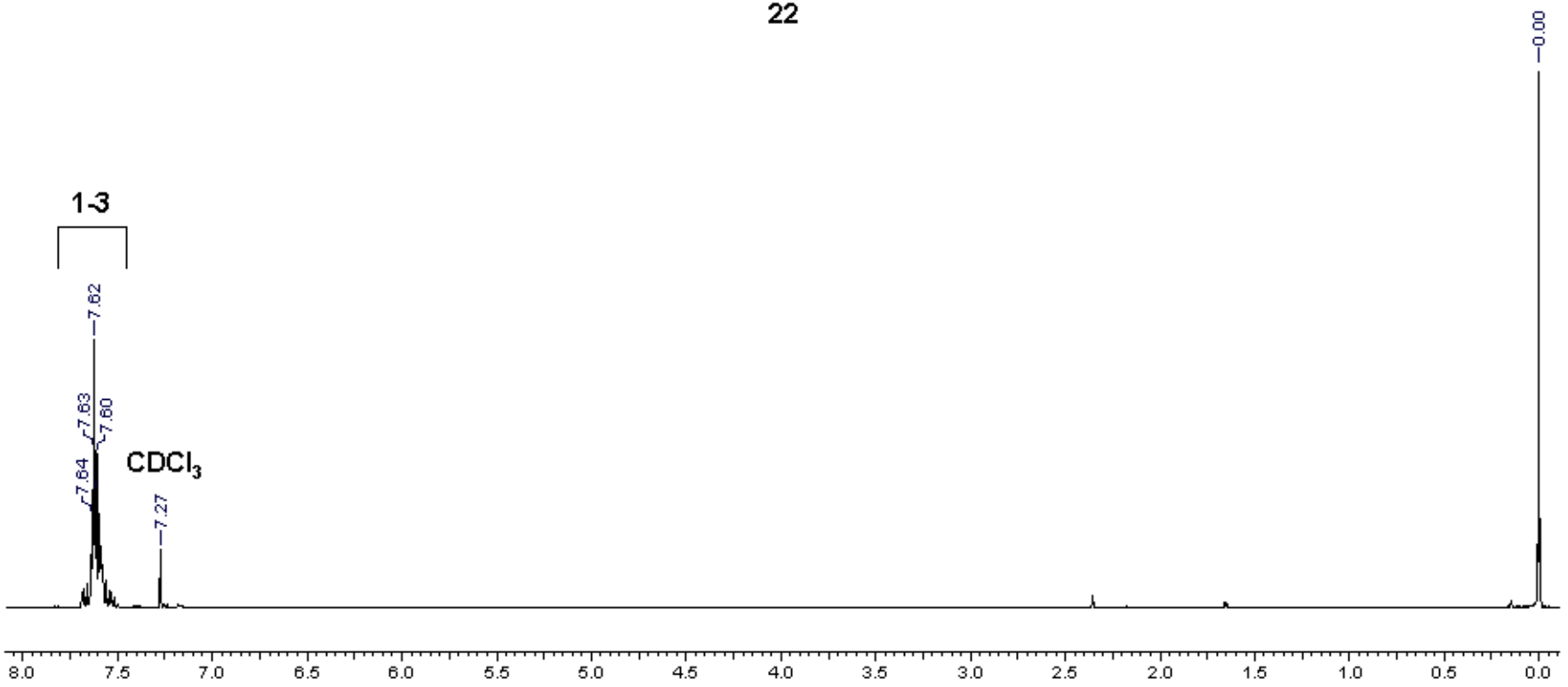
0.00
1-3
7.62
7.63
7.60
7.64
CDCl3
7.27
8.0
7.5
7.0
6.5
6.0
5.5
5.0
4.5
4.0
3.5
3.0
2.5
2.0
1.5
1.0
0.5
0.0

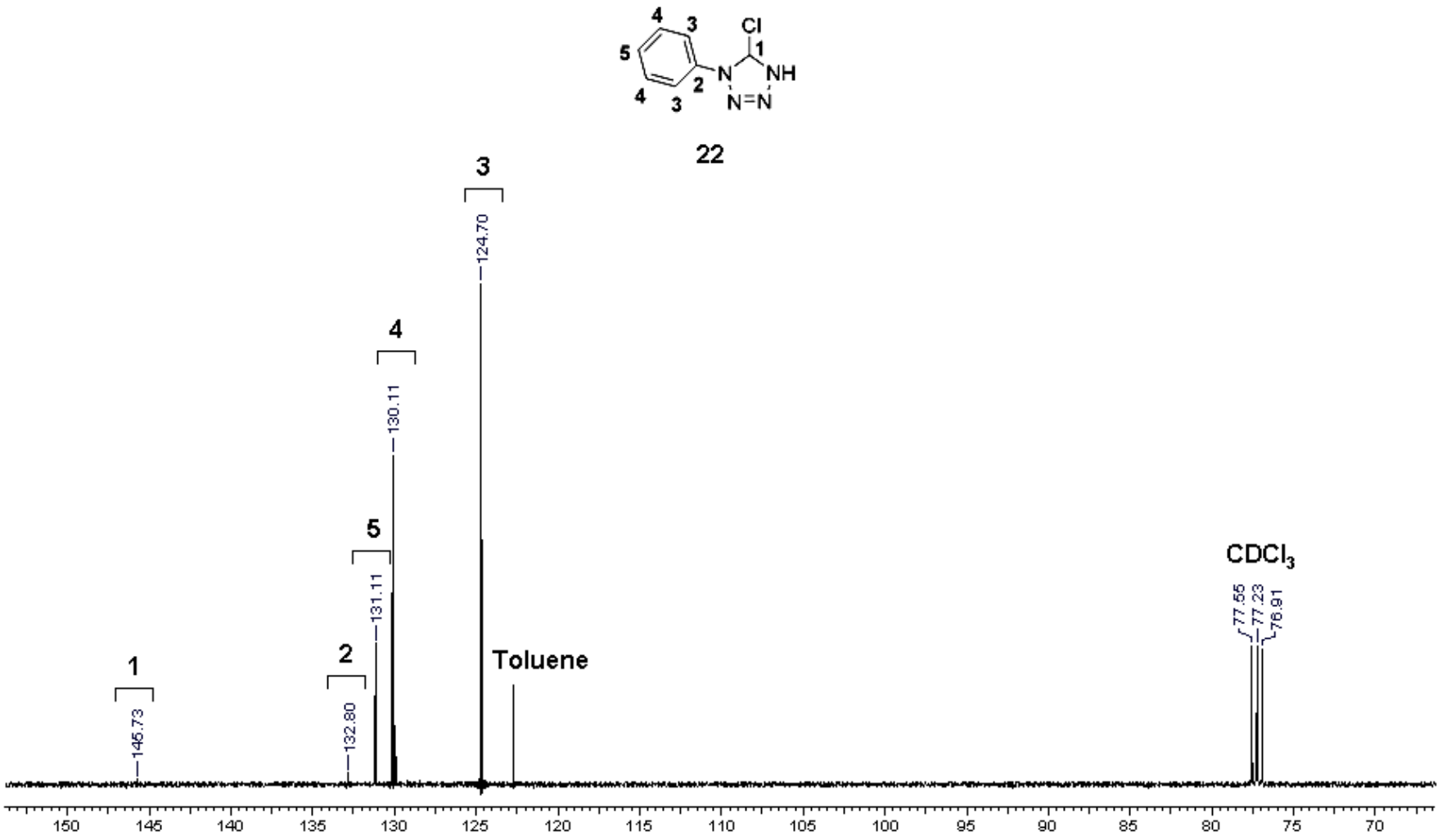
22
1
2
3
4
5
145.73
132.80
131.11
130.11
124.70
Toluene
CDCl3
77.55
77.23
76.91

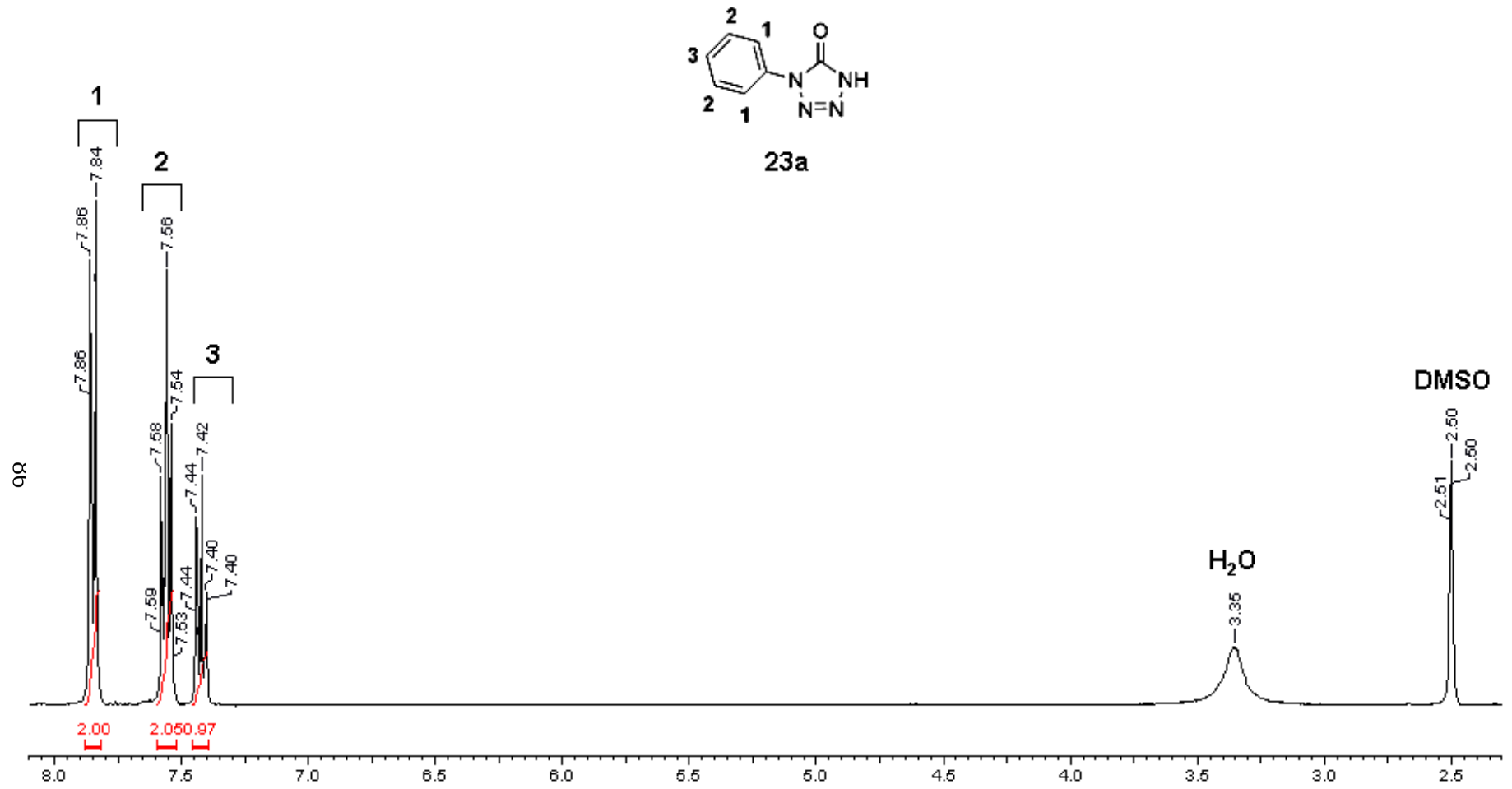
23a
1
2
3
7.84
7.86
7.86
7.56
7.58
7.54
7.42
7.44
7.40
7.40
7.59
7.44
7.53
H2O
3.35
DMSO
2.50
2.50
2.51
2.00
2.05
0.97
8.0
7.5
7.0
6.5
6.0
5.5
5.0
4.5
4.0
3.5
3.0
2.5

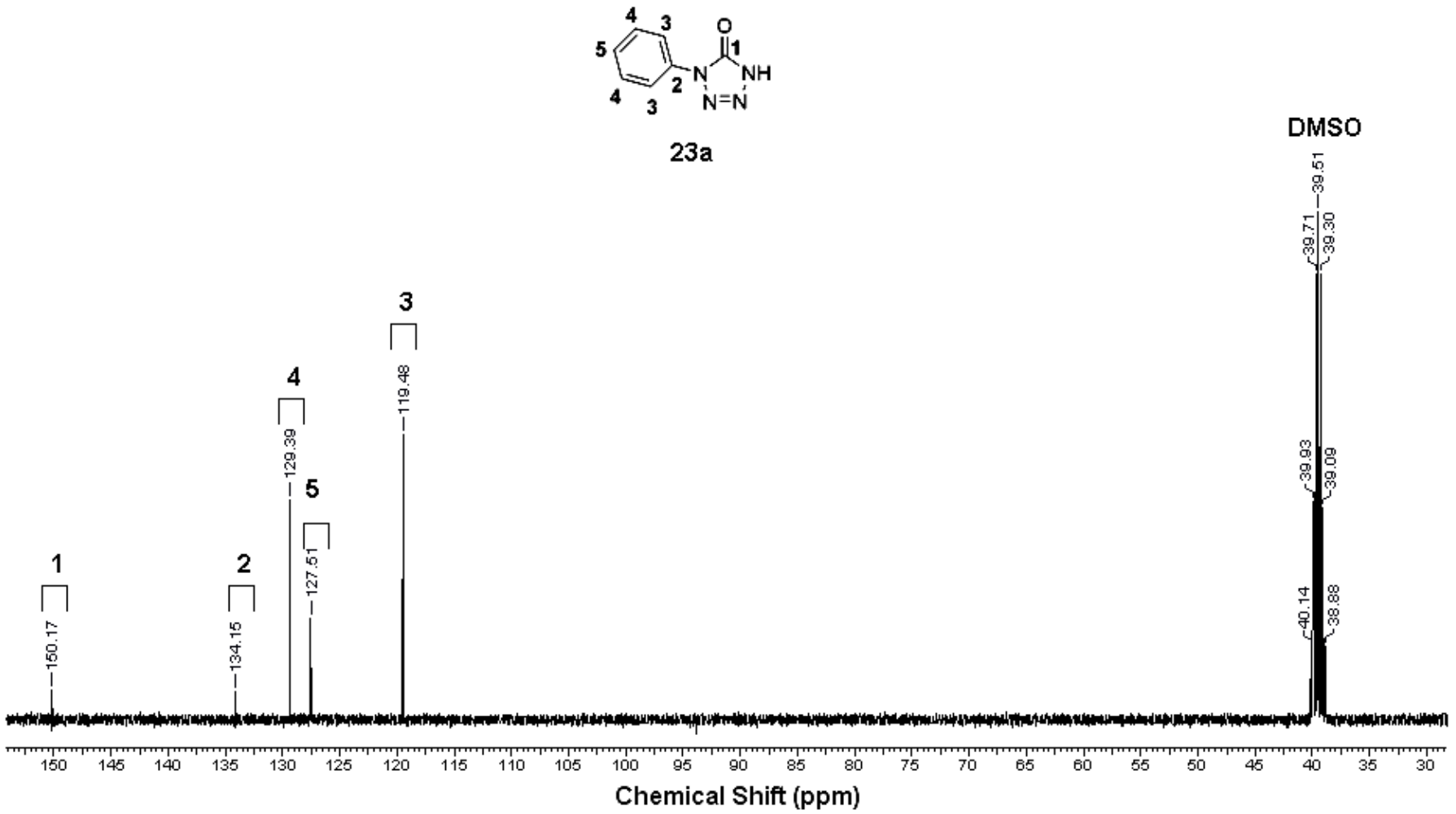
23a
DMSO
1
2
3
4
5
150.17
134.15
129.39
127.51
119.48
39.71
39.51
39.30
39.93
39.09
40.14
38.88
Chemical Shift (ppm)

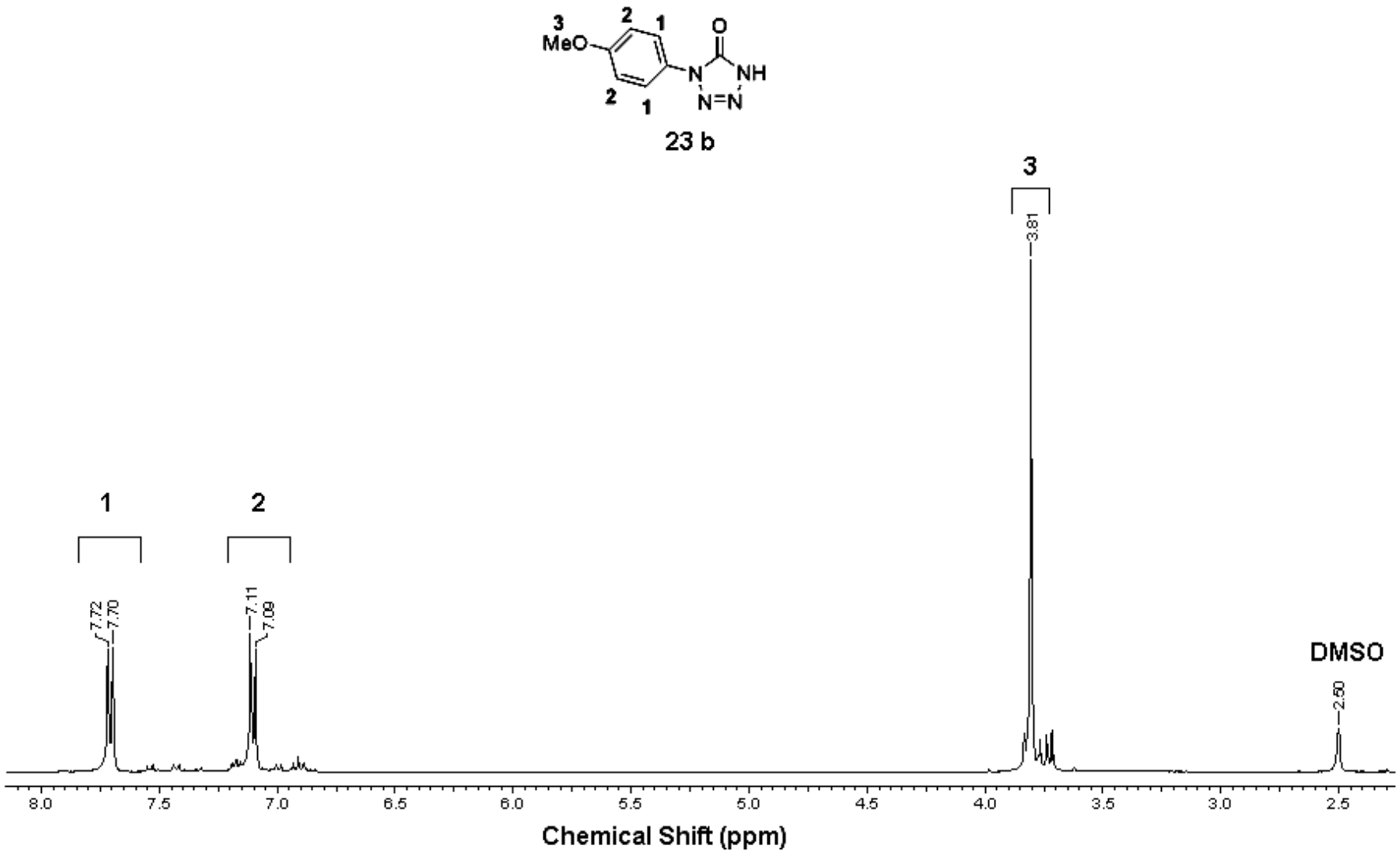
3
MeO
2
1
O
NH
N
N=N
2
1
23 b
3
3.81
1
2
7.72
7.70
7.11
7.09
DMSO
2.50
8.0
7.5
7.0
6.5
6.0
5.5
5.0
4.5
4.0
3.5
3.0
2.5
Chemical Shift (ppm)

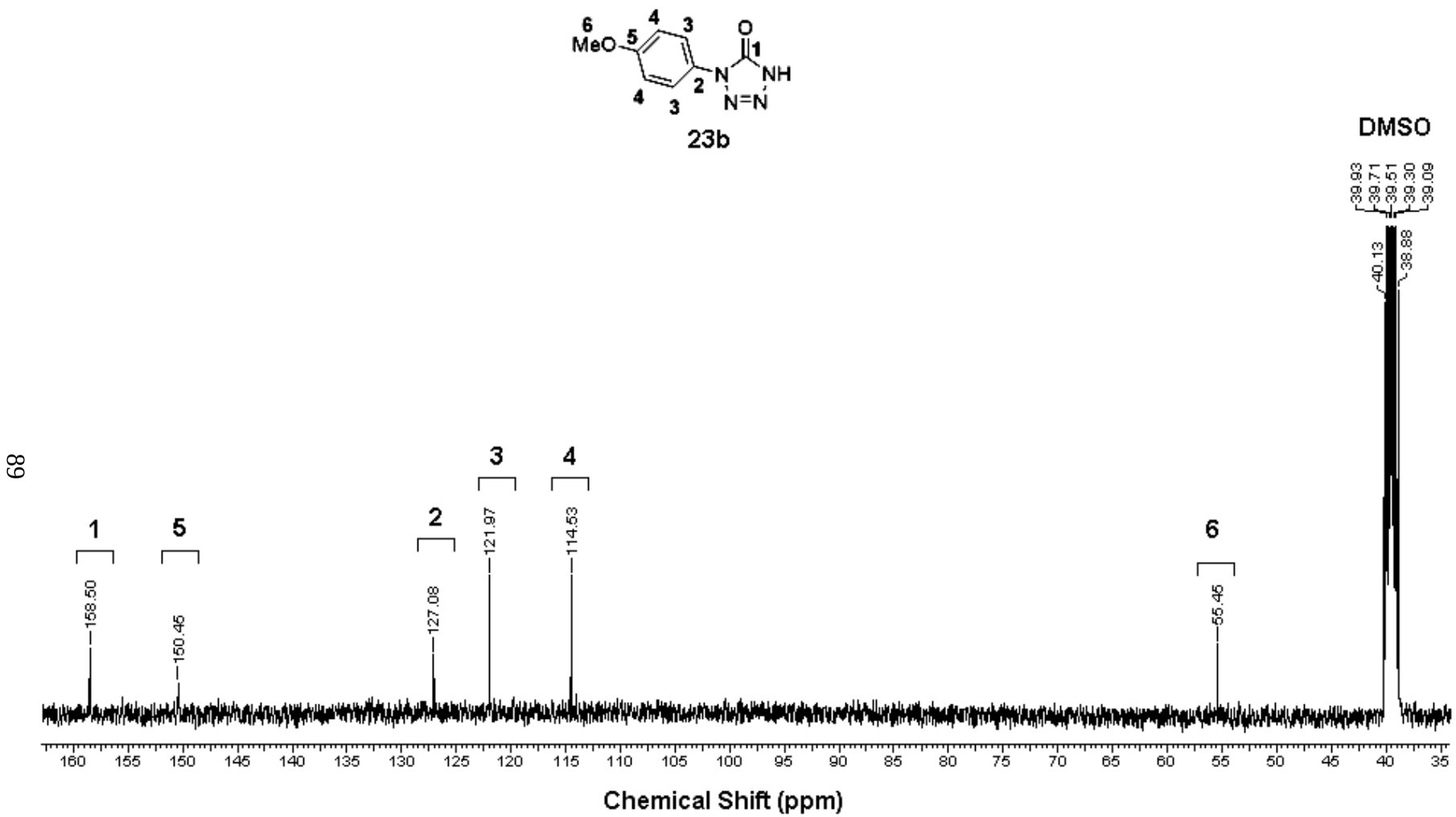
6
MeO
5
4
3
O
1
NH
N
2
N=N
4
3
23b
DMSO
39.93
39.71
39.51
39.30
39.09
40.13
38.88
1
5
2
3
4
6
158.50
150.45
127.08
121.97
114.53
55.45
160 155 150 145 140 135 130 125 120 115 110 105 100 95 90 85 80 75 70 65 60 55 50 45 40 35
Chemical Shift (ppm)

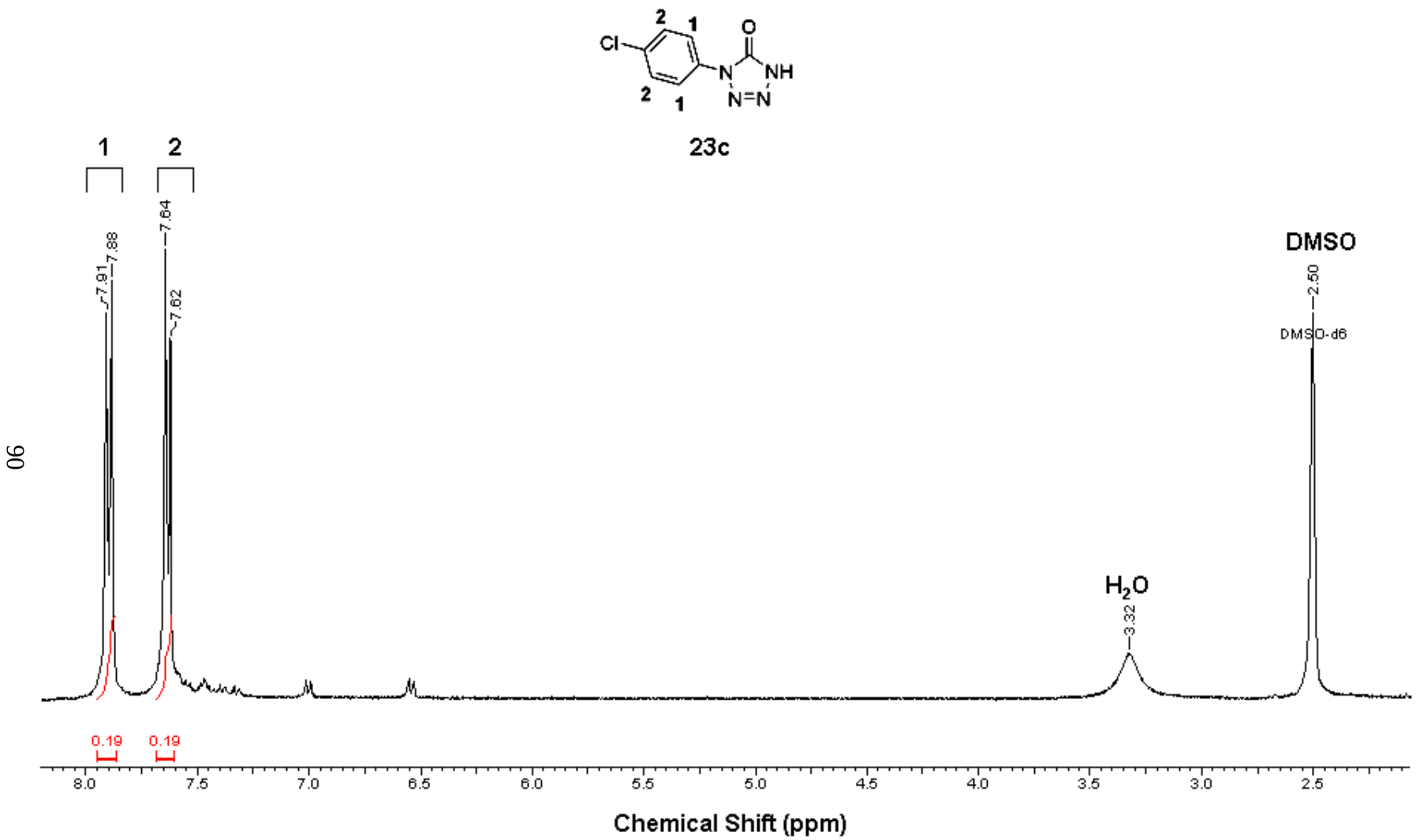
Cl
O
NH
N
N=N
1
2
23c
1
2
7.91
7.88
7.64
7.62
DMSO
2.50
DMSO-d6
H2O
3.32
0.19
0.19
8.0
7.5
7.0
6.5
6.0
5.5
5.0
4.5
4.0
3.5
3.0
2.5
Chemical Shift (ppm)

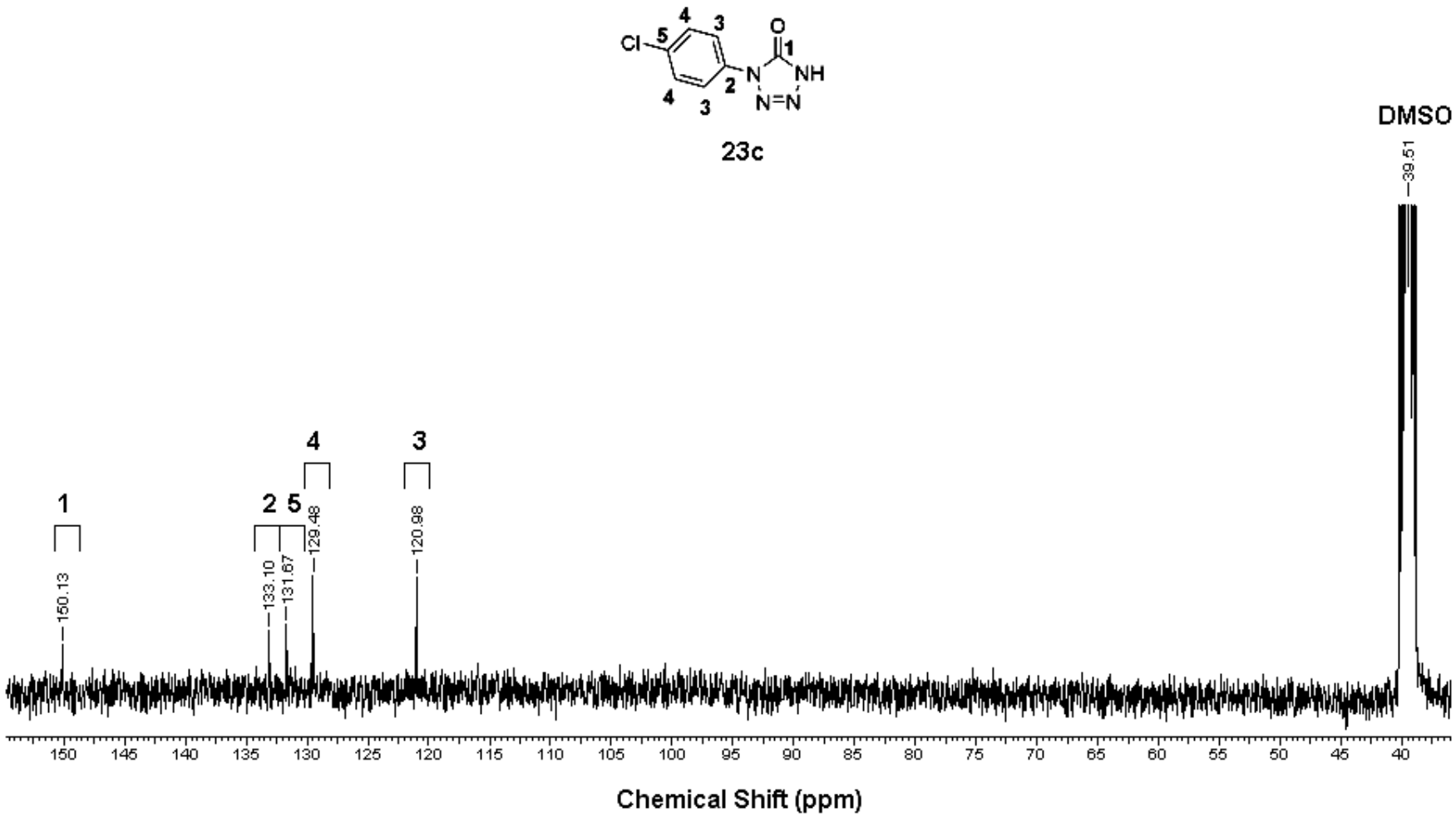
Cl
O
NH
N=N
23c
DMSO
39.51
1
2 5
4
3
150.13
133.10
131.67
129.48
120.98
Chemical Shift (ppm)

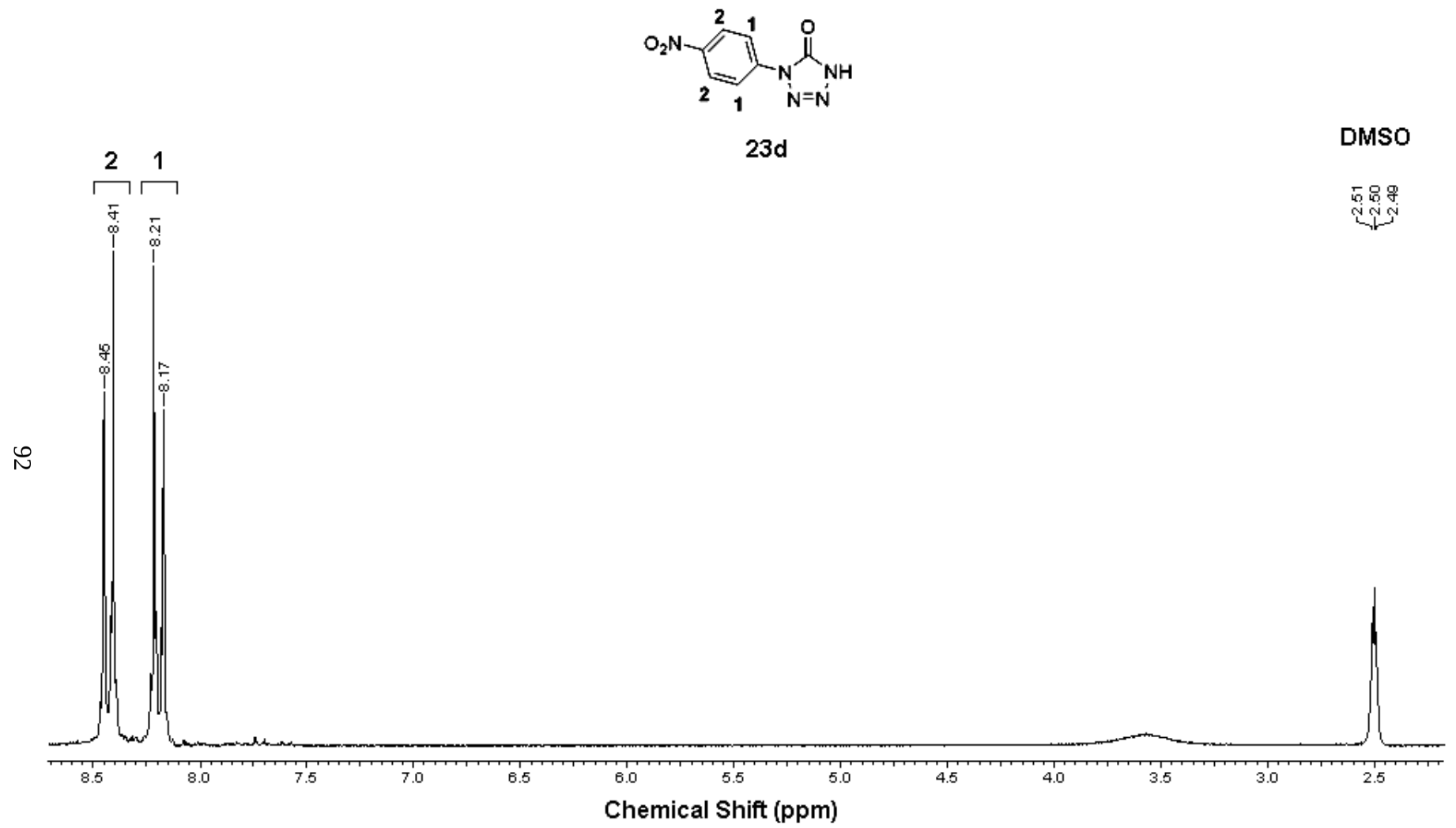
2
1
O
O_2N
NH
N
N=N
2
1
23d
DMSO
2.51
2.50
2.49
2
1
8.41
8.21
8.45
8.17
8.5
8.0
7.5
7.0
6.5
6.0
5.5
5.0
4.5
4.0
3.5
3.0
2.5
Chemical Shift (ppm)

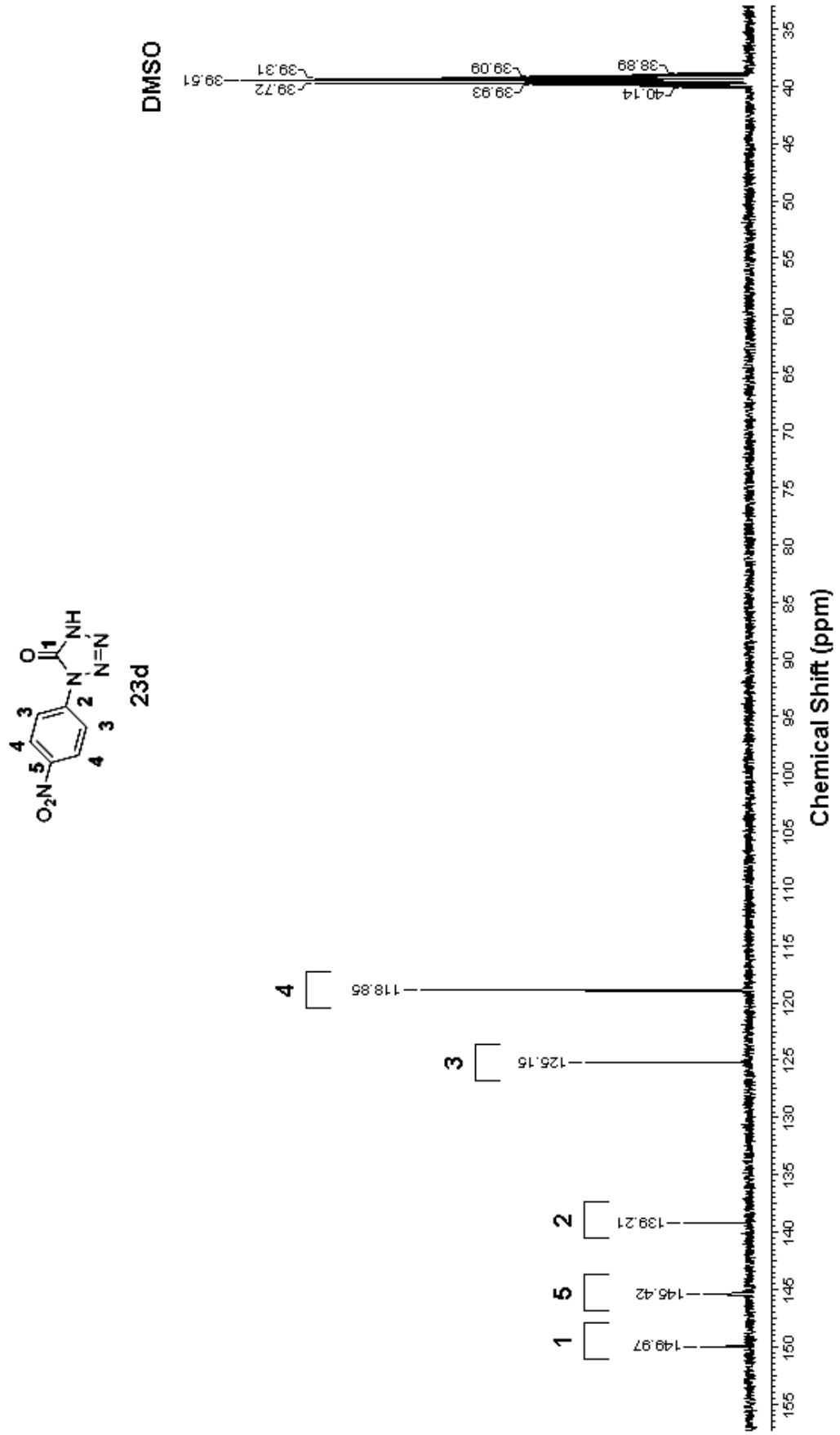
DMSO
39.51
39.72
39.93
40.14
38.89
39.09
39.31
23d
O
NH
N
N=N
O2N
1
2
3
4
5
4
118.86
3
125.15
2
139.21
5
145.42
1
149.97
Chemical Shift (ppm)

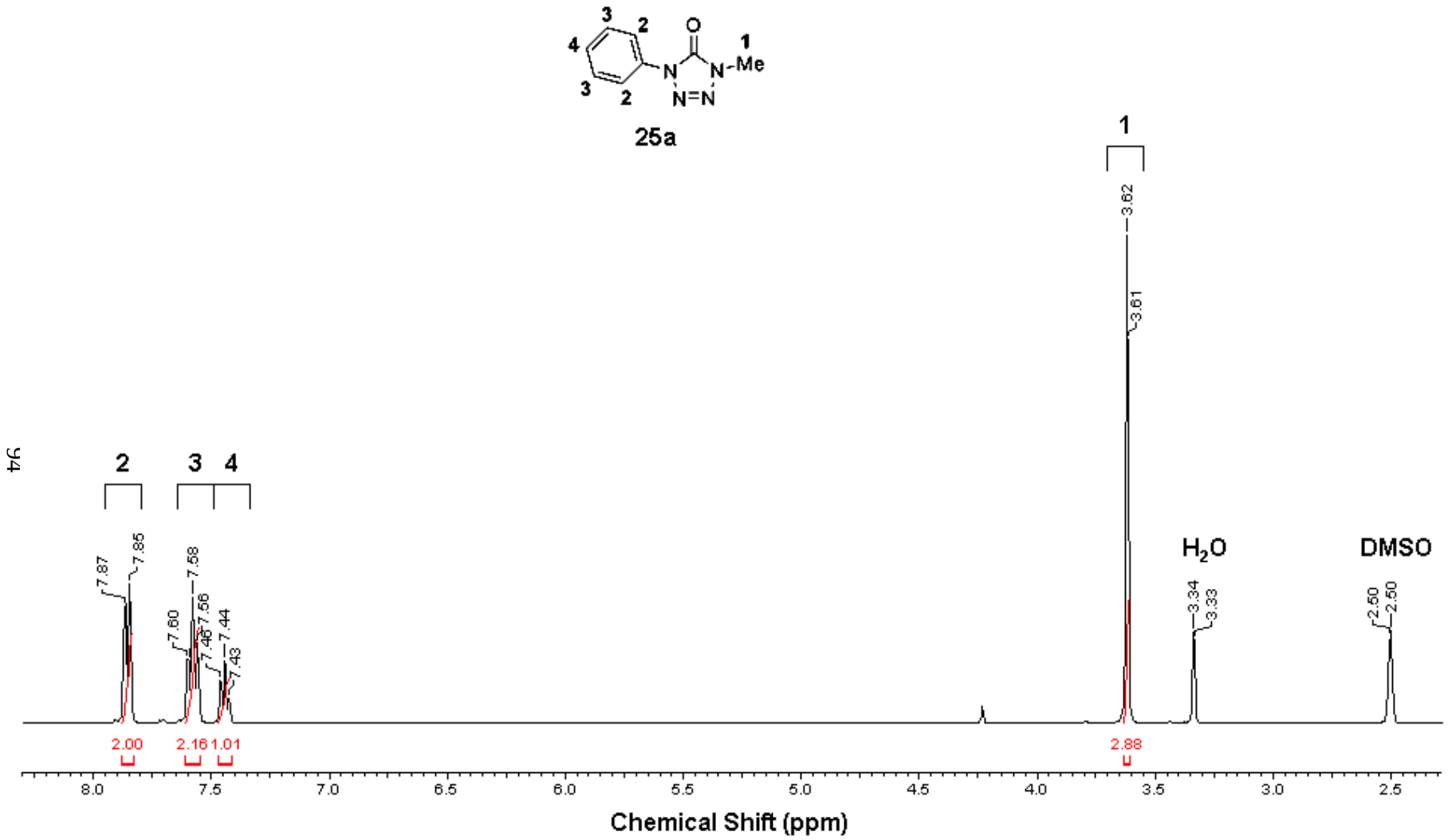
25a
1
2
3
4
Me
N
O
3.62
3.61
H2O
DMSO
3.34
3.33
2.50
2.50
7.87
7.85
7.60
7.58
7.56
7.46
7.44
7.43
2.00
2.16
1.01
2.88
8.0
7.5
7.0
6.5
6.0
5.5
5.0
4.5
4.0
3.5
3.0
2.5
Chemical Shift (ppm)

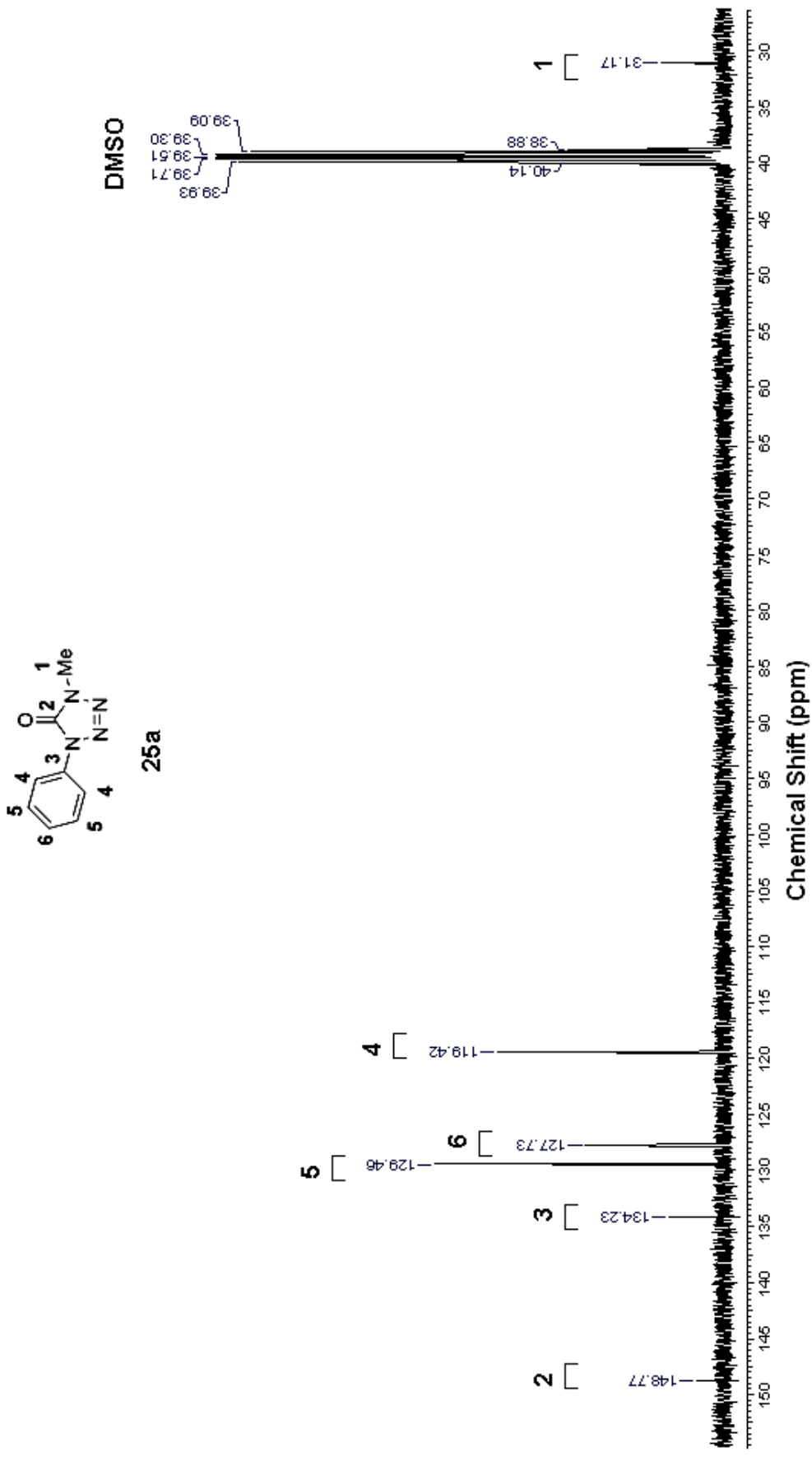
25a
DMSO
Chemical Shift (ppm)
31.17
38.88
39.09
39.30
39.51
39.71
39.93
40.14
119.42
127.73
129.46
134.23
148.77

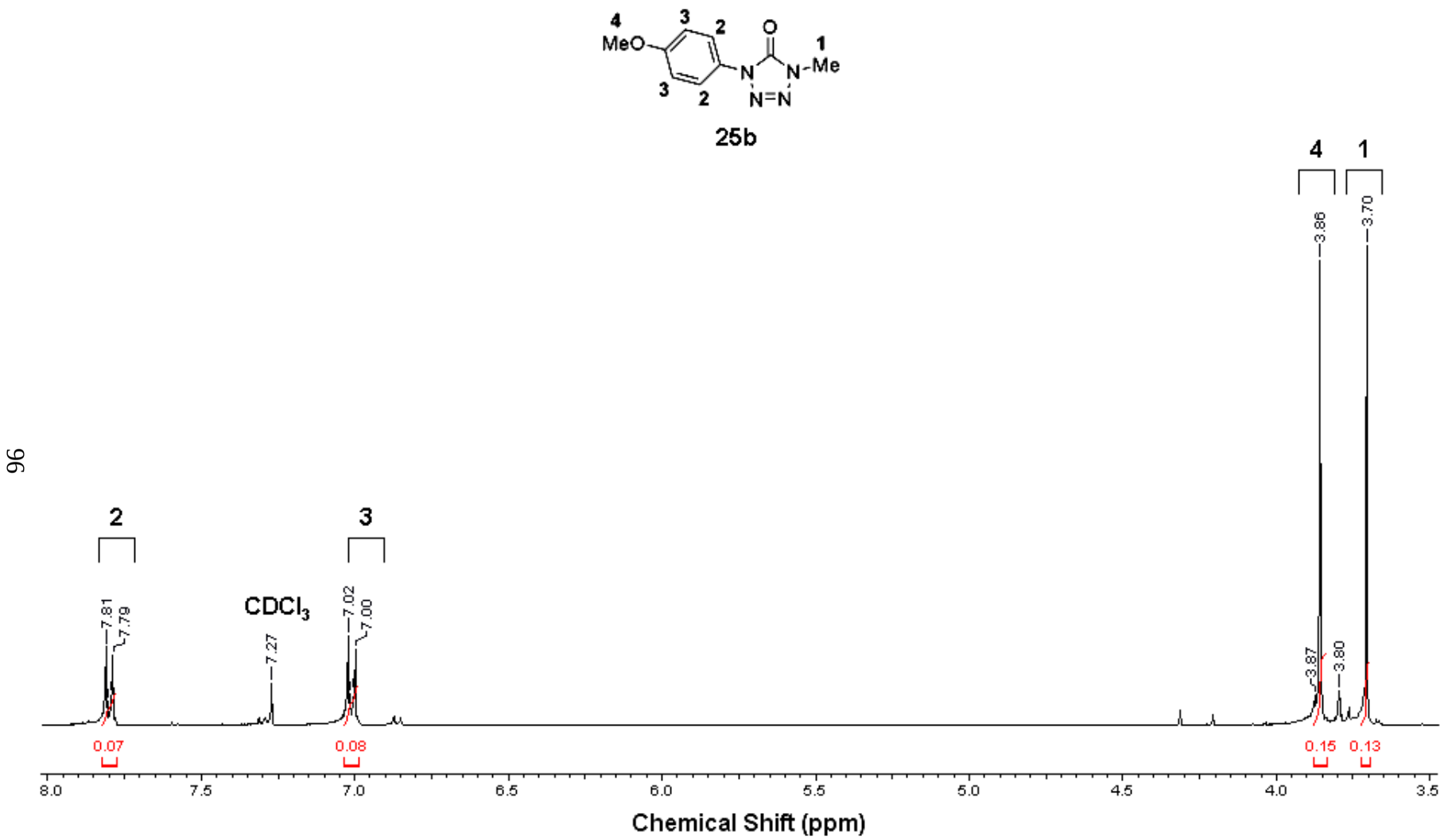
4
MeO
3
2
O
1
N-Me
N
N
N=N
3
2
25b
4
1
3.86
3.70
2
3
CDCl3
7.81
7.79
7.27
7.02
7.00
3.87
3.80
0.07
0.08
0.15
0.13
8.0
7.5
7.0
6.5
6.0
5.5
5.0
4.5
4.0
3.5
Chemical Shift (ppm)

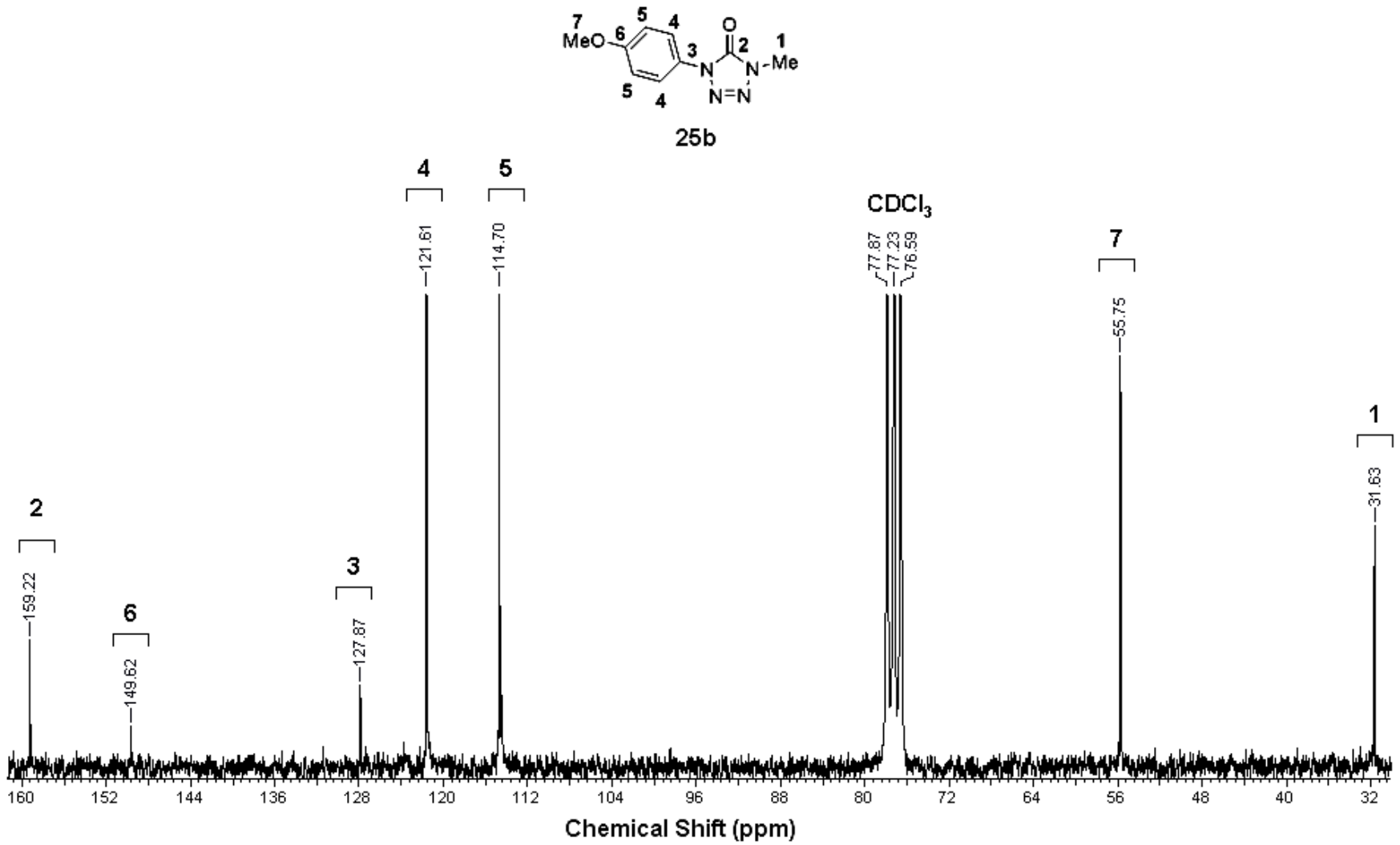
MeO
N
N
N=N
Me
O
25b
CDCl3
159.22
149.62
127.87
121.61
114.70
77.87
77.23
76.59
55.75
31.63
Chemical Shift (ppm)

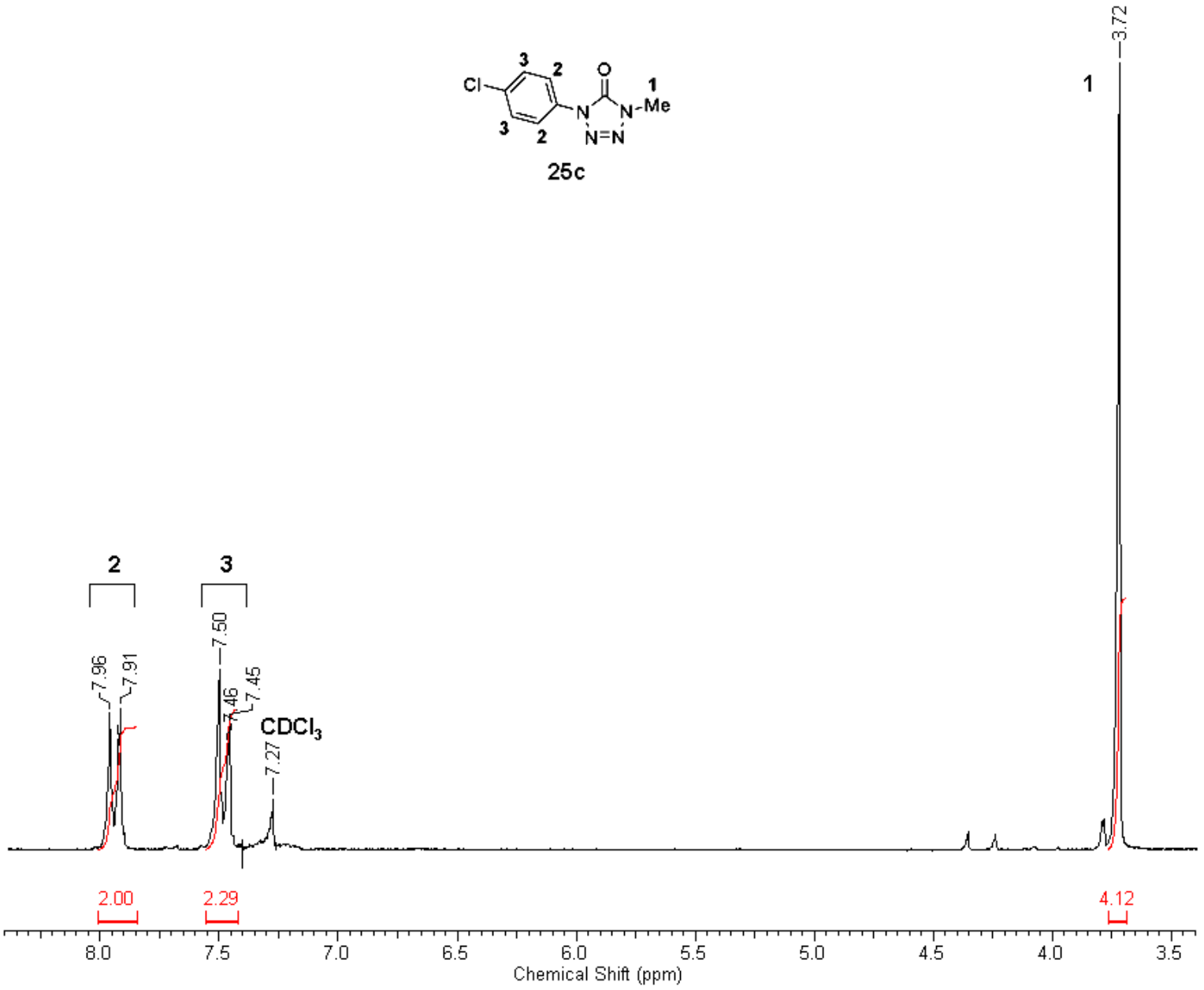
Cl
3
2
O
1
N
N-Me
3
2
N=N
25c
1
3.72
2
3
7.96
7.91
7.50
7.46
7.45
CDCl3
7.27
2.00
2.29
4.12
8.0
7.5
7.0
6.5
6.0
5.5
5.0
4.5
4.0
3.5
Chemical Shift (ppm)

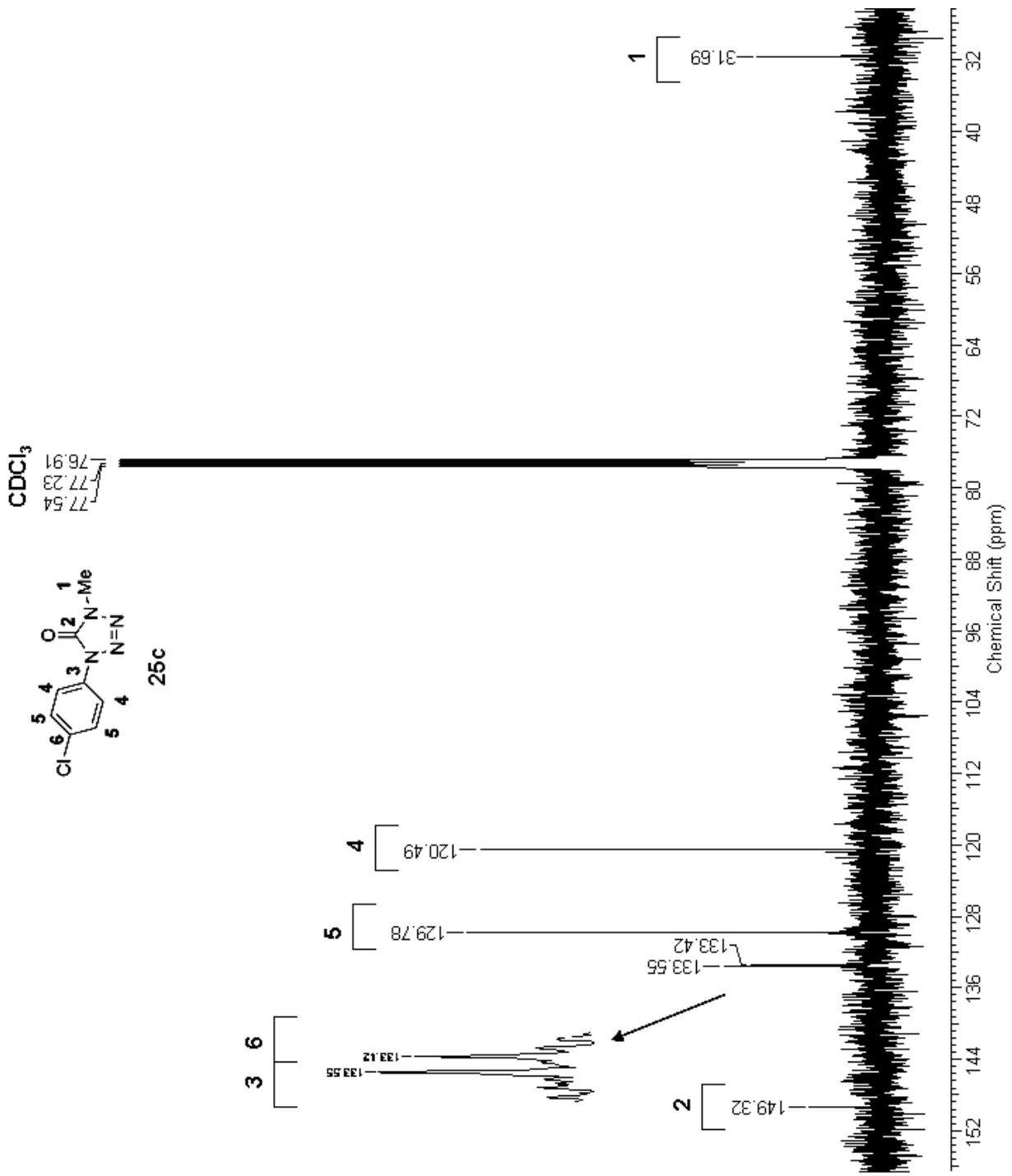
CDCl3
77.54
77.23
76.91
25c
1
31.69
2
149.32
3 6
133.55
133.42
4
120.49
5
129.78
133.55
133.42
Chemical Shift (ppm)

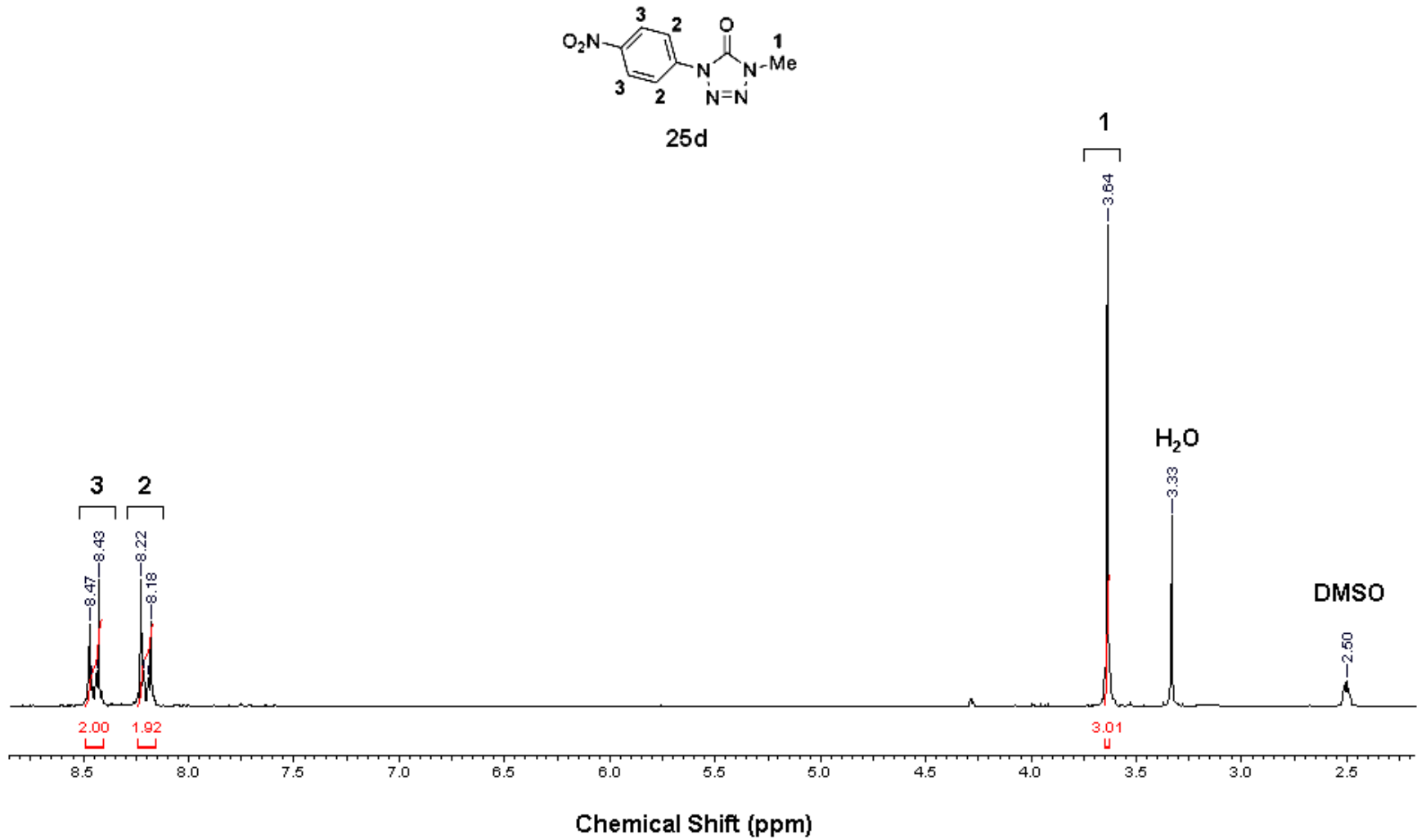
25d
1
3.64
H2O
3.33
DMSO
2.50
3
2
8.43
8.47
8.22
8.18
2.00
1.92
3.01
8.5
8.0
7.5
7.0
6.5
6.0
5.5
5.0
4.5
4.0
3.5
3.0
2.5
Chemical Shift (ppm)

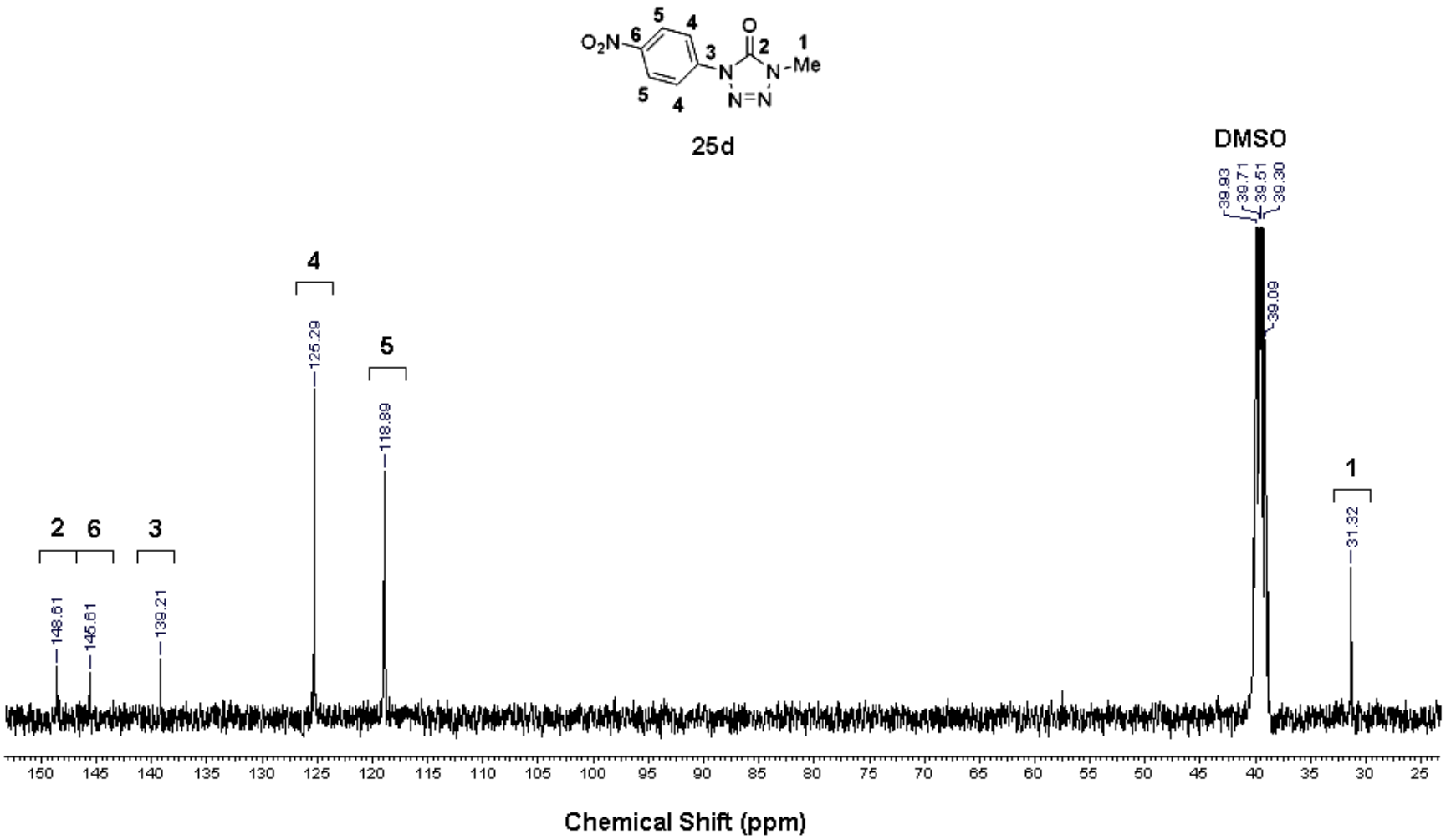
O2N
6
5
4
3
2
1
Me
N
N=N
O
25d
DMSO
39.93
39.71
39.51
39.30
39.09
125.29
118.89
148.61
146.61
139.21
31.32
Chemical Shift (ppm)

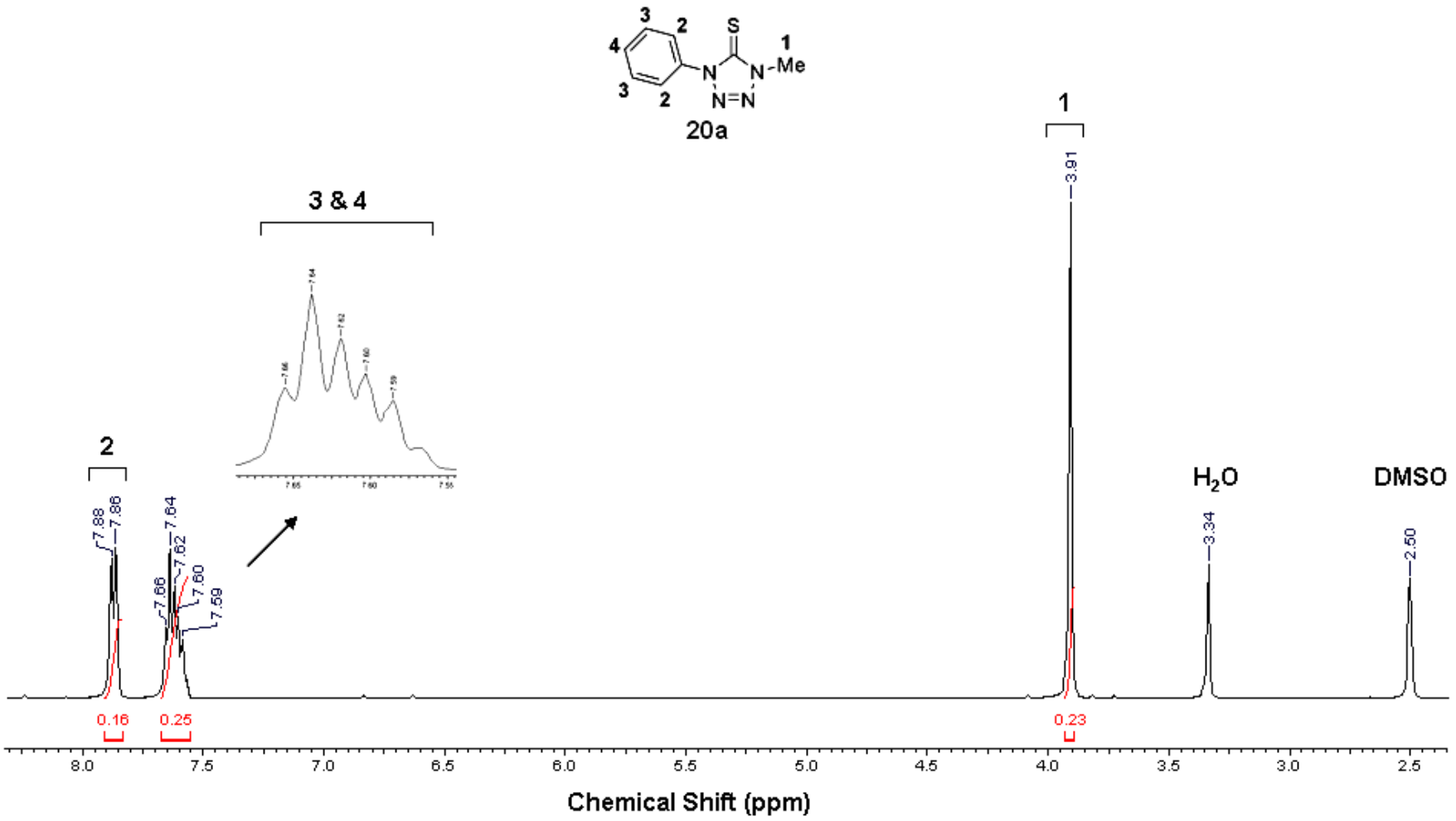
3
2
S
1
4
N
N-Me
3
2
N=N
20a
1
3.91
3 & 4
2
7.88
7.86
7.64
7.62
7.66
7.60
7.59
H2O
3.34
DMSO
2.50
0.16
0.25
0.23
8.0
7.5
7.0
6.5
6.0
5.5
5.0
4.5
4.0
3.5
3.0
2.5
Chemical Shift (ppm)

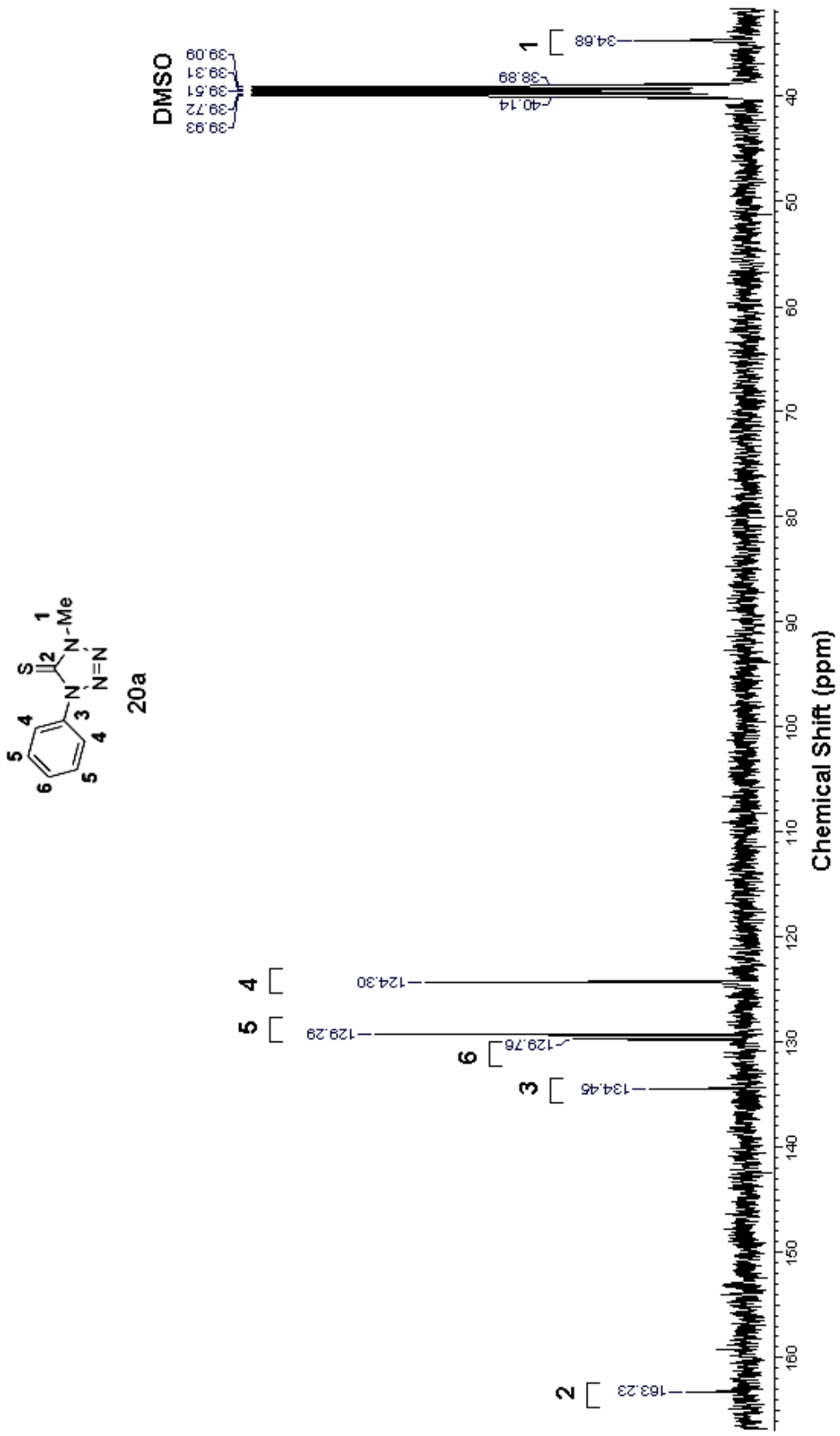
DMSO
39.93
39.72
39.51
39.31
39.09
40.14
38.89
34.68
1
124.30
4
129.29
5
129.76
6
134.45
3
163.23
2
Chemical Shift (ppm)
20a
S
N-Me
N=N

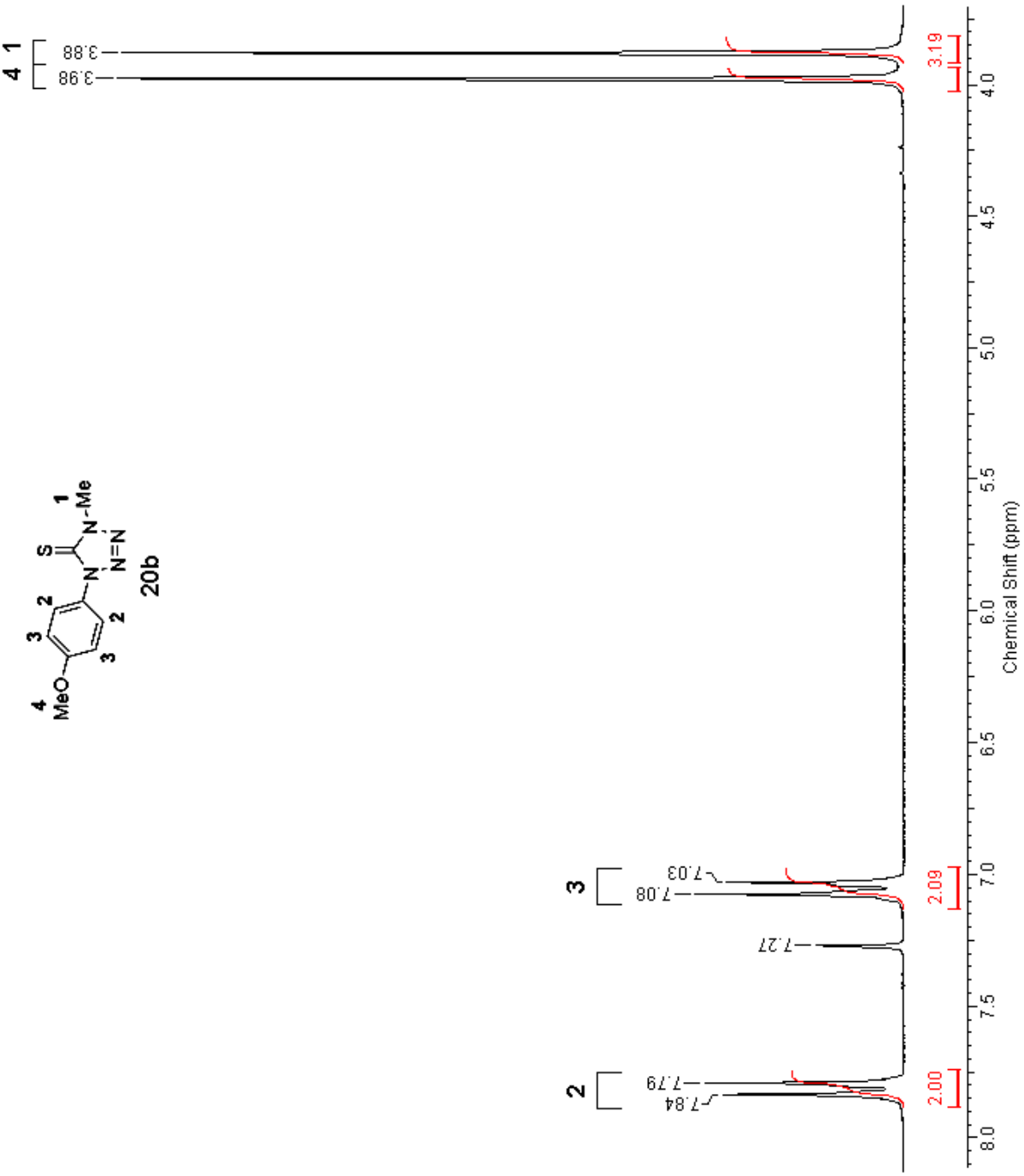
20b
Chemical Shift (ppm)

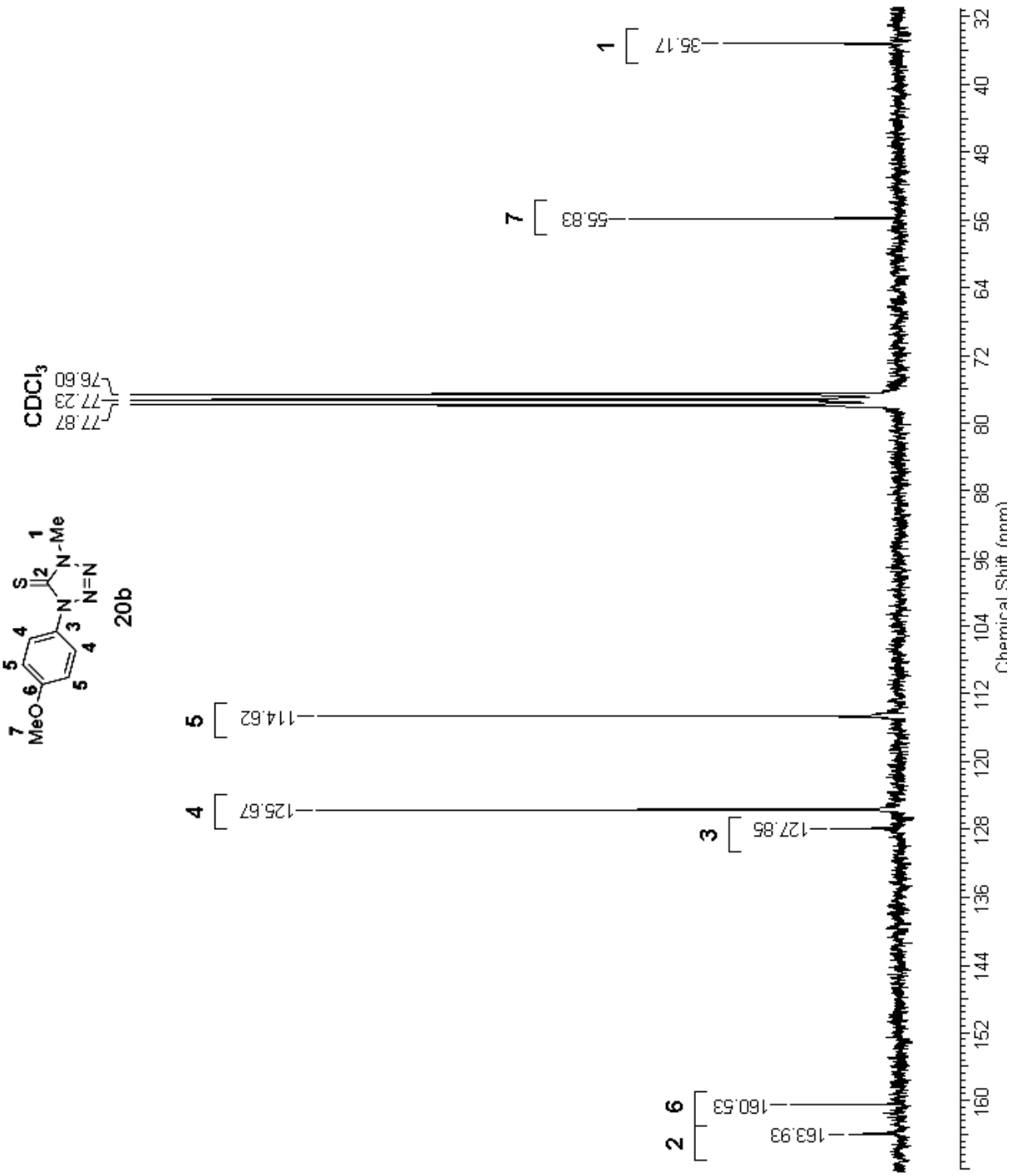
20b
CDCl3
77.87
77.23
76.60
35.17
55.83
114.62
125.67
127.86
160.53
163.93
Chemical Shift (ppm)

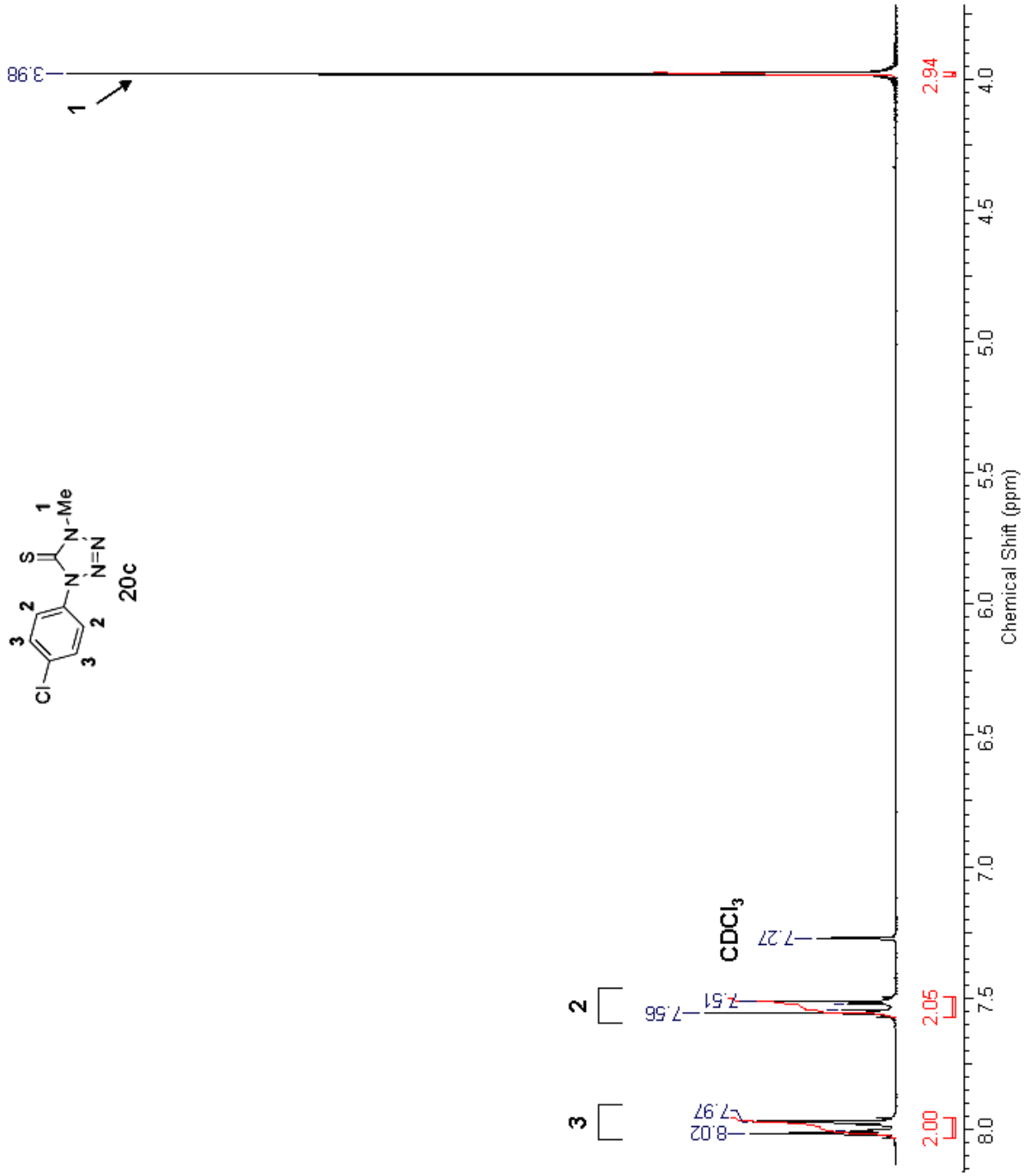
3.98
1
20c
S
N-Me
N
N=N
Cl
2
3
2
3
CDCl3
7.27
7.56
7.51
8.02
7.97
2
3
2.94
2.05
2.00
4.0
4.5
5.0
5.5
6.0
6.5
7.0
7.5
8.0
Chemical Shift (ppm)

20c
CDCl3
Chemical Shift (ppm)
35.05
163.57
124.71
129.56
133.36
135.50

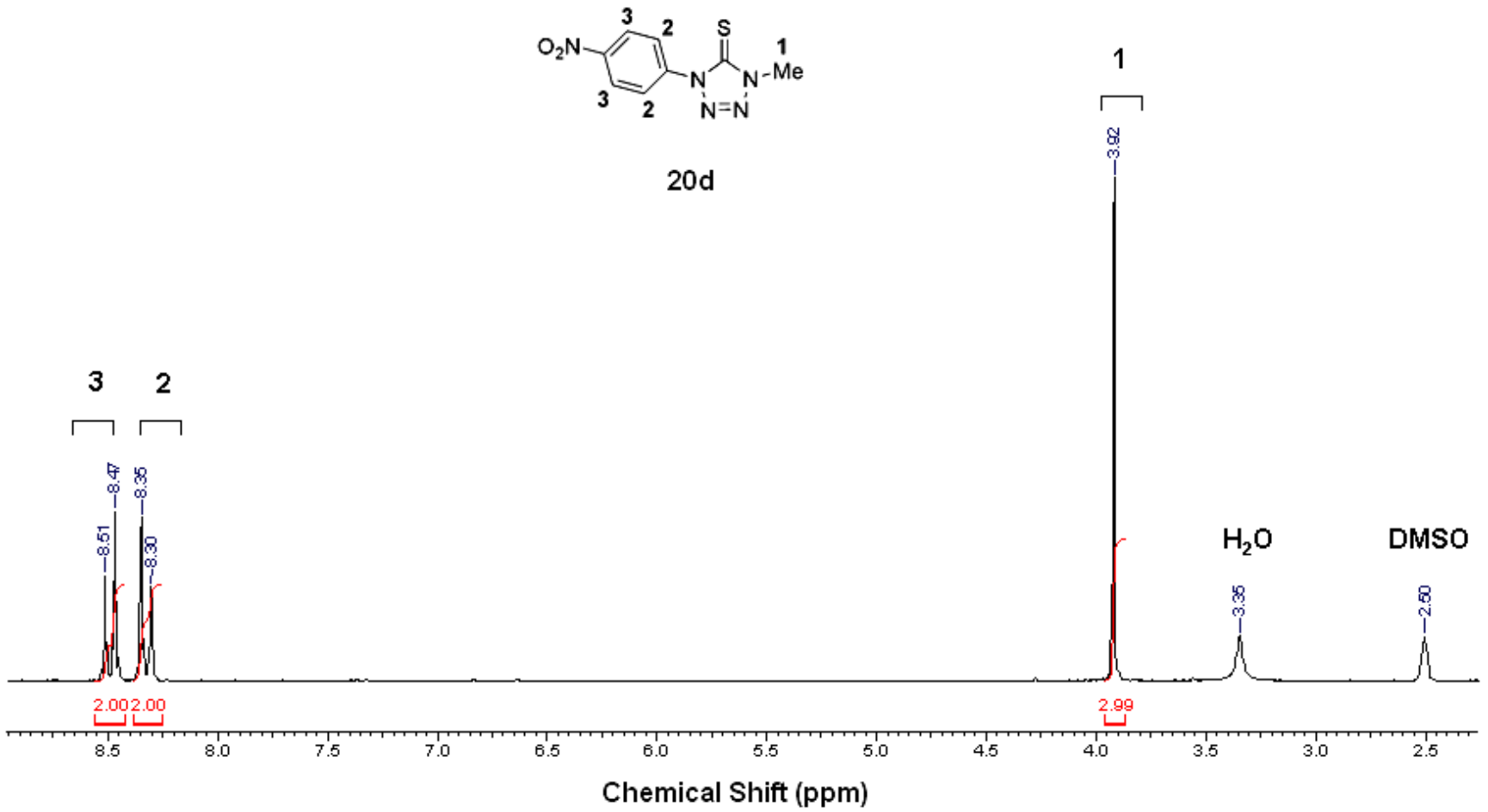
20d
1
3
2
3.92
H2O
DMSO
3.35
2.60
8.51
8.47
8.35
8.30
2.00
2.00
2.99
Chemical Shift (ppm)

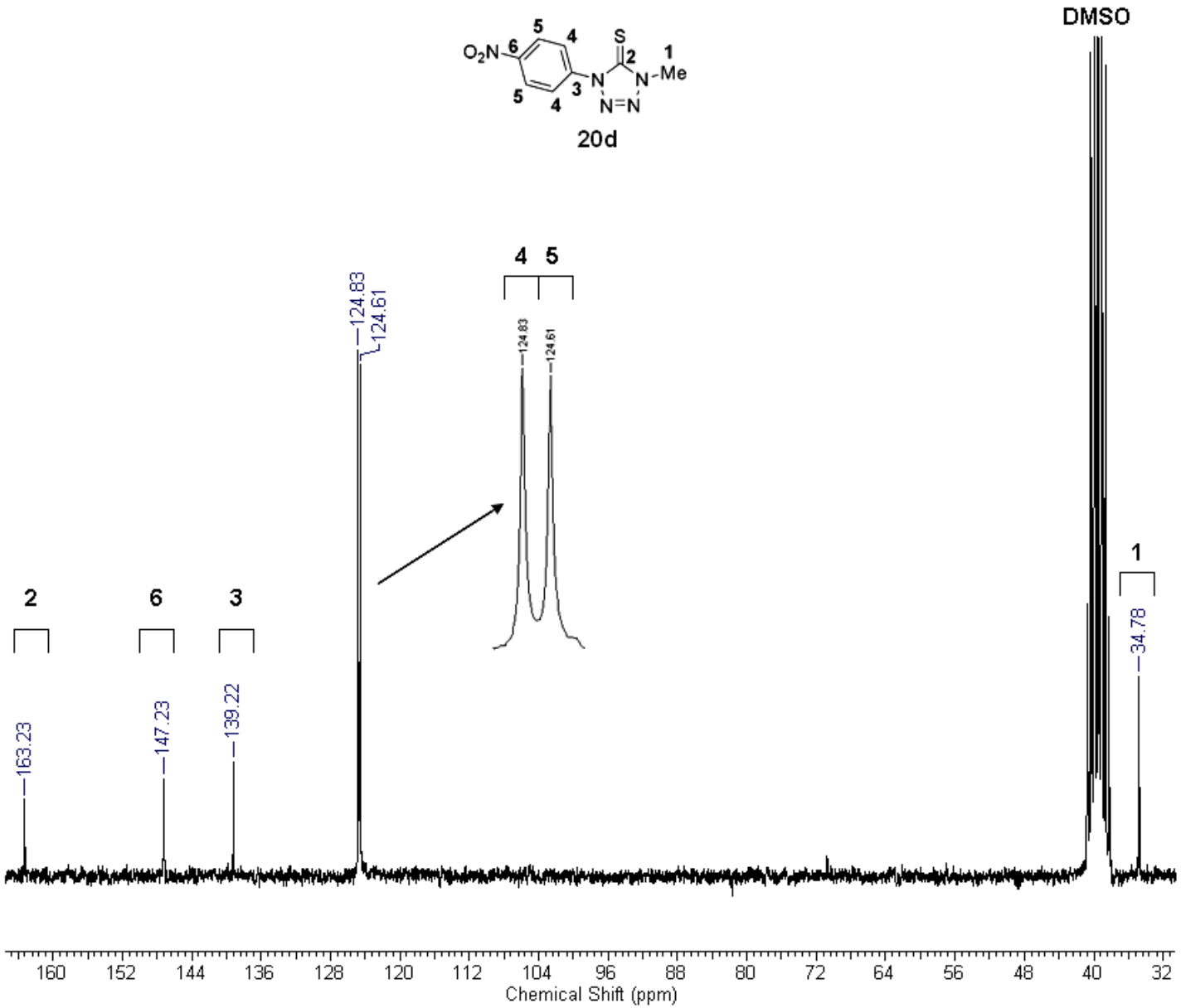
DMSO
20d
4 5
2
6
3
1
124.83
124.61
163.23
147.23
139.22
34.78
160 152 144 136 128 120 112 104 96 88 80 72 64 56 48 40 32
Chemical Shift (ppm)

APPENDIX II

IR SPECTRA

(Chapter -1)

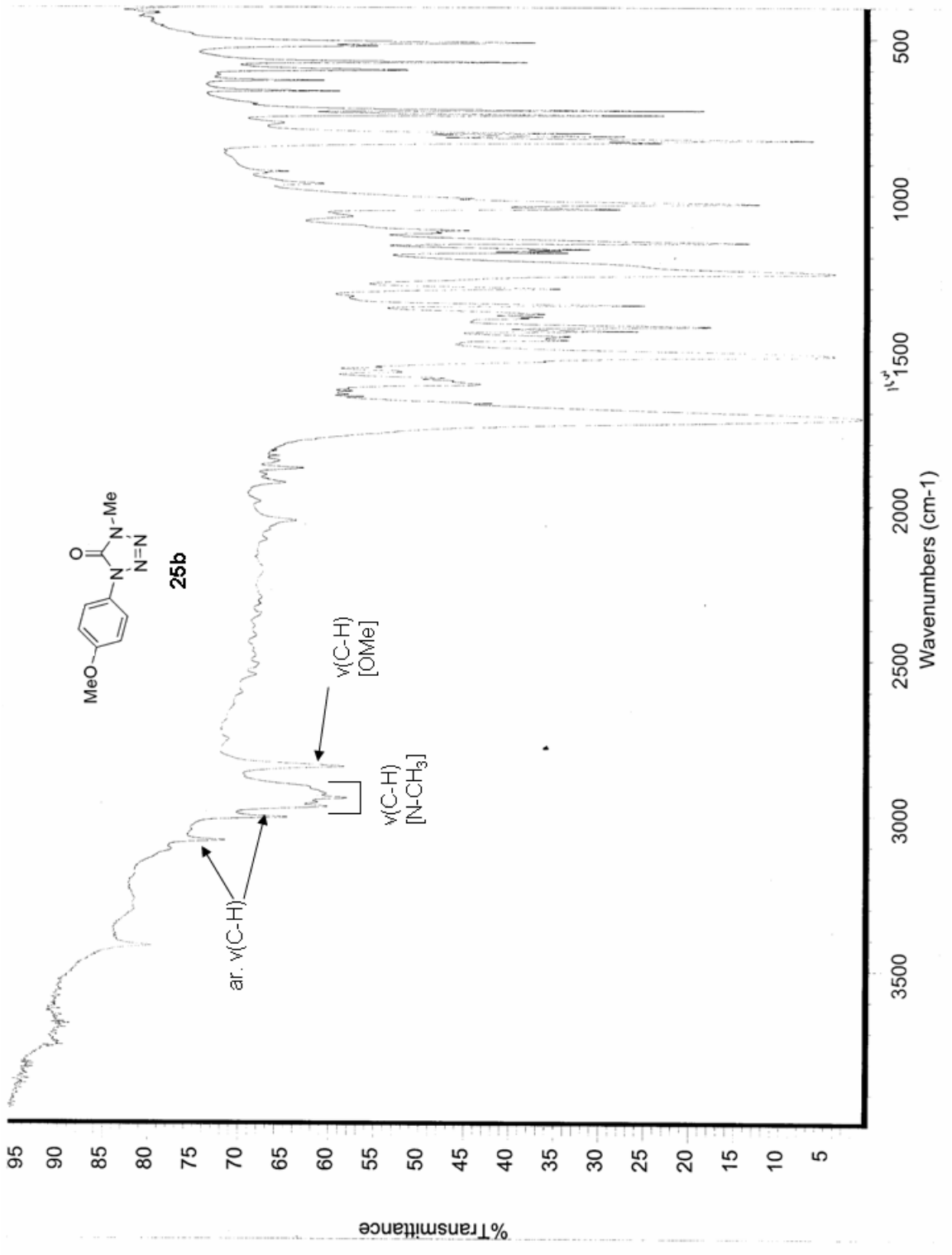
25b
MeO
N-Me
N=N
ar. ν(C-H)
ν(C-H)
[OMe]
ν(C-H)
[N-CH3]
%Transmittance
Wavenumbers (cm-1)
3500
3000
2500
2000
1500
1000
500
95
90
85
80
75
70
65
60
55
50
45
40
35
30
25
20
15
10
5

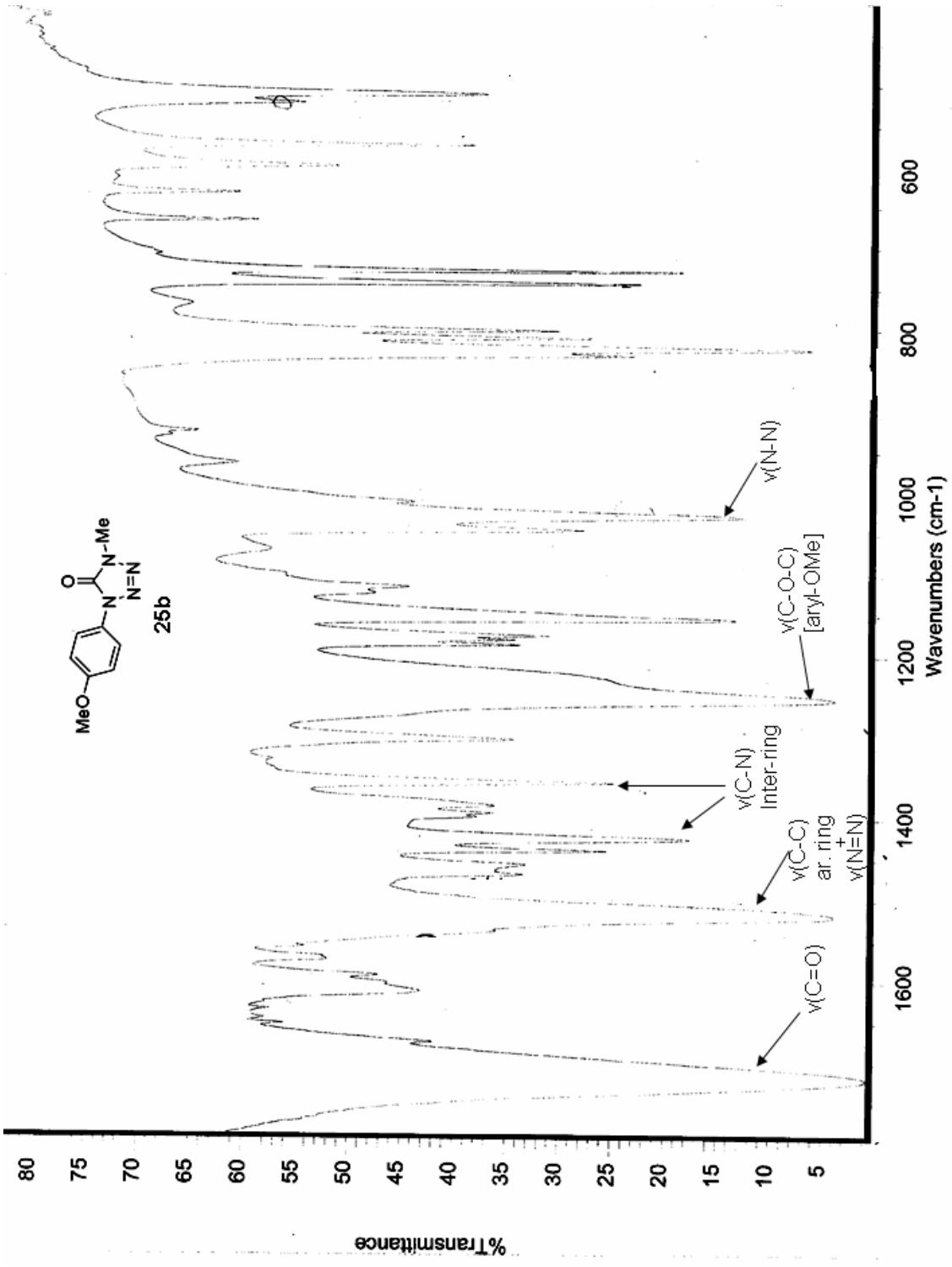
25b
MeO
N-Me
N=N
%Transmittance
Wavenumbers (cm-1)
v(C=O)
v(C-C) ar. ring + v(N=N)
v(C-N) Inter-ring
v(C-O-C) [aryl-OMe]
v(N-N)

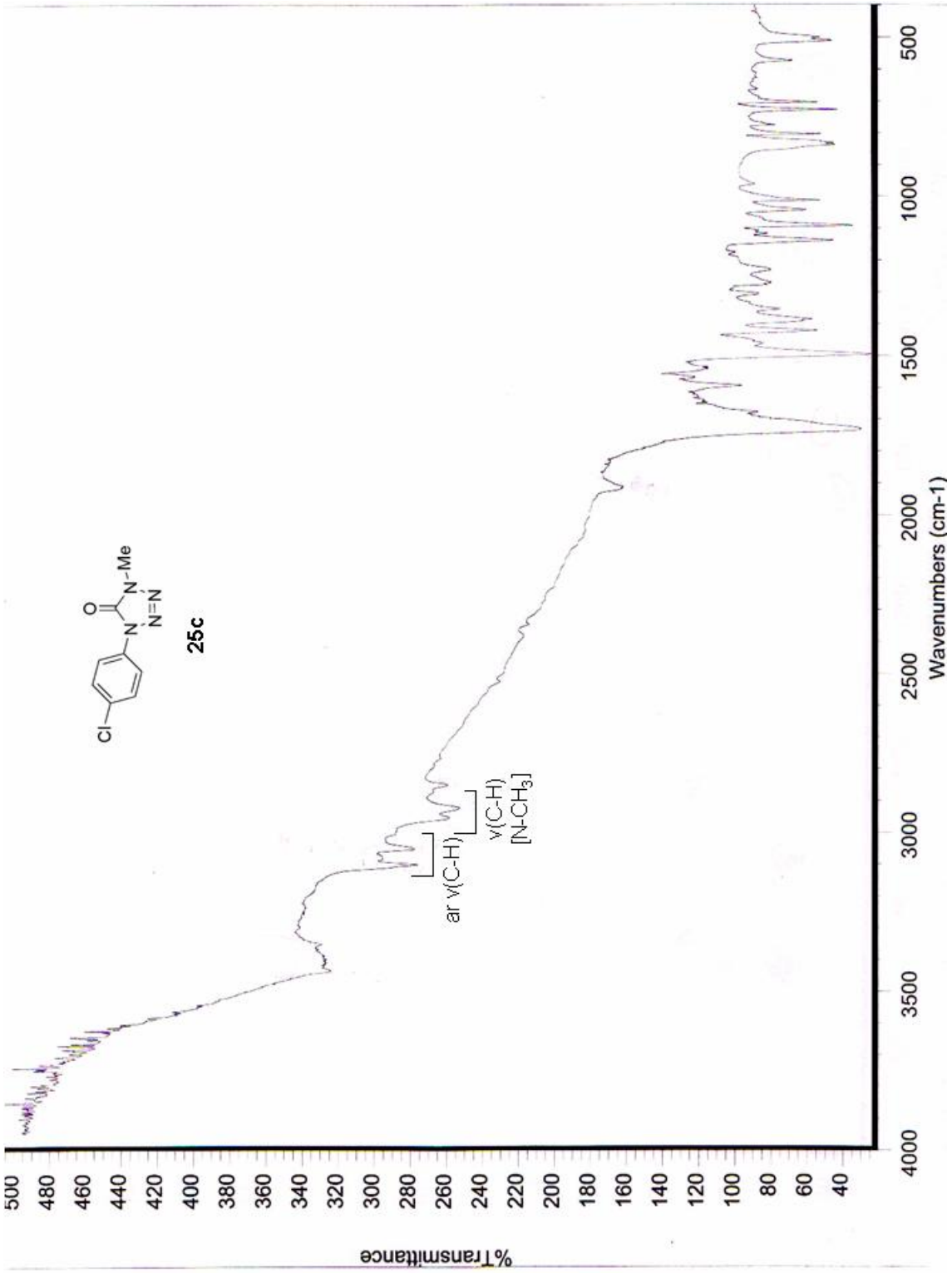
25c
ar ν(C-H)
ν(C-H)
[N-CH3]
%Transmittance
Wavenumbers (cm-1)

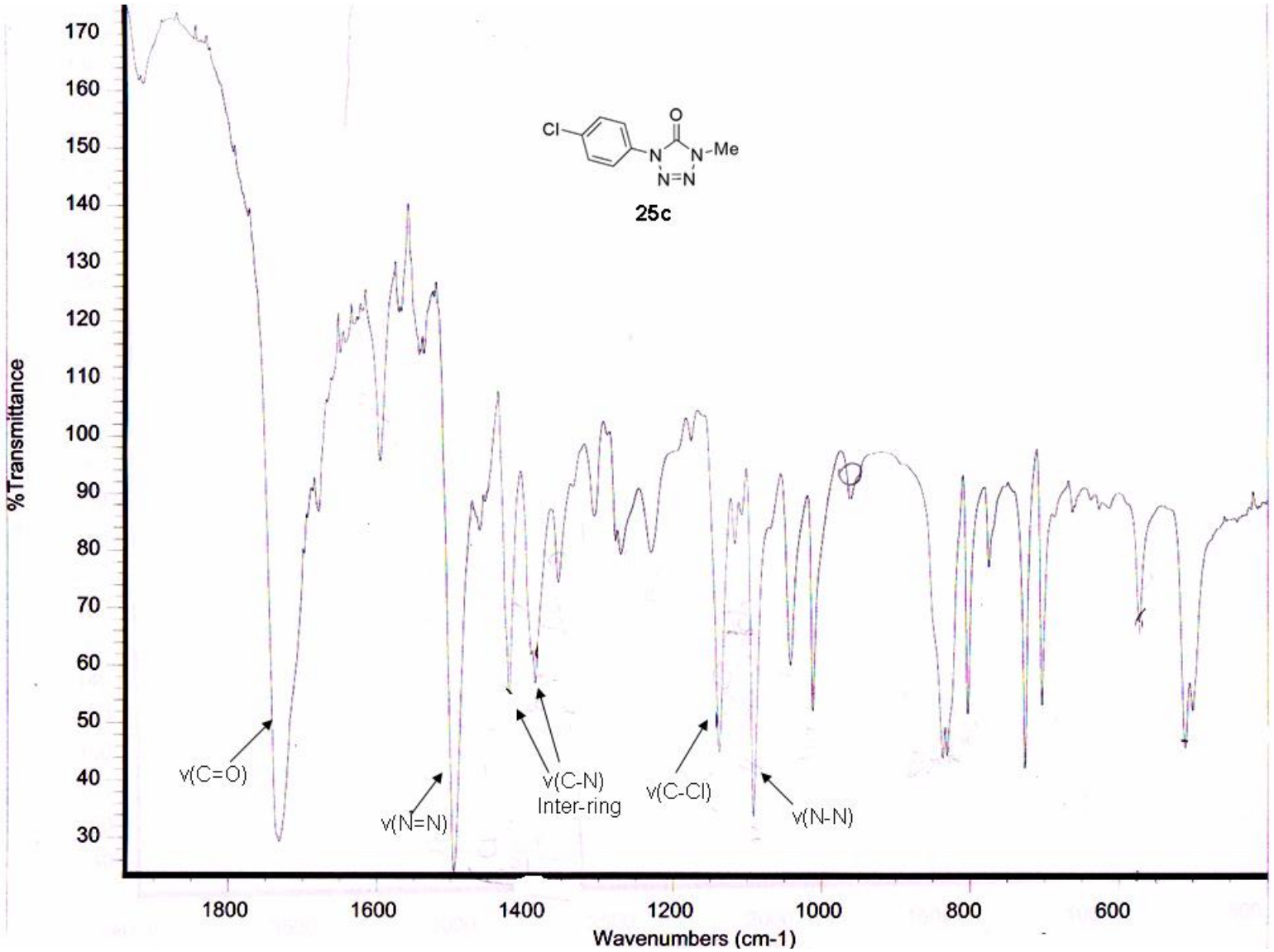
Cl
O
N
N-Me
N=N
25c
%Transmittance
170
160
150
140
130
120
110
100
90
80
70
60
50
40
30
1800
1600
1400
1200
1000
800
600
Wavenumbers (cm-1)
v(C=O)
v(N=N)
v(C-N)
Inter-ring
v(C-Cl)
v(N-N)

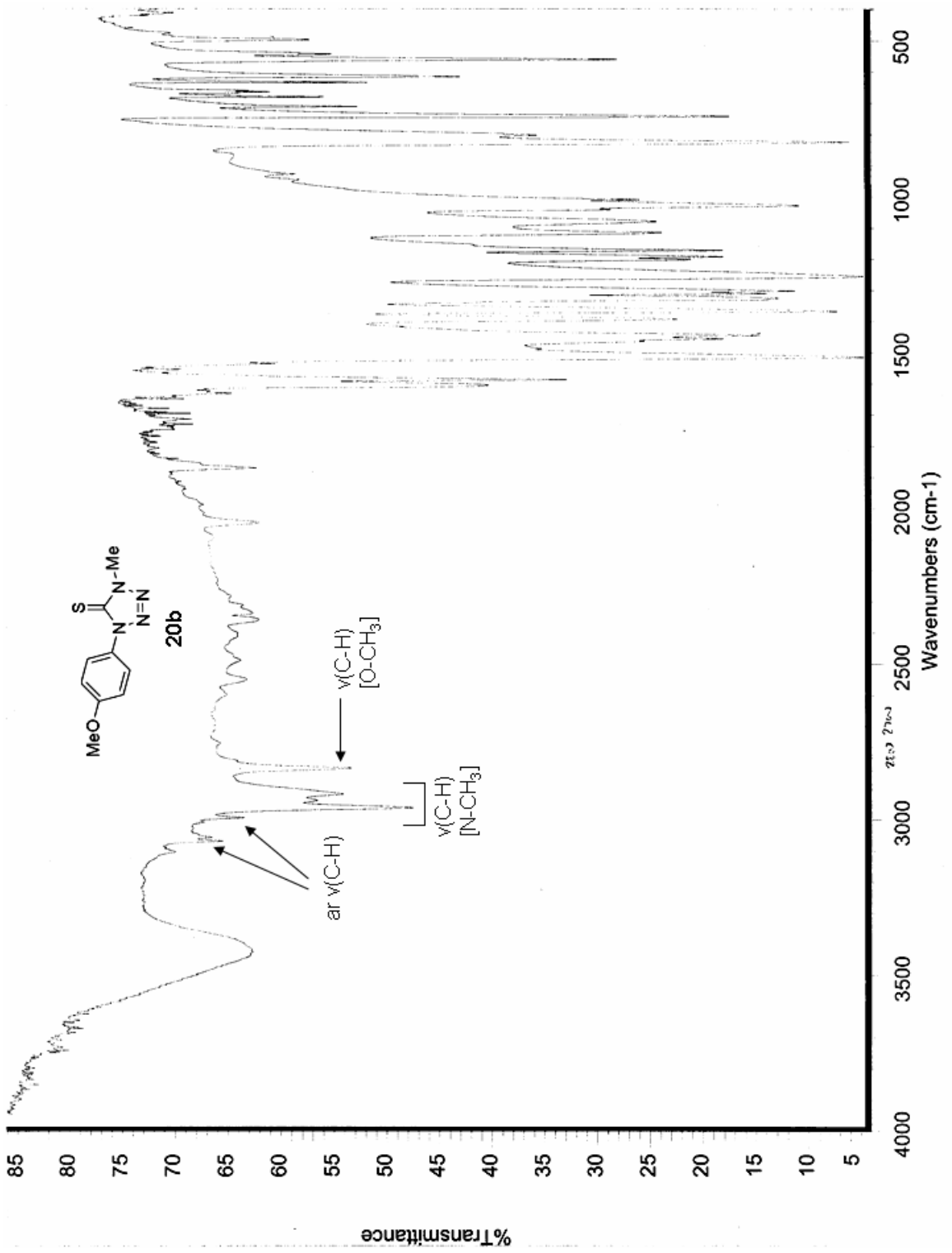
%Transmittance
Wavenumbers (cm-1)
20b
MeO
S
N-Me
N=N
ar ν(C-H)
ν(C-H)
[N-CH3]
ν(C-H)
[O-CH3]

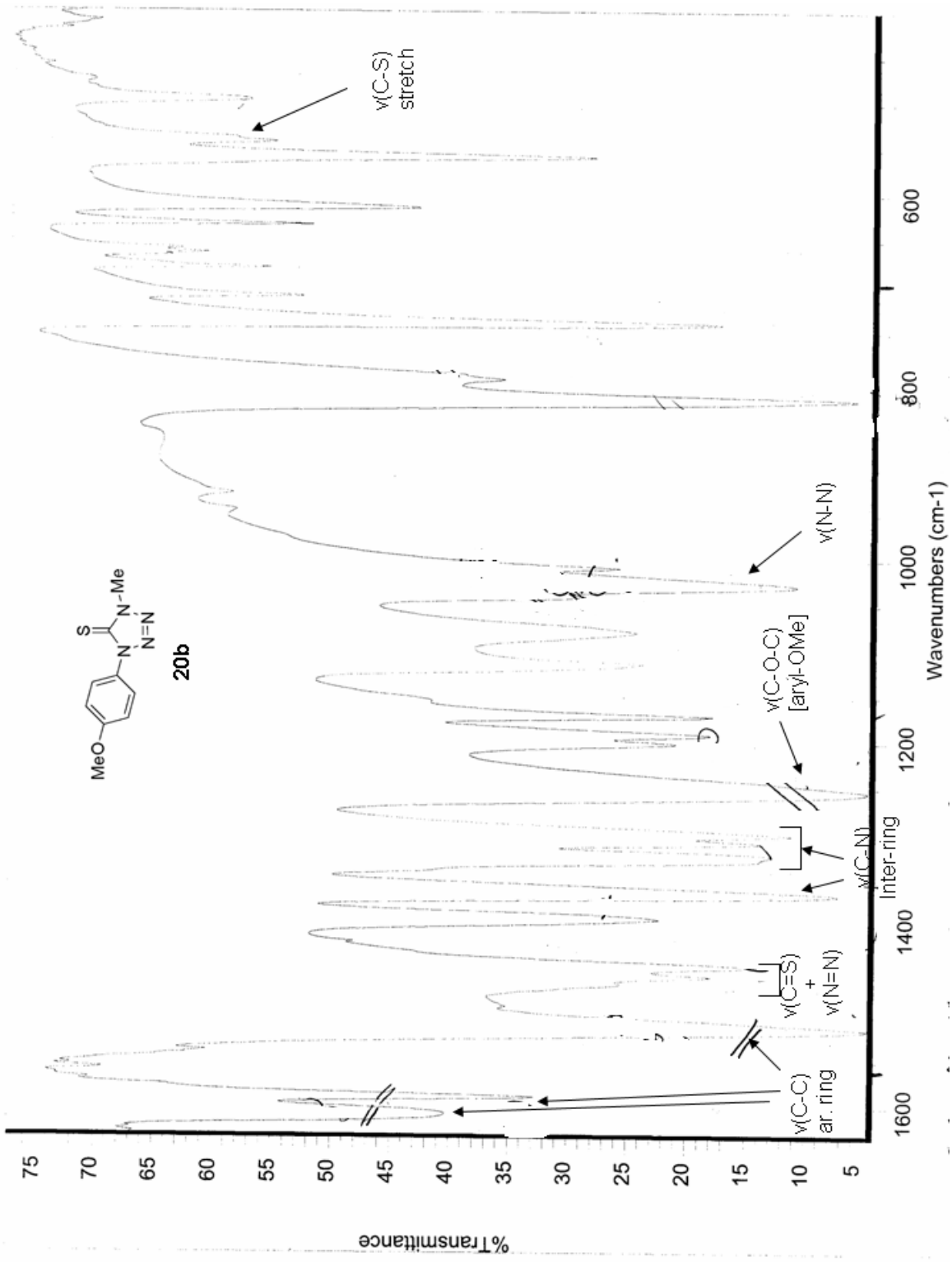
%Transmittance
Wavenumbers (cm-1)
v(C-S) stretch
v(N-N)
v(C-O-C) [aryl-OMe]
v(C-N)
Inter-ring
v(C=S) + v(N=N)
v(C-C) ar. ring
20b
MeO
N-Me
S
N=N

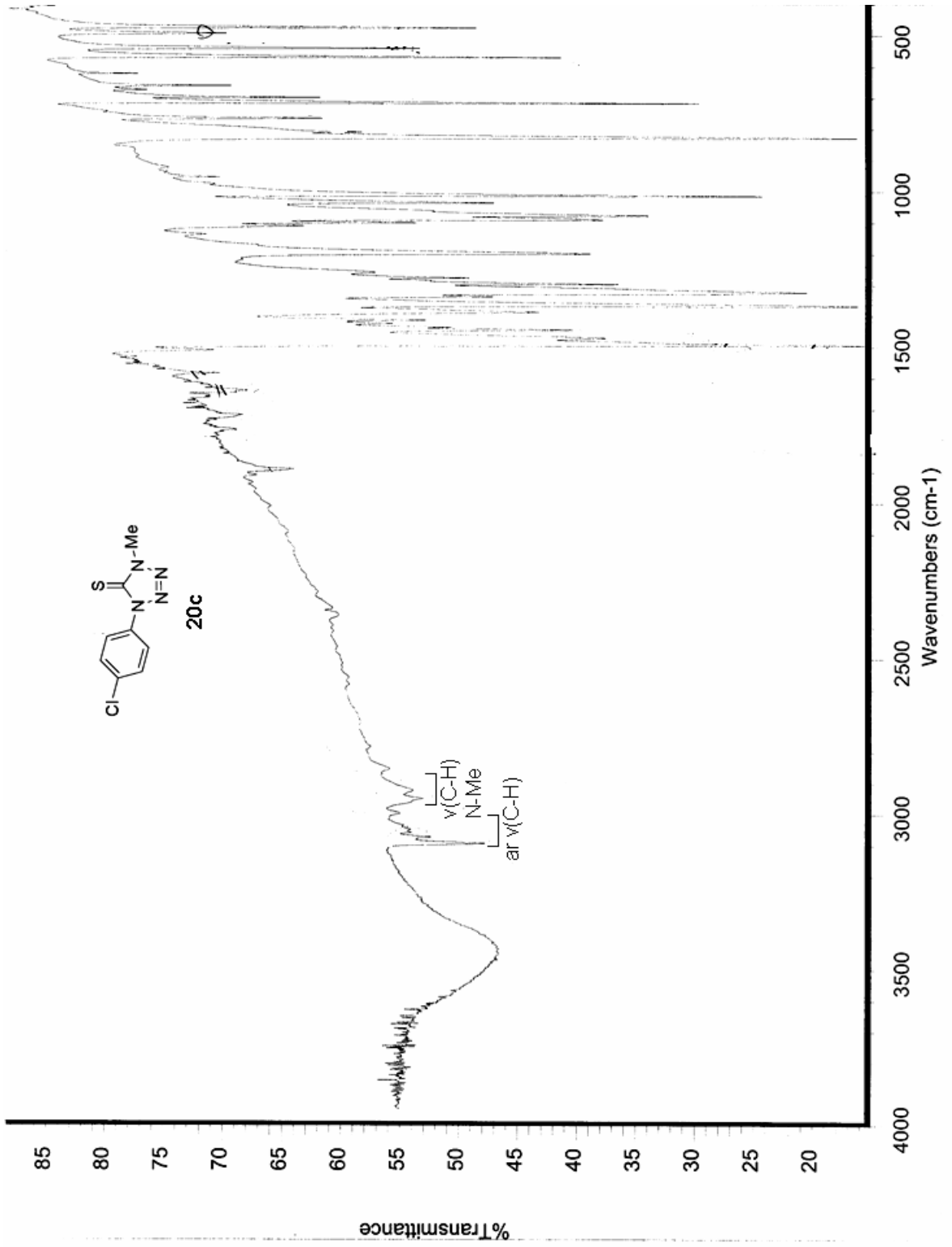
%Transmittance
Wavenumbers (cm-1)
4000
3500
3000
2500
2000
1500
1000
500
85
80
75
70
65
60
55
50
45
40
35
30
25
20
ν(C-H)
N-Me
ar ν(C-H)
20c
S
N-Me
N
N=N
Cl

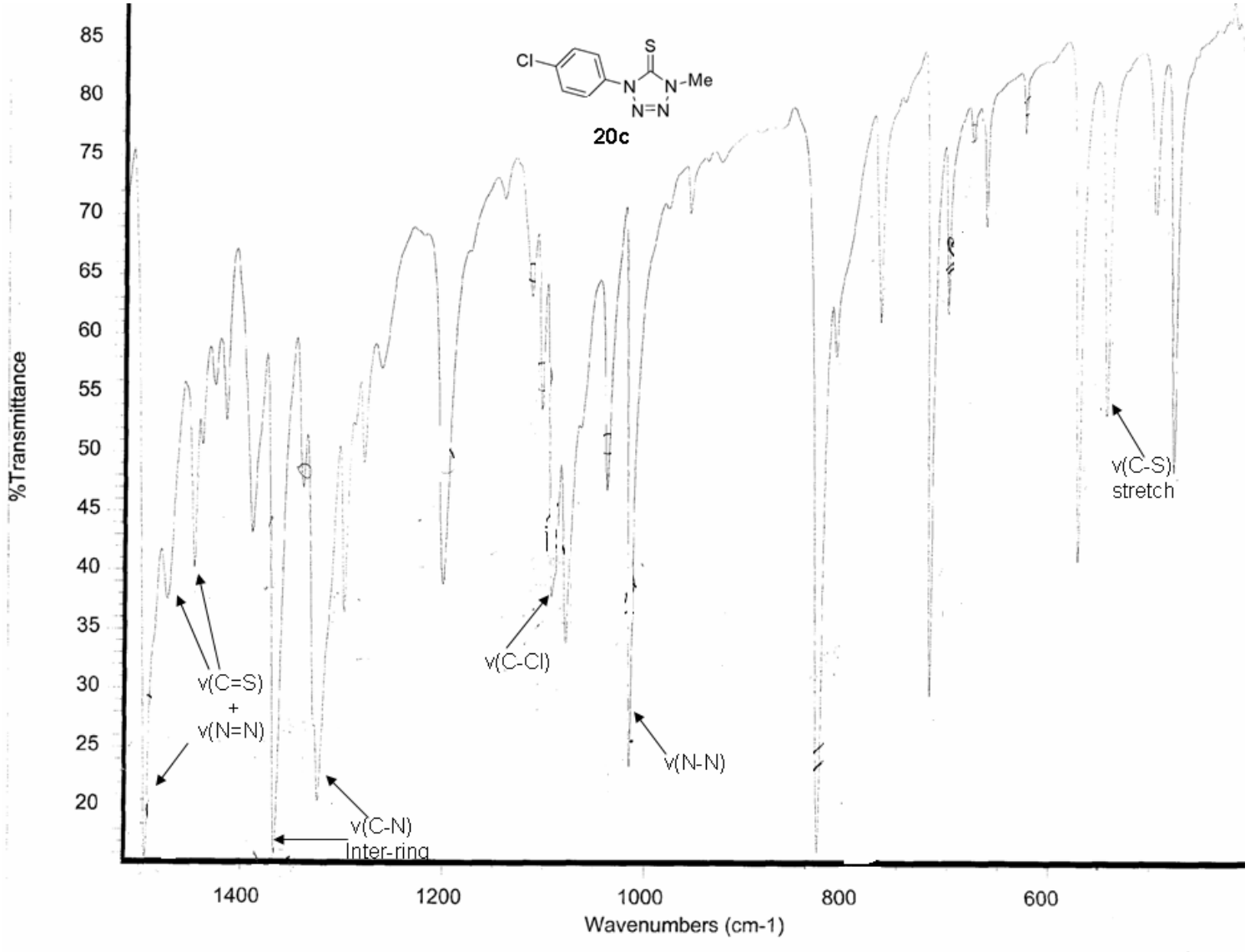
Cl
S
N
N
N
N=N
Me
20c
%Transmittance
85
80
75
70
65
60
55
50
45
40
35
30
25
20
v(C=S)
+
v(N=N)
v(C-Cl)
v(N-N)
v(C-S)
stretch
v(C-N)
Inter-ring
1400
1200
1000
800
600
Wavenumbers (cm-1)

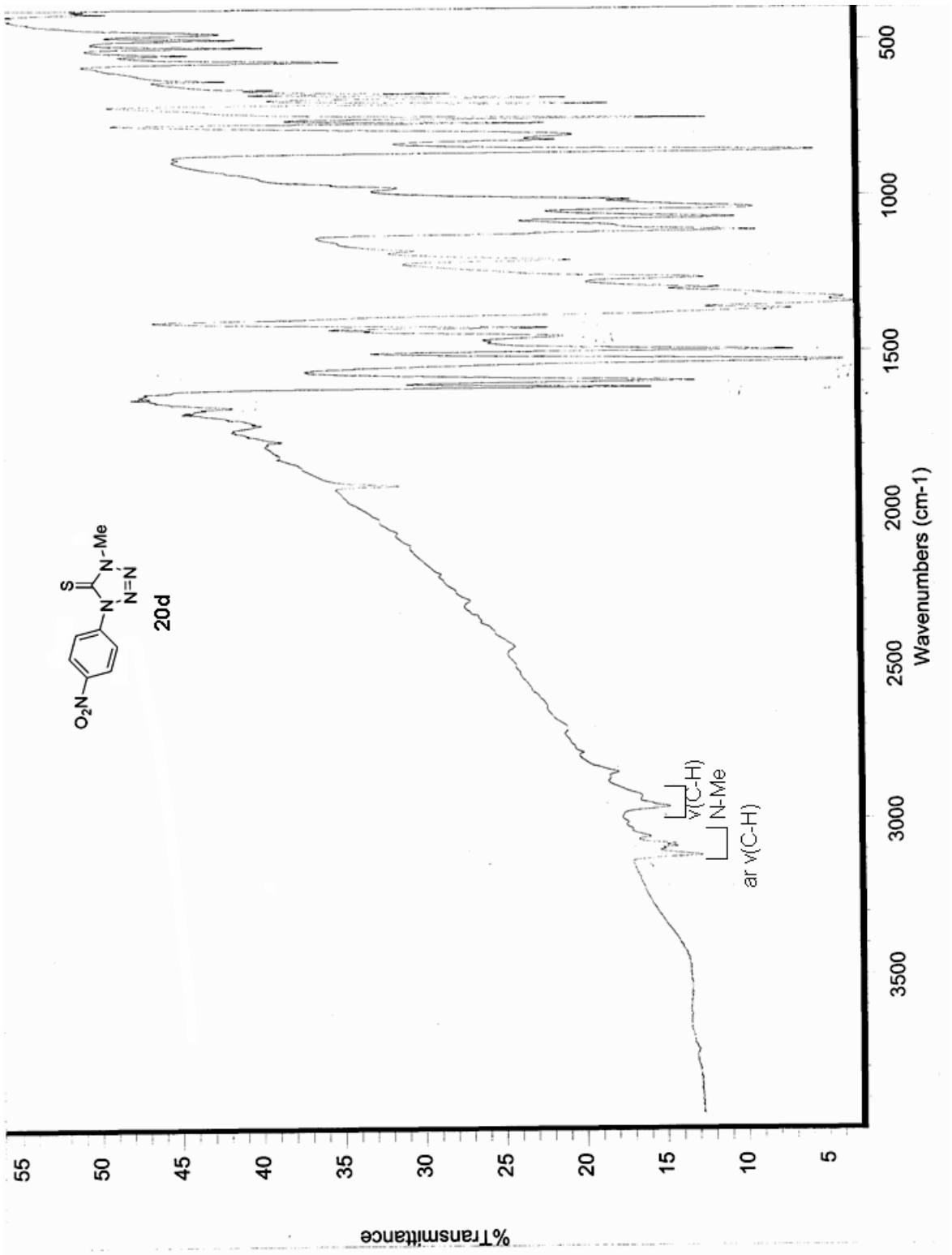
%Transmittance
Wavenumbers (cm-1)
20d
ν(C-H) N-Me
ar ν(C-H)

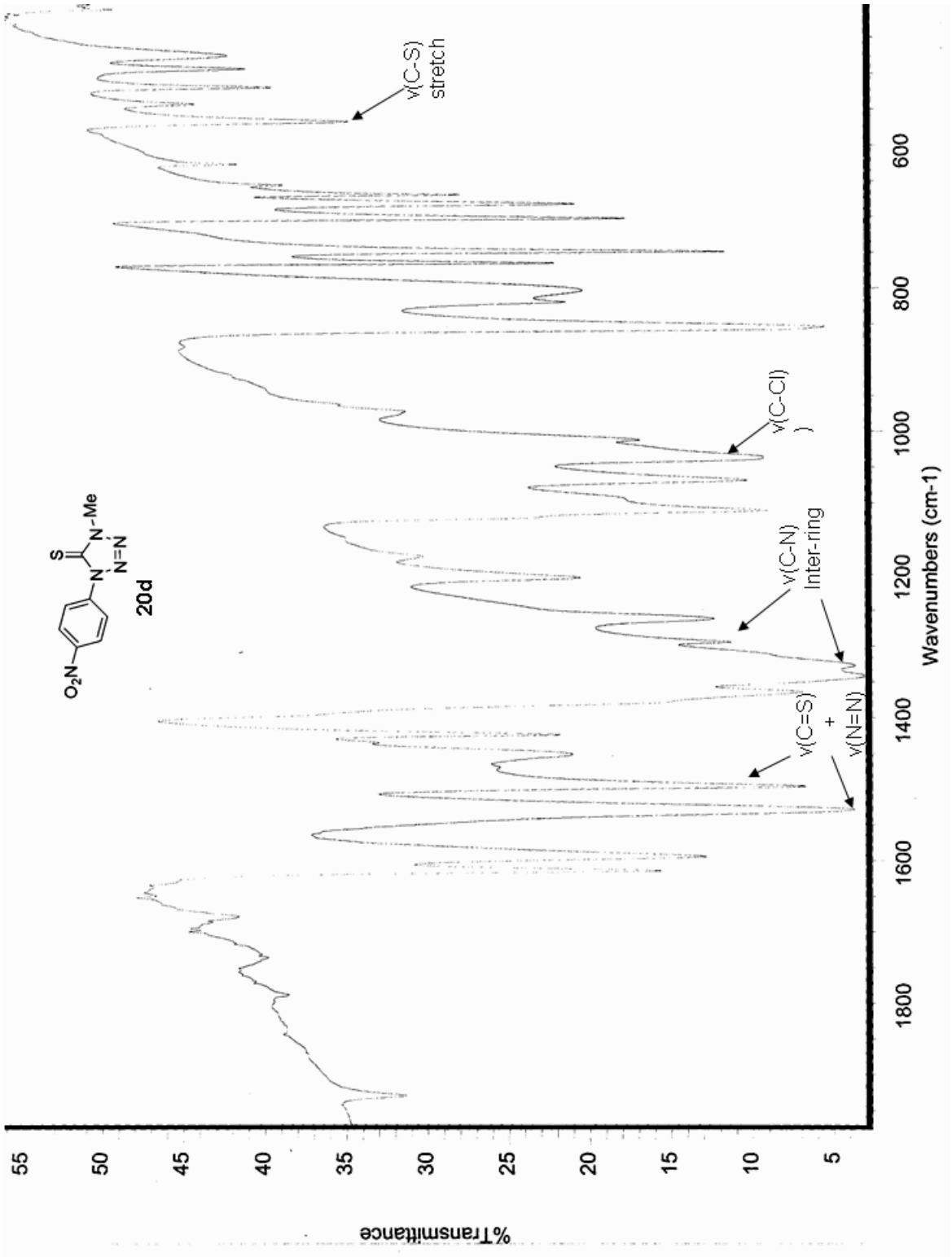
%Transmittance
Wavenumbers (cm-1)
ν(C=S) + ν(N=N)
ν(C-N) Inter-ring
ν(C-Cl)
ν(C-S) stretch
20d

APPENDIX III

MASS SPECTRA

(Chapter -1)

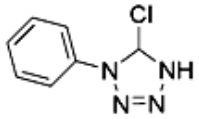

22

MS/ MS of [M+ NH_4^+]

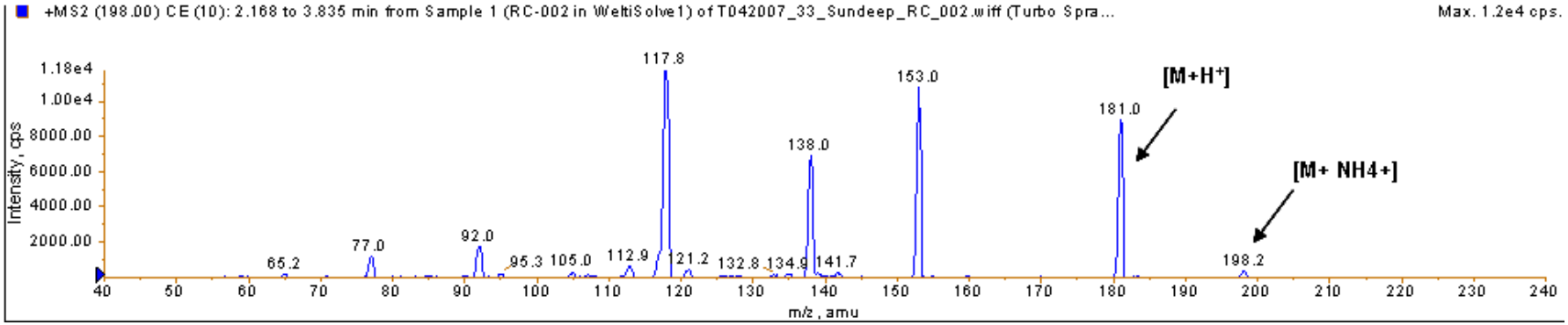

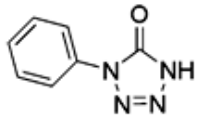

23a

MS/ MS of [M+ NH_4^+]

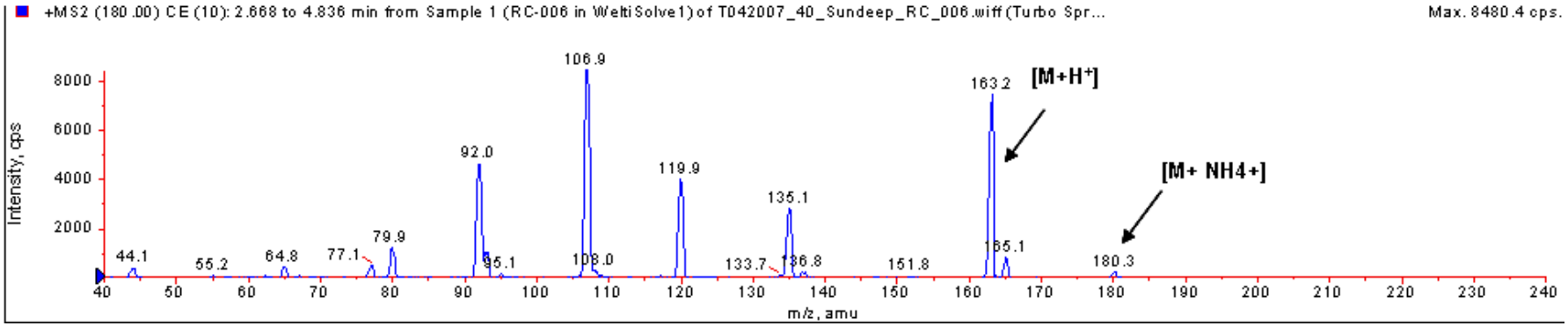

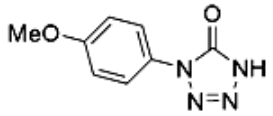

23b

MS/ MS of [M+ NH_4^+]

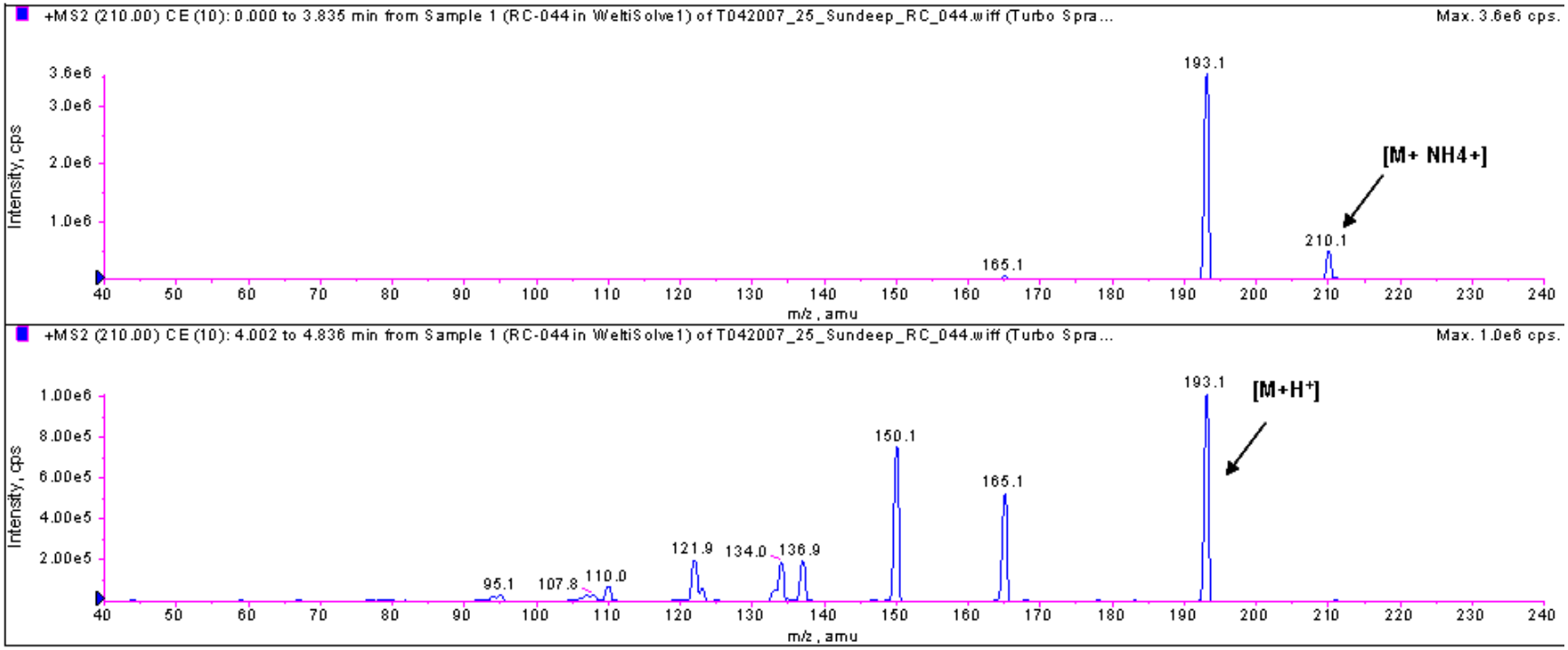

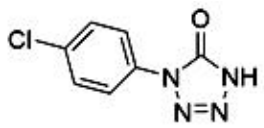

23c

MS/ MS of [M+ NH_4^+]

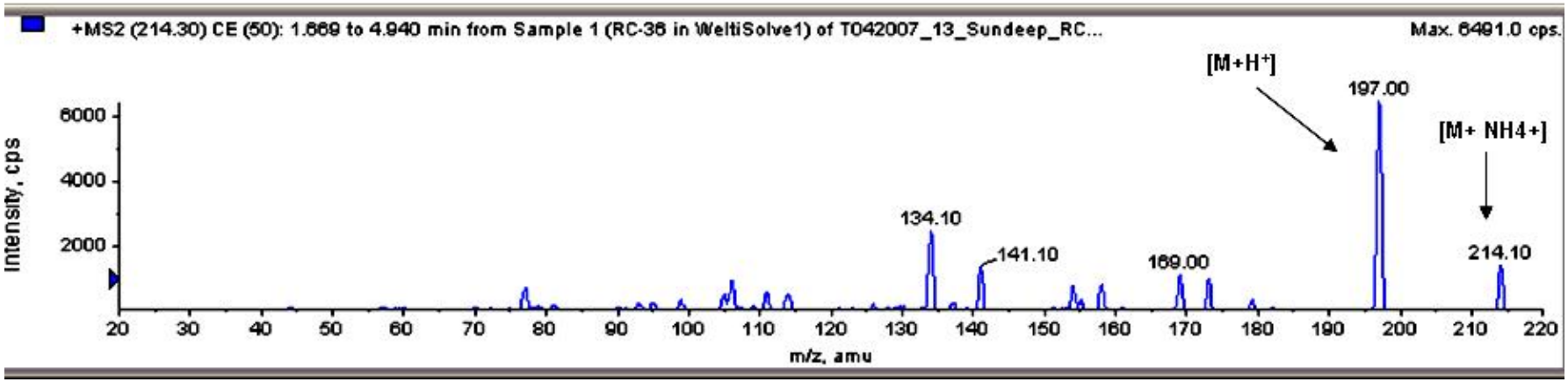

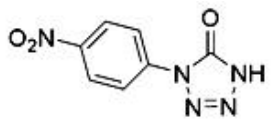

23d

MS/ MS of [M+ NH_4^+]

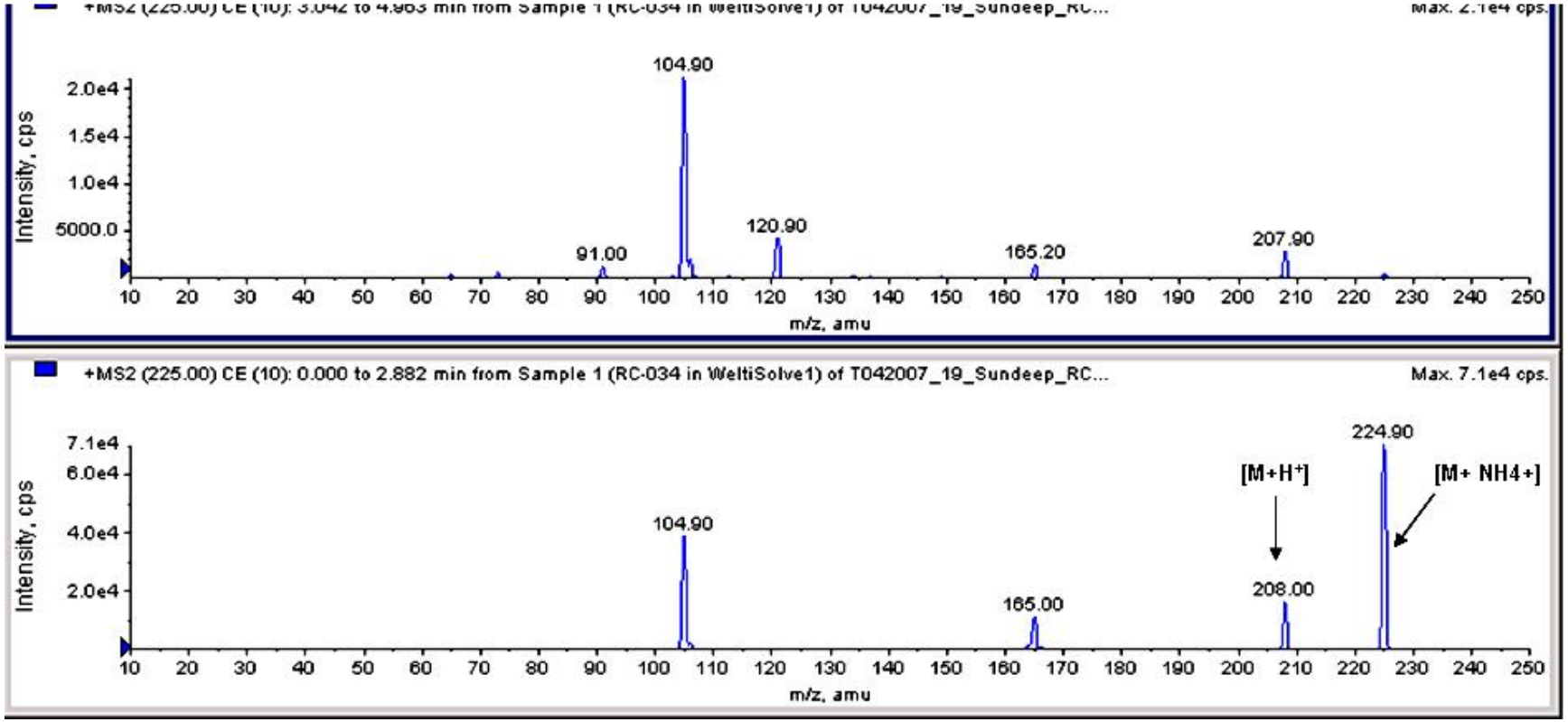

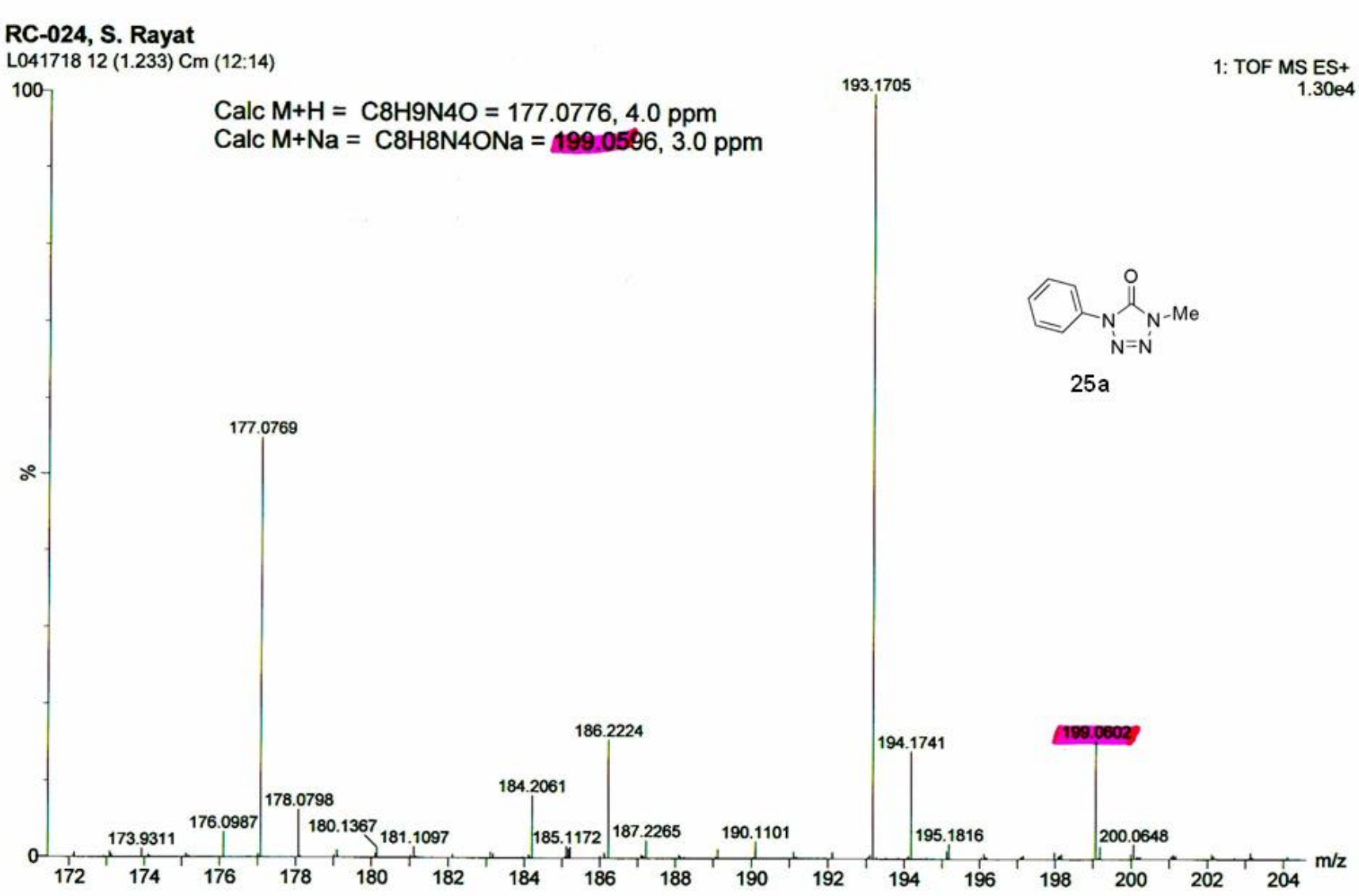
RC-024, S. Rayat
L041718 12 (1.233) Cm (12:14)
1: TOF MS ES+
1.30e4
Calc M+H = C8H9N4O = 177.0776, 4.0 ppm
Calc M+Na = C8H8N4ONa = 199.0596, 3.0 ppm
193.1705
177.0769
186.2224
194.1741
199.0602
184.2061
178.0798
176.0987
180.1367
173.9311
181.1097
185.1172
187.2265
190.1101
195.1816
200.0648
25a
100
%
0
m/z
172
174
176
178
180
182
184
186
188
190
192
194
196
198
200
202
204

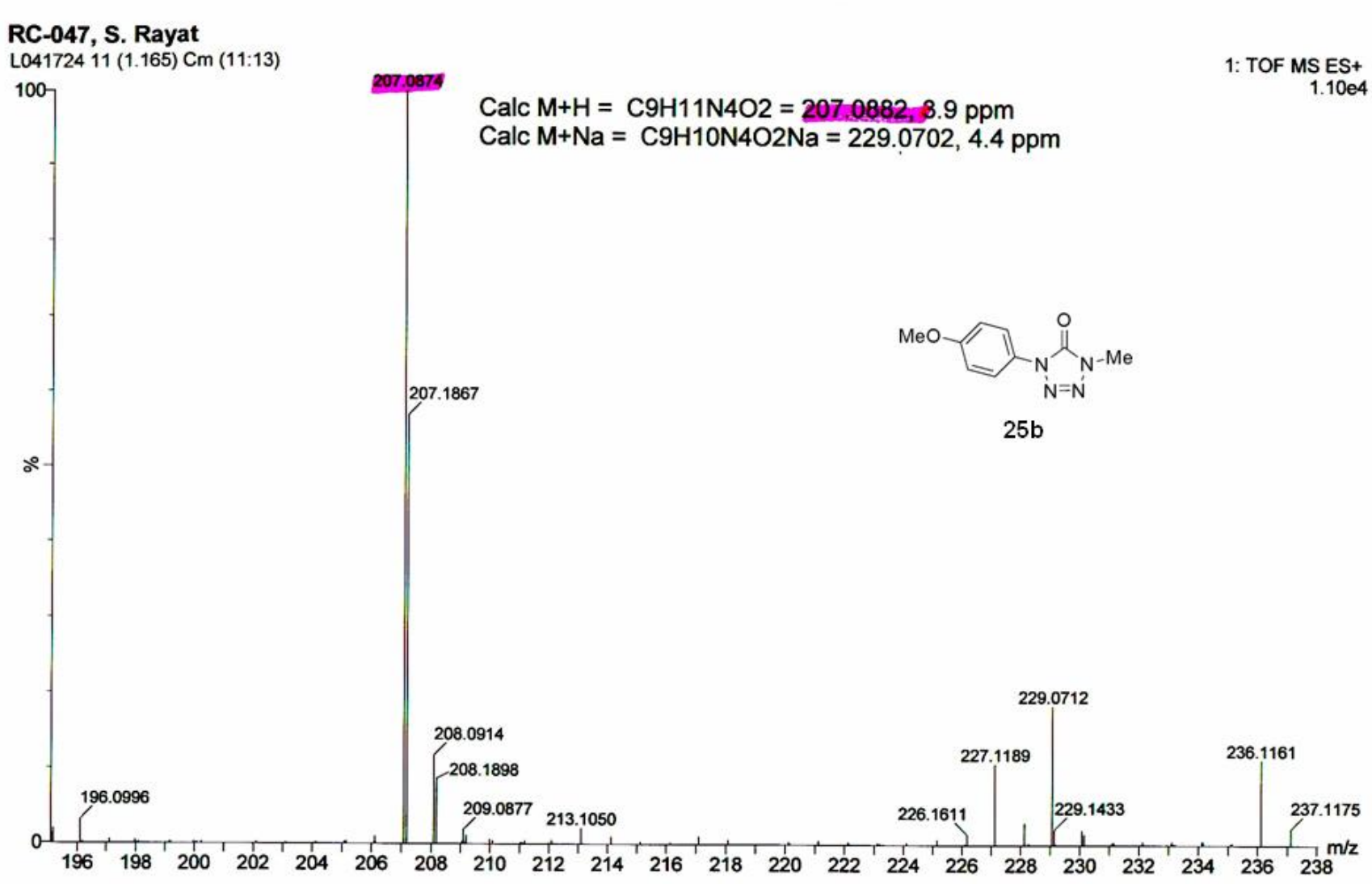
RC-047, S. Rayat
L041724 11 (1.165) Cm (11:13)
1: TOF MS ES+
1.10e4
Calc M+H = C9H11N4O2 = 207.0882, 8.9 ppm
Calc M+Na = C9H10N4O2Na = 229.0702, 4.4 ppm
MeO
N
N
N=N
Me
25b
207.0874
207.1867
208.0914
208.1898
196.0996
209.0877
213.1050
229.0712
227.1189
236.1161
226.1611
229.1433
237.1175
100
%
0
m/z
196 198 200 202 204 206 208 210 212 214 216 218 220 222 224 226 228 230 232 234 236 238

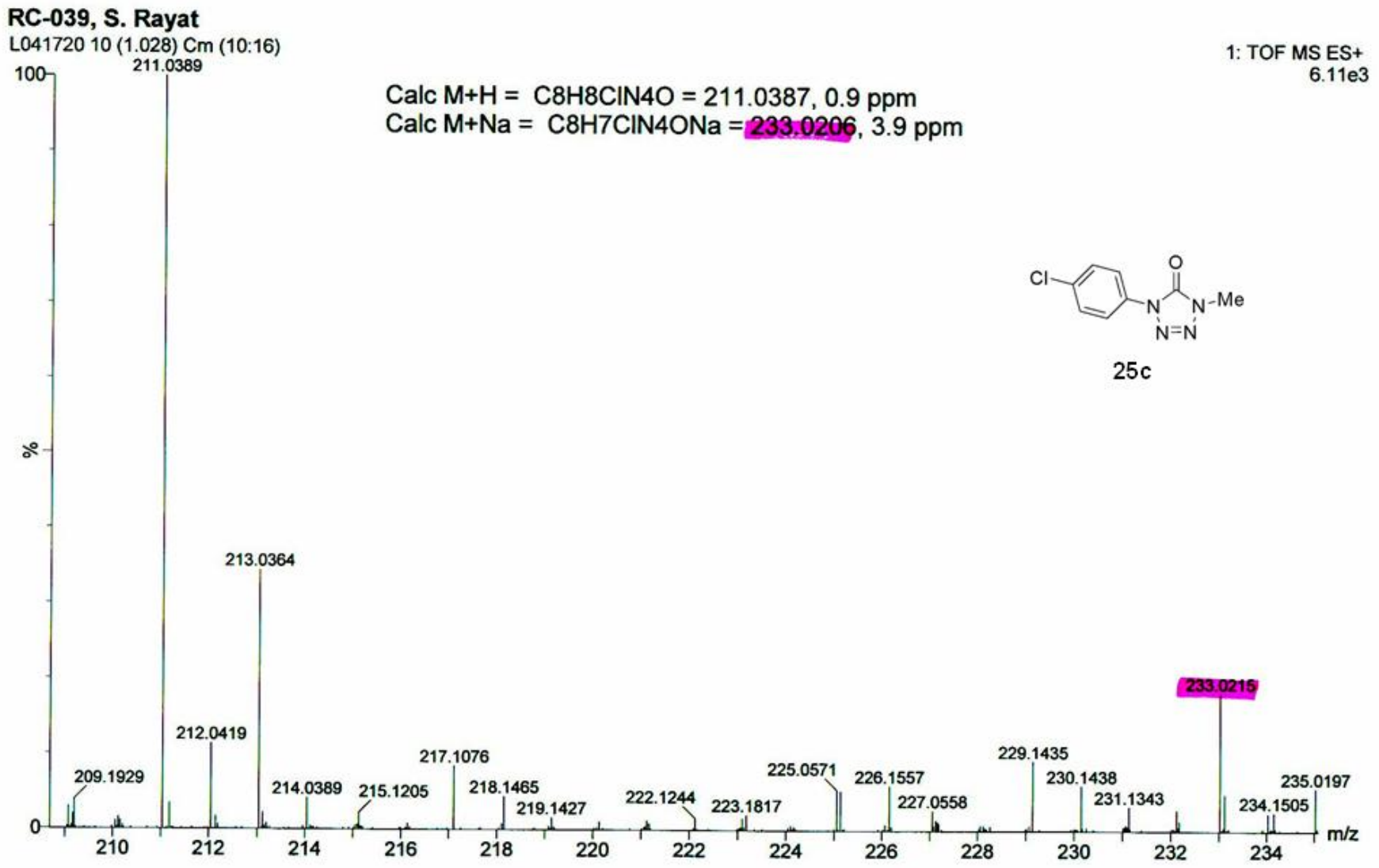
RC-039, S. Rayat
L041720 10 (1.028) Cm (10:16)
1: TOF MS ES+
6.11e3
Calc M+H = C8H8ClN4O = 211.0387, 0.9 ppm
Calc M+Na = C8H7ClN4ONa = 233.0206, 3.9 ppm
25c
100
%
0
211.0389
213.0364
212.0419
209.1929
214.0389
215.1205
217.1076
218.1465
219.1427
222.1244
223.1817
225.0571
226.1557
227.0558
229.1435
230.1438
231.1343
233.0215
234.1505
235.0197
210
212
214
216
218
220
222
224
226
228
230
232
234
m/z

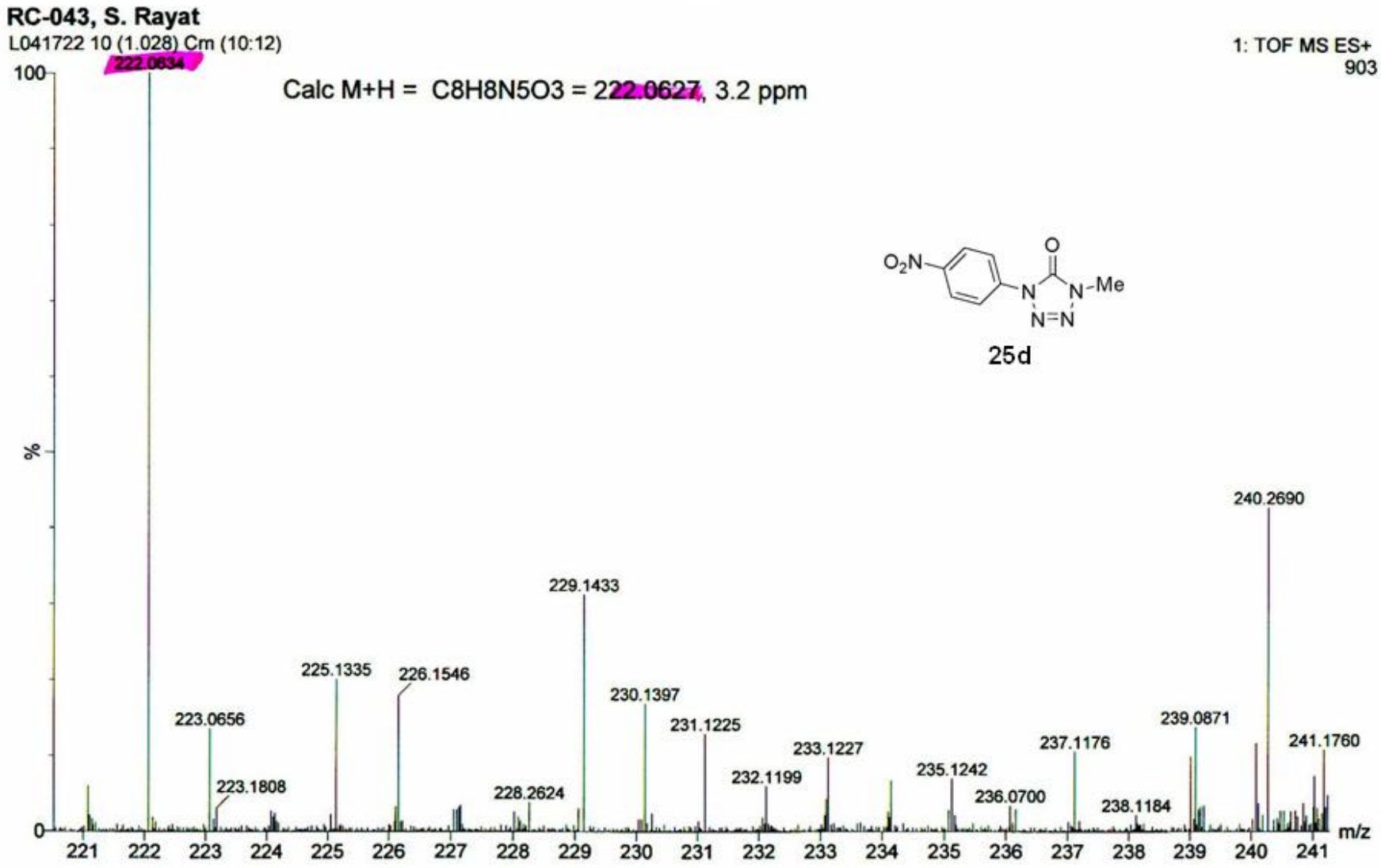
RC-043, S. Rayat
L041722 10 (1.028) Cm (10:12)
1: TOF MS ES+
903
222.0634
Calc M+H = C8H8N5O3 = 222.0627, 3.2 ppm
O2N
O
N
N
N=N
Me
25d
100
%
0
240.2690
229.1433
225.1335
226.1546
230.1397
223.0656
231.1225
239.0871
233.1227
237.1176
241.1760
232.1199
235.1242
223.1808
228.2624
236.0700
238.1184
m/z
221
222
223
224
225
226
227
228
229
230
231
232
233
234
235
236
237
238
239
240
241

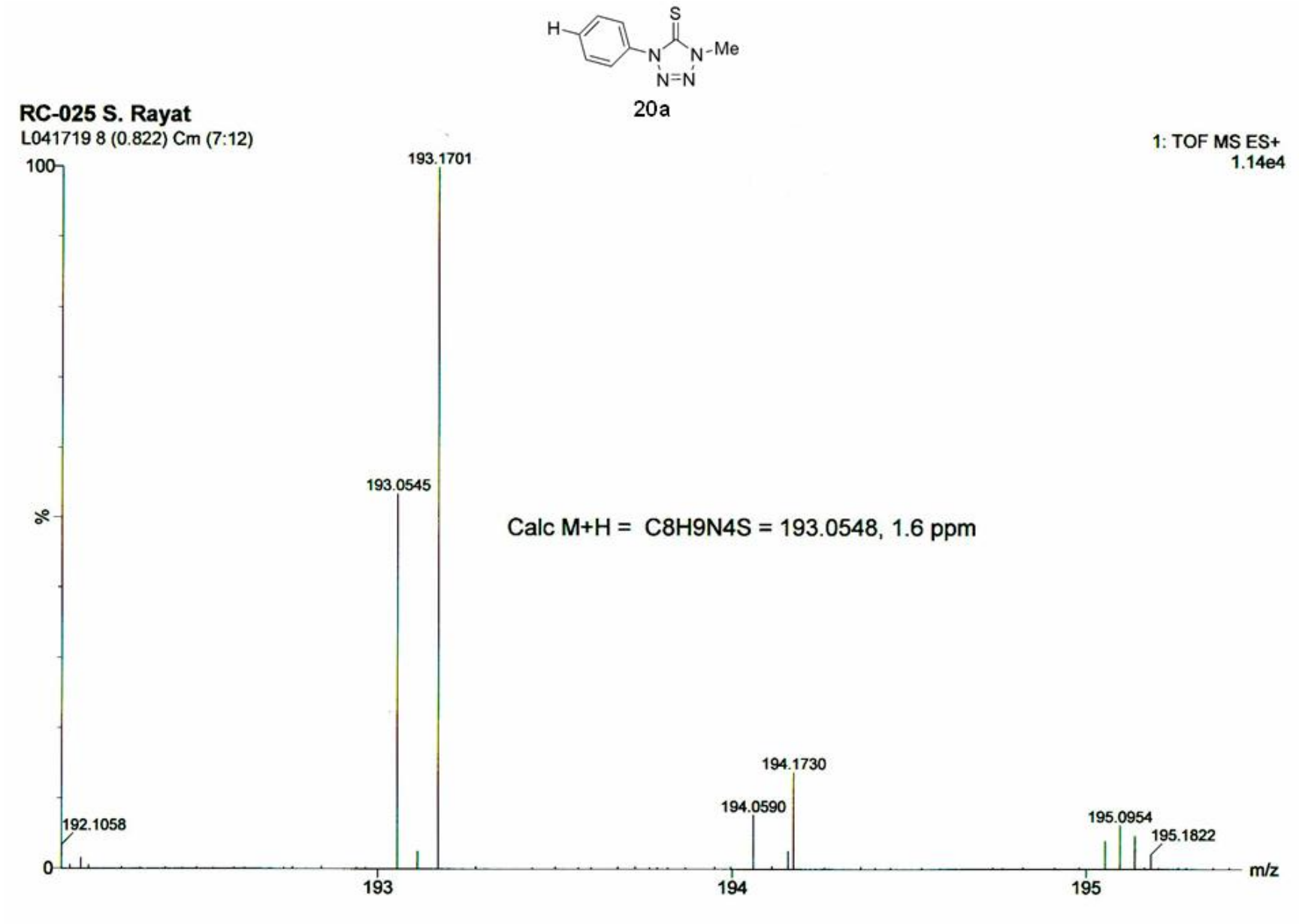
S
H
N
N
N-Me
N=N
20a
RC-025 S. Rayat
L041719 8 (0.822) Cm (7:12)
1: TOF MS ES+
1.14e4
100
%
0
193.1701
193.0545
192.1058
194.1730
194.0590
195.0954
195.1822
Calc M+H = C8H9N4S = 193.0548, 1.6 ppm
193
194
195
m/z

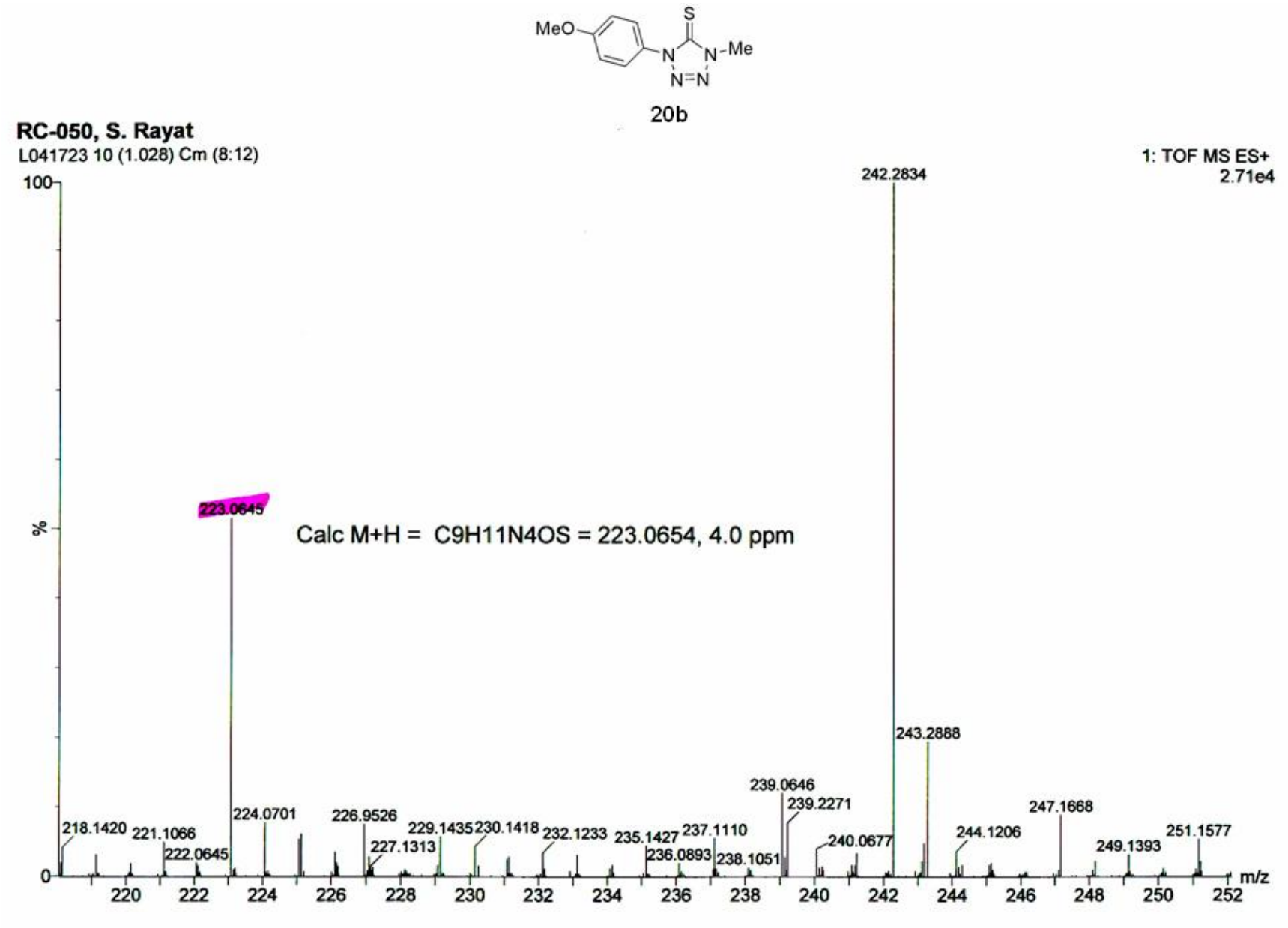
MeO
S
N
N
N
N=N
Me
20b
RC-050, S. Rayat
L041723 10 (1.028) Cm (8:12)
1: TOF MS ES+
2.71e4
100
%
0
242.2834
223.0645
Calc M+H = C9H11N4OS = 223.0654, 4.0 ppm
243.2888
239.0646
239.2271
247.1668
218.1420
221.1066
222.0645
224.0701
226.9526
227.1313
229.1435
230.1418
232.1233
235.1427
237.1110
236.0893
238.1051
240.0677
244.1206
249.1393
251.1577
m/z
220
222
224
226
228
230
232
234
236
238
240
242
244
246
248
250
252

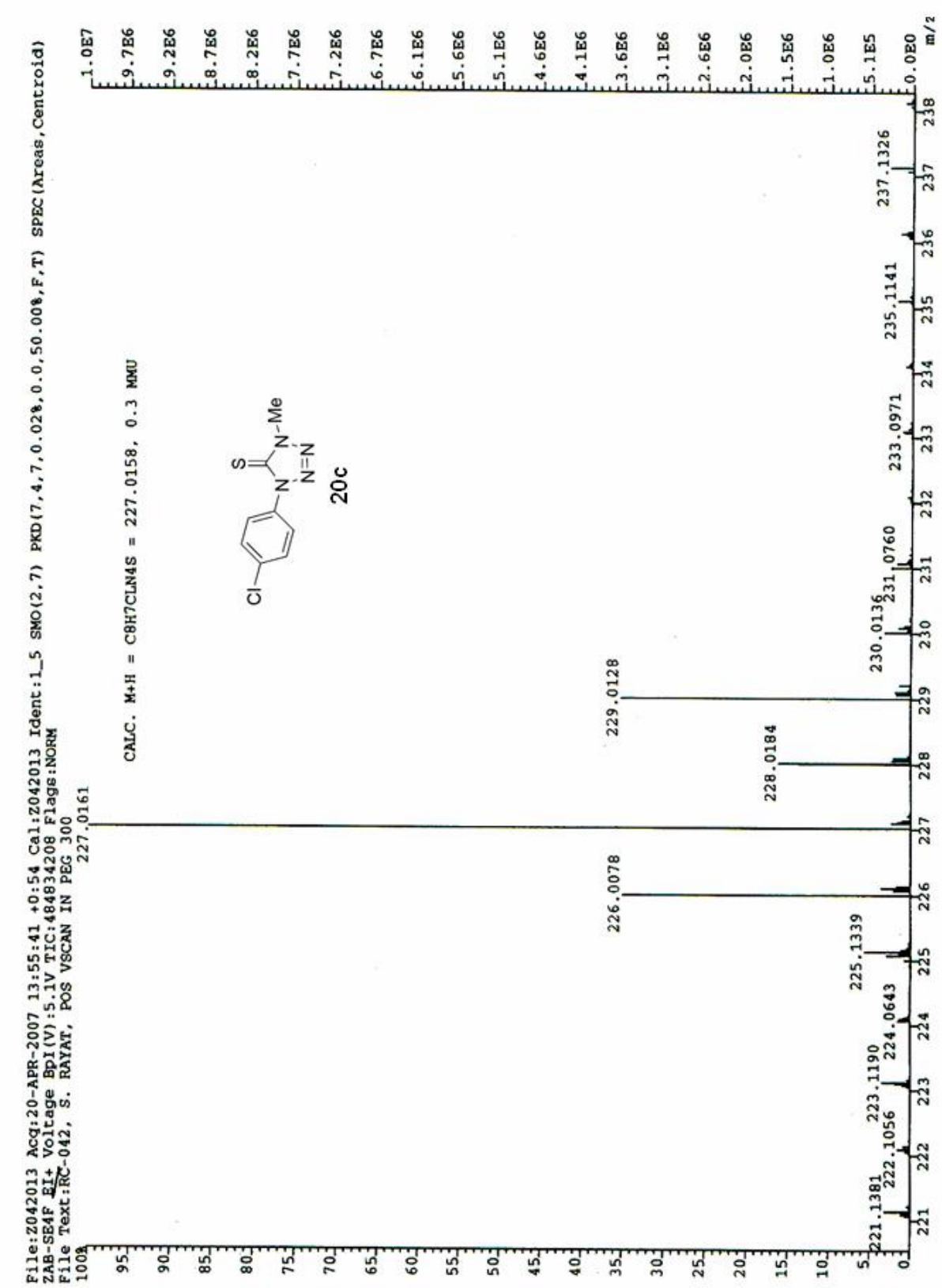
File:Z042013 Acq:20-APR-2007 13:55:41 +0:54 Cal:Z042013 Ident:1_5 SMO(2,7) PKD(7,4,7,0.02%,0.0,50.00%,F,T) SPEC(Areas,Centroid)
ZAB-SE4F EI+ Voltage BpI(V):5.1V TIC:48483208 Flags:NORM
File Text:RC-042, S. RAYAT, POS VSCAN IN PEG 300
CALC. M+H = C8H7ClN4S = 227.0158, 0.3 MMU
20c
227.0161
229.0128
228.0184
226.0078
230.0136
231.0760
233.0971
235.1141
237.1326
225.1339
221.1381
222.1056
223.1190
224.0643
m/z

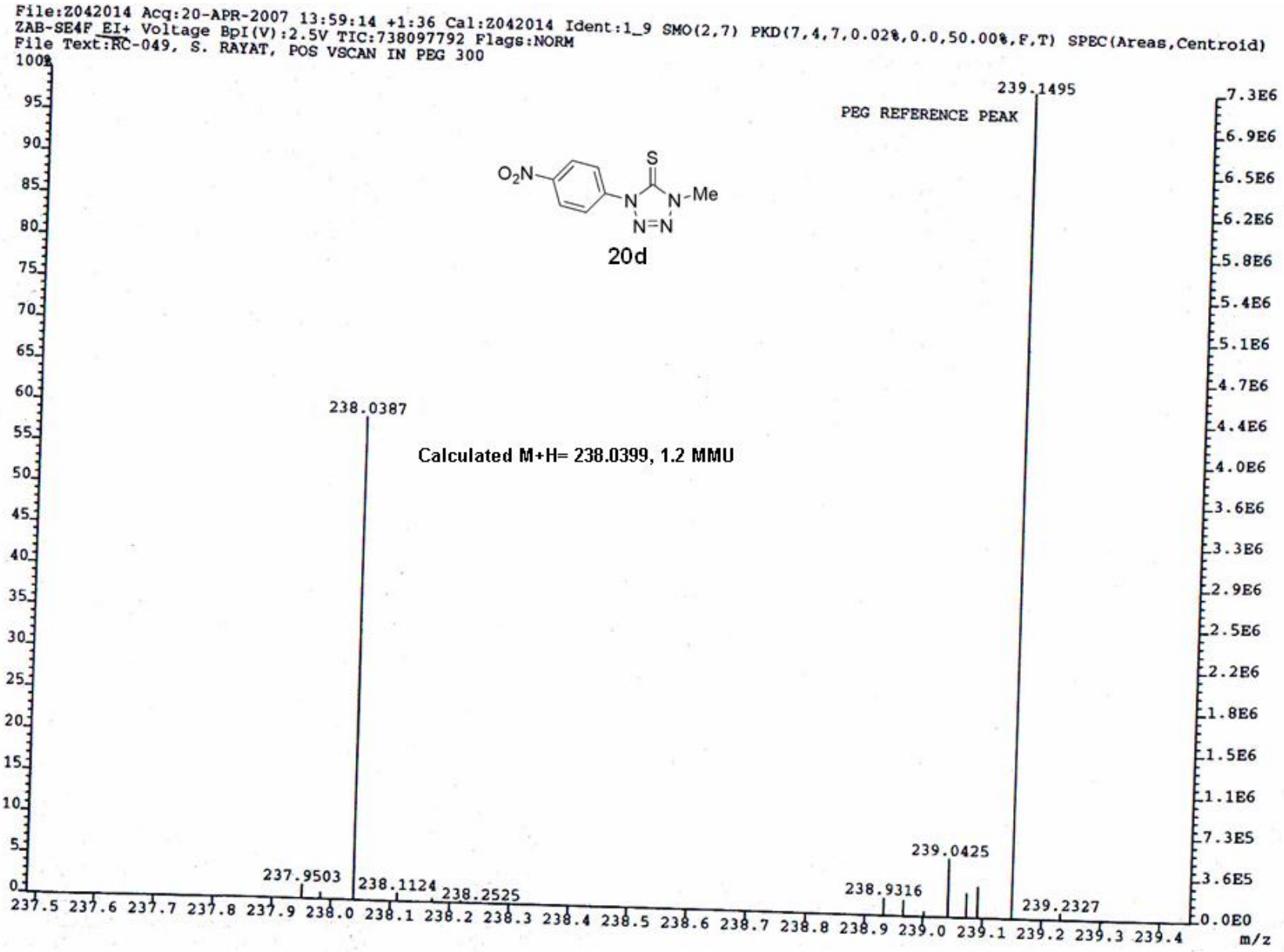
File:Z042014 Acq:20-APR-2007 13:59:14 +1:36 Cal:Z042014 Ident:1_9 SMO(2,7) PKD(7,4,7,0.02%,0.0,50.00%,F,T) SPEC(Areas,Centroid)
ZAB-SE4F_EI+ Voltage BpI(V):2.5V TIC:738097792 Flags:NORM
File Text:RC-049, S. RAYAT, POS VSCAN IN PEG 300
239.1495
PEG REFERENCE PEAK
20d
238.0387
Calculated M+H= 238.0399, 1.2 MMU
237.9503
238.1124
238.2525
238.9316
239.0425
239.2327
m/z

APPENDIX IV

OVERLAYED UV SPECTRA OF PHOTOLYSIS EXPERIMENTS

(Chapter -1)

I. Photolysis of 20a- c in THF

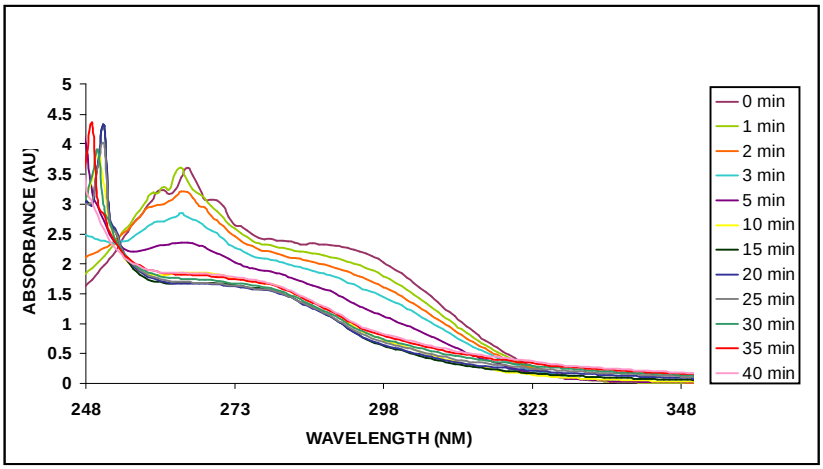

(i) Photolysis of 20a.

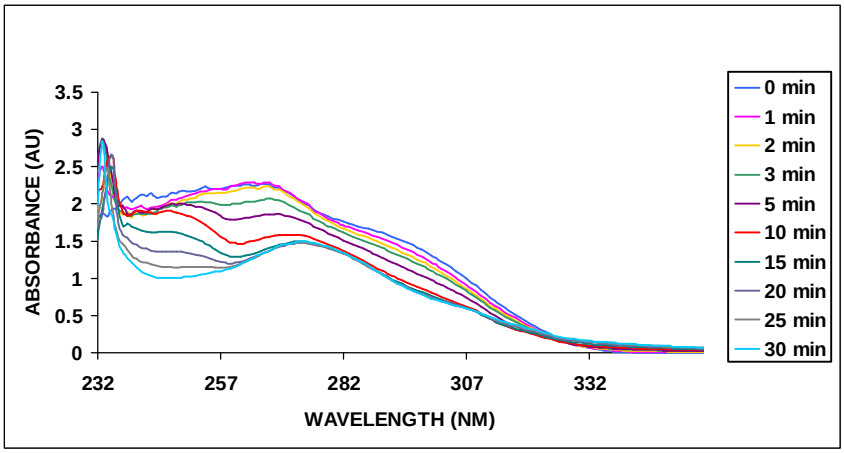

(ii) Photolysis of 20b

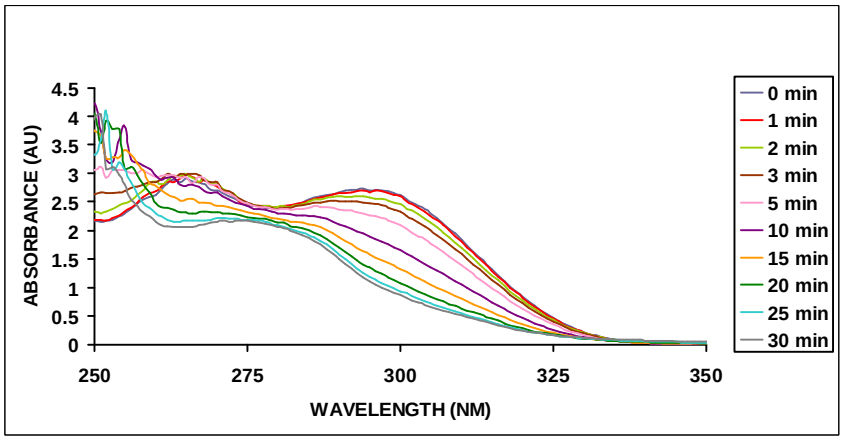

(iii) Photolysis of 20c

II. Photolysis of 20a- d in MeCN

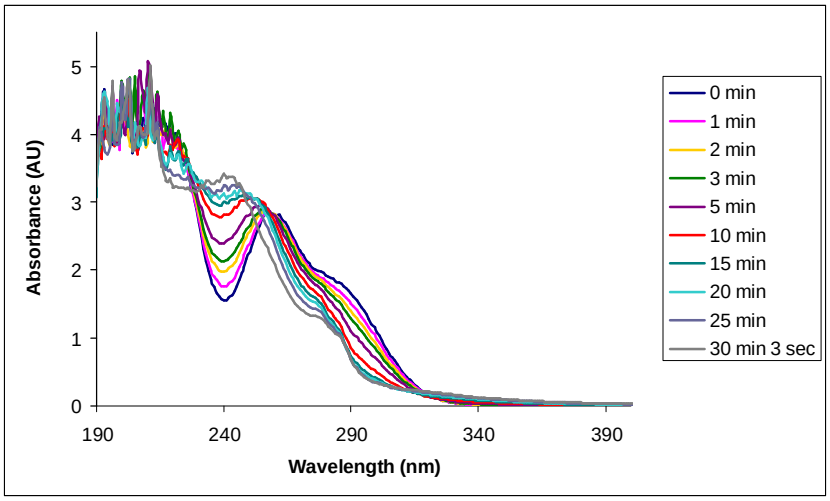

(i) Photolysis of 20a.

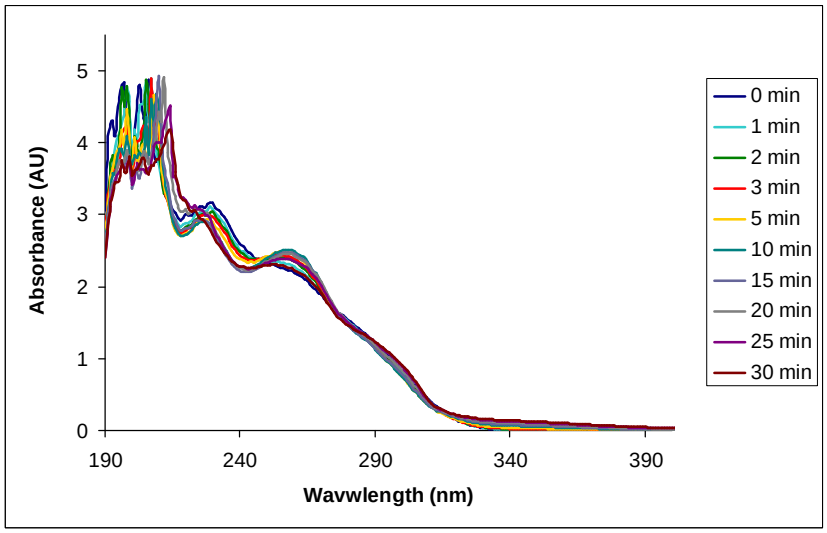

(ii) Photolysis of 20b.

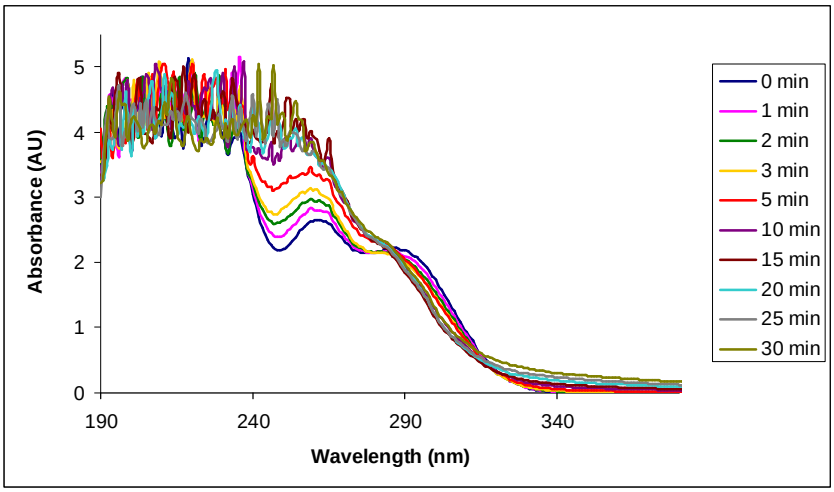

(iii) Photolysis of 20c.

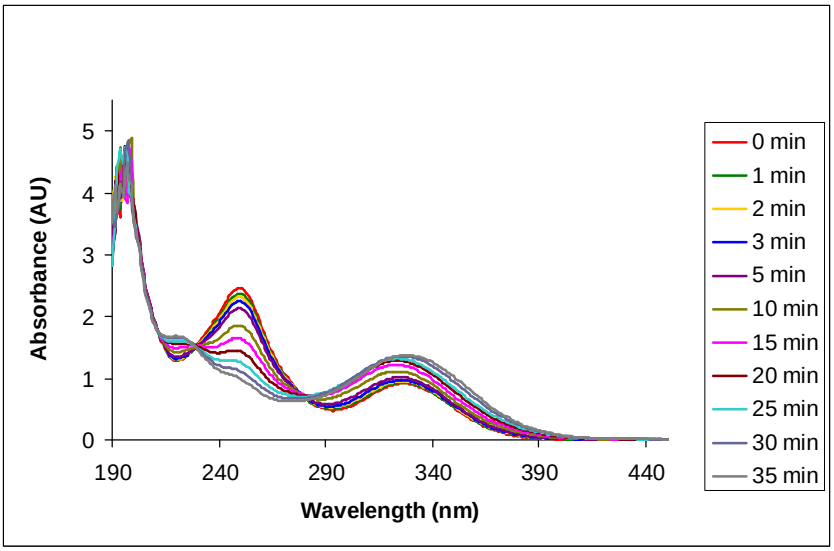

(iv) Photolysis of 20d.

APPENDIX V

OVERLAYED HPLC CHROMATOGRAMS OF PHOTOLYSIS EXPERIMENTS

(Chapter -1)

I. Photolysis of 20a- c in THF

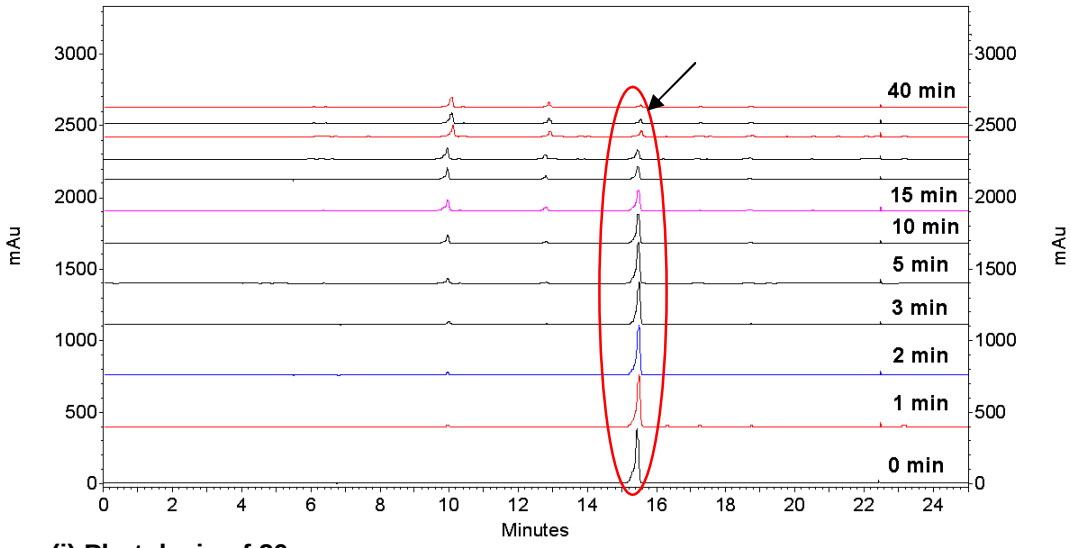

(i) Photolysis of 20a.

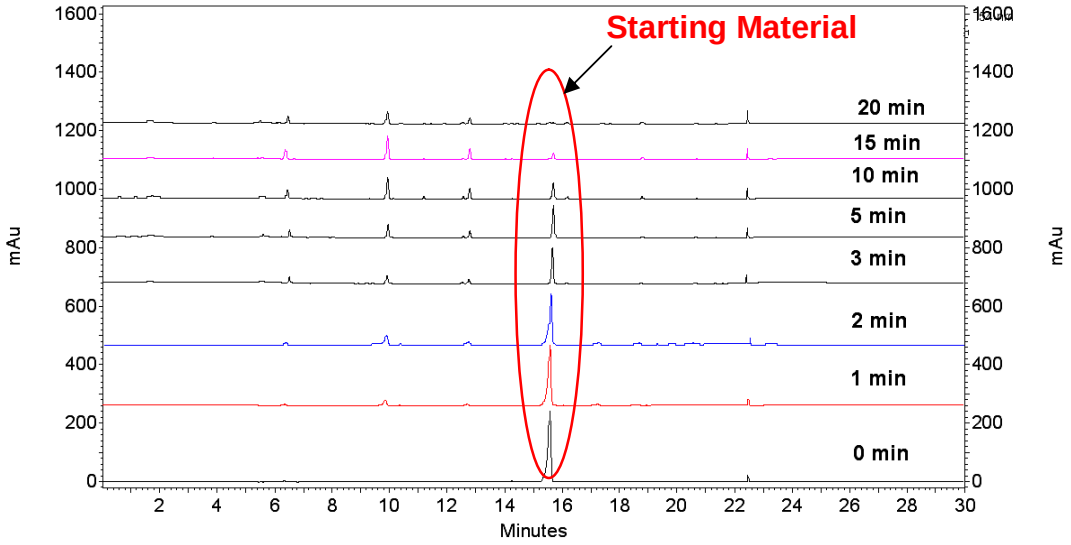

(ii) Photolysis of 20b.

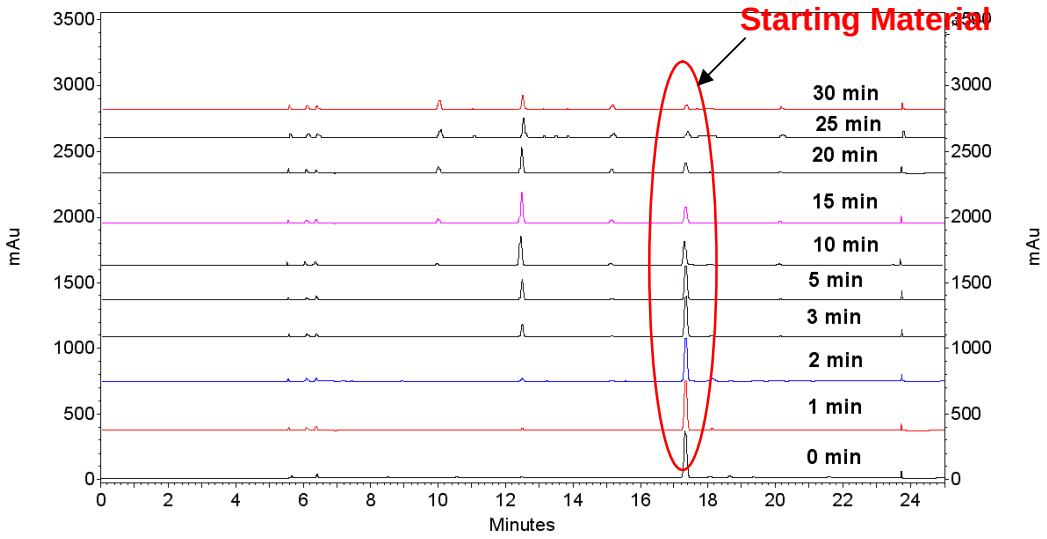

(iii) Photolysis of 20c.

II. Photolysis of 20a- d in MeCN

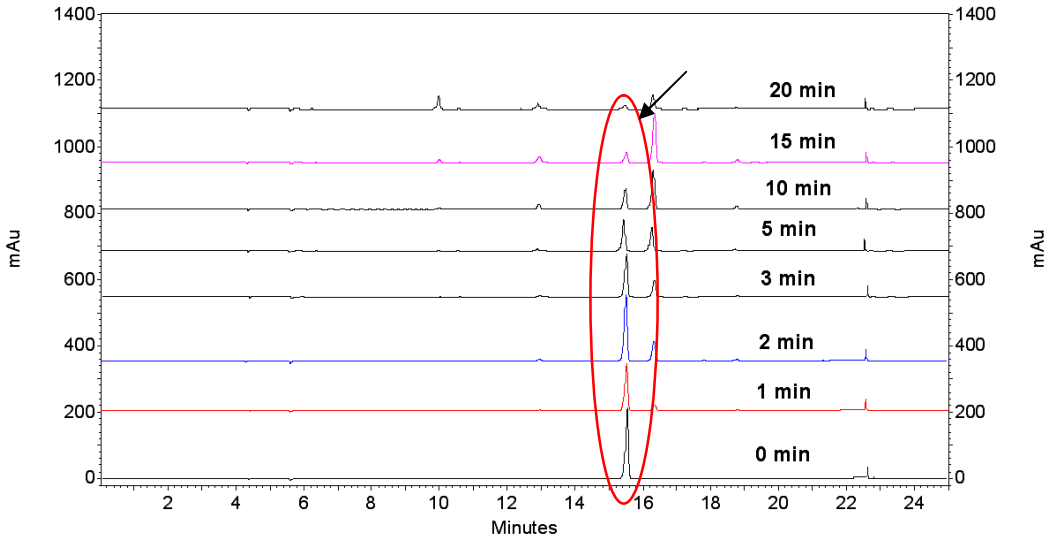

(i) Photolysis of 20a.

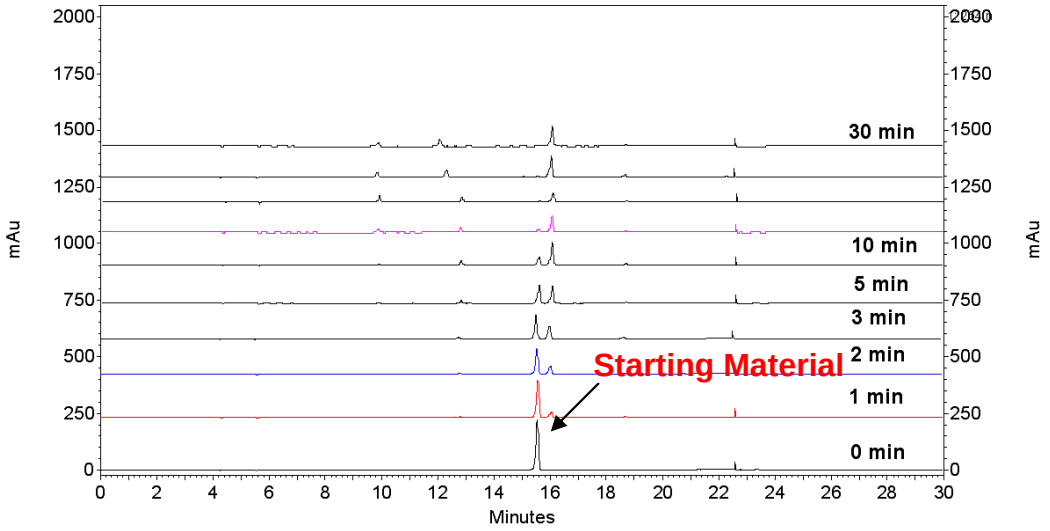

(ii) Photolysis of 20b.

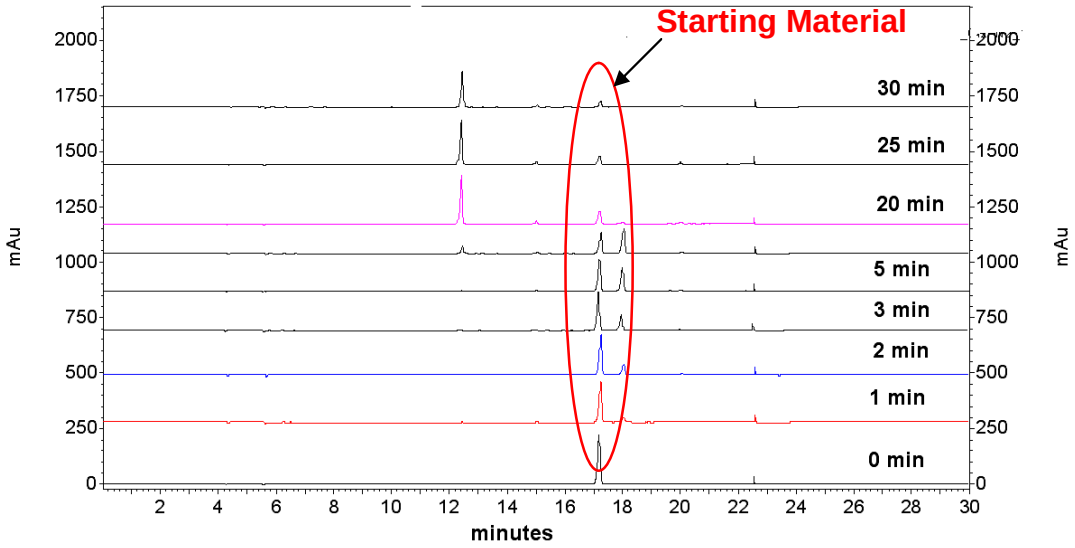

(iii) Photolysis of 20c.

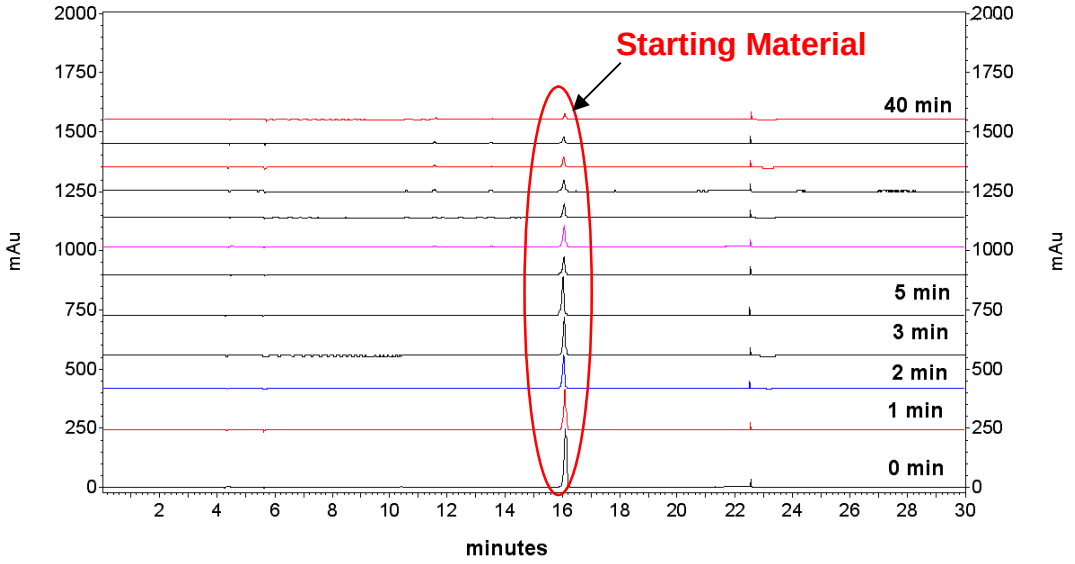

(iv) Photolysis of 20d.

APPENDIX VI

LCMS SPECTRA OF PHOTOLYSIS PRODUCTS

(Chapter -1)

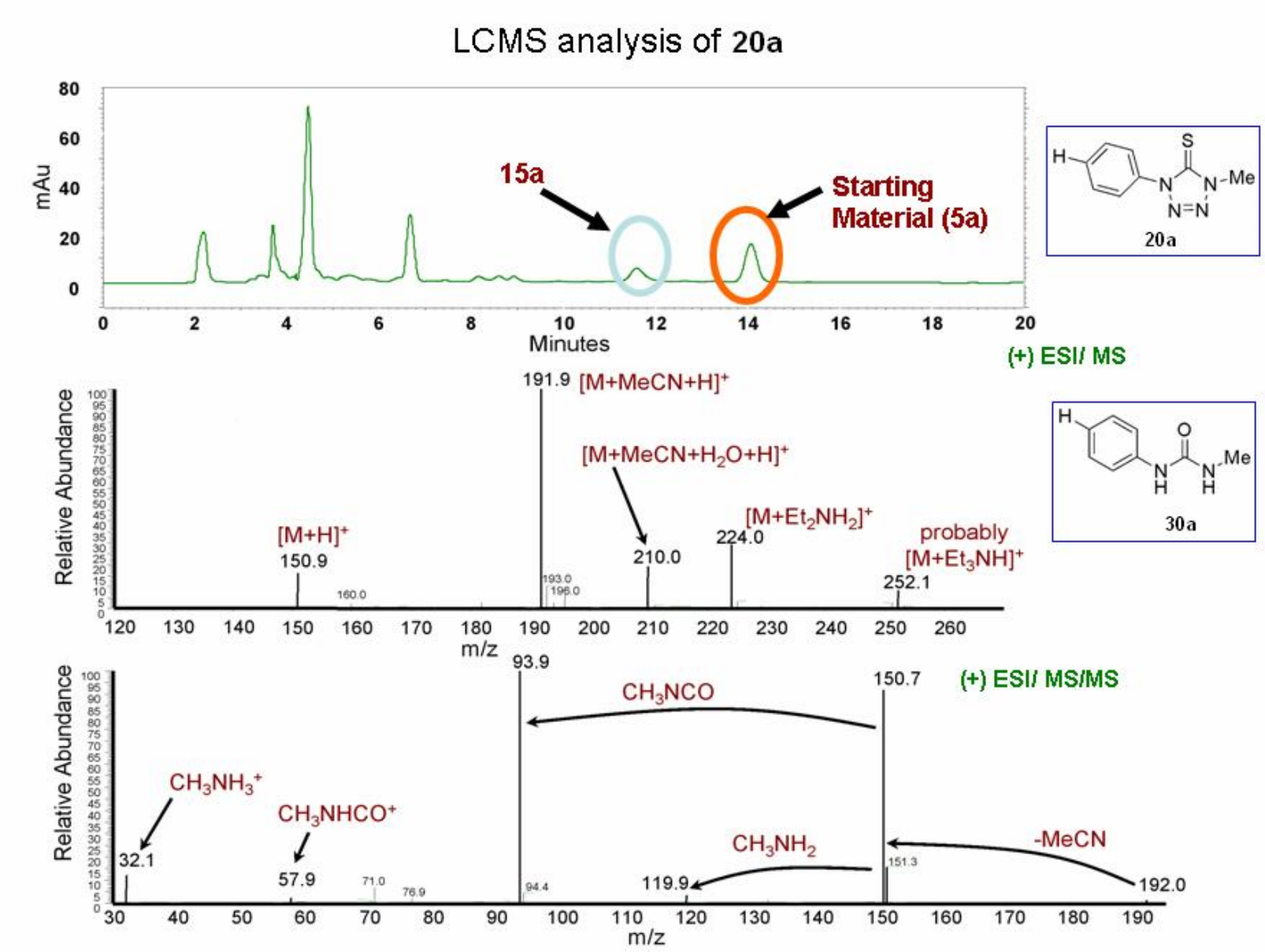
LCMS analysis of 20a
mAu
Minutes
15a
Starting Material (5a)
20a
(+) ESI/ MS
Relative Abundance
m/z
191.9 [M+MeCN+H]+
[M+MeCN+H2O+H]+
[M+H]+
150.9
210.0
[M+Et2NH2]+
224.0
probably [M+Et3NH]+
252.1
30a
(+) ESI/ MS/MS
93.9
CH3NCO
150.7
CH3NH3+
CH3NHCO+
32.1
57.9
CH3NH2
119.9
-MeCN
192.0

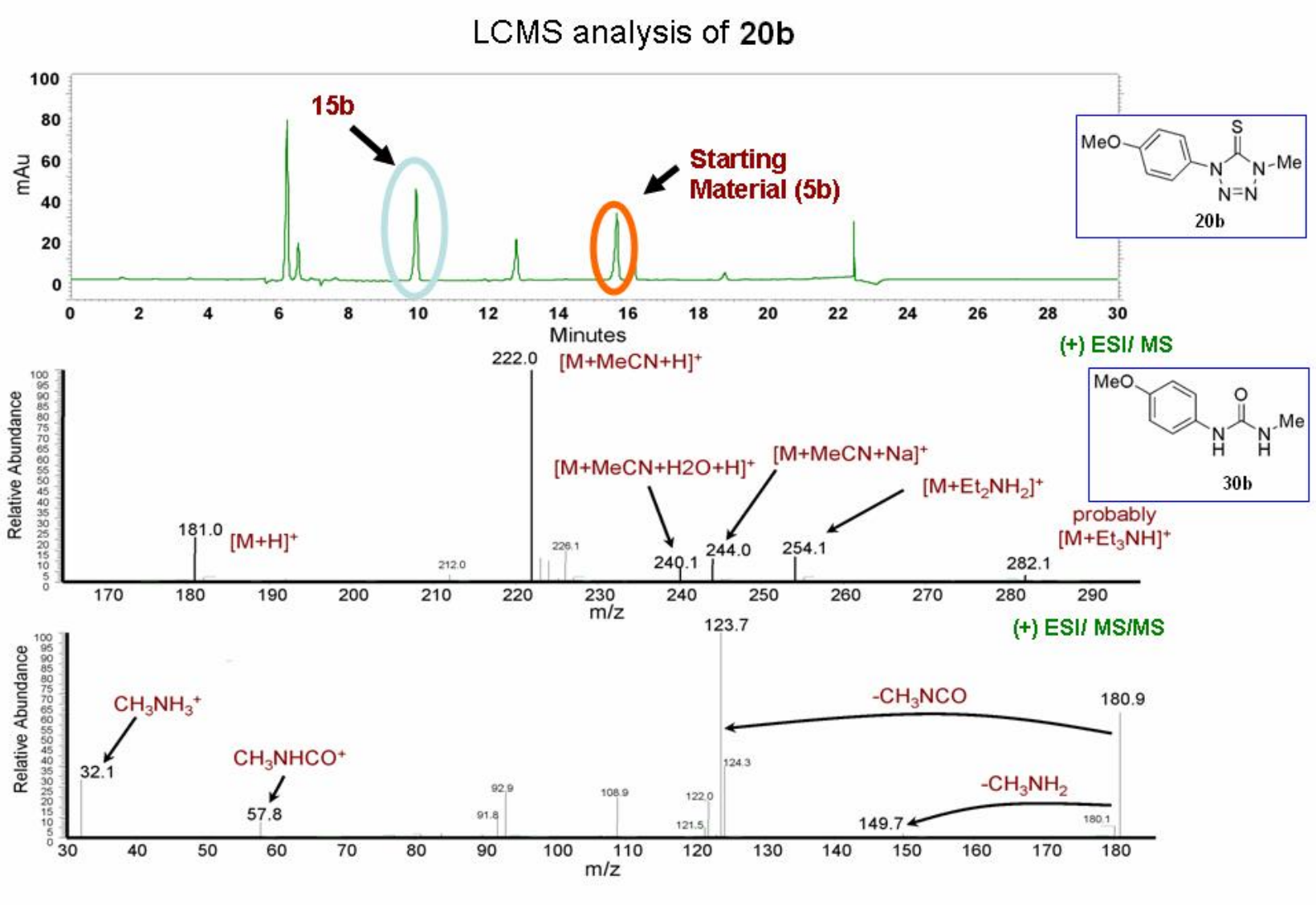
LCMS analysis of 20b
15b
Starting Material (5b)
mAu
Minutes
MeO
S
N
N-Me
N=N
20b
(+) ESI/ MS
222.0 [M+MeCN+H]+
[M+MeCN+H2O+H]+
[M+MeCN+Na]+
[M+Et2NH2]+
probably [M+Et3NH]+
181.0 [M+H]+
240.1
244.0
254.1
282.1
Relative Abundance
m/z
MeO
O
N
H
N
H
Me
30b
(+) ESI/ MS/MS
123.7
CH3NH3+
32.1
CH3NHCO+
57.8
-CH3NCO
180.9
-CH3NH2
149.7
124.3
92.9
91.8
108.9
122.0
121.5
180.1

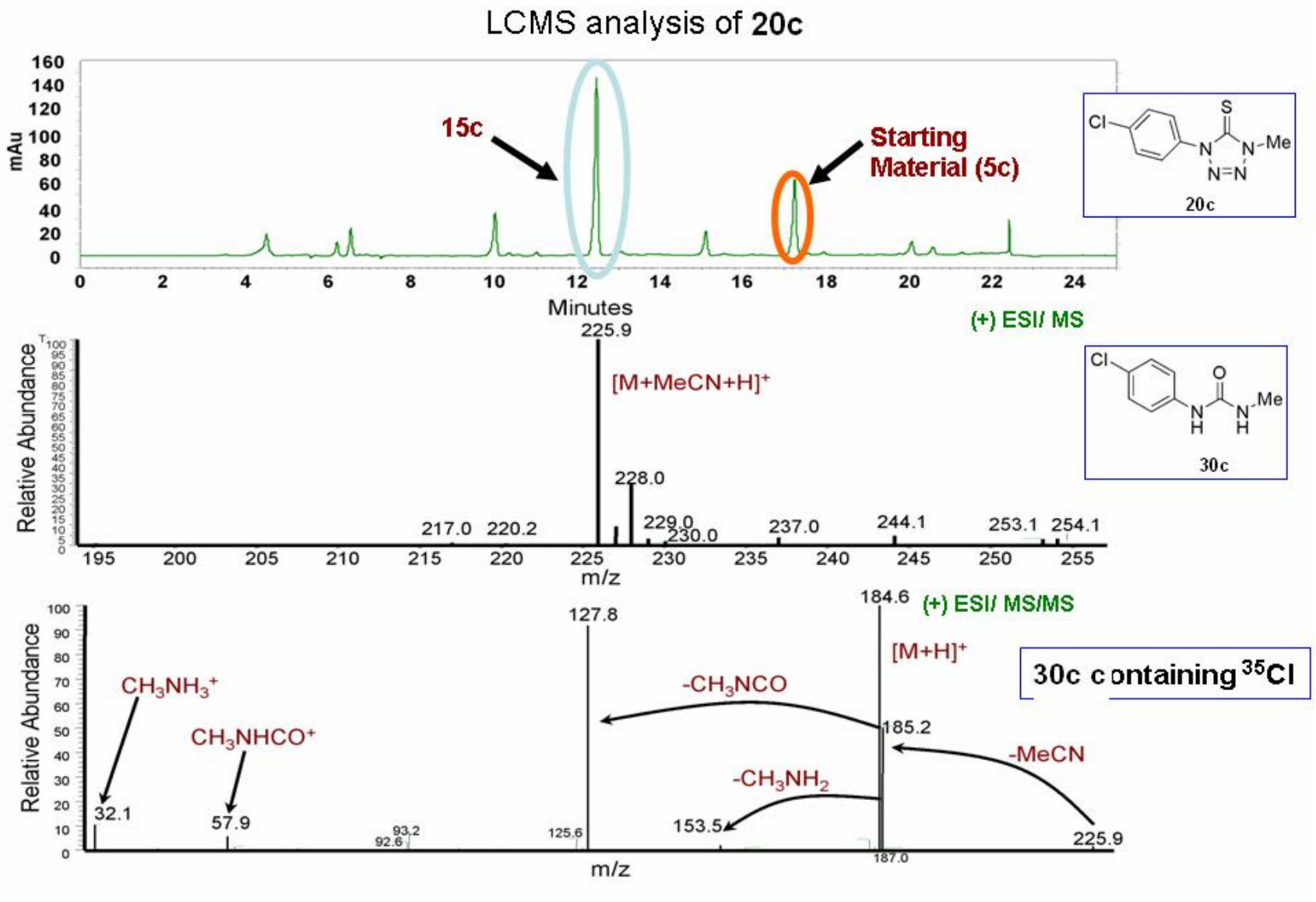
LCMS analysis of 20c
mAu
15c
Starting Material (5c)
Minutes
20c
(+) ESI/ MS
Relative Abundance
225.9
[M+MeCN+H]+
228.0
217.0
220.2
229.0
230.0
237.0
244.1
253.1
254.1
m/z
30c
(+) ESI/ MS/MS
184.6
127.8
[M+H]+
CH3NH3+
CH3NHCO+
-CH3NCO
185.2
-MeCN
-CH3NH2
153.5
225.9
32.1
57.9
93.2
92.6
125.6
187.0
30c containing 35Cl

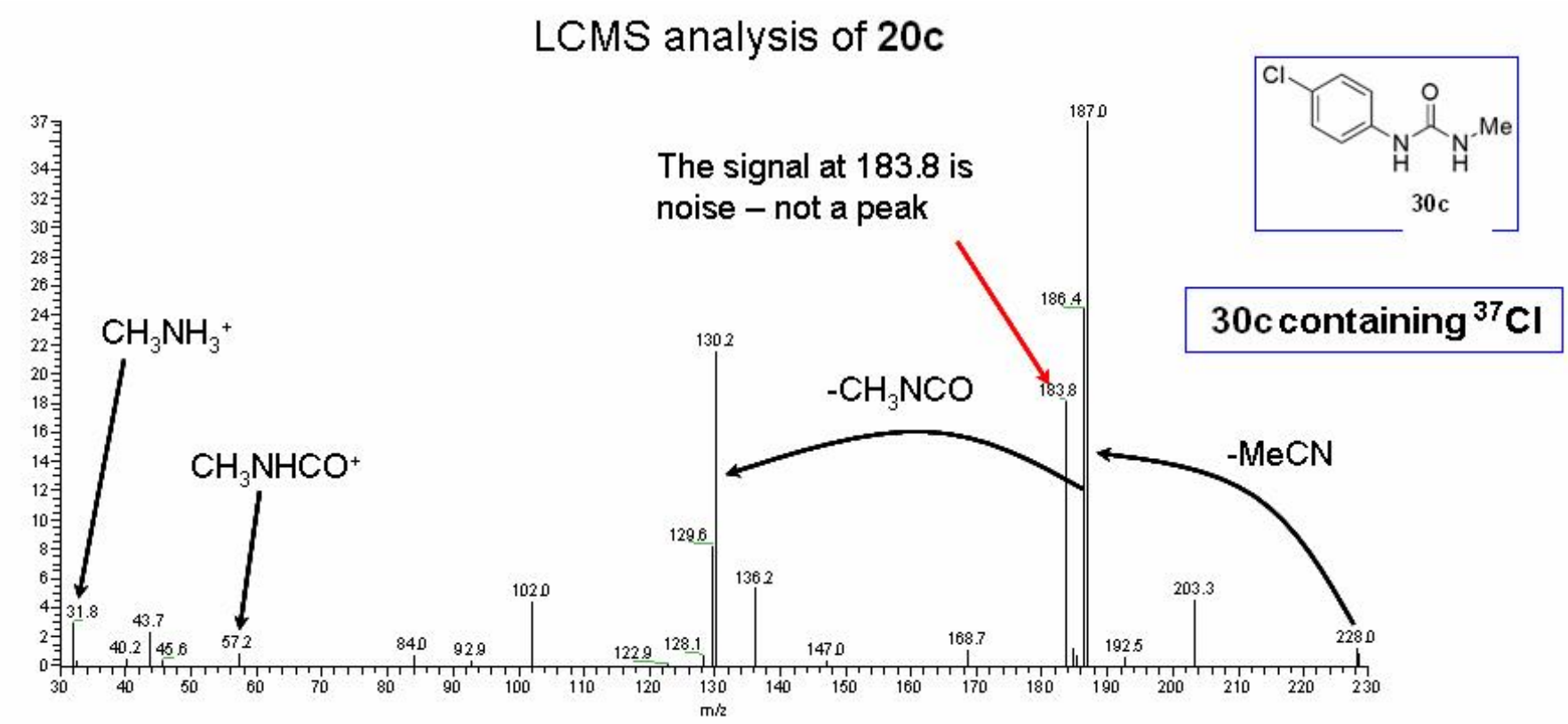
LCMS analysis of 20c
The signal at 183.8 is noise – not a peak
Cl
O
N
H
N
H
Me
30c
30c containing 37Cl
CH3NH3+
CH3NHCO+
-CH3NCO
-MeCN
187.0
186.4
130.2
183.8
129.6
136.2
102.0
203.3
31.8
43.7
40.2
45.6
57.2
84.0
92.9
122.9
128.1
147.0
168.7
192.5
228.0
m/z

APPENDIX VII

GCMS SPECTRA OF PHOTOLYSIS PRODUCTS

(Chapter -1)

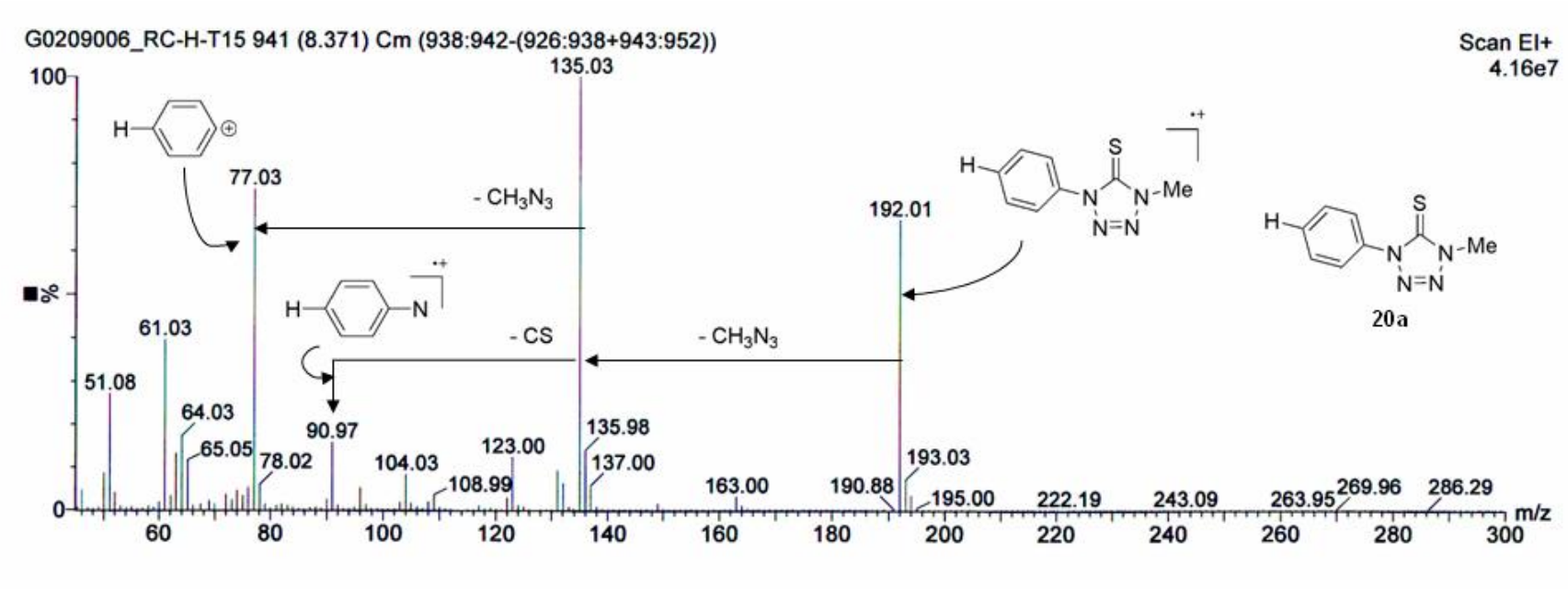
G0209006_RC-H-T15 941 (8.371) Cm (938:942-(926:938+943:952))
Scan EI+
4.16e7
100
%
0
135.03
77.03
- CH3N3
192.01
- CS
- CH3N3
61.03
51.08
64.03
65.05
78.02
90.97
104.03
108.99
123.00
135.98
137.00
163.00
190.88
193.03
195.00
222.19
243.09
263.95
269.96
286.29
m/z
60
80
100
120
140
160
180
200
220
240
260
280
300
20a

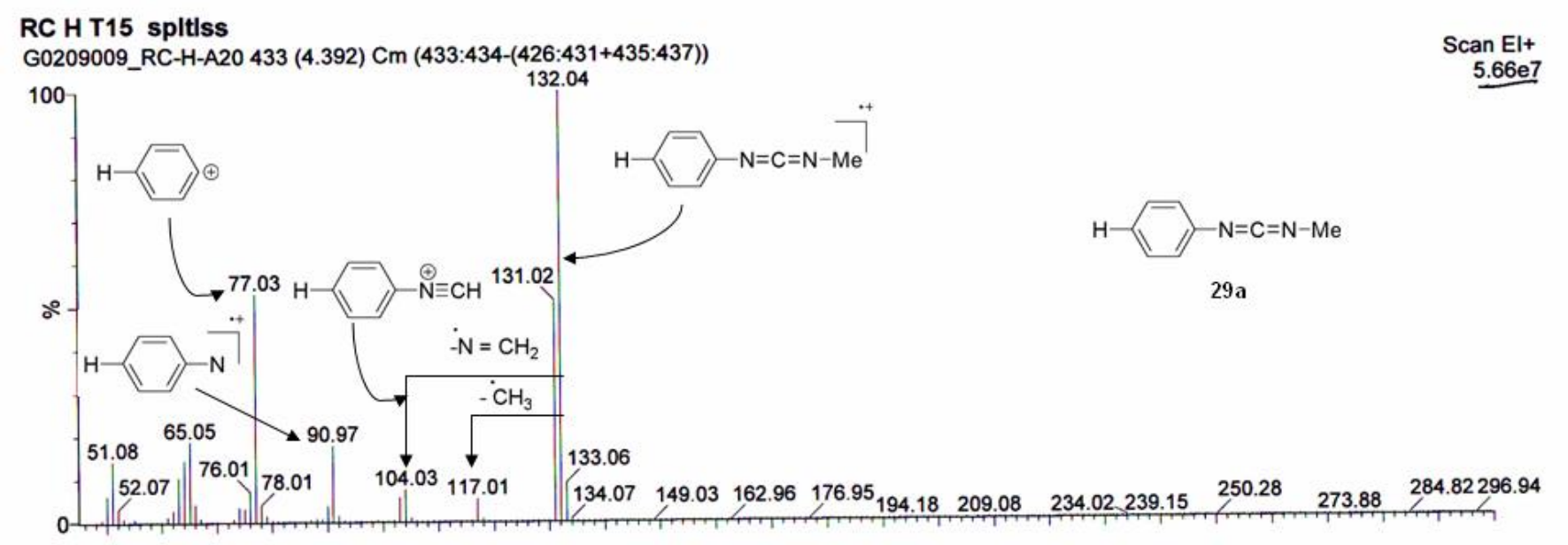
RC H T15 spltlss
G0209009_RC-H-A20 433 (4.392) Cm (433:434-(426:431+435:437))
Scan EI+
5.66e7
100
%
0
132.04
131.02
77.03
90.97
65.05
51.08
52.07
76.01
78.01
104.03
117.01
133.06
134.07
149.03
162.96
176.95
194.18
209.08
234.02
239.15
250.28
273.88
284.82
296.94
-N = CH2
- CH3
N=C=N-Me
29a

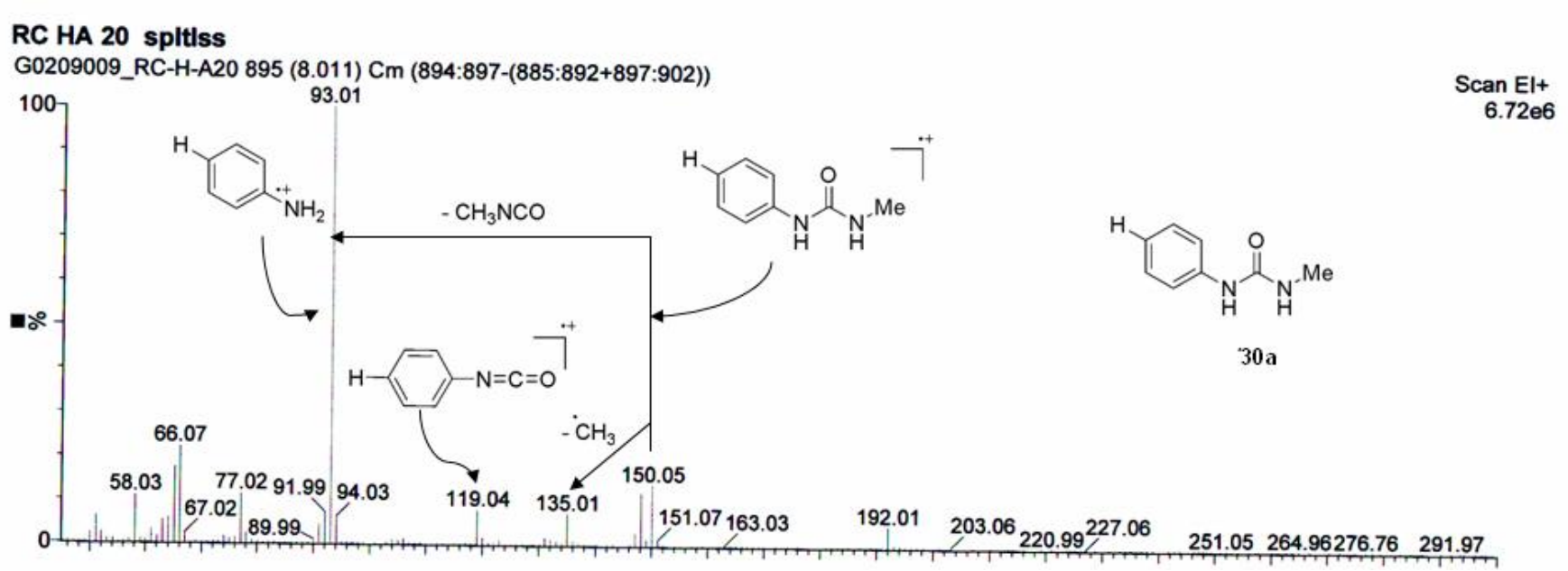
RC HA 20 spitiss
G0209009_RC-H-A20 895 (8.011) Cm (894:897-(885:892+897:902))
Scan EI+
6.72e6
100
%
0
93.01
66.07
58.03
77.02
67.02
91.99
89.99
94.03
119.04
135.01
150.05
151.07
163.03
192.01
203.06
220.99
227.06
251.05
264.96
276.76
291.97
- CH3NCO
- CH3
N=C=O
Me
30a

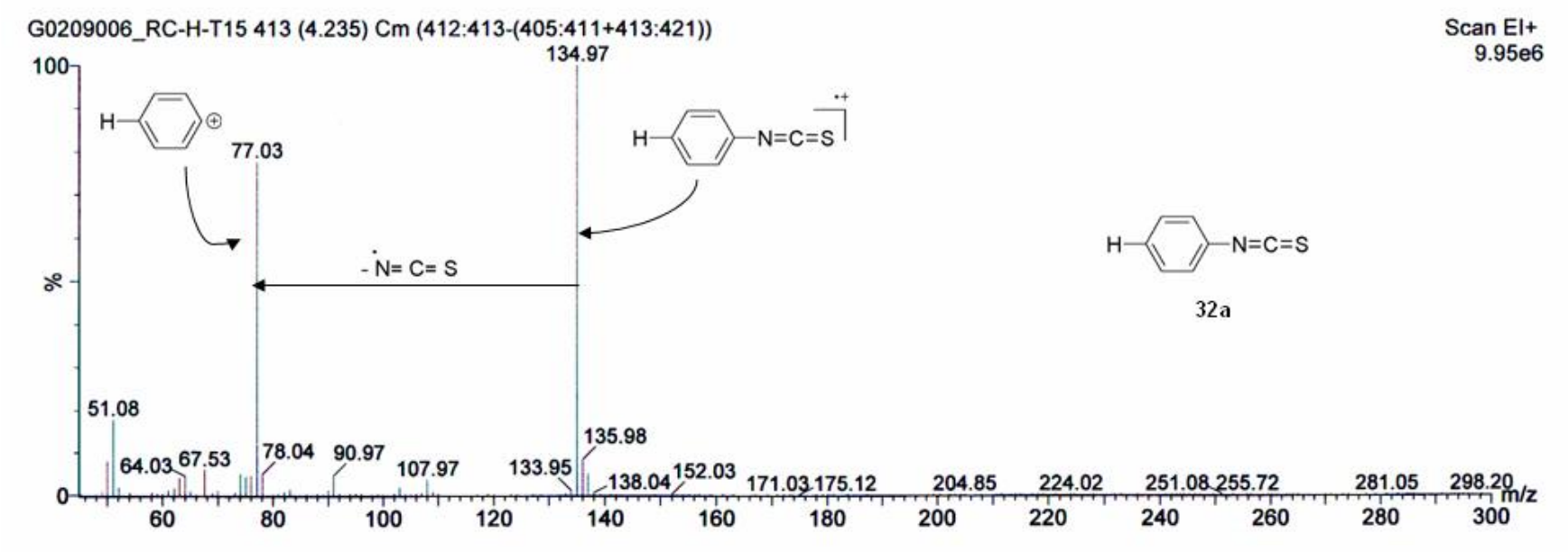
G0209006_RC-H-T15 413 (4.235) Cm (412:413-(405:411+413:421))
Scan EI+
9.95e6
100
%
0
134.97
77.03
- N= C= S
51.08
64.03
67.53
78.04
90.97
107.97
133.95
135.98
138.04
152.03
171.03
175.12
204.85
224.02
251.08
255.72
281.05
298.20
m/z
60
80
100
120
140
160
180
200
220
240
260
280
300
32a

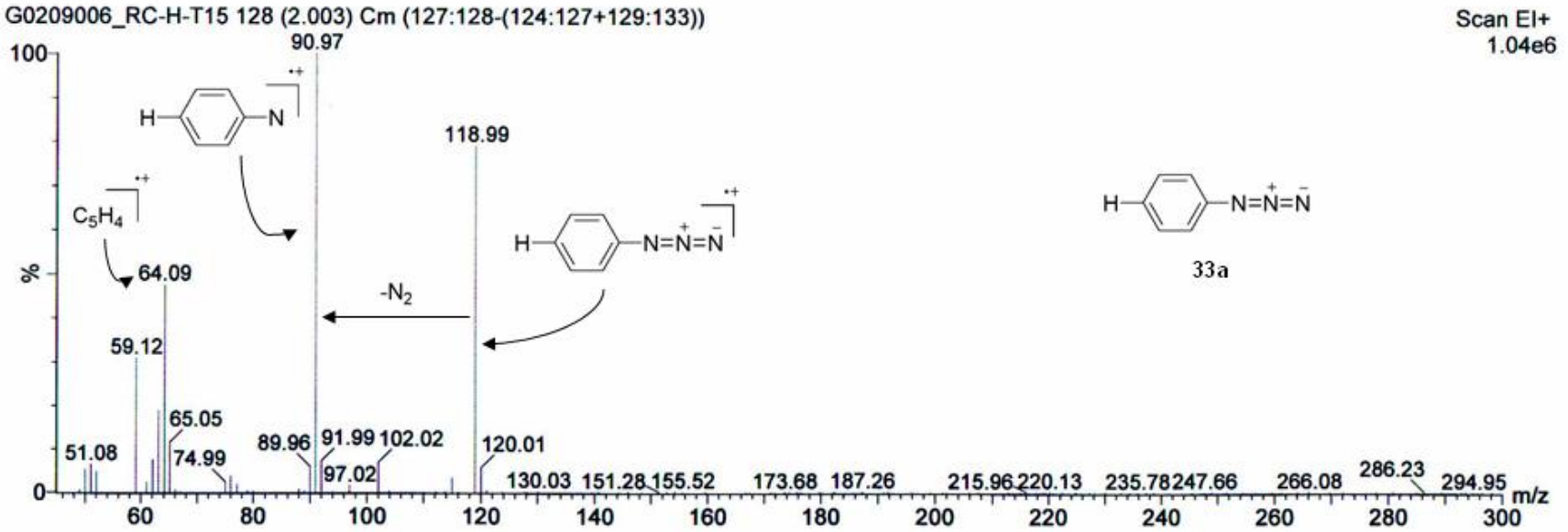
G0209006_RC-H-T15 128 (2.003) Cm (127:128-(124:127+129:133))
Scan EI+
1.04e6
100
%
0
90.97
118.99
64.09
59.12
65.05
51.08
74.99
89.96
91.99
97.02
102.02
120.01
130.03
151.28
155.52
173.68
187.26
215.96
220.13
235.78
247.66
266.08
286.23
294.95
m/z
60
80
100
120
140
160
180
200
220
240
260
280
300
C_5H_4
$-N_2$
33a

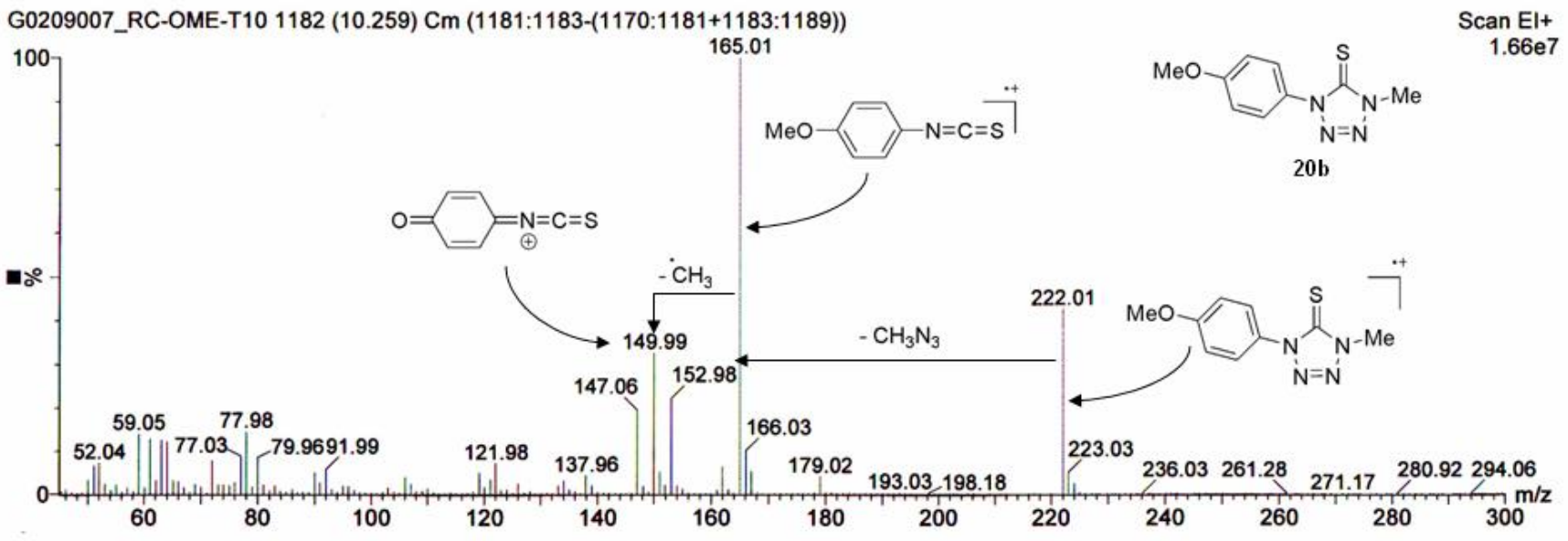
G0209007_RC-OME-T10 1182 (10.259) Cm (1181:1183-(1170:1181+1183:1189))
Scan EI+
1.66e7
100
%
0
165.01
MeO
N=C=S
20b
- ·CH3
149.99
222.01
- CH3N3
147.06
152.98
166.03
59.05
77.98
52.04
77.03
79.96
91.99
121.98
137.96
179.02
193.03
198.18
223.03
236.03
261.28
271.17
280.92
294.06
m/z
60
80
100
120
140
160
180
200
220
240
260
280
300

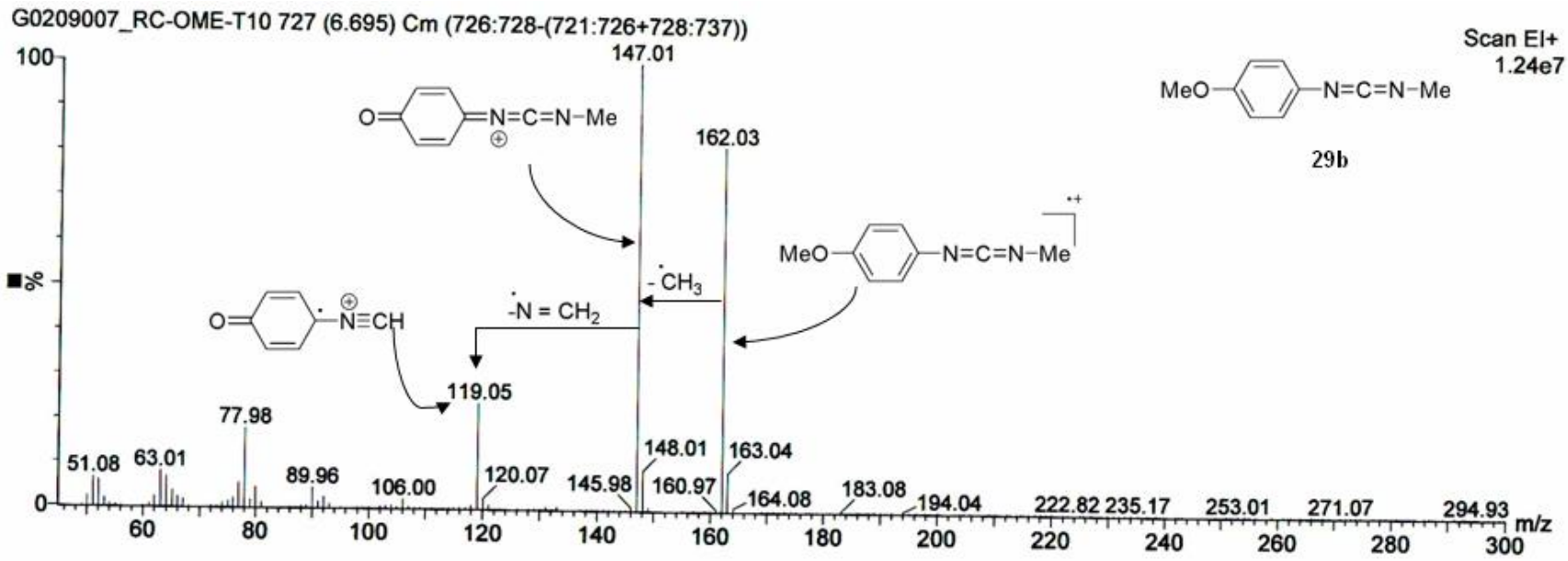
G0209007_RC-OME-T10 727 (6.695) Cm (726:728-(721:726+728:737))
Scan EI+
1.24e7
100
%
0
147.01
162.03
119.05
77.98
51.08
63.01
89.96
106.00
120.07
145.98
148.01
160.97
163.04
164.08
183.08
194.04
222.82
235.17
253.01
271.07
294.93
m/z
60
80
100
120
140
160
180
200
220
240
260
280
300
MeO
N=C=N-Me
29b
- CH3
-N = CH2

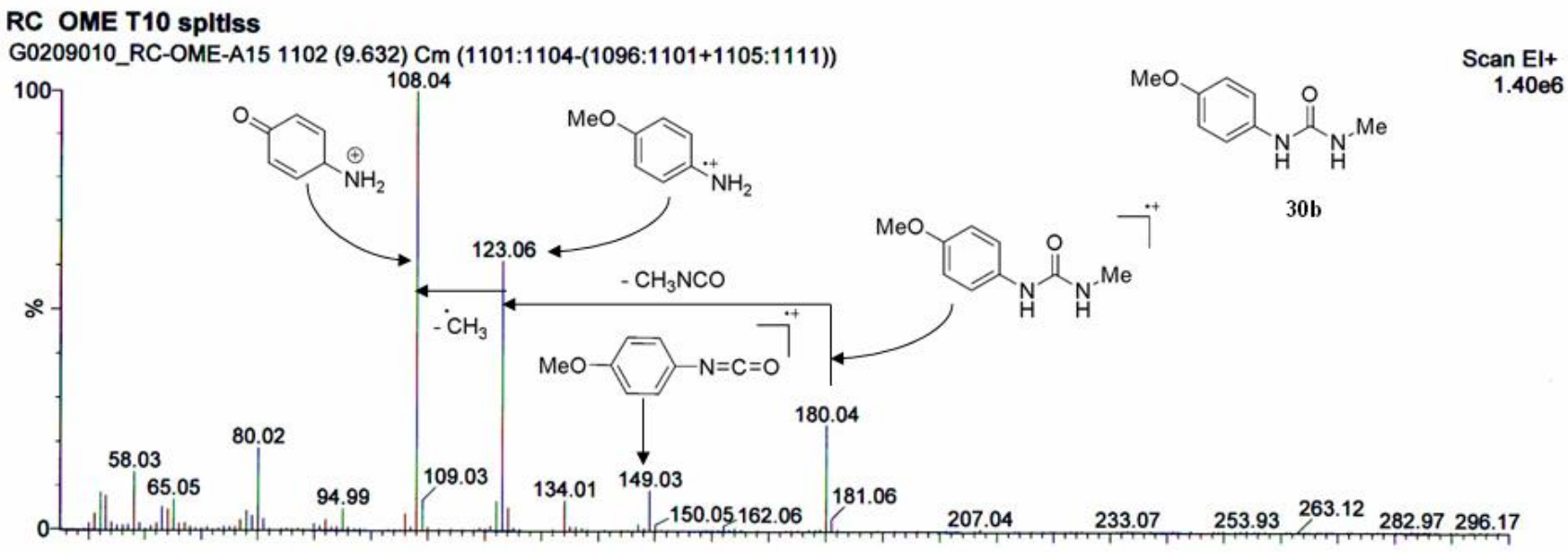
RC OME T10 spltlss
G0209010_RC-OME-A15 1102 (9.632) Cm (1101:1104-(1096:1101+1105:1111))
Scan EI+
1.40e6
100
%
0
108.04
123.06
- CH3NCO
- CH3
180.04
80.02
58.03
65.05
94.99
109.03
134.01
149.03
150.05
162.06
181.06
207.04
233.07
253.93
263.12
282.97
296.17
30b

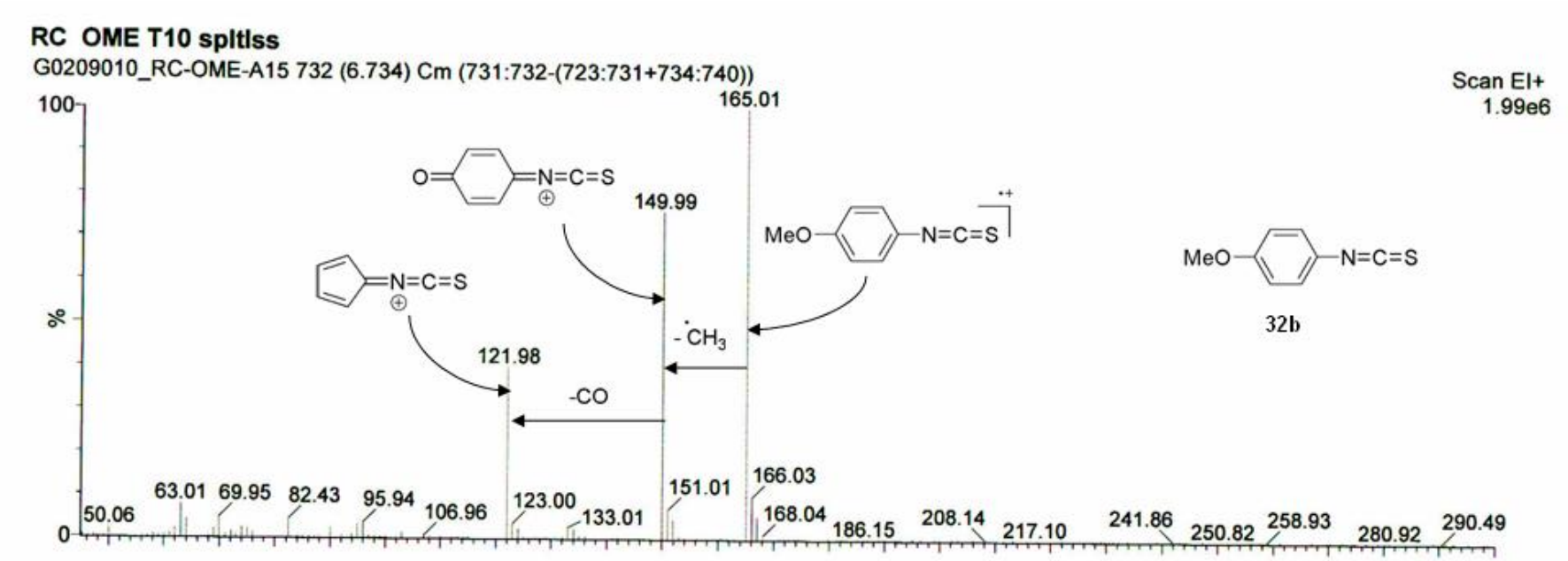
RC OME T10 spltlss
G0209010_RC-OME-A15 732 (6.734) Cm (731:732-(723:731+734:740))
Scan EI+
1.99e6
100
%
0
165.01
149.99
121.98
- ·CH3
-CO
MeO
N=C=S
32b
50.06
63.01
69.95
82.43
95.94
106.96
123.00
133.01
151.01
166.03
168.04
186.15
208.14
217.10
241.86
250.82
258.93
280.92
290.49

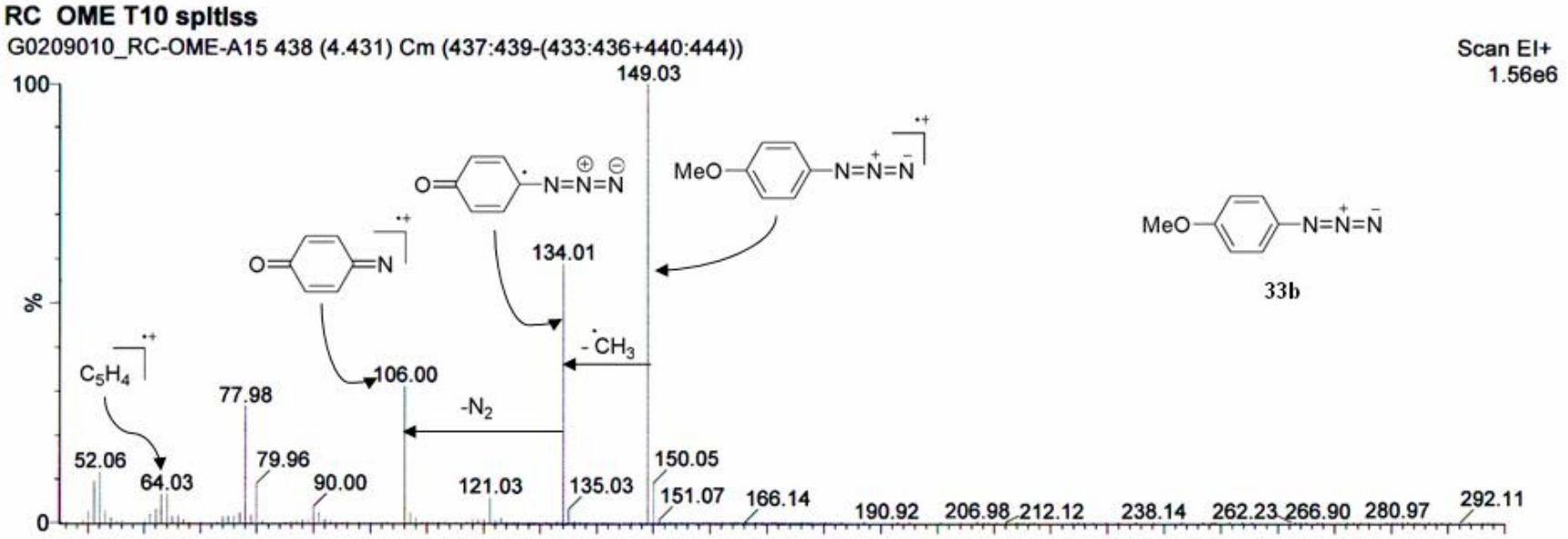
RC OME T10 spitlss
G0209010_RC-OME-A15 438 (4.431) Cm (437:439-(433:436+440:444))
Scan EI+
1.56e6
100
%
0
149.03
134.01
106.00
77.98
52.06
64.03
79.96
90.00
121.03
135.03
150.05
151.07
166.14
190.92
206.98
212.12
238.14
262.23
266.90
280.97
292.11
- CH3
-N2
C5H4
MeO
N=N=N
33b

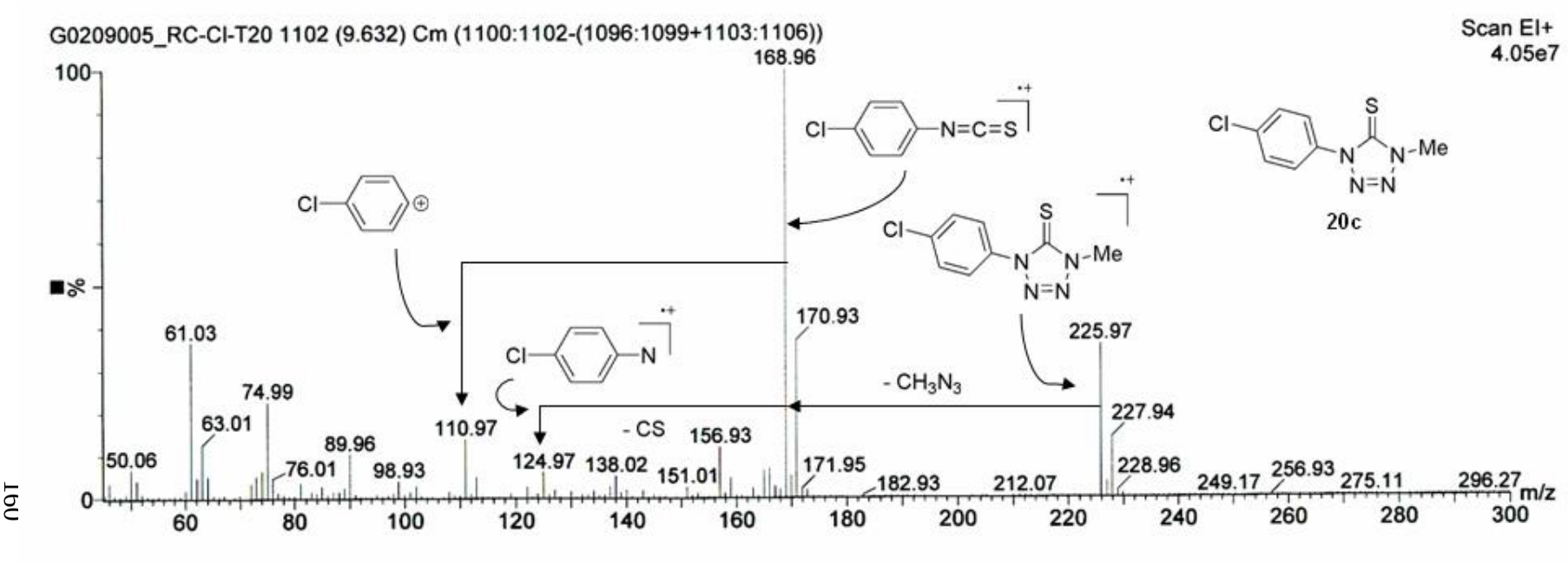
G0209005_RC-Cl-T20 1102 (9.632) Cm (1100:1102-(1096:1099+1103:1106))
Scan EI+
4.05e7
168.96
100
%
0
61.03
74.99
63.01
50.06
89.96
76.01
98.93
110.97
124.97
138.02
151.01
156.93
- CS
170.93
171.95
182.93
212.07
225.97
227.94
228.96
249.17
256.93
275.11
296.27
- CH3N3
m/z
60
80
100
120
140
160
180
200
220
240
260
280
300
Cl
N=C=S
N
S
N-Me
N=N
20c

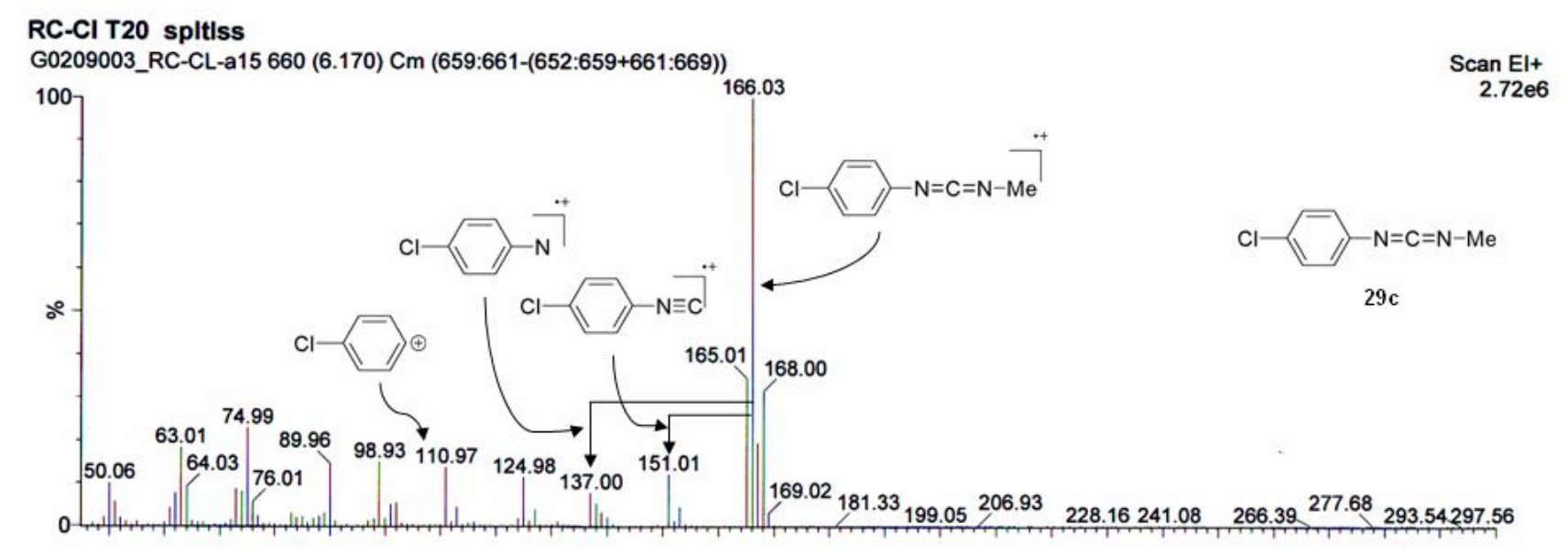
RC-Cl T20 spltlss
G0209003_RC-CL-a15 660 (6.170) Cm (659:661-(652:659+661:669))
Scan EI+
2.72e6
100
%
0
166.03
165.01
168.00
74.99
63.01
89.96
64.03
50.06
76.01
98.93
110.97
124.98
137.00
151.01
169.02
181.33
199.05
206.93
228.16
241.08
266.39
277.68
293.54
297.56
Cl
N
N≡C
N=C=N−Me
29c

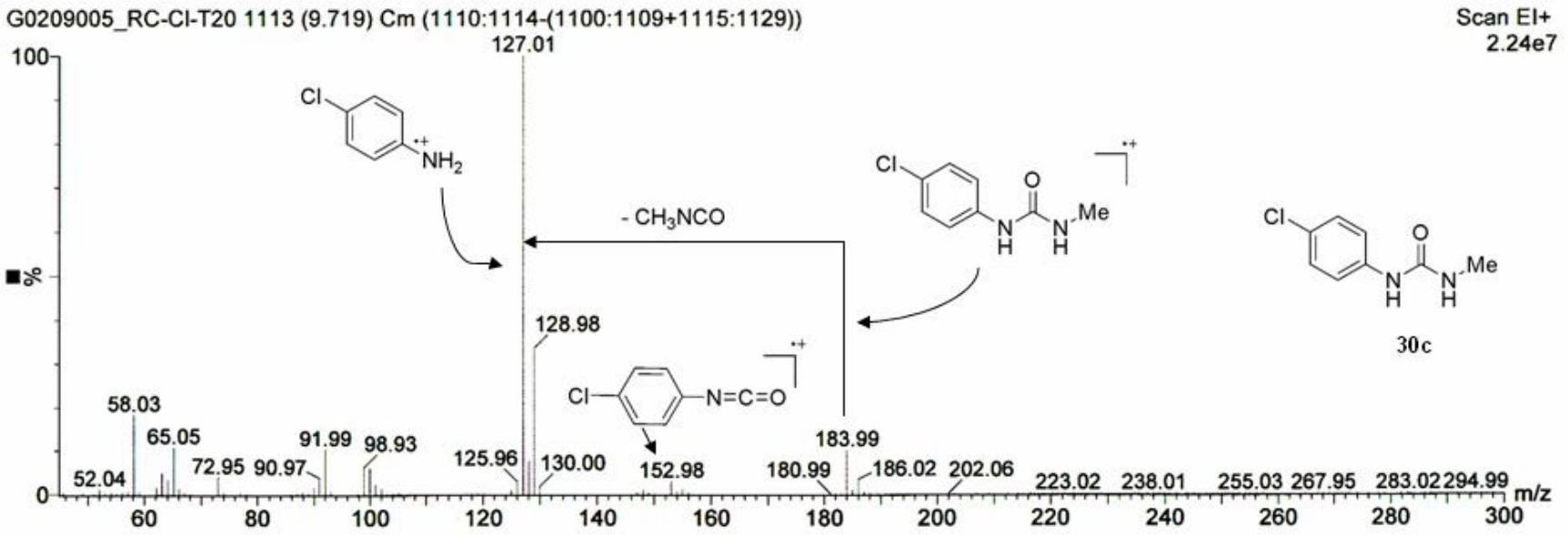
G0209005_RC-Cl-T20 1113 (9.719) Cm (1110:1114-(1100:1109+1115:1129))
Scan EI+
2.24e7
100
%
0
127.01
- CH3NCO
128.98
58.03
65.05
52.04
72.95
90.97
91.99
98.93
125.96
130.00
152.98
180.99
183.99
186.02
202.06
223.02
238.01
255.03
267.95
283.02
294.99
m/z
60
80
100
120
140
160
180
200
220
240
260
280
300
30c

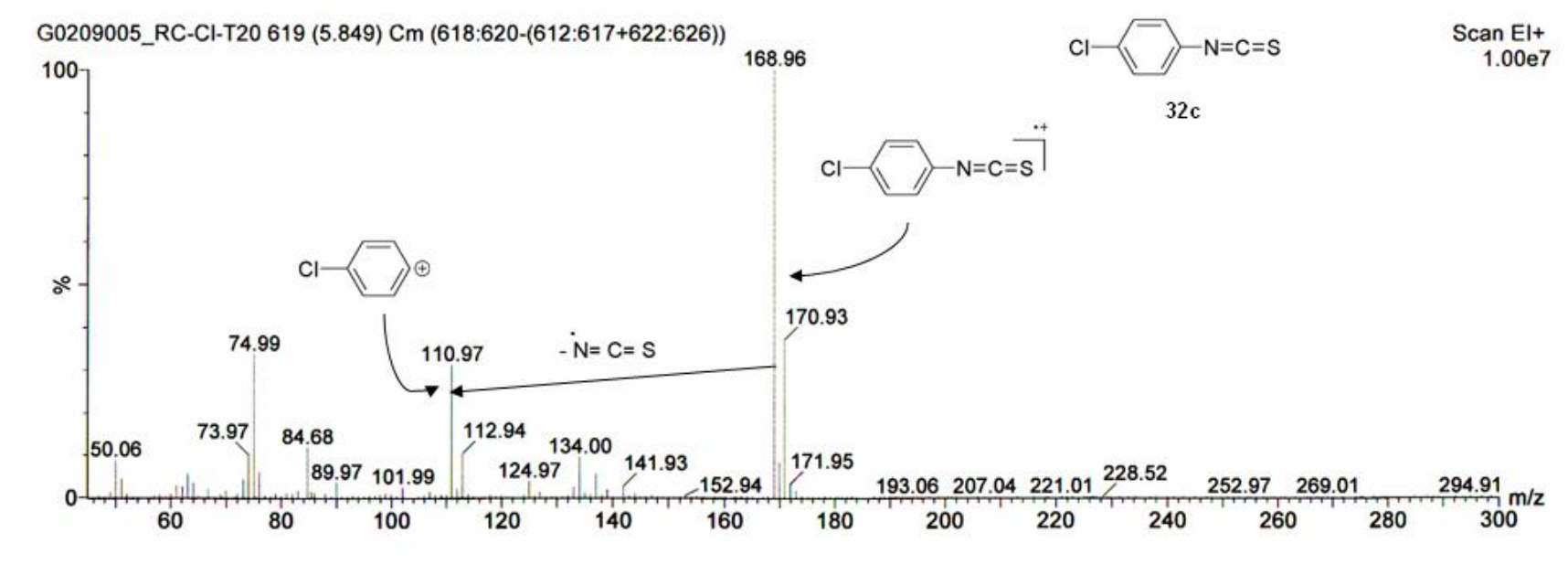
G0209005_RC-Cl-T20 619 (5.849) Cm (618:620-(612:617+622:626))
Scan EI+
1.00e7
168.96
Cl
N=C=S
32c
Cl
N=C=S
Cl
- N= C= S
170.93
110.97
74.99
73.97
84.68
50.06
89.97
101.99
112.94
124.97
134.00
141.93
152.94
171.95
193.06
207.04
221.01
228.52
252.97
269.01
294.91
100
%
0
60
80
100
120
140
160
180
200
220
240
260
280
300
m/z

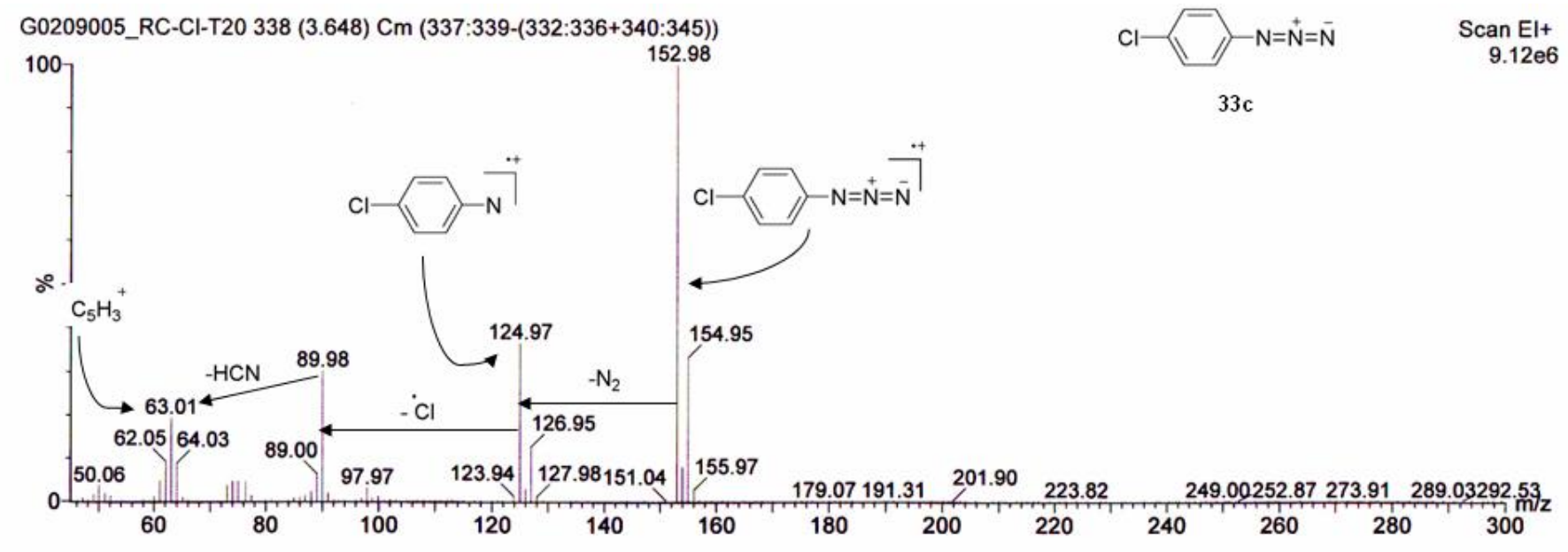
G0209005_RC-Cl-T20 338 (3.648) Cm (337:339-(332:336+340:345))
Scan EI+
9.12e6
33c
100
%
0
$C_5H_3^+$
-HCN
89.98
63.01
62.05
64.03
50.06
89.00
97.97
- Cl
124.97
123.94
126.95
127.98
-N_2
152.98
154.95
151.04
155.97
179.07
191.31
201.90
223.82
249.00
252.87
273.91
289.03
292.53
m/z
60
80
100
120
140
160
180
200
220
240
260
280
300

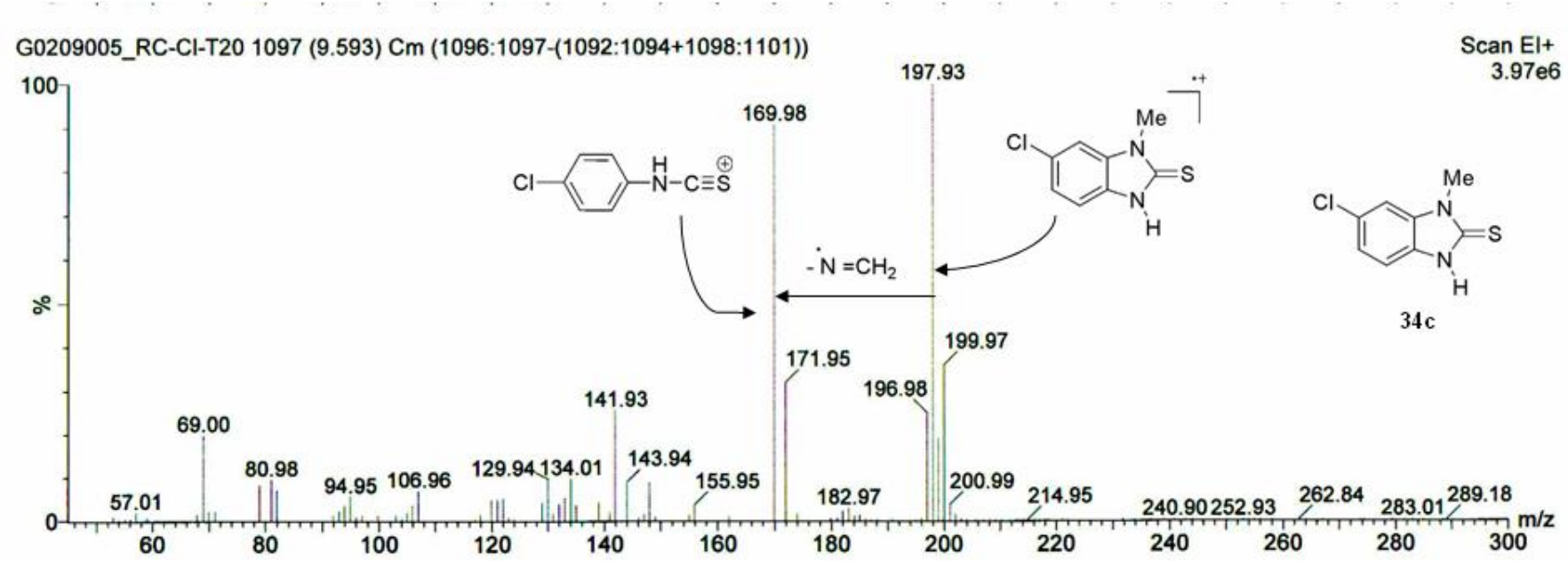
G0209005_RC-Cl-T20 1097 (9.593) Cm (1096:1097-(1092:1094+1098:1101))
Scan EI+
3.97e6
100
%
0
197.93
169.98
199.97
171.95
196.98
141.93
69.00
80.98
94.95
106.96
129.94
134.01
143.94
155.95
182.97
200.99
214.95
240.90
252.93
262.84
283.01
289.18
57.01
m/z
60
80
100
120
140
160
180
200
220
240
260
280
300
Cl
H
N–C≡S
- N =CH2
Me
N
S
N
H
34c

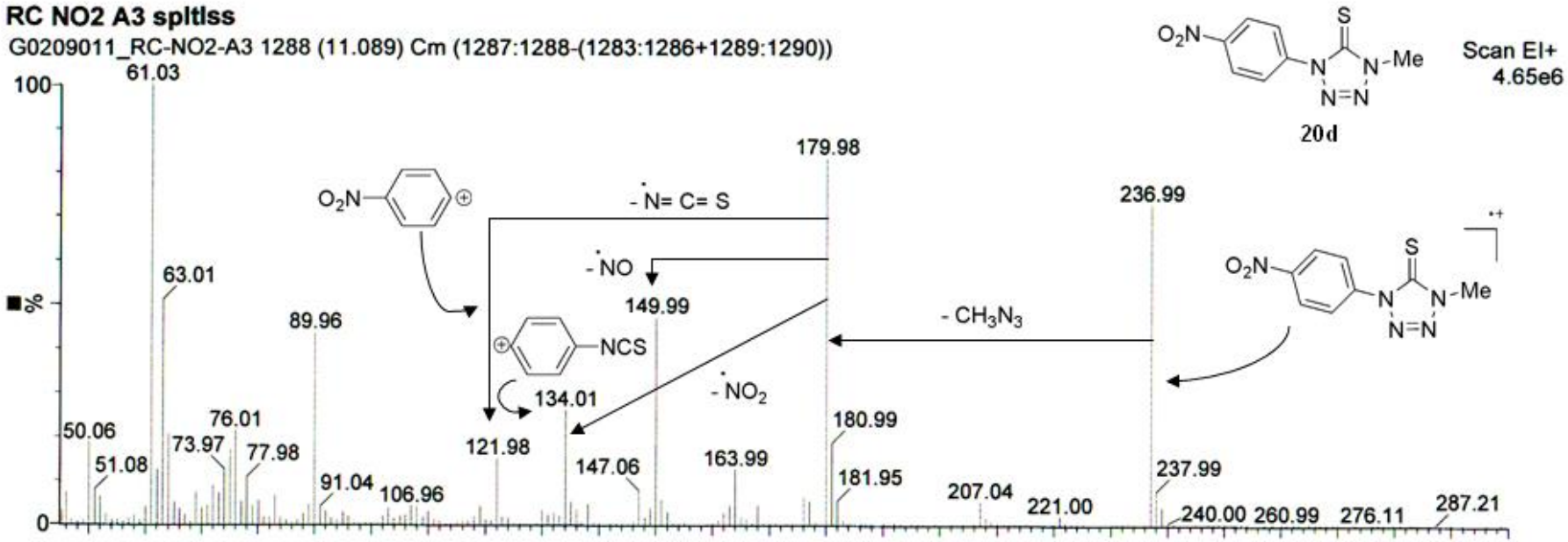
RC NO2 A3 spltlss
G0209011_RC-NO2-A3 1288 (11.089) Cm (1287:1288-(1283:1286+1289:1290))
Scan EI+
4.65e6
20d
100
%
0
61.03
63.01
89.96
50.06
51.08
73.97
76.01
77.98
91.04
106.96
121.98
134.01
147.06
149.99
163.99
179.98
180.99
181.95
207.04
221.00
236.99
237.99
240.00
260.99
276.11
287.21
- N= C= S
- NO
- NO2
- CH3N3
NCS
O2N
Me
N=N

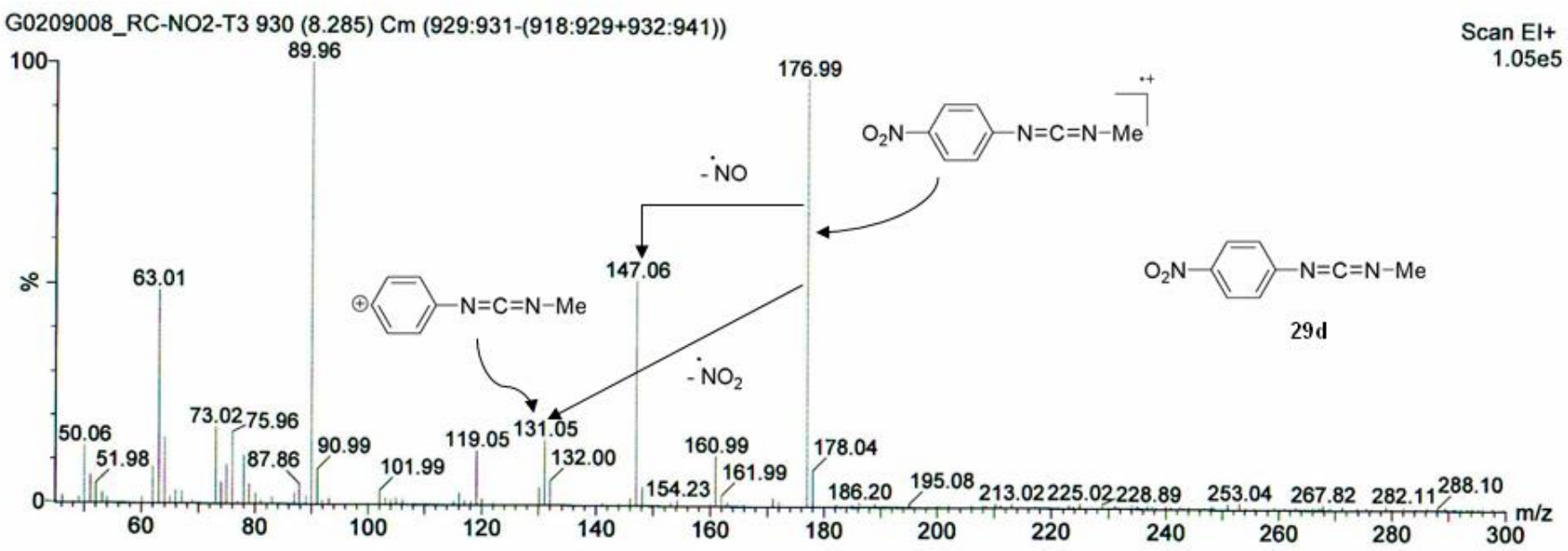
G0209008_RC-NO2-T3 930 (8.285) Cm (929:931-(918:929+932:941))
Scan EI+
1.05e5
100
%
0
89.96
176.99
63.01
147.06
131.05
50.06
51.98
73.02
75.96
87.86
90.99
101.99
119.05
132.00
154.23
160.99
161.99
178.04
186.20
195.08
213.02
225.02
228.89
253.04
267.82
282.11
288.10
m/z
60
80
100
120
140
160
180
200
220
240
260
280
300
- NO
- NO2
O2N
N=C=N-Me
29d

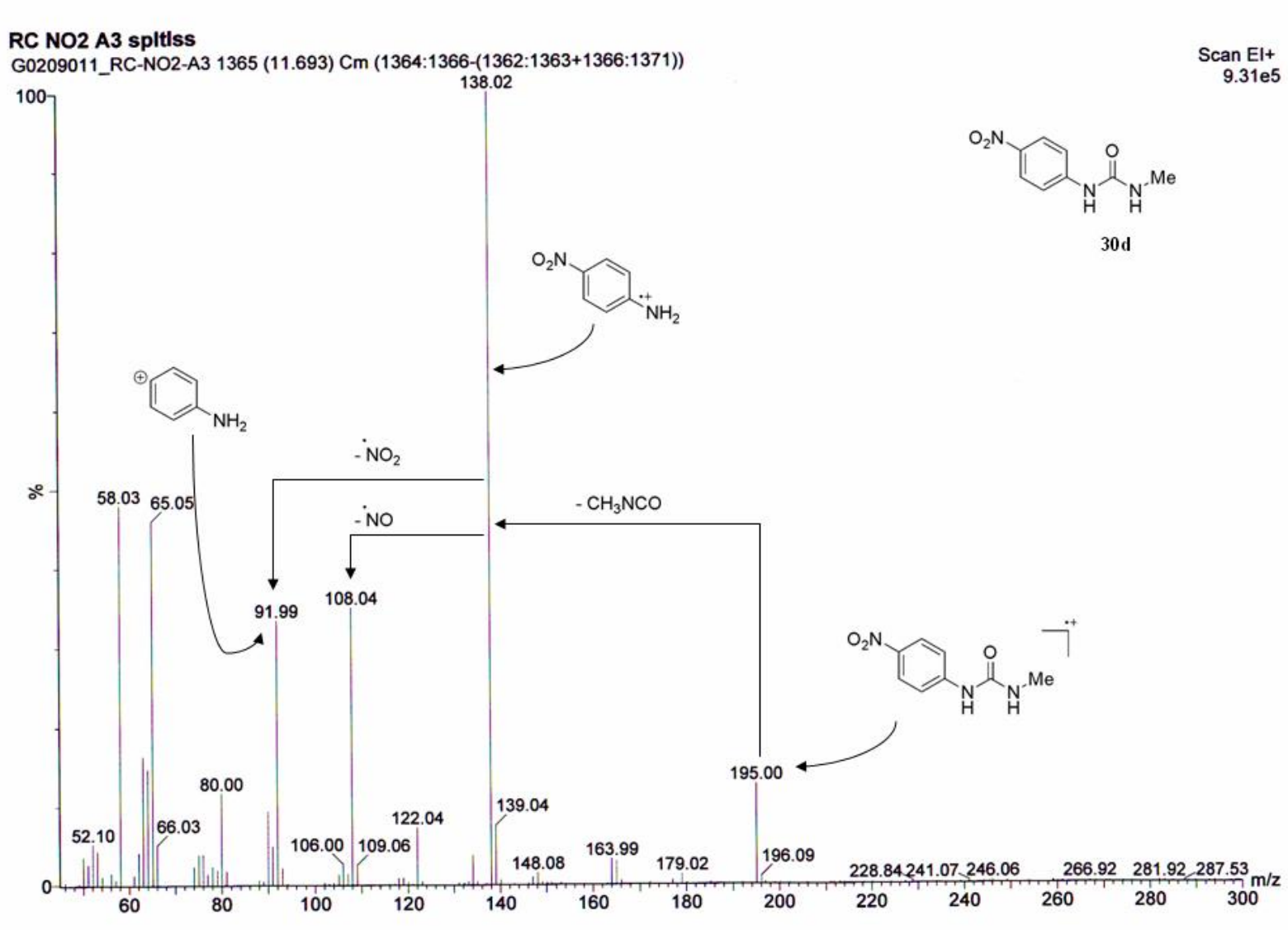
RC NO2 A3 spltlss
G0209011_RC-NO2-A3 1365 (11.693) Cm (1364:1366-(1362:1363+1366:1371))
Scan EI+
9.31e5
30d
- NO2
- NO
- CH3NCO
%
m/z
138.02
91.99
108.04
195.00
58.03
65.05
80.00
52.10
66.03
106.00
109.06
122.04
139.04
148.08
163.99
179.02
196.09
228.84
241.07
246.06
266.92
281.92
287.53

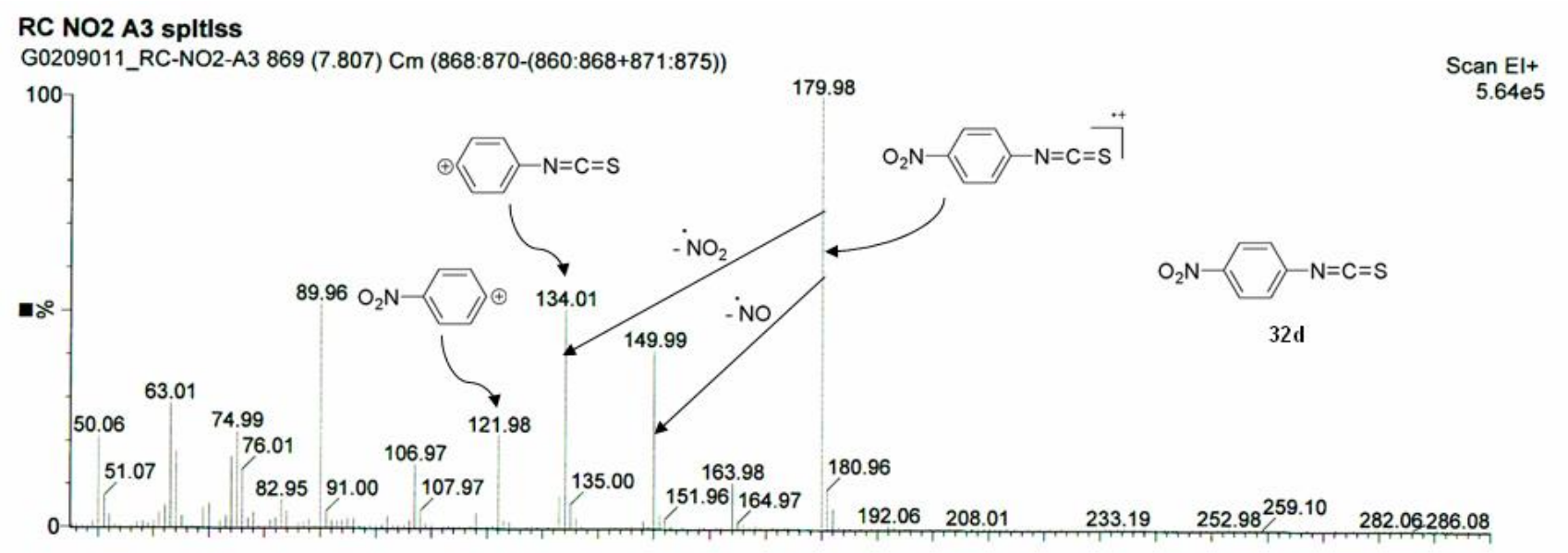
RC NO2 A3 spltlss
G0209011_RC-NO2-A3 869 (7.807) Cm (868:870-(860:868+871:875))
Scan EI+
5.64e5
100
%
0
179.98
134.01
89.96
149.99
121.98
63.01
50.06
74.99
76.01
51.07
106.97
82.95
91.00
107.97
135.00
163.98
151.96
164.97
180.96
192.06
208.01
233.19
252.98
259.10
282.06
286.08
- NO2
- NO
32d

APPENDIX VIII

NMR SPECTRA OF PHOTOLYSIS PRODUCTS

(Chapter -1)

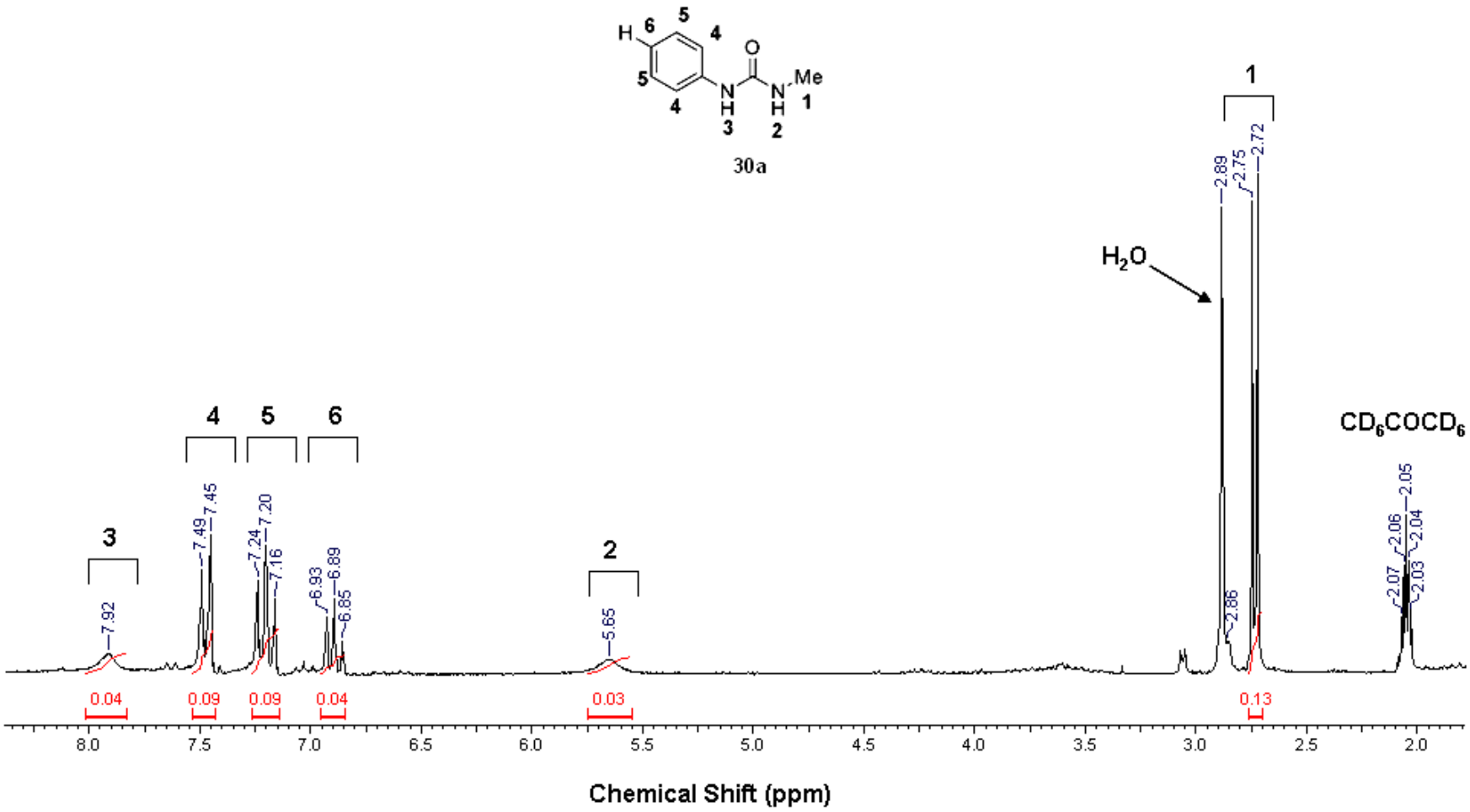
30a
H2O
CD6COCD6
Chemical Shift (ppm)

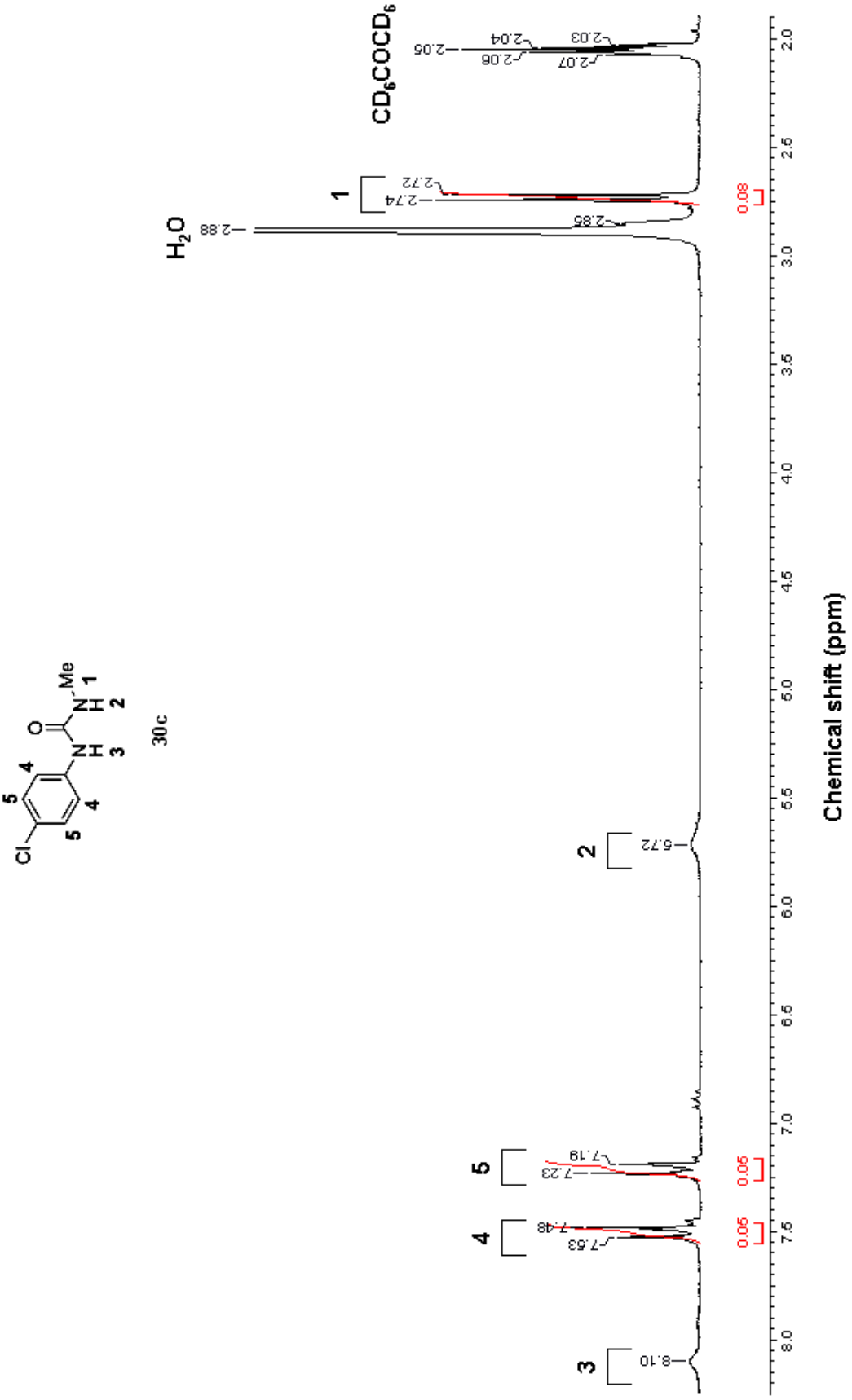
30c
Me
N
H
1
2
O
N
H
3
4
5
4
5
Cl
H_2O
2.88
CD_6COCD_6
2.05
2.04
2.06
2.03
2.07
1
2.74
2.72
2.85
0.08
2
6.72
5
7.19
7.23
0.05
4
7.48
7.53
0.05
3
8.10
2.0
2.5
3.0
3.5
4.0
4.5
5.0
5.5
6.0
6.5
7.0
7.5
8.0
Chemical shift (ppm)

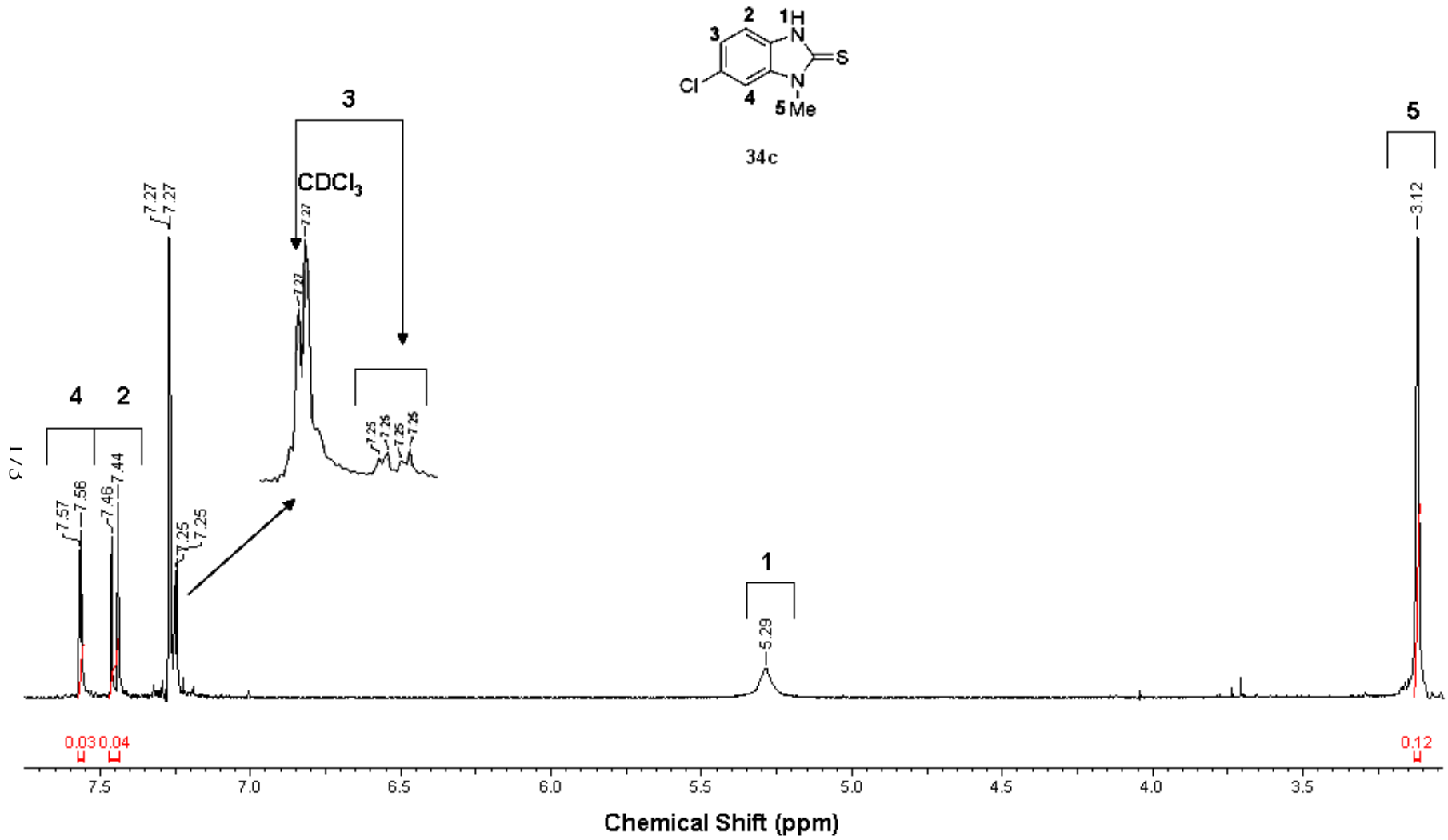
34c
CDCl3
Chemical Shift (ppm)

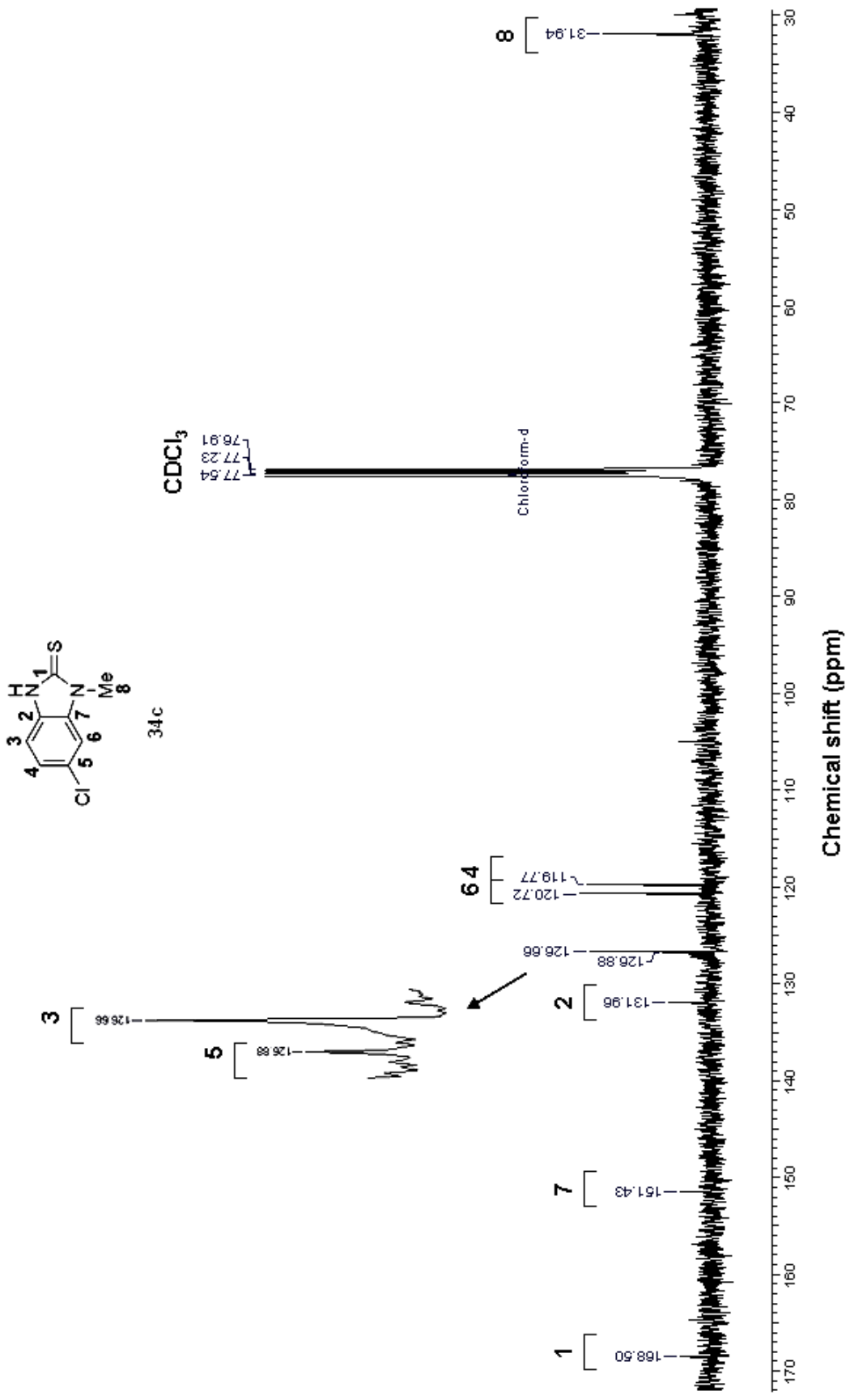
34c
CDCl3
Chloroform-d
Chemical shift (ppm)

APPENDIX IX

HRMS SPECTRUM:6-CHLORO-1,3-DIHYDRO-1-METHYL-2H-BENZIMIDAZOLE-2-THIONE **34c**

(Chapter -1)

+TOFMS- Sample #CA3|P3

Theoretical Mass ([M+H]+): 199.0091

Experimental Mass: 199.0091

Error: 0 ppm

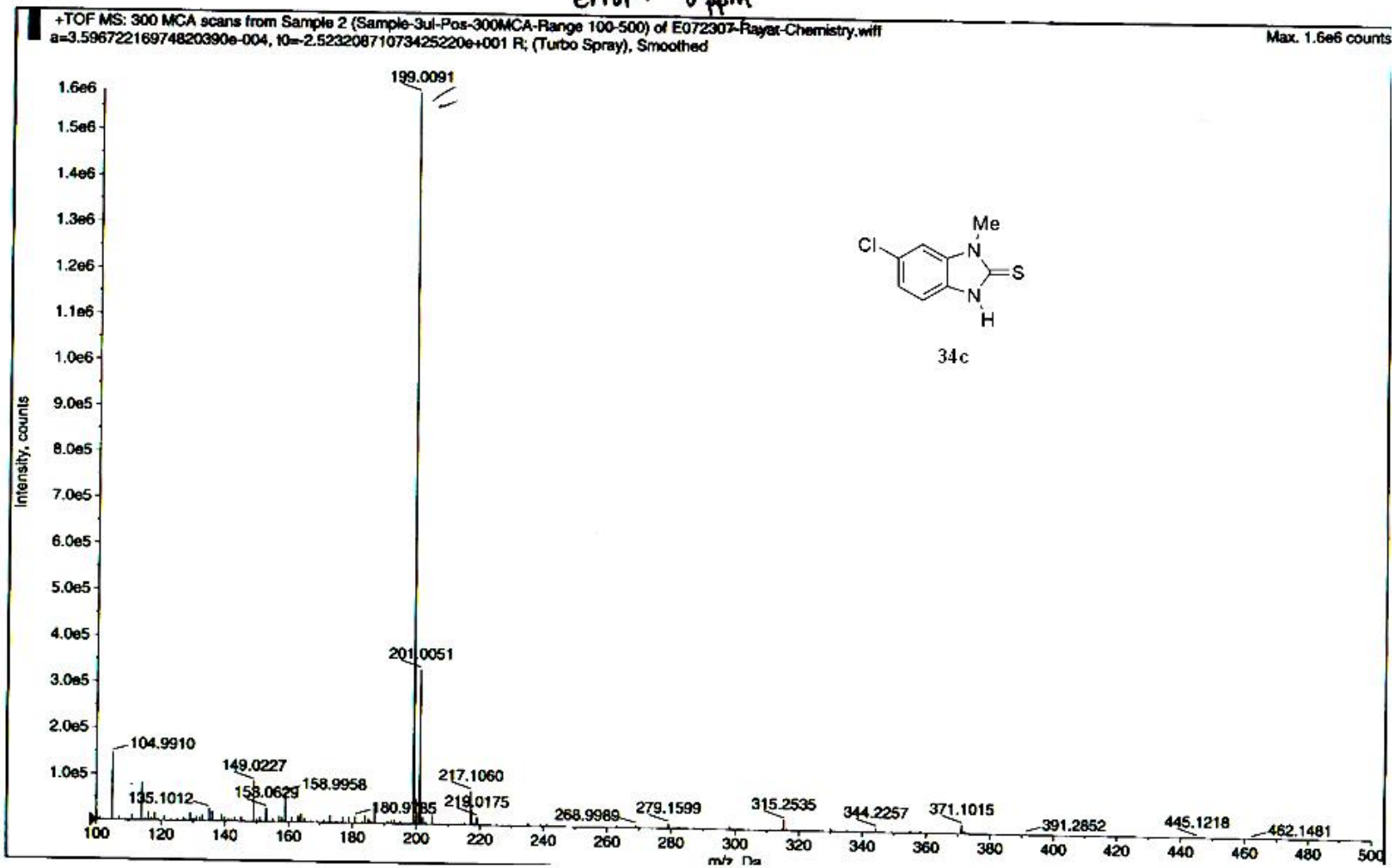

34c

APPENDIX X

OVERLAYED FLUORESCENCE SPECTRA FOR PHOTOLYSIS EXPERIMENTS

(Chapter -1)

Photolysis of MeCN solutions of 20a-d

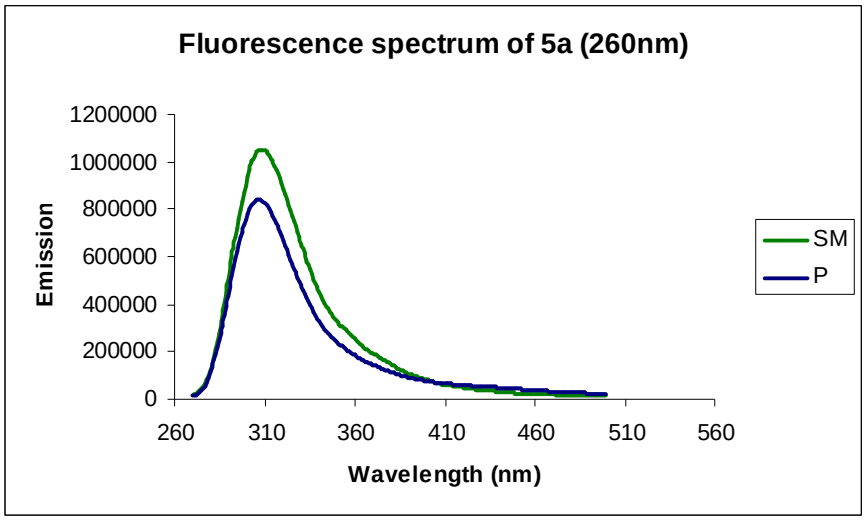

(i) Fluorescence collected before and after 20 min of irradiation of 20a. Excitation wavelength: 260 nm

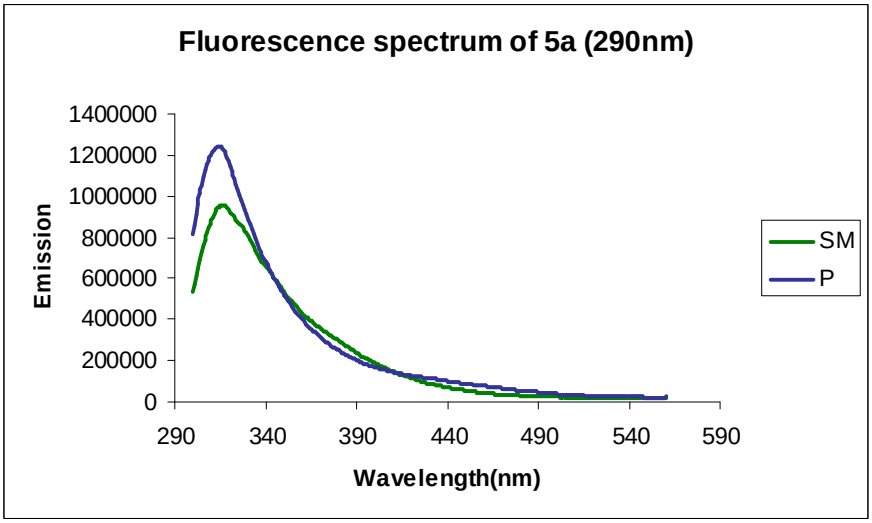

(ii) Fluorescence collected before and after 20 min of irradiation of 20a. Excitation wavelength: 290 nm

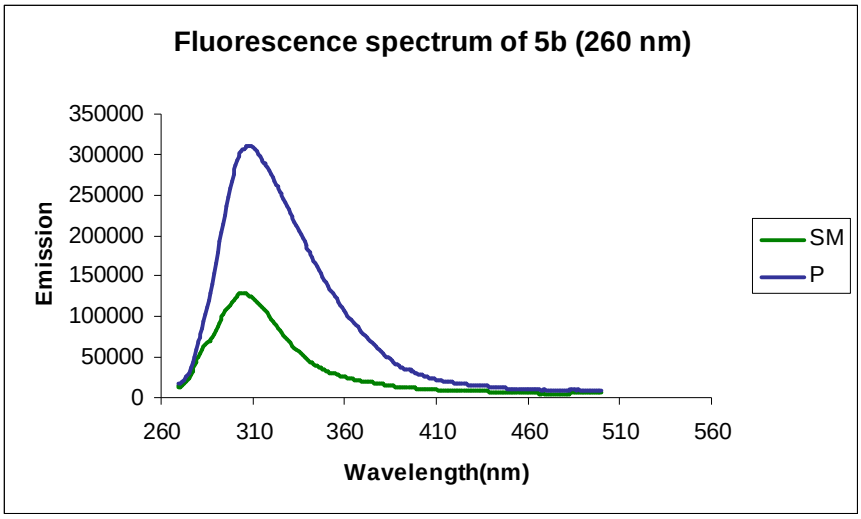

(iii) Fluorescence collected before and after 15 min of irradiation of 20b. Excitation wavelength: 260 nm

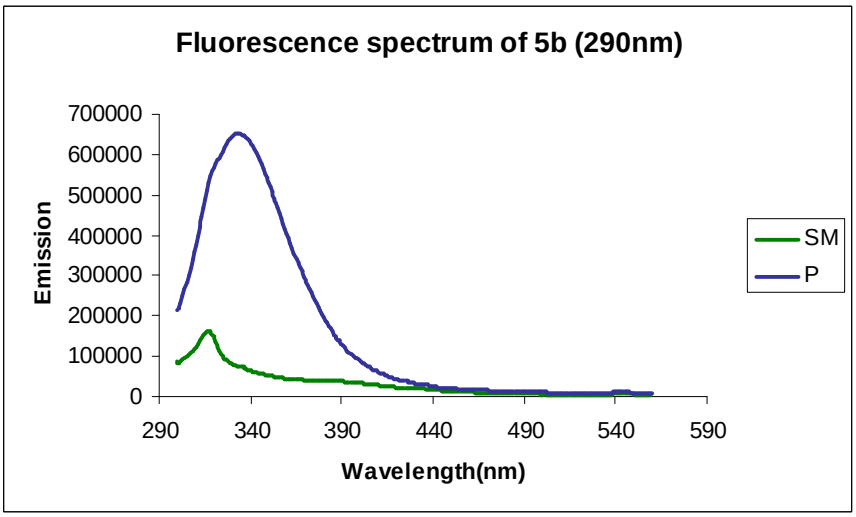

(iv) Fluorescence collected before and after 15 min of irradiation of 20b. Excitation wavelength: 290 nm

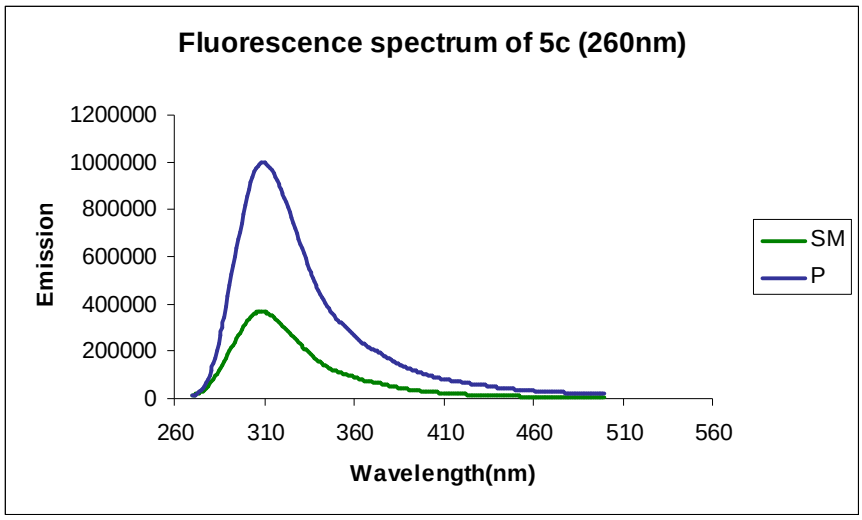

(v) Fluorescence collected before and after 15 min of irradiation of 20c. Excitation wavelength: 260 nm

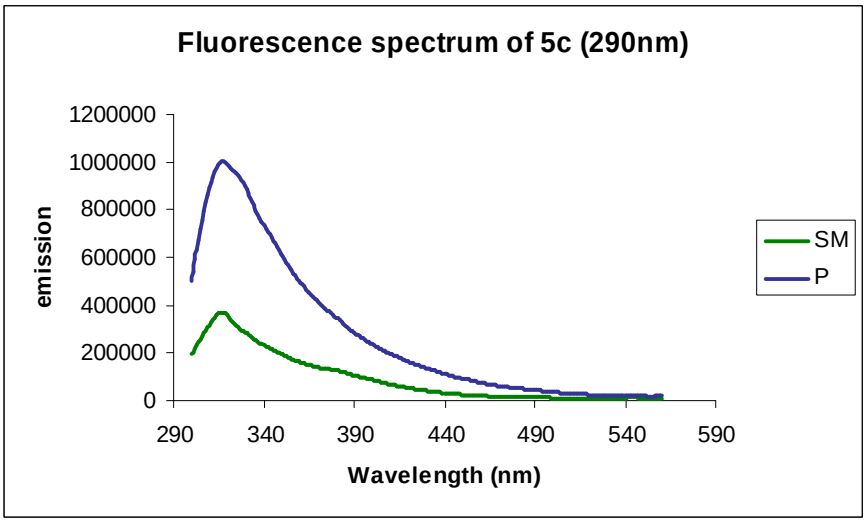

(vi) Fluorescence collected before and after 15 min of irradiation of 20c. Excitation wavelength: 290 nm

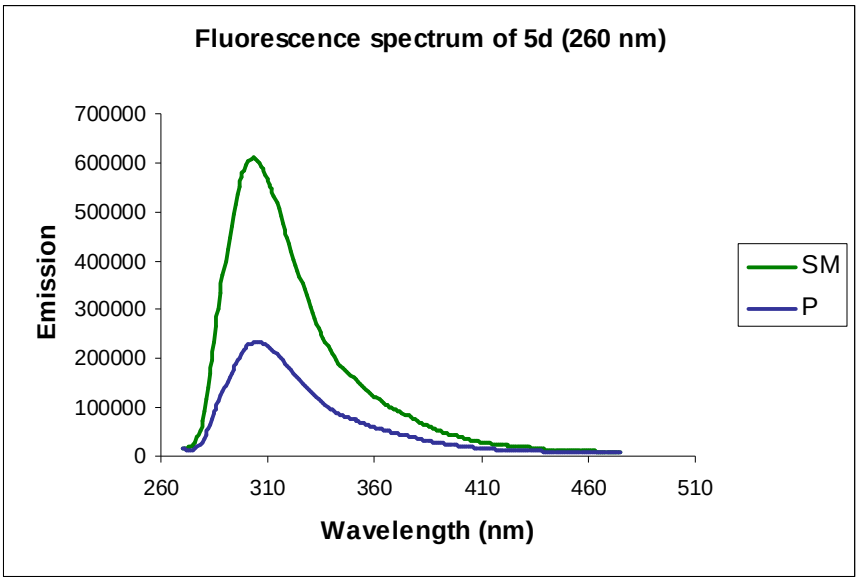

(vii) Fluorescence collected before and after 15 min of irradiation of 20d. Excitation wavelength: 260 nm

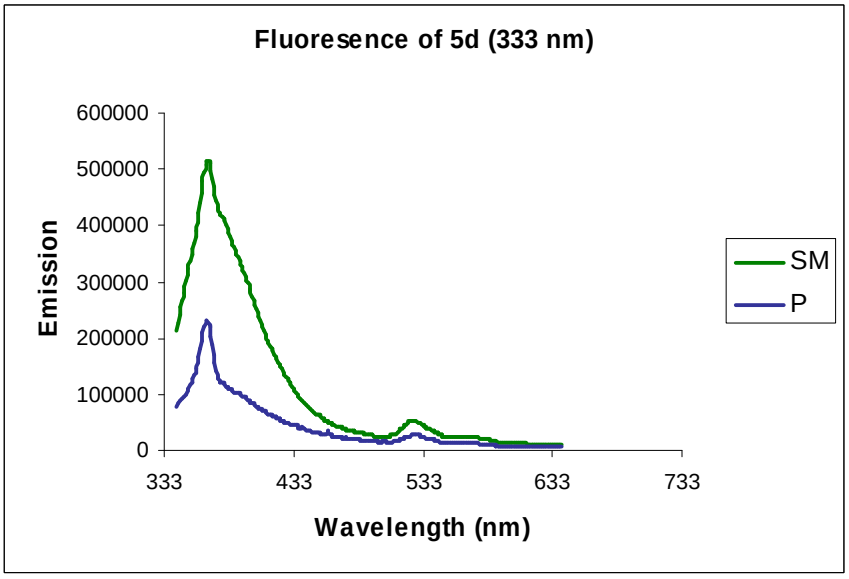

(viii) Fluorescence collected before and after 15 min of irradiation of 20d. Excitation wavelength: 333 nm

APPENDIX XI

^{1}H-NMR AND ^{13}C-NMR SPECTRA OF 2-(2-CYANOPHENYL) ACETIC ACID

(20)

(Chapter -3)

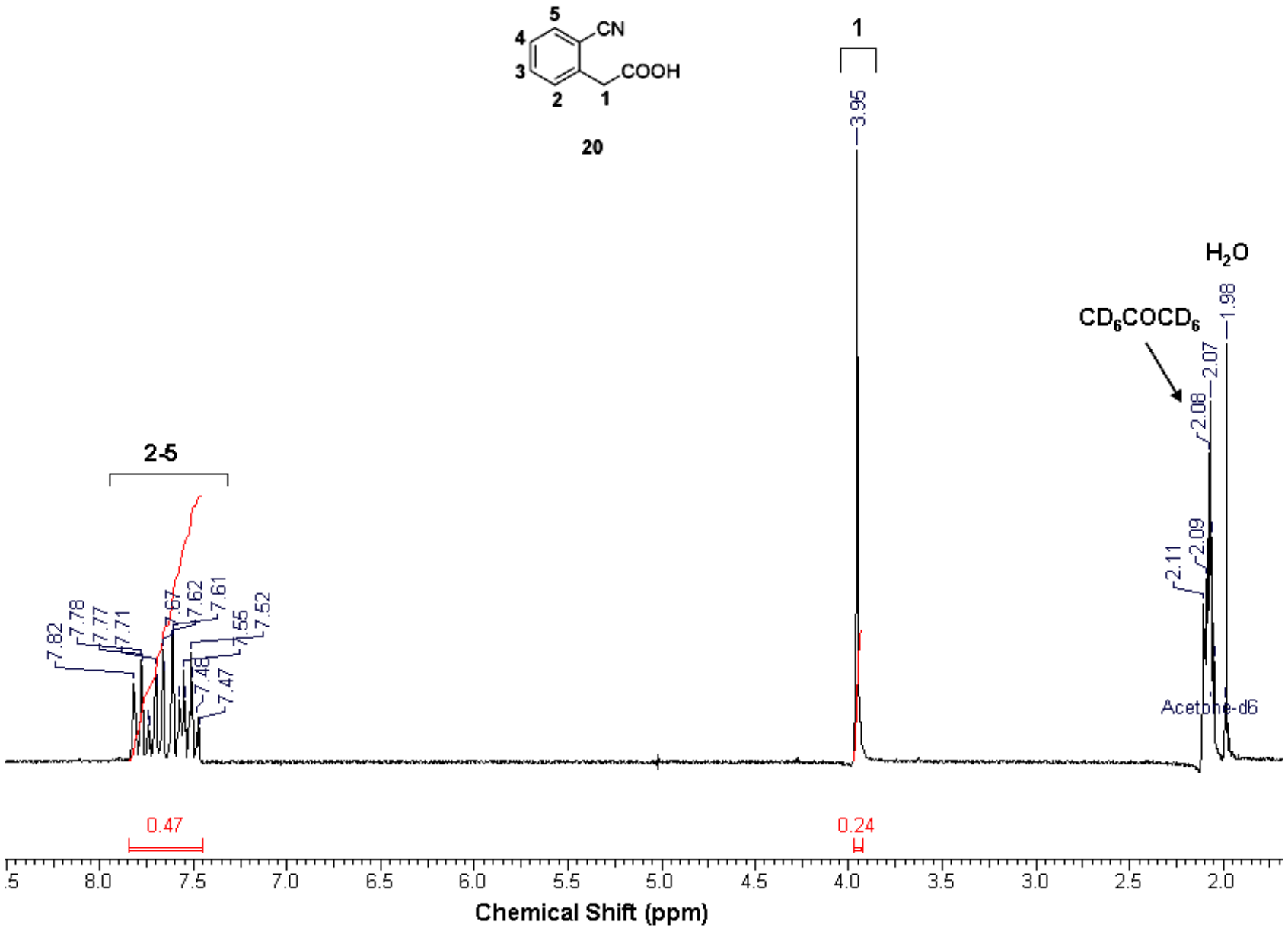
5
4
3
2
1
CN
COOH
20
1
3.95
H2O
CD6COCD6
1.98
2.07
2.08
2.09
2.11
2-5
7.82
7.78
7.77
7.71
7.67
7.62
7.61
7.55
7.52
7.48
7.47
Acetone-d6
0.47
0.24
Chemical Shift (ppm)

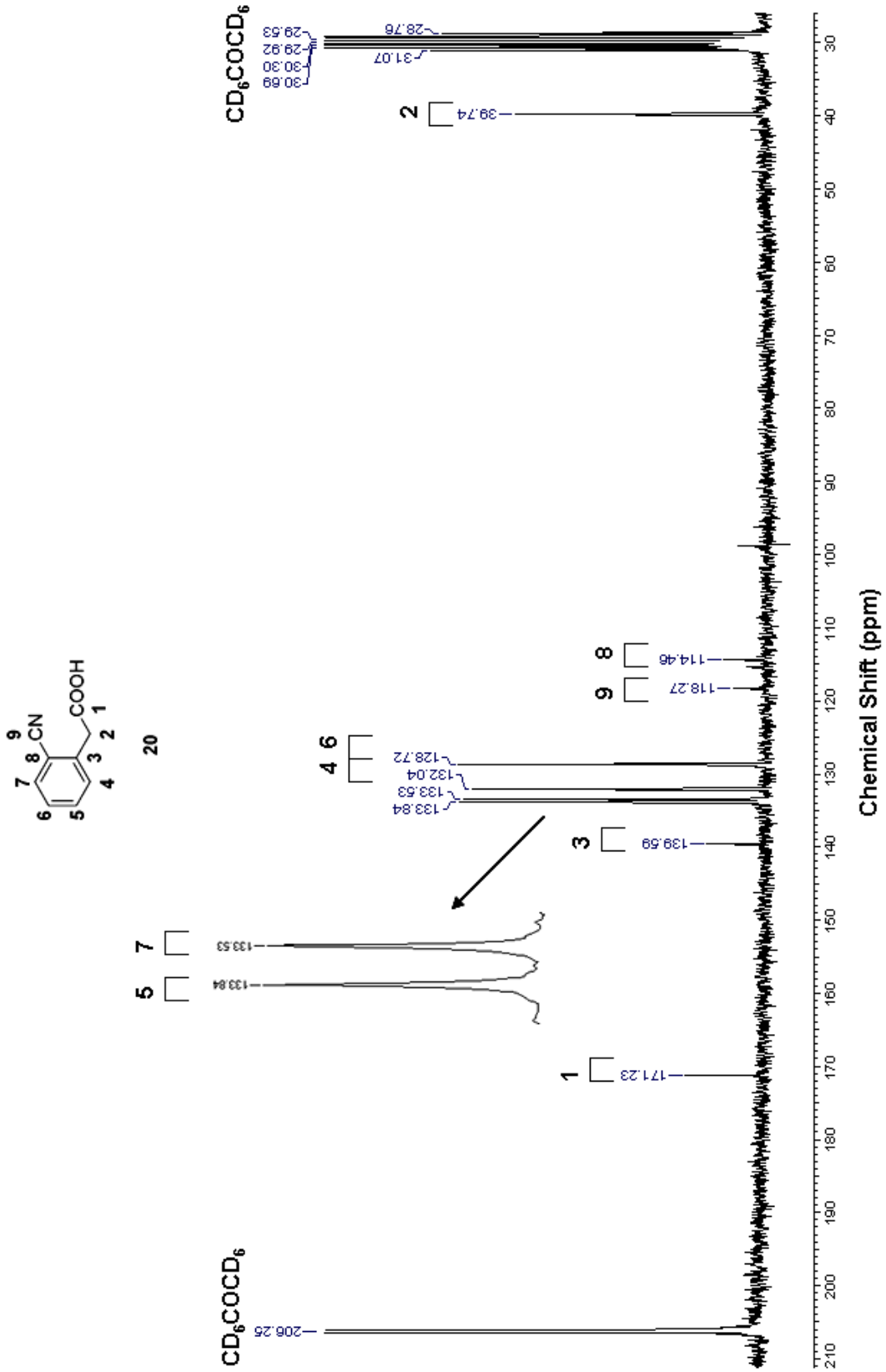
CD6COCD6
206.25
171.23
139.59
133.84
133.53
132.04
128.72
118.27
114.46
39.74
31.07
30.69
30.30
29.92
29.53
28.76
Chemical Shift (ppm)
20
COOH
CN